SYNTHESIS, ANTI-CANCER EVALUATION OF NEW MIXED-LIGAND GOLD(I) COMPLEXES WITH DITHIOCARBAMATES AND PHOSPHINES, AND INTERACTION STUDY OF GOLD(III)-1,2-DIAMINOCYCLOHEXANE COMPLEXES WITH SOME BIOMOLECULES

BY

ADAM AHMED ABDALLAH SULAIMAN

A Dissertation Presented to the

DEANSHIP OF GRADUATE STUDIES

KING FAHD UNIVERSITY OF PETROLEUM & MINERALS

DHAHRAN, SAUDI ARABIA

In Partial Fulfillment of the
Requirements for the Degree of

DOCTOR OF PHILOSOPHY

In

CHEMISTRY

MAY, 2016

KING FAHD UNIVERSITY OF PETROLEUM & MINERALS

DHAHRAN- 31261, SAUDI ARABIA

DEANSHIP OF GRADUATE STUDIES

This thesis, written by **ADAM AHMED ABDALLAH SULAIMAN** under the direction his thesis advisor and approved by his thesis committee, has been presented and accepted by the Dean of Graduate Studies, in partial fulfillment of the requirements for the degree

DOCTOR OF PHILOSOPHY IN CHEMISTRY

Dr. Anvar Husein A. Isab

(Advisor)

2/6/2016

Dr. Abdulaziz Al-Saadi

Department Chairman

Dr. Mohammed I. M. Wazeer
(Member)

Dr. Salam A. Zummo
Dean of Graduate Studies

Dr. Mohammed B. Fettouhi
(Member)

9/6/16

Date

Dr. Hassan A. Al-Muallem
(Member)

Dr. Akhtar A. Naqvi
(Member)

This dissertation is dedicated to my lovely parents, my wife Lana, my kids (Razzan and Aamin) and to who taught me a letter

ACKNOWLEDGMENTS

My first and foremost thanks to Almighty Allah for giving me strength, power and patience to complete my postgraduate study successfully. My special thanks to King Fahd University of Petroleum and Minerals (KFUPM) for providing me an opportunity to achieve my Ph.D. degree in Chemistry Department.

My appreciation connected to the formal Chairman Dr. Abdullah Al-Hamadan for his great efforts that enable me to complete my study. Also, I would like to express my special thanks to current Chairman Dr. Abdulaziz Al-Saadi and Graduate Coordinator Prof. Bassam El-Ali for their supports and facilities provided by Chemistry Department.

I would like to connect my gratitude and special thanks to my advisor Prof. Anvar Husein A. Isab for his encouragement, he accepted me when I was in my sixth semester. I want to thank him for his support, guidance and wisdom words without his enthusiasm and dedication this work could not be possible by Allah's willing.

I wish to appreciate and acknowledge my committee members Dr. Mohammed Fettouhi, Dr. Hassan Al-Muallem, Prof. Mohammed I. M. Wazeer and Prof. Akhtar Naqvi for their help, advice, guidance and revision of my dissertation. Further, I need to give my thanks to Mr. Mohammed Arab and Mr. Mansour Al-Zaki for their support to use IR, Elemental analyzer, and NMR. Heartfelt thanks to Dr. Musa M. Musa and Dr. Abdel-Nasser Kawde for their help beside a permission to do a part of my work in their labs. Many thanks to Dr. Mohammed Altaf for his help and advice.

Thank you kindly, my parents for your sacrifices, my wife Lana, my kids Razzan and Aamin for your prayers, support, and advice. Thanks to Sudanese Students in KFUPM.

TABLE OF CONTENTS

LIST OF TABLES

LIST OF FIGURES

LIST OF ABBREVIATIONS

A549	Human lung carcinoma cell line
[Au(Ipr)Cl]	1,3-bis(2,6-di-isopropylphenyl) imidazol-2-ylidenegold(I) chloride
CV	Cyclo voltammetry
Cy	Cyclohexyl group
DACH	1,2-Diaminocyclohexane
DEDTC	Diethyldithiocarbamate
DBDTC	Dibenzyldithiocarbamate
DMDTC	Dimethyldithiocarbamate
DMEM	Dulbecco's Modified Eagle's Medium
Diap	1,3-diazepine-2-thione
Diaz	1,3-diazinane-2-thione
DiapSe	1,3-diazepane-2-selone
DiazSe	1,3-diazinane-2-selone
en	Ethylenediamine
FT-IR	Fourier transformer infra-red
H-His-Met-OH (D)	Peptide
H-Gly-Gly-Met-OH (T)	Peptide
HCT15	Human colon cancer cell line
ImSe	1,3-imidazolidine-2-selone
Imt	1,3-imidazolidine-2-thione

L0	2-(diphenylphosphino)ethylamine
L1	(1R,2R)-2-(diphenylphosphino)-2,3-dihydro-1H-inden-1-amine
L2 = L4	(1R, 2R)-2-(diphenylphosphino)-1-aminocyclohexane
L3	Bis(2-cyanoethyl)phenylphosphine
L5	(1R, 2R)-2-(diphenylphosphino)-1,2-diphenylethylamine
L6	(R)-2-(diphenylphosphino)-1-phenylethylamine
L7	(R)-1-(diphenylphosphino)-2-amino-3,3-dimethylbutane
L8	Tricyclohexylphosphine
L9	3-(Diphenylphosphino)propylamine
L10	1,3-Bis(Diphenylphosphino)propane
L11	1,2-Bis(Diphenylphosphino)ethane
L12	Bis[2-(Dicyclohexylphosphino)ethyl]amine
MCF7	Human breast adenocarcinoma cell line
MTT	3-(4,5-dimethylthiazol-2-yl)-2,5-diphenyltetrazolium bromide
NHC	N-heterocyclic carbene
PipDTC	Piperidinyldithiocarbamate
R_3P	Trialkyl/aryl phosphine
TMS	Tetramethylsaline
Thiourea	Thiourea
SWSV	Square wave stripping voltammetry

ABSTRACT

Name: **Adam Ahmed Abdallah Sulaiman**

Title of Study: **Synthesis, Anti-Cancer Evaluation of New Mixed-Ligand Gold(I) Complexes with Dithiocarbamates and Phosphines, and Interaction Study of Gold(III)-1,2-Diaminocyclohexane Complexes with Some Biomolecules**.

Major Field: **Chemistry**

Date of Degree: **May, 2016**

Recent advancement in the field of drug formulation and discovery of gold(I) compounds is leading to the innovation of new and unusual gold(I) molecules with linear structure and geometry around the cation. The gold(I) dithiocarbamate complexes, (**2-17**), (**18-22**), (**23-26**), (**27-30**) and (**31-34**), type ([Au(R_3P)(R_2NCS_2)] (where R_2= dimethyl, diethyl and dibenzyl) were prepared by the reaction of R_3PAuCl compound with sodium dimethyldithiocarbamate monohydrate and sodium diethyl dithiocarbamate trihydrate and dibenzyldithiocarbamate, respectively. The precusors have been prepared by the reaction of $(CH_3)_2SAuCl$ **(1)** with equimolar amount of R_3P. In addition, the complexes of gold(I) phosphine (**35-37**), gold(I) carbene (**38-50**), gold(I) thione (**51-55**) and gold(I) carbene (**56-65**) have been prepared. These complexes were characterized by FT-IR, ^{1}H, ^{13}C, ^{31}P, ^{77}Se NMR spectroscopy and elemental analysis. Complexes **27, 39, 44, 46, 48, 49, 54, 55, 56, 61, 63** and **65** were characterized by X-ray diffraction analysis, showing linear geometrical structure around gold center atom. Gold(I) complex **(20-22)** (IC_{50}

19.56 ± 0.85, 29.25 ± 1.81 and 34.42 ± 1.02 μM) showed potent *in vitro* cytotoxicity one-to-two fold higher than *cisplatin* (IC_{50} 42.2 ± 2.01 μM) against A549 (human lung carcinoma). Furthermore, complex **48 (**IC_{50} 27.97 ± 1.67) showed better *in vitro* cytotoxicity than *cisplatin* (IC_{50} 32.04 ± 2.12 μM) against HCCT15. All other studied complexes exhibited similar and moderate to lower in *vitro* cytotoxicity against A549, HCT15 (human colon cancer) and HeLa (human cervical cancer) cell lines.

The interactions of the synthesized [Au(*cis*-DACH)Cl_2]Cl and [Au(*cis*-DACH)$_2$]Cl_3 complexes, (DACH=*cis*-1,2-diaminocyclohexane), with enriched (^{13}C,^{15}N) thiourea and 1,3-diazinane-2-thione ligands were investigated. The progress of these reactions was monitored with NMR (^1H, ^{13}C and ^{15}N) and UV-Vis spectroscopy as well as square wave stripping voltammetry. The kinetics of the substitution reactions between the above-mentioned complexes with thione ligands were studied in aqueous solutions containing 30 mM KCl, which is used to suppress hydrolysis of the chloride complex. The reactions were followed under pseudo first-order conditions as a function of ligand concentration, pH and temperature in the range of 15-37 °C. The activation parameters ($\Delta H^{\#}$, $\Delta S^{\#}$) were calculated from Eyring plot and the negative values of $\Delta S^{\neq}$ lend support for an associative mechanism. The kinetic data also indicate a relatively higher reactivity of [Au(*cis*-DACH)Cl_2]Cl than [Au(*cis*-DACH)$_2$]Cl_3 towards the thiones.

The interaction of [Au(*cis*-DACH)Cl_2]Cl and [Au(*cis*-DACH)$_2$]Cl_3 complexes [where *cis*-DACH: is *cis*-1,2-diaminocyclohexane] with enriched (^{13}C,^{15}N) KCN were carried out in CD_3OD and D_2O, respectively. The reaction pathways of these complexes were studied by ^1H, ^{13}C, ^{15}N NMR, UV spectrophotometry and electrochemistry. The kinetic data of the reaction of cyanide ion with [Au(*cis*-DACH)$_2$]Cl_3 are found to be k = 18

$M^{-1}s^{-1}$, $\Delta H^{\neq}$ = 11 $kJmol^{-1}$, $\Delta S^{\neq}$ = -185 $JK^{-1}mol^{-1}$, and E_a = 13 kJ mol^{-1} with SWV peak +1.35 V, whereas the kinetic data for the reaction of cyanide ion with [Au(*cis*-DACH)Cl_2]Cl are found to be k = 148 $M^{-1}s^{-1}$, $\Delta H^{\neq}$ = 39 $kJmol^{-1}$, $\Delta S^{\neq}$ = -80 $JK^{-1}mol^{-1}$, and E_a= 42 $kJmol^{-1}$ along with SWV peak +0.82 V, indicating the much higher reactively of [Au(*cis*-DACH)Cl_2]Cl toward cyanide ligand than [Au(*cis*-DACH)$_2$]Cl_3. The interaction of these complexes with potassium cyanide resulted in an unstable $[Au(^{13}CN)_4]^-$ specie, which readily underwent reductive elimination reaction to generate $[Au(^{13}CN)_2]^-$ and cyanogen (NCCN).

Kinetic measurements revealed the rate constants of the interaction between [Au(*cis*-DACH)Cl_2]Cl with Tu and DIAZ are 49.50; 121.70 and 24.31; 46.65 $M^{-1}s^{-1}$, respectively, at 288 K and 310 K. Similarly, the rate constants for [Au(*cis*-DACH)$_2$]Cl_3 with Tu and DIAZ are found to be 41.88; 64.86 and 21.68; 40.89 $M^{-1}s^{-1}$, respectively at 288 K and 310 K. [Au(*cis*-DACH)Cl_2]Cl reacted faster towards thione ligands than [Au(*cis*-DACH)$_2$]Cl_3 complex; also Tu reacted faster than DIAZ towards these complexes. The negative values of $\Delta S^{\neq}$ for these reactions lend support for an associative mechanism.

DEGREE OF PHILOSOPHY OF DOCTRATE IN CHEMISTRY

KING FAHD UNIVERSITY OF PETROLEUM AND MINERALS

DHAHRAN, SAUDI ARABIA

ملخص الرسالة

الاسم الكامل: آدم أحمد عبدالله سليمان

عنوان الرسالة: اصطناع وتقييم تضاد السرطان لمعقدات الذهب(+1) المشتقة من لاقطات الفوسفينات مع كاربومات ثنائية الكبريت ودراسة تفاعلات معقدات الذهب(+3) المشتقة من لاقطة 2,1-ثنائى أمين الهكسان الحلقي مع بعض الجزيئات الحيوية

التخصص: علوم الكيمياء

تاريخ الدرجة العلمية: مايو 2016

التقدم المتزايد حديثا في مجال صناعة أدوية السرطان مع أكتشاف معقدات الذهب(+1) أدي الى اختراع معقدات ذهب(+1) جديدة ذات تركيبة خطية حول أيون الذهب المركزي. حضرت مجموعات متسلسلة من معقدات الذهب(+1) (**2-17**)، (**18-22**)، (**23-26**)، (**27-30**) و(**31-34**) مشتقة من لاقطات ثنائي ميثيل ثنائي كبريت-الكاربومات وثنائي ايثيل ثنائي كبريت-الكاربومات وثنائي بنزيل ثنائي كبريت-الكاربومات بالاضافة الي لاقطات فوسفينات مختلفة. هذه المعقدات آنفة الذكر تم تحضيرها من تفاعل مركب الذهب(+1) المشتق من كلوريد وثلاثي ألكيل/اريل الفوسفين مع لاقطات الكاربومات المذكورة سابقا. المركب الاولي ثلاثي ألكيل/أريل فوسفين كلوريد الذهب(+1) حضر من تفاعل مركب ثنائي ميثيل كبريتيد كلوريد الذهب(+1) مع مختلف لاقطات آحادية وثنائية الفوسفين.

بالاضافة الي هذه المعقدات تم تحضير معقدات أخرى وهي فوسفينات الذهب(+1) (**35-37**)، كاربينات سيلونات الذهب(+1) (**39-50**)، ثيونات الذهب(+1) (**51-55**) وكاربينات الذهب(+1) المرتبطة بفوسفينات احادية وثنائية (**56-65**). درست خصائص هذه المعقدات بواسطة مطيافية الاشعة تحت الحمراء والرنين النووى المغنطيسى لأنوية الهيدروجين والكربون والفسفور والسيلينيوم بالاضافة الي تحليل العناصر ومطيافية حيود الاشعة السينية للبلورات. المعقدات بالارقام **27**, **39**, **44**, **46**, **48**, **49**, **54**, **55**, **56**, **61**, **63** و**65** درست خصائصها بواسطة مطيافية حيود الاشعة السينية وقد أظهرت تركيبة هندسية خطية حول أيون الذهب(+1) المركزي.

أجريت دراسة فاعلية هذه المعقدات مختبريا علي ثلاثة انواع من خلايا السرطان المصنعة وهي سرطان الرئة والقولون وعنق الرحم. أظهرت المعقدات بالارقام **20-22** فاعلية قوية جدا ضد خلية سرطان الرئة أكثر من تلك التي أعطيت بواسطة معقد سيس بلاتين(+2) كعلاج قياسي لمعظم أنواع السرطانات. كذلك المعقد **48** أظهر فاعلية قوية

ضد خلية سرطان القولون أكثر من معقد السيس بلاتين(+2). بينما المعقدات الاخري اعطت فاعلية اقل من تلك التي وجدت لمعقد السيس بلاتين(+2) ضد خلايا سرطان الرئة والقولون وعنق الرحم.

من جهة أخرى حضرت معقدات الذهب(+3) المشتقة من 2,1-ثنائي أمين الهكسان الحلقي ودرست تفاعلاتها مع لاقطات السيانيد والثيويوريا و3,1-ثنائي ازانين-2-ثيون بواسطة مطيافية الضوء المرئي-الاشعة فوق البنفسجية والرنين النووي المغنطيسي لأنوية الهيدروجين والكربون والنتروجين بالاضافة الي فولتية تعرية الموجة المربعة.

درست حركية تفاعلات الاستبدال لمعقدات الذهب(+3) مع اللاقطات الآنفة الذكر، عن طريق الرتبة الأولي الكاذبة في درجات حرارة تتراوح بين 37-15 درجة مئوية في محاليلها المائية، والتي احتوت علي كلوريد البوتاسيوم بتركير 30 مليمولار لمنع ايونات كلوريد هذه المعقدات من التحلل.

حسبت معدلات سرعة التفاعل بالاضافة الي حركية التنشيط لطاقات المحتوى الحراري والانتروبيا لهذه المعقدات باستخدام معادلة ارينج. اوضحت الدراسة بان معقدات الذهب(+3) المشتقة من 2,1-ثنائي أمين الهكسان الحلقي المرتبطة بأيونات الكلوريد أسرع تفاعلا تجاه لاقطات السيانيد والثيويوريا و3,1-ثنائي ازانين-2-ثيون من تلك التي لا تحتوي علي الكلوريد وكذلك السيانيد اسرع من الثيويوريا و3,1-ثنائي ازانين-2-ثيون. كما اوضحت الدراسة ان معقدات الذهب(+3) غير مستقرة حينما تختزل الى معقدات الذهب(+1) في وجود هذة اللاقطات.

درجة الدكتوراة في فلسفة علوم الكيمياء

جامعة الملك فهد للبترول والمعادن

الظهران- المملكة العربية السعودية

CHAPTER 1

INTRODUCTION

1.1. Gold(III) complexes

Gold was discovered as shining yellow chunks, its symbol derived from Latin name *Aurum*. In early civilizations, humans almost spontaneously attribute a high value to gold associating it with power of beauty. In the ancient time 2500 BC, Chinese and Arab have used gold in medicine. Gold possesses special characteristic features that make it unique, such as high chemical and thermal stability, mechanical softness and high electrical conductivity. Gold(III) has electronic configuration d^8 ([Xe]$4f^{14}5d^8$) and forms diamagnetic four coordinate $16e^-$ species with predominantly square-planar geometry analogue to Pt(II) complexes. Five coordinate gold(III) complexes are rare [1-2].

The unexpected disclosure of cisplatin by Rosenberg in 1965 proclaimed another region of anticancer medication research on metal-based medication [3]. Cisplatin has been a standout amongst the best chemotherapies in the most recent 30 years, and has been utilized to treat various sorts of tumor diseases. In spite of having great usefulness as a chemotherapeutic, cisplatin has downsides; tumors regularly create imperviousness to the medication, and patients routinely encounter serious symptoms over the span of treatment [4]. Subsequently, scientists are consistently searching for remedial options that may

enhance these constraints. Common problems include cumulative toxicities of nephrotoxicity and cytotoxicity [5–8]. Notwithstanding the genuine symptoms, the remedial adequacy is additionally constrained by regular or treatment-impelled resistance tumor cells. These drawbacks have given the inspiration to select chemotherapeutic procedures. To stay away from the issue of medication resistance in cisplatin, gold(III)_ based compounds have been outlined as a potential distinct option for cisplatin [9–13].

Gold(III) derivatives have significantly pulled in researcher's consideration in the most recent decade for their exceptional cytotoxic activities. It is a metal ion which normally has a four-coordinate, square-planar geometry and anticipated to emulate the structure and electronic properties of platinum(II). Late studies have demonstrated that few gold(III) compounds are exceptionally cytotoxic against various tumor cells [10, 14–16], including some which are active even against the cisplatin-resistance cell lines [17–19]. A few lines of confirmation propose that gold (III) complexes produce their anti-proliferative impacts through innovative and nonconventional modes of activity. Case in point, the speculation that their biological impacts are mediated by an antimitochondrial mechanism rather than by direct DNA damage, as it is the situation for cisplatin and its analogs, has increased much credit amid the most recent couple of decades [12].

The stringent relationship to Pt(II) complexes makes Au(III) compounds great possibility for improvement and testing as anticancer medications, despite the fact that the generally high kinetic lability and the normally high redox possibilities have to a great extent ruined such investigations. These drawbacks can be dodged by shaping gold(III) derivatives with one or more multi-dentate nitrogen ligands to upgrade the strength and stability of gold(III) complexes [20–22]. Some recent studies point out that novel gold(III) complexes show

good antitumor properties both *in-vitro* and in *vivo*, have bringing new enthusiasm up in this research field [23–25].

A number of structurally analogues of cisplatin [26] have been tested, later utilized in clinical practice [27], one of these is trans-1,2-diaminocyclohexane dichloridoplatinum(II) (DACH) [28]. Since the molecule is chiral, the pertinence of stereochemistry has been addressed by researchers [29]. The ligand DACH has three isomeric structures: (1R, 2R-DACH) (*trans*-DACH), (lS, 2S-DACH) (*trans*-DACH) and (1R,2S-DACH) (*cis*-DACH). Disregarding conflicting perspectives [30 –34], the agreement is that the (R, R) isomer is more active than the (S,S) isomer [35-36], in spite of the fact that activity has additionally been shown for the (R, S) isomer [37]. As the stereochemistry of the complexes, the DACH platinum compounds of Pt(IR,2R-DACH) and Pt(1S,2S-DACH) have a higher antitumor activity than Pt(1R,2S-DACH) complex [38–40].

1.2 Gold(I) complexes

Gold(I) has d^{10} electron configuration which is divided into three distinct classes of co-ordination environments: linear two coordination, so far the most important co-ordination environment along with trigonal three-coordination and tetrahedral four-coordination.

Gold(I) is a soft cation with susceptibility for soft ligands such as: cyanide, thiolate, halide (e.g. iodide), and phosphine to form stable species of AuX_2^-, and AuL_2^+, respectively [41–43]. During the last two decades, a large variety of gold(I) and gold(III) compounds have been reported to possess anti-proliferative properties *in vitro* against several human tumor cell lines, qualifying them as excellent candidates for further pharmacological evaluation.

The recent literature shows a high number of papers reporting gold(I) phosphine complexes with sulphur ligands with application in catalysis, biological activities, luminescence, and the medical field. Moreover, the aurophilic interaction is well known in gold compounds containing P-, S-, and N- ligands [44–48], Fortman et al. studied thermodynamics of ligand exchange reactions in [(tht)AuCl] (tht= tetrahydrothiophene) with a series of tertiary phosphines and phosphites. They found that P─Au bond formed to be largely dependent on electronics parameters of phosphorus donor, whereas steric of ligand seems to play only a minor role in affecting enthalpy and BDE (bond disassociation energy). The phosphite ligands bind more weakly to Au centre than phosphine [49].

Gold(I) can be oxidized to gold(III) in vivo e.g. by myeloperoxidase system in white cells, that may be responsible for side-effects of gold(I) drugs [50]. On the other hand, gold(I) predominates the biochemistry of gold compounds, which is stabilized via π-acceptor ligands.

Auranofin is the first gold(I) phosphine lipophilic complex utilized into clinical practice for the treatment of rheumatoid arthritis. Also some of mixed ligands phosphine and thiolate gold(I) complexes have been tremendously shown to induce cell death, with varying characteristics depending on the cell type such as: solganol, myocrisin, sanocrysin, and allocrysin (Scheme 1).

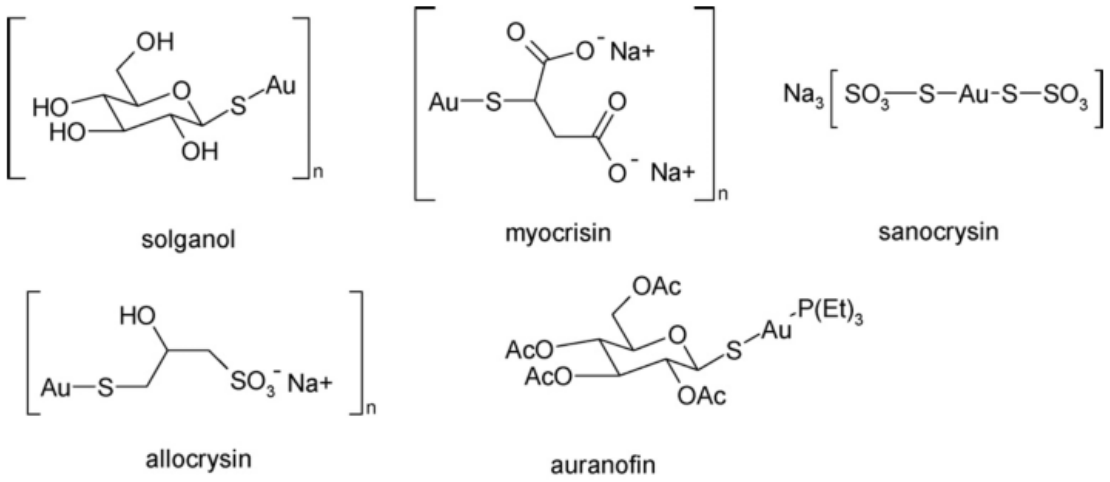

***Scheme 1**: Some gold(I) complexes are used in rheumatic arthritis treatment.*

These complexes and other gold(I) compounds including phosphine ligands such as Gopl (Scheme 2) have been reported to show bioactivities and anticancer activity [43, 51-52].

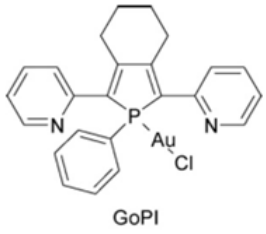

***Scheme 2:** Gold(I) phosphine anticancer drug (GoPl)*

Gold(I) N-heterocyclic carbene (NHC) complexes were obtained in good yields from the corresponding silver complexes by treatment with [AuCl(PPh_3)]. These complexes have been characterized by ^{1}H, ^{13}C-NMR, IR spectroscopy and elemental analysis. Au-NHC complexes were evaluated for their in vitro antimicrobial activity against a variety of Gram-positive and Gram-negative bacteria and fungal species [53].

A series of gold(I) phosphine complexes containing naphtha-imide ligand have been shown promising properties of antica2ncer drugs development, along with strong

anti-proliferative effects in MCF-7 breast cancer cells and HT-29 colon carcinoma cells [54].

In this thesis, I would like to explore the nature of bonding in Au(III) *cis*-DACH type complexes and to study their stability, when exposed to cyanide, thiones. Cyanide occurs naturally and blood of smokers contains high amount of SCN^-. Myeloperoxidase (MPO) converts SCN^- to cyanide. ^{1}H, ^{13}C, and ^{15}N solution NMR were used to study these interactions. In addition, different types of [(R_3P-Au-S_2CNR], gold(I)_carbene with selones, gold(I)_ter-t-butylphosine with thione, and gold(I)_carbene with phosphine complexes were synthesized, and then were characterize by using ^{1}H, ^{13}C, ^{31}P solution and solid NMR.

1.3 RESEARCH OBJECTIVES

1. Preparation of the two complexes, [*cis*-1,2-(DACH)$AuCl_2$]Cl and [*cis*-1,2-$(DACH)_2Au]Cl_3$.

2. Study of interactions of the complexes prepared in objective 1 with thiones such as IMT, DIAZ, and DIAP along with thiourea and cyanide using UV spectroscopy, ^{1}H NMR, ^{13}C NMR, and ^{15}N NMR.

3. Study of interactions of these complexes with labeled nucleobases: Guanine (8-^{13}C, 7, 9 $^{15}N_2$), Adenine (8-^{13}C, 6-amino and 1, 9 $^{15}N_2$), Cytosine (2,4-$^{13}C_2$, $^{15}N_3$) and Uracil (1,3 $^{15}N_2$) using UV spectroscopy, ^{1}H NMR, ^{13}C NMR, and ^{15}N NMR methods.

4. Synthesis of complexes of the type $[R_3P\text{-}Au\text{-}PR_3]^+$ and $[R_3P\text{-}Au\text{-}S_2CNR_2]$, where PR_3 = (1R,2R)-2-(diphenylphosphino)-1-aminocyclohexane, (R)-1-(diphenylphosphino)-2-amino-3,3-dimethylbutamine, (S)-1-(diphenylphosphino)-2-amino-3,3-dimethylbutane, (1R,2R)-2-(diphenylphosphino)-2,3-dihydro-1H-inden-1-amine, (1R,2R)-2-(diphenylphosphino)-1,2diphenylethylamine, 2-(diphenylphosphino) ethylamine, (R)-1-[(2-diphenylphosphino)phenyl]ethylamine, (S)-1-[(2-diphenylphosphino)phenyl]ethylamine, (R)-[(2-diphenylphosphino) phenyl]-1-phenylethylamine, (3-diphenylphosphino)propylamine, 2-(D-i-propylphosphino)ethylamine, and 3-(D-i-propylphosphino)propylamine and $NR_2CS_2^-$ = dimethyldithiocarbamate (DMTC), diethyldithiocarbamate (DETC), and dibenzyldithiocarbamate (DBTC).
5. Characterization of gold(I) phosphine complexes using ^1H, ^{13}C, ^{31}P NMR, IR, elemental analysis, and single crystal X-ray.
6. Study of their cytotoxic activity against A549 (human lung cancer), MCF7 (human breast cancer), and HCT15 (human colon cancer) cell lines.

CHAPTER 2

LITERATURE REVIEW

2.1. Gold(III) complexes

Since early 1990s, the chemistry of gold has been a well-established area of research. The metal and its complexes have special characteristic features that make them suitable for several research fields. For instance, a huge number of these complexes have antitumor action with positive results [55, 56]. Recently, using various Au(III) complexes with novel functionality has elicited more interest due to their distinct physical and chemical properties, stability under physiological conditions, and outstanding cytotoxic effects [57,58]. Cis-diamminedichloridoplatinum(II) (cisplatin) is one of the most widely used anticancer drugs today. However, platinum compounds possessing the 1,2-diaminocyclohexane (DACH) carrier ligand offer advantages over cisplatin with regard to bioavailability, activity and decreased renal toxicity [59]. Furthermore, success of oxaliplatin, (1R,2R-DACH)PtC_2O_4 complex, raised considerable research interest over the past three decades in platinum–DACH complexes [60].

2.1.1. Complexes formed from (C, N) donor ligands

Bugarčić et. al. [61] recently have studied the kinetics of the substitution reactions of gold(III) compounds bearing 3-azapentane-1,5-diamine, 2,2′,6′,2″-terpyridine, 2.2′-bipyridine and 1,2-diaminocyclohexaneligands associated with biologically applicable ligands, for example, L-histidine (L-His), inosine (Ino), inosine-5′-monophosphate (5′-IMP) and guanosine-5′-monophosphate (5′-GMP). Their outcomes demonstrated that the [Au(terpyridine)Cl]$^{2+}$ complex is the most reactive one, which was affirmed by (DFT) computations [61]. The nucleophiles reactivity order are: L-His > 5′-GMP > 5′-IMP > Ino.

As per the deliberate activation parameters, all studied reactions affiliated an associative substitution mechanism. The outcomes show strong association between the reactivity of these complexes toward biological pertinent ligands and their chemical and electronic characteristics. Hence, the binding of gold(III) compounds to 5′-GMP, constituent of DNA, is exceptionally compelling since this connection is thought to be in charge of their anticancer activity.

Over the past several years, significant effort has been devoted to study the antitumor activity of platinum-DACH complexes, whereas, gold-DACH complexes [62] have generally little consideration despite the fact that gold(III) has a genuinely rich biological nature. For instance, it has redox activity, can be facilitated by amino acids and proteins [63]. As on account of cisplatin, the anticancer activity of platinum–DACH is associted by some toxicity. The rise of resistance and low water solubility that can influence the pharmacokinetics are extra components that should be enhanced in the mission for more successful analogues [64].

Promising results were obtained with a class of gold(III) compounds with 2-(dimethylamino)methylphenyl ligand synthesized in such an approach to settle gold in its +3 oxidation state. These compounds showed cytotoxic impacts against a few human tumor cell lines, tantamount to, or more noteworthy than cis-platin [65].

In recent literature Messori et al. brought up the in vitro test of a series of gold(III) compounds, such as $[Au(en)_2]Cl_3$ against the A2780 ovarian malignancy cell line and a cisplatin safe variation [10, 65]. A number of other gold(III) compounds have been prepared and their cytotoxicity has been assessed. Calamai et al. studied gold(III) compounds containing no less than two gold-chloride bonds in cis-position [66, 67].

Arsenijevic et al [68] studied the kinetics of the reaction of $[Au(en)Cl_2]Cl$, $[Au(bipy)Cl_2]Cl$ and $[Au(DACH)Cl_2]Cl$ with 5'-GMP. They observed the spectral changes upon mixing of the complex with the 5'-GMP in λ_{max} in the range (280─350 nm). All kinetics measurements were performed under pseudo-first order conditions. The activation parameters suggest an associative mechanism. They measured their reactions at three different temperatures and reported the rate constants and activation parameters.

In biological systems, the imidazole group of histidine is frequently found in combination with copper ions, but also with nickel and zinc ions whereas the cobalt ion, in vitamin B_{12}, is coordinated to the benzimidazole group [69, 70]. In the blue copper protein, the Cu(II) is ligated in a distorted-tetrahedral arrangement of two histidine nitrogens, a cysteine thiolate sulfur and a methionine thioether sulfur [71]. For the modeling of this active site, imidazole- and thioether containing ligands are relevant.

Imidazole as shown below is a planar 5-membered aromatic molecule [72]. The electrons in the unhybridized p-orbital of N1 form part of the aromatic sextet. The all-electron computation for the imidazole [73] molecule was reported previously, and the net charges at the nitrogen atoms obtained from ab initio calculations are calculated.

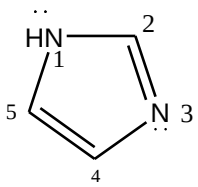

Scheme 3*. Basic imidazole structure (both N1 and N3 has one lone pair each).*

The nitrogen atoms in imidazole are in two different environments. The N1 electrons are not available for bonding, since the aromicity of the imidazole molecule will be compromised, unless this nitrogen deprotonates and has an available pair of electrons. The N3 nitrogen displays fractionally negative σ and π electron charges, indicating that it is a modest σ-donor and a weak π-acceptor when involved in bonding. Therefore, the imidazole molecule presents a single energetically favorable coordination site for a metal ion, namely the unshared electron pair on N3.

A metal ion can bind at N3, thereby forming a metal ion complex containing a neutral imidazole. In fact, there are extensive studies of biological systems with the imidazole core, especially with N-alkylated derivatives, and these models display the coordination of the N3 nitrogen to the metal ions [69, 70, 73-74]. However, the neutral imidazole can be deprotonated at N1 in strongly basic solutions.

Megumu et al. [75] have already studied the interactions of imidazole with Cd^{2+} in solution. Barbarossou et al. [76] have studied the interaction of the mononucleotides guanosine-5'- monophosphate (5'-GMP^{2-}) and inosine-5'-monophosphate (5'-IMP^{2-}) with Na^{+}, Ba^{2+}, and Cd^{2+} by ^{15}N and ^{113}Cd CP MAS NMR spectra in the solid state at natural abundance. The ^{15}N CP MAS NMR spectrum of Cd(5'-GMP)·$5H_2O$ shows sharp single resonances for all the purine nitrogens in agreement with the X-ray structure, which demonstrates the presence of one nucleotide and one metal ion per crystal unit [77]. The X-ray structure is typical for transition and heavy metal complexes with a 1:1 ratio of metal to guanosine-5'-monophosphate monomeric structure with the general formula $[M(5'\text{-}GMP)(H_2O)_5]\cdot nH_2O$. The common features of this type of structure are the M-N (7) metal bonding and three intramolecular hydrogen bonds; one between a water molecule and O(6) and two between water molecules and phosphate oxygens. The N(7) resonance absorption in Cd^{2+} complex is strongly shielded by -29.6 and -31.9 ppm compared to that of the Na^{+} and Ba^{2+} complexes, respectively. This demonstrates significantly different binding modes to N(7), although X-ray structural data have been interpreted in terms of direct metal ion-N(7) interaction for Na^{+}, Ba^{2+}, and Cd^{2+} complexes [78-79]. Unambiguous demonstration of a direct Cd-N coordination bond is provided by the ^{113}Cd CP MAS NMR spectrum, which indicates the presence of an asymmetric 1:1:1 triplet due to (^{113}Cd, ^{14}N) indirect and residual dipolar spin-spin interactions [80–82].

2.1.2 Complexes formed from (N, S) donor ligands

Thiolate complexes are of great importance from a bioinorganic point of view, mainly due to the presence of thiolate donors in the coordination sphere of many metal ions in very diverse metalloproteins [83, 84].

Complexes of heterocyclic thiones such as imidazolidine-2-thione (Imt), diazinane-2-thione (Diaz) and their derivatives with transition metals are of interest in bioinorganic chemistry because of the search for simple model compounds for metal proteins [84–86]. In view of this, copper(I) [89], silver(I) [88, 89], gold(I) [90–92], mercury(II) [93, 94] and cadmium(II) [95] complexes with thiones have been widely studied in recent years. the coordination chemistry of >C=S ligands with d^{10} metal ions have been investigated in an attempt to assess their mode of binding and to study their physical properties [96–97]. In biological systems, the imidazole group of histidine is frequently found in combination with copper ions, but also with nickel and zinc ions whereas the cobalt ion in vitamin B_{12} is coordinated to the benzimidazole group [69, 70]. In the blue copper protein, the Cu(II) is ligated, in a distorted-tetrahedral arrangement to two histidine nitrogens, a cysteine thiolate sulfur and a methionine thioether sulfur [96]. For the modeling of this active site, imidazole- and thioether containing ligands are relevant. Mononuclear Au(III) compounds of the peptides H-His-Met-OH (D) and H-Gly-Gly-Met-OH (T) were structurally characterized by IR, MS and NMR [86]. In Au(III) complexes with dipeptides, Au(III) is bonded to S of imidazole, N of methionine and histidine ligands shaping macrochelate rings [98].

The dithiocarbamate gold(III) compounds have additionally been analyzed lately [99]. Dimethyl dithiocarbamate (DMDT) which forms [(DMDT)AuX_2] demonstrate more cytotoxic action than cisplatin even toward human tumor cell lines naturally impervious to cisplatin itself.

Dinger and Henderson [100] have additionally shown the potential pharmacological action of gold(III) compounds. They portrayed the synthesis of cycloaurated N,N-dimethyl-

benzylamine compounds, these compounds showed better cytotoxic action in vitro. These compounds were assessed against the P388 leukemia cell line, and subsequently their potential activity against human tumors requires further examination.

El-Maythalony et al. monitored the interaction of auricyanide $[Au(CN)_4]^-$ with biologically important thiols, thioether and selenoether using ^1H and ^{13} C NMR and UV spectroscopy. These ligands include L-cysteine, glutathione, captopril, L-methionine and DL-seleno-methionine. They pointed out L-cysteine reaction mechanism with $[Au(CN)_4]^-$ was found to be dependent on reactants mole ratio. While L-methionine was completely inert toward auricyanide, DL-Se-methionine showed some reactivity with $[Au(CN)4]^-$ after raising solution pH to 12 that facilitated cyanide exchange [101].

Kouroulis et al. showed that the reaction of tetrachloroauric(III) with the thioamides ligands leads to the desulfuration of these ligands. They demonstrated that the reaction of $HAuCl_4$ with 2-mercapto-nicotinic acid, leads to of 2-sulfonate-nicotinine with the synchronous oxidation of the sulfur molecule. While the reactions of the gold(I) complex $[Au(Ph_3P)Cl]$ (Ph_3P = triphenylphosphine) with the thioamides, 2-mercapto- thiazolidine (mtzdH), 2-mercapto-benzothiazole (mbztH) and 5-chloro-2-mercapto- benzothiazole (ClmbztH) in the presence of potassium hydroxide brought about the arrangement of the gold(I) complexes without ligand desulfuration and were investigated by spectroscopic methods such as FT-IR, far-FT-IR, ^1H-NMR and X-ray crystallography. These complexes were tested in vitro for their cytotoxicity against leiomyosarcoma cells [102].

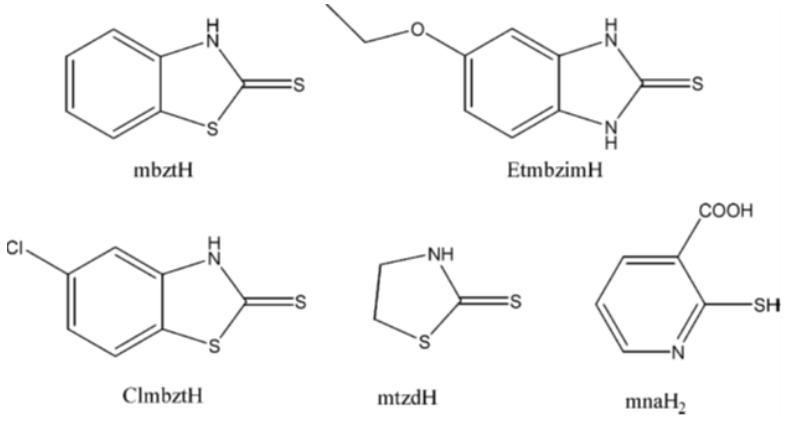

***Scheme 4**: Thioamide ligands.*

Glišić et al. used spectroscopic (^{1}H-NMR and UV-vis) and electrochemical (CV) techniques to study the interaction of Gly-Met dipeptide with $[Au(en)Cl_2]^+$ complex resulting Gly-Met sulfoxide, formed by the oxidation of methionine residue with $[Au(en)Cl_2]^+$. The formation of Gly-Met sulfoxide proceeds through two steps including the monodentate coordination of thioether sulfur atom of methionine residue and release of en ligand from Au(III). In addition, the obtained kinetic data showed that oxidation of methionine residue in Gly-Met was 200 times slower in comparison to the same process with $[AuCl_4]^-$ complex. The variation in the oxidation rate of Gly-Met between these two complexes was attributed to the presence of chelated ethylenediamine ligand in $[Au(en)Cl_2]^+$ [103].

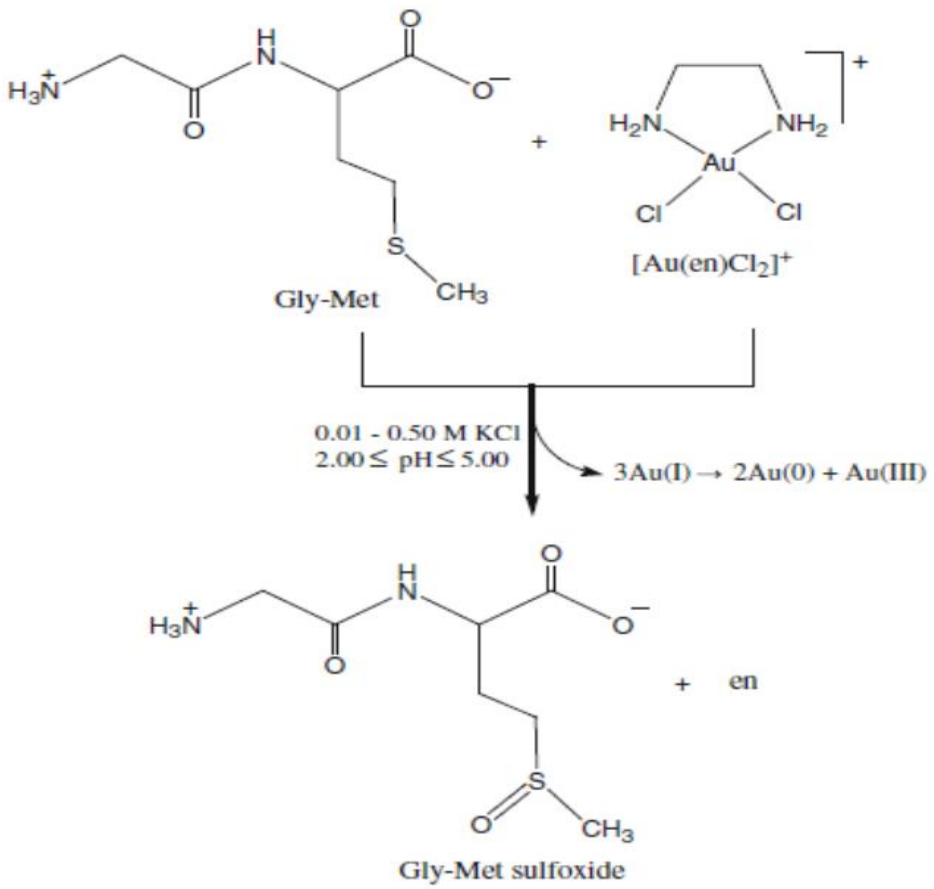

***Scheme** 5: Oxidation of methionine residue in Gly-Met dipeptide in the presence of $[Au(en)Cl_2]^+$ [103].*

Chi et al. prepared a series of new potential anticancer Au(III) complexes such as $[(PipDTC)AuCl_2]$ with macro-cyclic amine-based dithiocarbamate ligands. These complexes were characterized by elemental analysis, IR, UV, NMR, conductivity measurements and X-ray diffraction analysis. They have selective cytotoxic effects against a panel of human cancer cells lines. All these complexes show higher cytotoxicity than *cisplatin* against all examined cell lines. The nature of cyclic amine and the number of metal centers have important impacts on cytotoxicity of these complexes [104].

In 2012, a series of new gold(III)-dithiocarbamato (dtc) complexes of oligopeptides as promising potential anticancer drugs were synthesized to obtain metal peptidomimetics compounds. In vitro cytotoxicity studies pointed out some of them to be the most effective toward the four evaluated human tumor cell lines (PC3, 2008, C13, and L540), for which the IC_{50} values were lower than *cisplatin* [105].

In 2014, M. D. Đurović et al. studied the effect of tridentate, nitrogen donor ligands on stability of gold(III) complexes under physiochemical conditions. They have monitored the interaction of $[Au(terpy)Cl]^{2+}$ (terpy = 2.2':6, 2" terpyridine), $[Au(bpma)Cl]^{2+}$ (bpma = bis(pyridyl-methyl)amine), $[Au(dien)Cl]^{2+}$ (dien=diethylenetriamine) and $[AuCl_4]^-$ with biological thiols, L-cysteine (L-Cys), glutathione (GSH) and L-methionine (L-Met) using UV-Vis and ^1H NMR spectroscopy techniques, cyclic voltammetry and ESI-MS. The obtained second-order rate constants were determined at different initial concentrations of reactants, chloride ions, pH and constant ionic strength [106].

2.2 Gold(I) Complexes

2.2.1 Complexes formed from (P, S, Se) donor ligands

Dithiocarbamates are versatile ligands used in a wide range of application such as medicine, industry, agriculture and catalysis. Recently, gold(I) phosphine complexes have exhibited promising results as novel antitumor drugs against a wide variety of different malignancies.

Scheffler et al. reported a series of chlorido gold(I) phosphine complexes (Cl-Au-PR_3) R= Me, Et, tert-But, Ph). They showed the influence of R group on cytotoxicity, cellular and

nuclear uptake in HT-29 colon carcinoma and MCF-7 breast cancer cells. These complexes showed significant cytotoxicity results [107]. Four-coordinate gold(I) complexes, containing mono-phosphine ligands, these complexes showed strongly luminescence in liquid nitrogen and weakly at room temperature in addition to high cytotoxicity against a panel of cancer cell lines [108].

Gold(I) thiolate complexes are used extensively in medicine. For instance, gold(I) thiosemicarbazone complexes exhibited high efficacy as antimalarial agent [109]. In addition, a series of gold(I) complexes with mixed phosphine and dithiocarbamate ligands have been synthesized. The stability of these complexes depends on the nature of phosphine used. Bis(phenylphosphino) ligands, with alkyls higher than ethyl give stable gold(I) complexes in solution (Scheme 6). All these complexes showed promising anticancer activity against HeLa cancer cell lines [110].

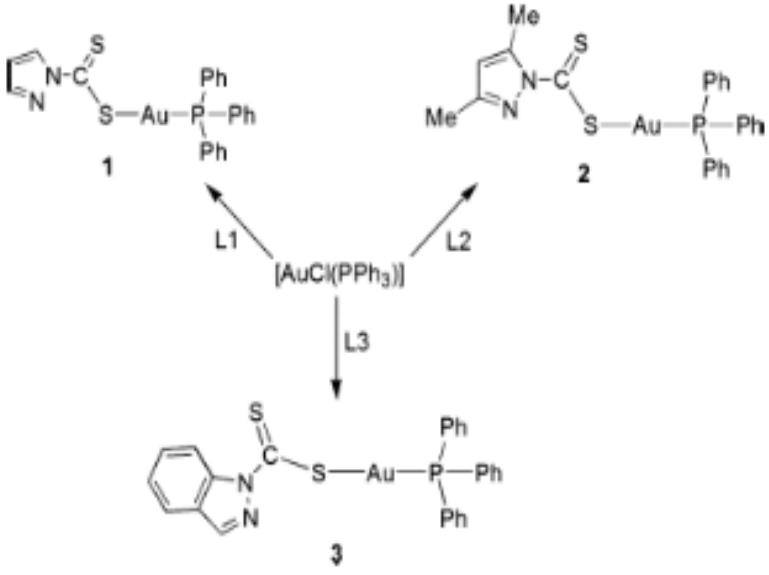

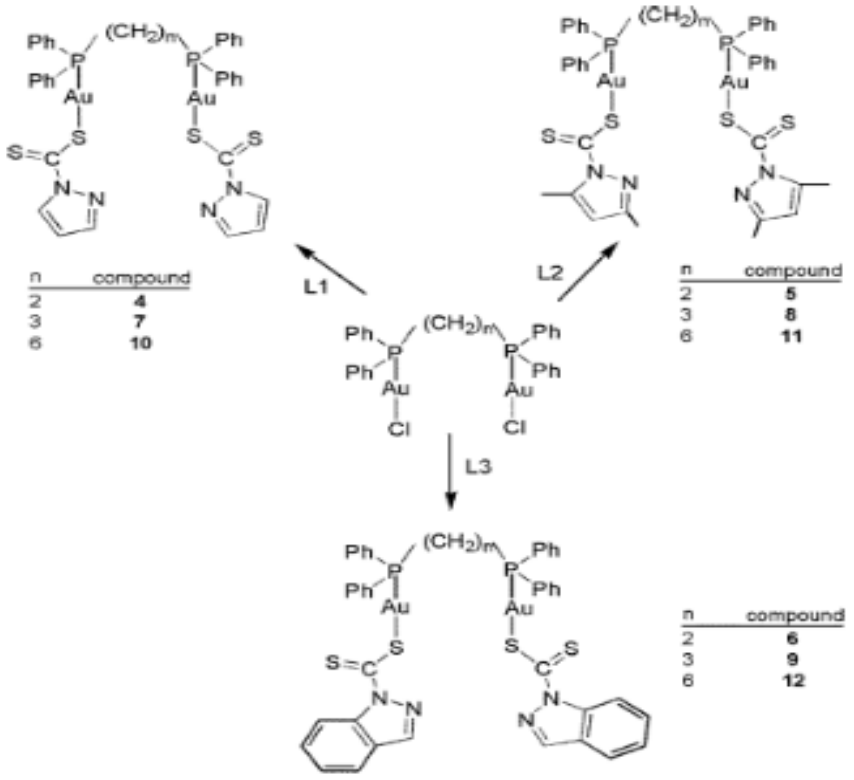

Scheme 6: *Gold(I) with monophosphosphine and dithiocarbamte complexes (1-3), gold(I) with (bis-phosphino)alkyl and dithiocarbamate complexes(4-12)[110].*

Jamaludin et al. [111] reported three $R_3PAu[S_2CN(ipr)CH_2CH_2OH]$ complexes, where R is Ph(1), Cy(2) and Et (3). They showed influence of substituted phosphine on in vitro cytotoxic activity against breast cancer cell line and death of cell pathways. They found that complex (1) is the most efficient even more than cisplatin and fallows apoptotic pathway for cell death, whereas for complexes 2 and 3, the cell death is caused by necrosis (Figure 1).

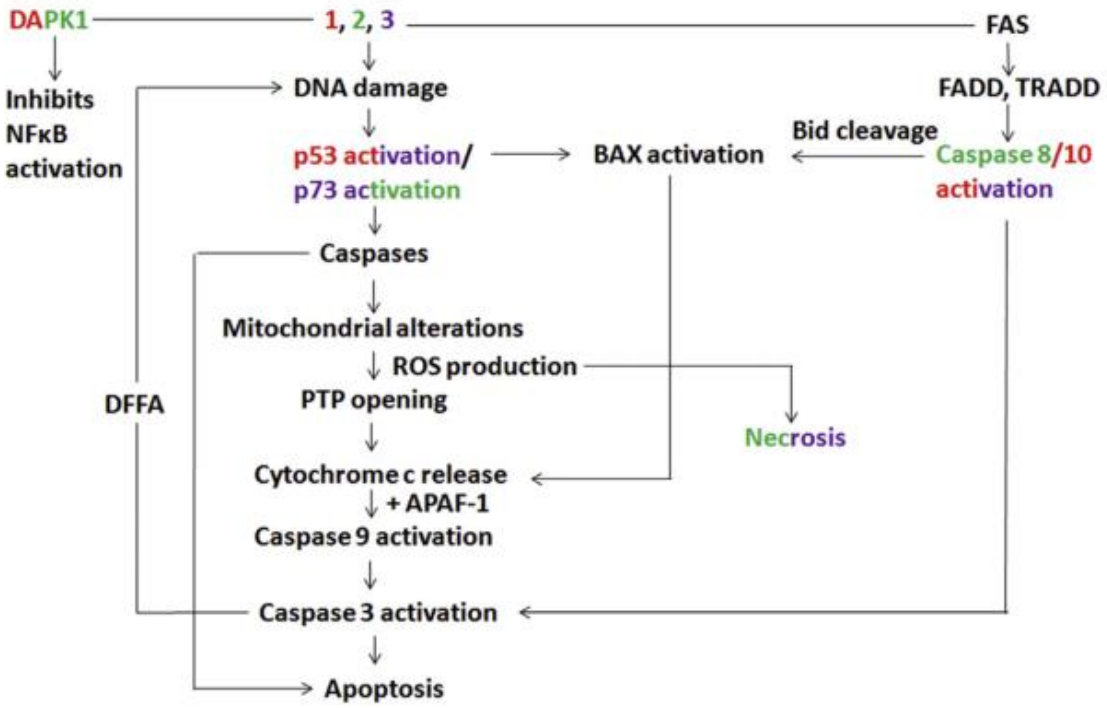

Figure 2.1. *Signaling pathway of apoptosis induced by 1, 2 and 3. This diagram collates and summarizes the results of the PCR array analysis, caspase activity study, DNA fragmentation and ROS production measurements [111].*

Recently, phosphinogold(I) organoselenium complexes have emerged as a new area in drugs delivery and medicinal applications due to the facts that selenopropteins play important role in the metabolism and antioxidant [112–114]. A series of organoselenogold(I) complexes (Scheme 7) were reported to have antimalarial activity. These complexes showed moderate activity compared to chloroquine [115].

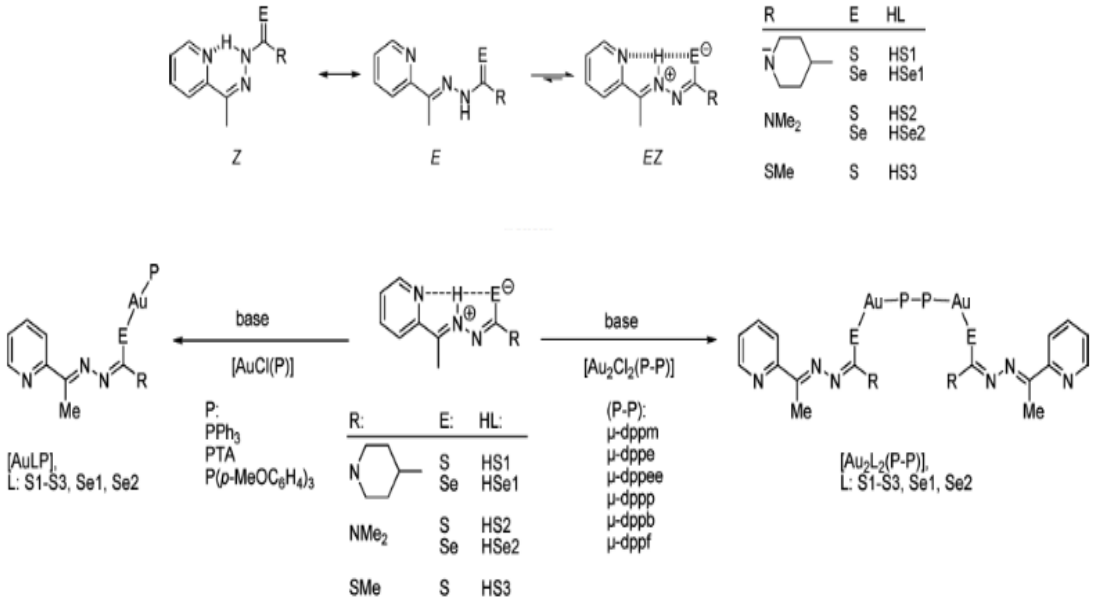

Scheme 7: *Mono- and binuclear gold(I)phosphine complexes containing monoanionic seleno-and thiosemicarbazone ligands [115].*

Abdulah et al. reviewed important biological roles of selenium in cancer prevention worldwide. They reported that the first clinical trials with Se to induce DNA damage and repair were performed in China [116].

Al-Maythalony et al. reported $Hg(SeCN)_2$ and $Cd(SeCN)_2$ complexes with histidine and glycine, they studied their anti-bacterial activities and they found that histidine ligates more strongly than glycine. Cd(II) complexes have exhibited significant antimicrobial activity [117]. Isab et al. demonstrated that Me_3PAu^+ moiety coordinates more strongly to Se containing ligands than Et_3PAu^+ and Ph_3PAu^+ moieties, therefore, Me_3PAu^+ with selenium ligands lend to less side effects as anticancer agents [118].

Gold complexes bearing N-Heterocyclic carbene (NHC) ligands have been extensively used in the fields of catalysis [119], anticancer [120] and antimicrobial [121]. Water

soluble NHC complexes with coinage metals (Cu, Ag, Au) have been prepared and their biological activity evaluated against A549 lung cancer, HCT-15 colon cell line and selenocystiene TrxR (Scheme 8). Au and Ag complexes were found more active than Cu complexes [122].

2.2.2 Complexes fromed from (P, C, N) donor ligands

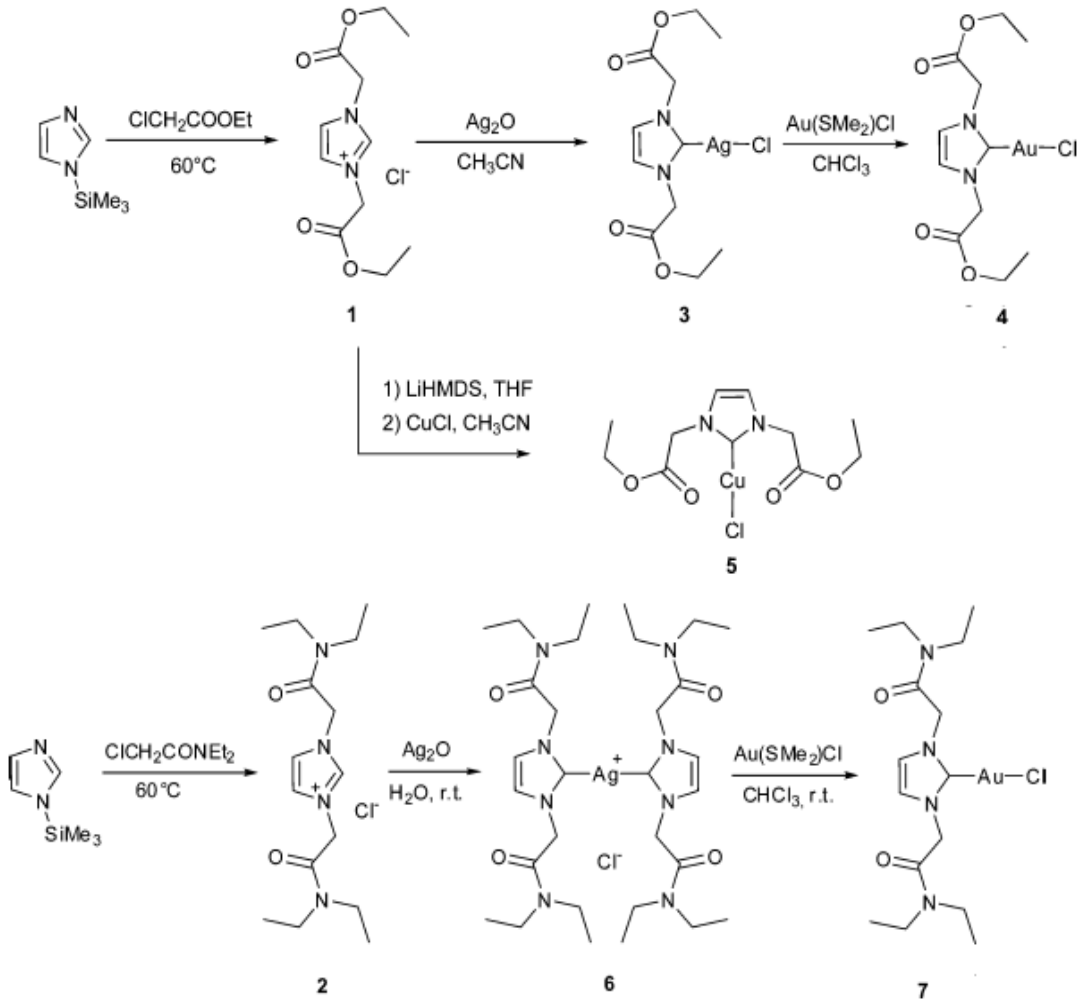

Scheme 8. *Reaction scheme of complexes from* ***2*** *to* ***7*** [123].

Messori et al. synthesized a series of Au(I)- NHC compounds. They further functionalized these compounds as useful actively esters to enhance their cytotoxicity and selectivity towards human ovarian cancer A2780 cells and HEK-293T cells (Scheme 9). The functionalized compounds exposed promising anti-proliferate properties and significant selectivity to these cells (Scheme 10) [123].

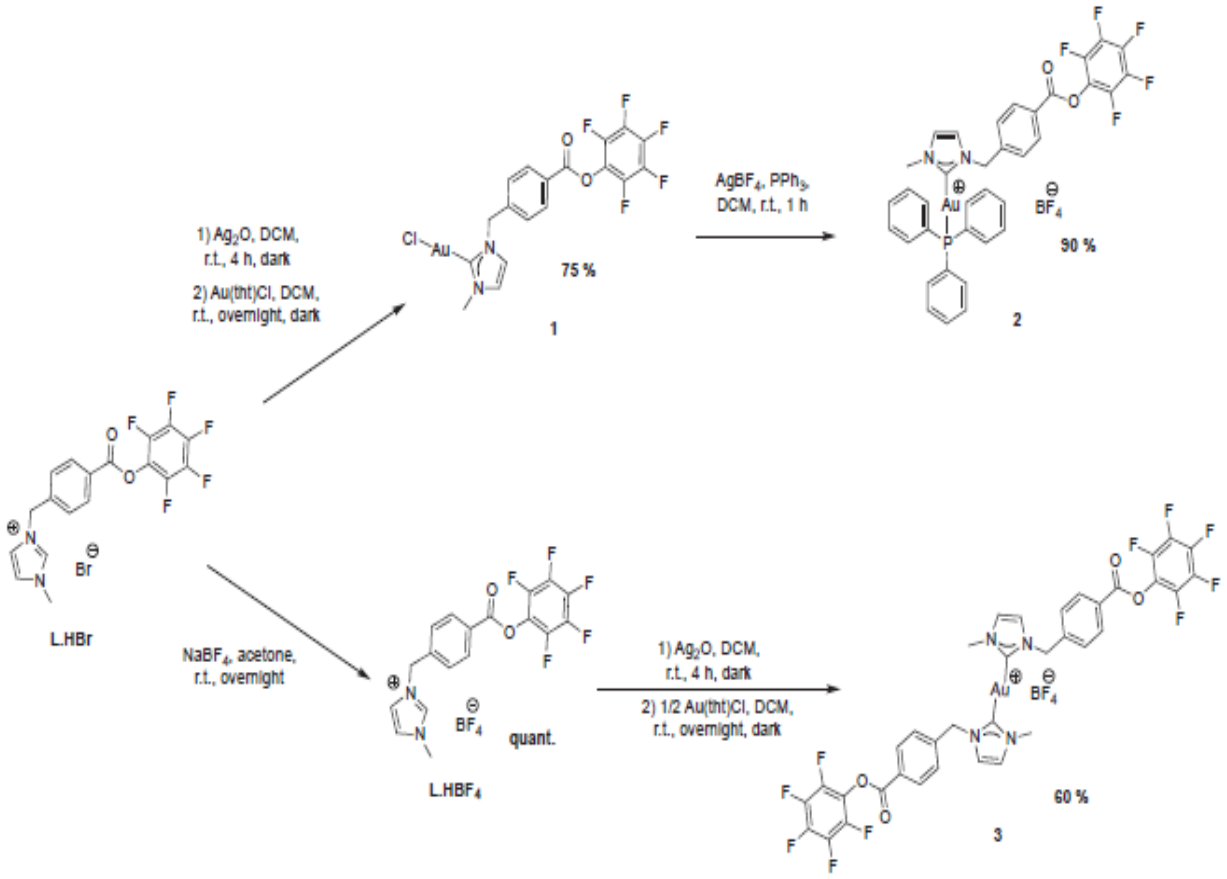

Scheme 9*. Synthesis of different Au(I)-NHC compounds bearing pentafluorophenol ester moiety.*

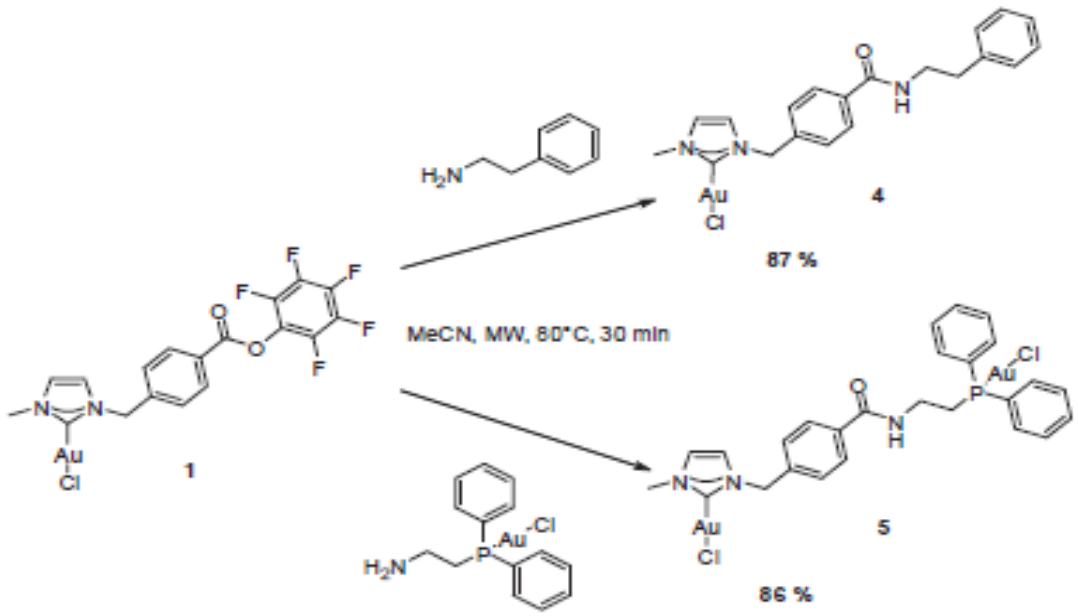

Scheme 10. *Synthesis of different Au(I)-NHC compounds through reaction of activated ester moiety.*

Two novel Au(I)-NHC complexes with high solubility in physiological media have been prepared (Scheme 11). These complexes completely overcome the resistance of cisplatinum against A2780 cell line, and their activity against three types of proteins were observed [123].

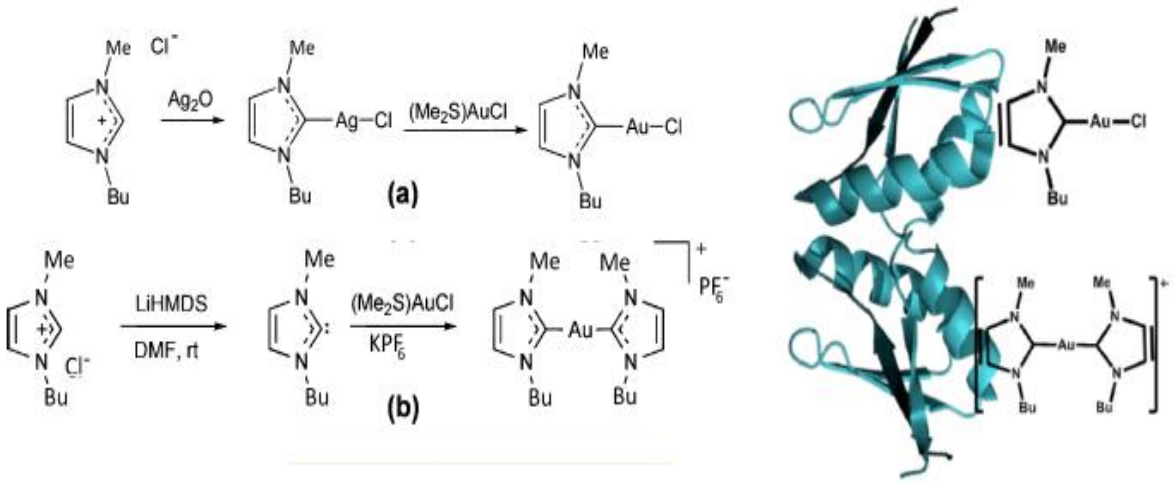

Scheme 11*. (a) Synthesis of compound* ***1*** *(b) Synthesis of compound* ***2****.*

The high *in vitro* and *in vivo* proficiency binuclear gold(I) complex (**1-PF_6**) with mixed diphosphine and bis-(NHC) ligands, with selective thiol reactivity has been prepared (Figure 2.2). Bis-(N-heterocyclic carbene) to enhance thiol stability and biphosphine to tune thiol reactivity. The stability of this complex allows selective inhibition of thioredoxin reductase (TrxR) without reacting with blood thiol. *In vitro* studies were performed against cancer stem cells and *in vivo* against tumor *HeLa xenograft* in mice and mouse *B16- F10 melanoma* [124].

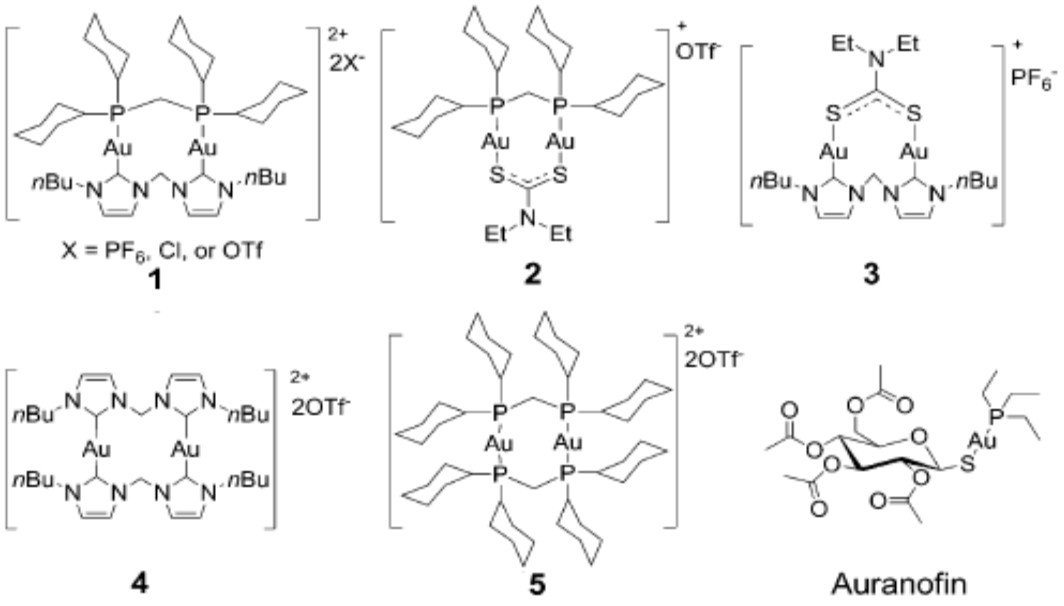

Figure 2.2. *Chemical structures of* ***1–5*** *complexes and auranofin.*

CHAPTER 3

SYNTHESIS, ANTI-CANCER EVALAUTION OF NEW MIXED-LIGAND GOLD(I) COMPLEXES WITH DITHIOCARBAMATES AND PHOSPHINES

3.1 EXPERIMENTAL SECTION

3.1.1 Materials and Instrumentation

All solvents are analytical grade used without further purification. (1R, 2R)-N, N-Bis[2-(diphenylphosphino)benzyl]cyclohexane 1,2-diamine, bis[2-(dicyclophosphino)ethyl]amine, bis[(2-diphenylphosphino)ethyl]ammonium chloride, (1S, 2S)-N, N-Bis[2-(diphenylphosphino)benzyl]cyclohexane 1,2-diamine, 2-(diphenylphosphino) ethylamine, (1R,2R)-2-(diphenylphosphino)-2,3-dihydro-1H-inden-1-amine, (R_1, R_2)-2-(diphenylphosphino)-1-aminocyclohexane, triphenylphosphine,

tri(o-methoxyphenyl)phosphine and 2-(di-isopropylphosphino)ethylamine, bis(2-cyanoethyl)phenyl phosphine were purchased from Stream Chemicals Inc. (Newburyport, Massachusetts, United States). Dimethylsulfide, sodium tetrachloroaurate(III), ethanol, diethyl ether, dichloromethane from Fluka AG (St. Gallen, Switzerland).

^{1}H and ^{13}C NMR spectra were recorded on a JEOL-LA 500 NMR spectrophotometer, operating at 500.0 and 125.65 MHz, respectively, corresponding to a magnetic field of 11.74 T. The spectral conditions included 32 k data points, a 3.2 s acquisition time, and a 5.75 μs pulse width. ^{13}C NMR spectra were obtained with ^{1}H broadband decoupling and following spectral conditions: 32 k data points, a 1 s acquisition time, a 2.5 s pulse delay, and a 5.12 μs pulse width. ^{31}P NMR spectra were obtained at 200.0 MHz, with phosphoric acid as an external standard. All spectra were recorded at 297 K in $CDCl_3$ using tetramethylsilane (TMS) as an internal standard.

Elemental analyses were obtained on Perkin Elmer Series 11 (CHNS/O), Analyzer 2400. The solid state FT-IR spectra of the free ligands and their gold(I) complexes were recorded on a Perkin Elmer FT-IR 180 spectrophotometer, using KBr pellets over the range 4000-400 cm^{-1}. Single crystal X-ray crystallography.

3.2 Synthesis of binuclear Gold(I) complexes with mixed bis-phosphine and dithiocarbamate ligands

3.2.1 [Au_2((1R,2R)-N,N-Bis[2-(diphenylphosphino)benzyl]cyclohexane-1,2-di amine)Cl_2] with dialkyl and diaryldithiocarbamate ligands (1-5)

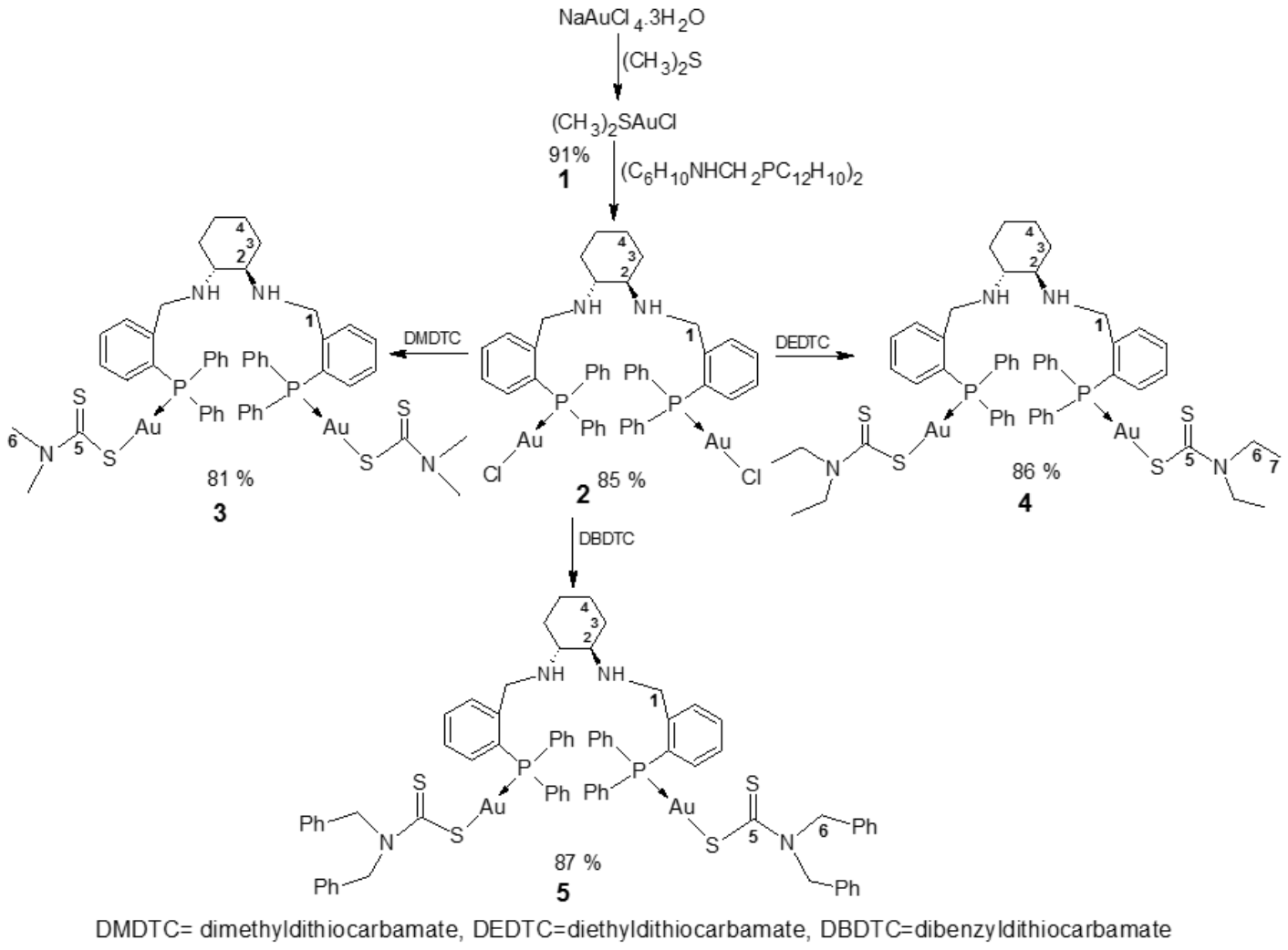

Scheme 12. *Synthesis of gold(I) bis-phosphine complexes* ***(1-5)***

$(CH_3)_2SAuCl$ **(1)**

Complex (**1**) was synthesized by a modified previously reported method [125]. In a fume hood, dimethylsulfide was added dropwise with stirring to reduce a yellow ethanolic $NaAuCl_4.3H_2O$ solution at 0-5 ºC until a white precipitate was formed. The product was washed twice with ethanol (5 mL) and three times with diethyl ether (10 mL), then dried in the dark and stored in fridge. The yield was 0.268 g (91%). Anal. calc. for C_2H_6SAuCl= 294.55 g/mol: C, 8.35; H 2.13. Found: C, 8.12; H, 1.83. ^{1}H NMR ($CDCl_3$, ppm), δ 2.75 (s, 6H). ^{13}C NMR ($CDCl_3$, ppm) δ 25.3.

$[C_{44}H_{44}Au_2Cl_2N_2P_2]$ **(2)**

Precursor (**1**) (295 mg, 1 mmol) in 5 mL of dichloromethane was added dropwise to a solution of *(1R,2R)-N,N-Bis[2-(diphenylphosphino)-benzyl]cyclohexane-1,2-diamine* (331.4 mg, 0.5 mmol) in 10 mL of dichloromethane. A clear colorless solution appeared and was stirred for 30 min; then, the solvent was concentrated by low evaporation at room temperature. The dichloro(bisphosphino)digold(I) intermediate **(2),** was obtained as a white solid, recrystallized from acetone /dichloromethane and dried overnight in vacuum. The yield was 0.479 g (85%). M.P. 127-130 ℃. Anal. calc. for $C_{44}H_{44}Au_2Cl_2N_2P_2$ (1127.62 g/mol): C, 46.42; H, 3.39; N, 2.41. Found: C, 46.87; H, 3.93; N, 2.48. IR (cm^{-1}) ν(N-H) 3442, ν(=CH) 3055, ν(CH_2) 2923_{asym}, 2854_{sym}, ν(C-H) 1436_{bend}, ν(Ar-C=C) 1633, ν(N-C) 1478. ^{1}H NMR ($CDCl_3$, ppm) δ 9.06 (s, NH); 4.79, 4.54 (d, C(1)H, H'); 4.11 (m, C(2)H, H'); 2.31, 2.14 (m, C(3)H); 1.86, 1.32 (m, C(4)H); 6.77-8.25 (m, 28H, C_6H_5). ^{13}C NMR ($CDCl_3$, ppm) δ 46.22 C(1); 63.89, 59.05 C(2); 29.68, 29.40; C(3); 23.64, 22.97 C(4); 127.28-163.76 C(C_6H_5). ^{31}P NMR ($CDCl_3$, ppm) δ -11.25.

$[Au_2(C_{44}H_{44}N_2P_2)(C_2H_6NCS_2)_2]$ **(3)**

This complex was prepared by a previously reported method [126], intermediate **(2)** (281.9 mg, 0.25 mmol) in 10 mL of dichloromethane was added to sodium dimethyldithiocarbamate monohydrate (72 mg, 0.5 mmol) in 10 mL of ethanol at room temperature with continuous stirring for 2h. The mixture was filtered, and the clear pale yellow solution was stored for low evaporation. A yellow solid was obtained, recrystallized from acetone/dichloromethane and dried overnight in vacuum. The yield 0.263 g (81%). M.P. 110-112℃. Anal. calc. for $C_{50}H_{56}Au_2N_4P_2S_4$ (1297.15 g/mol): C, 46.32; H, 4.31; N, 4.21; S, 9.79. Found: C, 46.29; H, 4.35; N, 4.31; S, 9.88. IR (cm^{-1}) ν(N-H) 3434, ν(CH) 2923; ν(CH_2) 2925_{asym}, 2852_{sym}, ν(C-H) 1435_{bend}; ν(Ar-C=C) 1629; ν(N-C) 1478; ν(C=S) 1099. ^{1}H NMR ($CDCl_3$, ppm) δ 1.61 (s, NH); 4.00, 3.81 (d, C(1)H, H'); 3.46 (m, C(2)H, H'); 2.13, 1.62 (m, C(3)H); 1.26, 1.10 (m, C(4)H); 4.35(s, C(6)H);6.80-7.58 (m, 28H, C_6H_5). ^{13}C NMR ($CDCl_3$, ppm) δ 49.56 C(1); 59.10 C(2); 31.58, 30.93; C(3); 24.84, 22.64 C(4); 207.37 (C=S); 45.37 C(6); 127.24-134.66 C(C_6H_5). ^{31}P NMR ($CDCl_3$, ppm) δ 29.77.

$[Au_2(C_{44}H_{44}N_2P_2)(C_4H_{10}NCS_2)_2]$ **(4)**

This complex was synthesized with **s**odium diethyldithiocarbamate trihydrate (112.7 mg, 0.5 mmol) by steps similar to **(3)**. An orange solid was obtained, recrystallized from acetone/dichloromethane and dried overnight in vacuum. Yield 0.291 g (86%). M.P. 99-101 ºC. Anal. calc. for $C_{54}H_{64}$ $Au_2N_4P_2S_4$ (1353.25 g/mol): C, 47.63; H, 4.65; N, 4.03; S, 9.21. Found: C, 47.92; H, 4.76; N, 4.14; S, 9.47. IR (cm^{-1}) ν(N-H) 3424, ν(=CH_2) 3052; ν(CH_2) 2925_{asym}, 2853_{sym}, ν(C-H) 1435_{bend}, ν(Ar-C=C) 1587, ν(N-C) 1480, ν(C=S) 1099.

^{1}H NMR ($CDCl_3$, ppm) δ 2.35 (s, NH); 4.07, 3.89 (d, C(1)H, H'); 3.74 (m, C(2)H, H'); 2.08, 1.78 (m, C(3)H);1.49, 1.02 (m, C(4)H); 4.19 (q, C(6)H); 1.30 (q, C(7)H); 6.74-8.03 (m, 28H, C_6H_5). ^{13}C NMR ($CDCl_3$, ppm) δ 50.78 C(1); 61.21 C(2); 30.93 C(3); 24.85 C(4); 205.71 (C=S); 49.31 C(6); 12.28 C(7) 126.71-145 C(C_6H_5). ^{31}P NMR ($CDCl_3$, ppm) δ 26.80.

$[Au_2(C_{44}H_{44}N_2P_2)(C_{14}H_{14}NCS_2)_2]$ **(5)**

This complex was synthesized with **s**odium dibenzyldithiocarbamate trihydrate (153.6 mg, 0.5 mmol) by steps similar to **(3)**. A yellow solid was obtained, recrystallized from acetone/dichloromethane and dried overnight in vacuum. Yield 0.348 g (87%). M.P. 101-103 ºC. Anal. calc. for $C_{74}H_{72}Au_2N_4P_2S_4$ (1601.53 g/mol): C, 55.13; H, 4.21; N, 3.11; S, 7.78. Found: C, 55.49; H, 4.53; N, 3.49; S, 8.00. IR (cm^{-1}) ν(N-H) 3418, ν(=CH_2) 3047, ν(CH_2) 2920, 2848_{sym}; ν(C-H) 1443_{bend}, ν(Ar-C=C) 1639, ν(N-C) 1203, ν(C=S) 1099. ^{1}H NMR ($CDCl_3$, ppm) δ 2.62 (s, NH); 4.90, 4.45 (d, C(1)H, H'); 4.22 (m, C(2)H, H'); 2.81, 1.99 (m, C(3)H); 1.59, 1.16 (m, C(4)H); 5.24, 5.07 (d, C(6)H); 6.81-7.91 (m, 38H, C_6H_5). ^{13}C NMR ($CDCl_3$, ppm) δ 51.19 C(1); 63.99 C(2); 29.40 C(3); 24.01 C(4); 198.54 (C=S); 56.14 C(6); 12.28 C(7) 127.94-136.71 C(C_6H_5). ^{31}P NMR ($CDCl_3$, ppm) δ 23.00.

3.2.2 [Au_2(Bis[(2-diphenylphosphino)ethyl]ammonium chloride)Cl_2] with dialkyl and diaryldithiocarbamates (6-9)

[$Au_2(C_{28}H_{30}ClNP_2)Cl_2$] **(6)**

This complex was synthesized with *bis[(2-diphenylphosphino)ethyl]ammonium chloride* (239 mg, 0.5 mmol) by a procedure similar to **(2)**. A white solid was obtained, recrystallized from acetone/dichloromethane and dried overnight in vacuum. Yield 0.391 g (83%). M.P. 159-161 ºC. Anal. calc. for $C_{28}H_{30}Au_2Cl_3NP_2$ (942.78 g/mol): C, 35.11; H, 2.99; N, 1.31. Found: C, 35.67; H, 3.20; N, 1.48. IR (cm^{-1}) ν(N-H) 3429, ν(=CH) 3051, ν(CH_2) 2936, ν(C-H) 1315_{bend}, ν(Ar-C=C) 1625, ν(N-C) 1435. ^{1}H NMR ($CDCl_3$, ppm) δ 10.10(s, NH); 3.67, 3.17 (m, C(1)H, H'); 2.81, 2.16 (m, C(2)H, H'); 7.42-7.70 (m, 20H, C_6H_5). ^{13}C NMR ($CDCl_3$, ppm) δ 44.04 C(1), 25.18 C(2),126.98-133.45 C(C_6H_5). ^{31}P NMR ($CDCl_3$, ppm) δ 21.90.

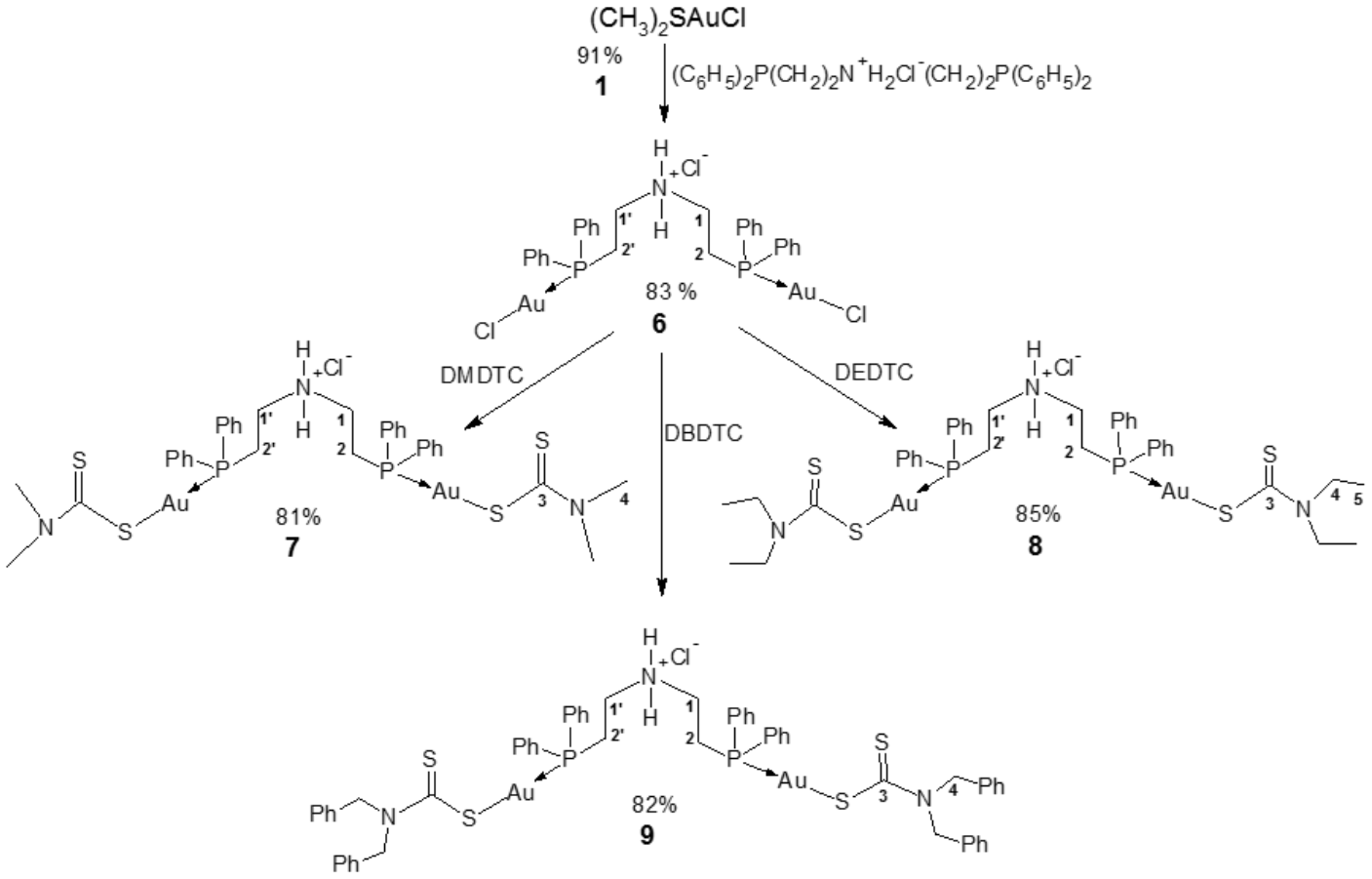

Scheme 13*. Synthesis of gold(I) bis-phosphine complexes* ***(6-9).***

$[Au_2(C_{28}H_{30}ClNP_2)(C_2H_6NCS_2)_2]$ **(7)**

This complex was synthesized with **s**odium dimethyldithiocarbamate monohydrate (71.6 mg, 0.5 mmol) by a procedure similar to **(3)**. A yellow solid was obtained, it was recrystallized from acetone/dichloromethane and dried overnight in vacuum. Yield 0.225 g (81%). M.P. 99-101 ºC. Anal. calc. for $C_{34}H_{42}Au_2ClN_3P_2S_4$ (1112.31 g/mol): C, 36.33; H, 3.45; N, 3.31; S, 11.21. Found: C, 36.71; H, 3.80; N, 3.77; S, 11.53. IR (cm^{-1}) ν(N-H) 3420, ν(=CH_2) 3045, ν(CH_2) 2920, ν(C-H) 1242_{bend}, ν(Ar-C=C) 1629, ν(N-C) 1490, ν(C=S) 1108. ^{1}H NMR ($CDCl_3$, ppm) δ 9.45 (s, NH); 3.92, 3.21 (m, C(1)H, H'); 2.99, 2.10 (m, C(2)H, H'), 3.56(s, C(4)H), 7.50-7.75 (m, 20H, C_6H_5). ^{13}C NMR ($CDCl_3$, ppm) δ 43.81 C(1), 22.68 C(2), 201.49 C=S(3), 45.66 C(4), 124.63-132.69 C(C_6H_5). ^{31}P NMR ($CDCl_3$, ppm) δ 27.50.

$[Au_2(C_{28}H_{30}ClNP_2)(C_4H_{10}NCS_2)_2]$ **(8)**

This complex was synthesized with **s**odium diethyldithiocarbamate trihydrate (112.7 mg, 0.5 mmol) by a procedure similar to **(3)**. An orange solid was obtained, it was recrystallized from acetone/dichloromethane and dried overnight in vacuum. Yield 0.248 g (85%). M.P. 95-97 ºC. Anal. calc. for $C_{38}H_{50}Au_2ClN_3P_2S_4$ (1168.42 g/mol): C, 38.93; H, 4.00; N, 3.32; S, 10.41. Found: C, 39.06; H, 4.31; N, 3.59; S, 10.97. IR (cm^{-1}) ν(N-H) 3425, ν(=CH_2) 3049, ν(CH_2) 2970, ν(CH_2) 2825_{sym},ν(C-H) 1262_{bend}, ν(Ar-C=C) 1624, ν(N-C) 1480, ν(C=S) 1103. ^{1}H NMR ($CDCl_3$, ppm) δ 9.45 (s, NH); 3.92, 3.12 (m, C(1)H, H'); 2.56, 2.43 (m, C(2)H, H'), 3.55 (s, C(4)H), 1.26 (s, C(5)H), 7.28-7.75 (m, 20H, C_6H_5). ^{13}C NMR ($CDCl_3$, ppm) δ 42.34 C(1), 27.36 C(2), 200.09 C=S(3), 52.32 C(4), 11.29 C(5), 128.95-133.41 C(C_6H_5). ^{31}P NMR ($CDCl_3$, ppm) δ 29.49.

$[Au_2(C_{28}H_{30}ClNP_2)(C_{14}H_{14}NCS_2)_2]$ **(9)**

This complex was synthesized with **s**odium dibenzyldithiocarbamate trihydrate (153.6 mg, 0.5 mmol) by a procedure similar to **(3)**. A yellow solid was obtained, recrystallized from acetone/dichloromethane and dried overnight in vacuum. Yield 0.291 g (82%). M.P. 93-95 ºC. Anal. calc. for $C_{58}H_{58}Au_2ClN_3P_2S_4$ (1416.69 g/mol): C, 38.69; H, 3.93; N, 2.32; S, 8.75. Found: C, 39.17; H, 4.12; N, 2.96; S, 9.05. IR (cm^{-1}) ν(N-H) 3425, ν(=CH_2) 3049, ν(CH_2) 2970, ν(CH_2) 2825_{sym},ν(C-H) 1256_{bend}, ν(Ar-C=C) 1624, ν(N-C) 1480, ν(C=S) 1103. ^{1}H NMR ($CDCl_3$, ppm) δ 9.03 (s, NH); 3.64, 3.19 (m, C(1)H, H'); 2.65, 2.18 (m, C(2)H, H'), 5.08, 4.47 (d, C(4)H), 7.30-7.76 (m, 30H, C_6H_5). ^{13}C NMR ($CDCl_3$, ppm) δ 44.12 C(1), 25.81 C(2), 209.55 C=S(3), 58.72 C(4), 127.83-135.68 C(C_6H_5). ^{31}P NMR ($CDCl_3$, ppm) δ 24.68.

3.2.3 [Au_2(Bis[2-(dicyclophosphino)ethyl]amine)Cl_2] with dialkyl and diaryldithiocarbamates (10-13)

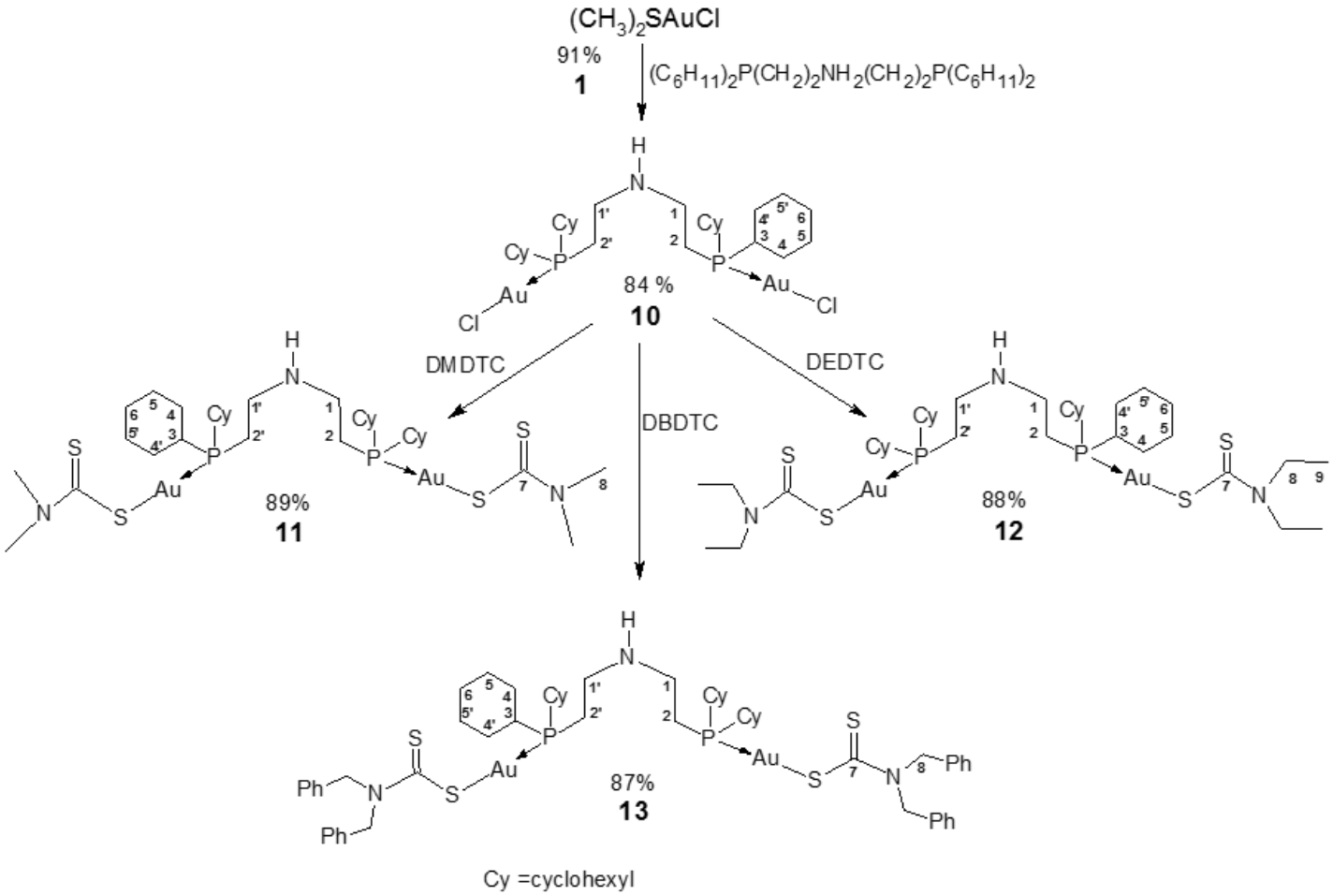

Scheme 14*. Synthesis of gold(I) bis-phosphine complexes* ***(10-13).***

$[Au_2(C_{28}H_{53}NP_2)Cl_2]$ **(10)**

This complex was synthesized with *bis[2-(dicyclophosphino)ethyl]amine* (23 3mg, 0.5 mmol) by a procedure similar to **(2)**. A white solid was obtained, recrystallized from acetone/dichloromethane and dried overnight in vacuum. Yield 0.195 g (84%). Anal. calc. for $C_{28}H_{53}Au_2Cl_2NP_2$ (930.51 g/mol): C, 35.71; H, 5.34; N, 1.21. Found: C, 36.14; H, 5.74; N, 1.50. IR (cm^{-1}) ν(N-H) 3434, ν(CH_2) 2934_{asym}, ν(CH_2) $2847_{sym,}$ ν(C-H) 1342_{bend}, ν(N-C) 1446. ^{1}H NMR ($CDCl_3$, ppm) δ 1.76 (s, NH); 3.94, 3.87 (m, C(1)H, H'); 2.51, 2.18 (m, C(2)H, H'); 3.47 (m, C(3) H,H'), 1.90 (m, C(4)H), 1.71 (m, C(5)H,H'), 1.35 (m, C(6)H,H'). ^{13}C NMR ($CDCl_3$, ppm) δ 46.23 C(1), 29.97 C(2), 34.47 C(3), 29.16 C(4,4'), 26.48 C(5,5'), 25.57 C(6). ^{31}P NMR ($CDCl_3$, ppm) δ -11.26.

$[Au_2(C_{28}H_{53}NP_2)(C_2H_6NCS_2)_2]$ **(11)**

This complex was synthesized with **s**odium dimethyldithiocarbamate monohydrate (71.6 mg, 0.5 mmol) by a procedure similar to **(3)**. A light yellow solid was obtained, recrystallized from acetone/dichloromethane and dried overnight in vacuum. Yield 0.245 g (89%). Anal. calc. for $C_{34}H_{65}Au_2N_3P_2S_4$ (1100.04 g/mol): C, 36.73; H, 5.31; N, 3.33. Found: C, 37.12; H, 5.95; N, 3.81. IR (cm^{-1}) ν(N-H) 3420, ν(CH_2) 2920, ν(C-H) 1242_{bend}, ν(N-C) 1449, ν(C=S) 1108. ^{1}H NMR ($CDCl_3$, ppm) δ 1.56 (s, NH); 3.88, 3.74 (m, C(1)H, H'); 3.35, 2.64 (m, C(2)H, H'); 3.48 (m, C(3) H,H'), 1.87 (m, C(4)H,H'), 1.45 (m, C(5)H,H'), 1.29 (m, C(6)H,). ^{13}C NMR ($CDCl_3$, ppm) δ 45.10 C(1), 30.10 C(2), 34.80 C(3), 29.82 C(4,4'), 26.21 C(5,5'), 25.82 C(6), 202.64 C=S(7), 45.23 C(8). ^{31}P NMR ($CDCl_3$, ppm) δ 38.36.

$[Au_2(C_{28}H_{53}NP_2)(C_4H_{10}NCS_2)_2]$ **(12)**

This complex was synthesized with **s**odium diethyldithiocarbamate trihydrate (112.7 mg, 0.5 mmol) by a procedure similar to **(3)**. A yellow solid was obtained, recrystallized from acetone/dichloromethane and dried overnight in vacuum. Yield 0.254 g (88%). Anal. calc. for $C_{38}H_{73}Au_2N_3P_2S_4$ (1156.15 g/mol): C, 39.21; H, 5.91; N, 3.29; S, 10.49. Found: C, 39.74; H, 6.36; N, 3.63; S, 11.09. IR (cm^{-1}) ν(N-H) 3436, ν(CH_2) 293, ν(C-H) 1242_{bend}, ν(N-C) 1446, ν(C=S) 1118. ^{1}H NMR ($CDCl_3$, ppm) δ 1.70 (s, NH); 3.88, 3.02 (m, C(1)H, H'), 2.02 (m, C(2)H, H'), 3.25 (m, C(3) H,H'), 1.84 (m, C(4)H,H'), 1.46 (m, C(5)H,H'), 1.21 (m, C(6)H). ^{13}C NMR ($CDCl_3$, ppm) δ 47.03 C(1), 31.98 C(2), 34.45 C(3), 28.42 C(4,4'), 26.64 C(5,5'), 25.74 C(6), 205.90 C=S(7), 49.02 C(8), 12.02 C(9). ^{31}P NMR ($CDCl_3$, ppm) δ 39.18.

$[Au_2(C_{28}H_{53}NP_2)(C_{14}H_{14}NCS_2)_2]$ **(13)**

This complex was synthesized with **s**odium dibenzyldithiocarbamate trihydrate (153.6 mg, 0.5 mmol) by a procedure similar to **(3)**. A yellow solid was obtained, recrystallized from acetone/dichloromethane and dried overnight in a vacuum. Yield 0.305 g (87%). Anal. calc. for $C_{58}H_{81}Au_2N_3P_2S_4$ (1404.42 g/mol): C, 49.21; H, 5.21; N, 2.29; S, 8.81. Found: C, 49.60; H, 5.81; N, 2.99; S, 9.13. IR (cm^{-1}) ν(N-H) 3425, ν(CH_2) 2970, ν(C-H) 1256_{bend}, ν(Ar-C=C) 1624, ν(N-C) 1480, ν(C=S) 1103. ^{1}H NMR ($CDCl_3$, ppm) δ 1.67 (s, NH); 3.07 (m, C(1)H, H'), 2.02 (m, C(2)H, H'), 3.14 (m, C(3) H,H'), 1.84 (m, C(4)H,H'), 1.45 (m, C(5)H,H'), 1.26 (m, C(6)H). ^{13}C NMR ($CDCl_3$, ppm) δ 47.30 C(1), 29.53 C(2), 34.52 C(3), 28.54 C(4,4'), 26.63 C(5,5'), 25.70 C(6), 210.11 C=S(7), 55.81 C(8), 127.81-135.94 C(C_6H_5). ^{31}P NMR ($CDCl_3$, ppm) δ 39.20.

3.2.4 [Au_2((1S,2S)-N,N-Bis[2-(diphenylphosphino)benzyl]cyclohexane-1,2-diamine)Cl_2] with dialkyl and diaryldithiocarbamates (14-17)

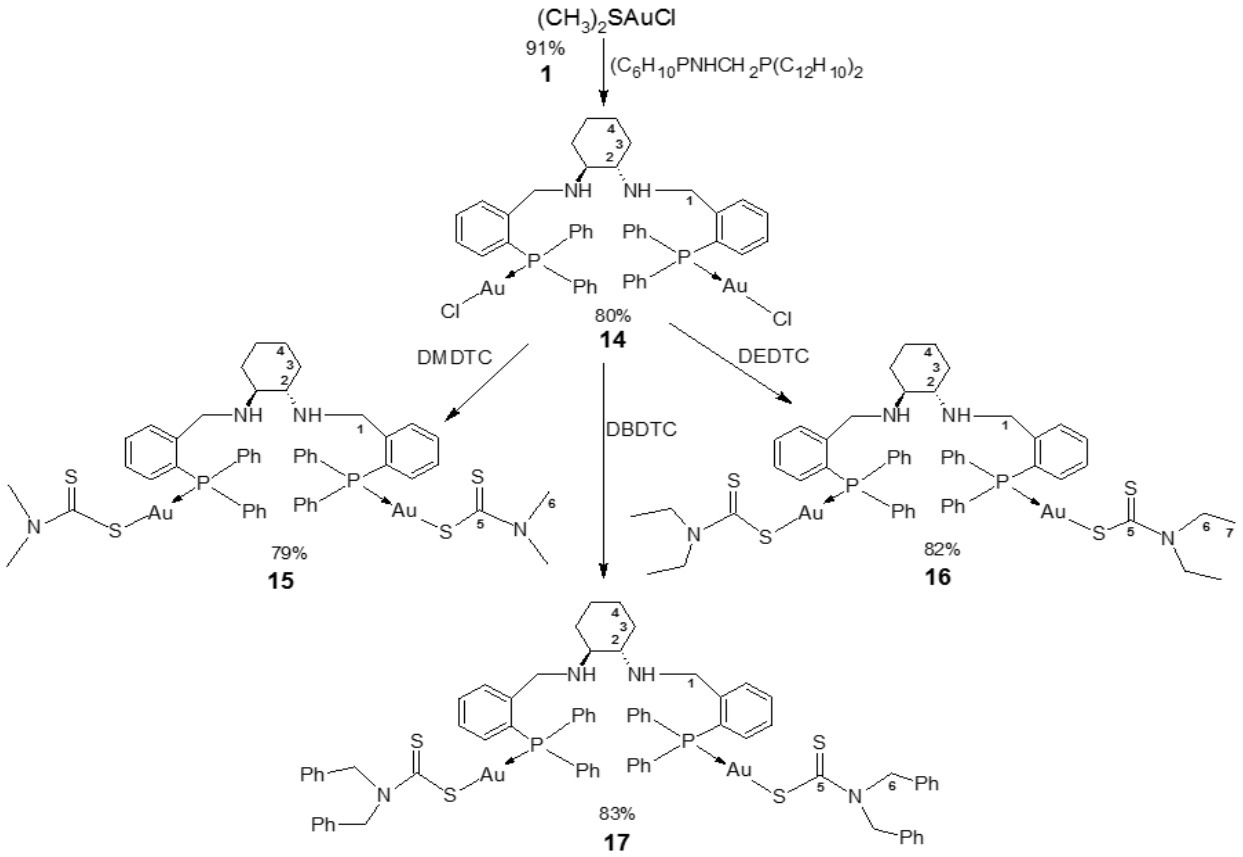

Scheme 15. *Synthesis of gold(I) bis-phosphine complexes* ***(14-17)***

$[C_{44}H_{44}Au_2Cl_2N_2P_2]$ **(14**)

This complex was synthesized with *(1S,2S)-N,N-bis[2-(diphenylphosino)benzyl]-cyclohexane 1,2-diamine* (331.4 mg, 0.5 mmol) by steps similar to **(2)**. A white solid was obtained, recrystallized from acetone/dichloromethane and dried overnight in a vacuum. Yield 0.451 g (80%). Anal. calc. for $C_{44}H_{44}Au_2Cl_2N_2P_2$ (1127.62 g/mol): C, 46.31; H, 3.41; N, 2.11. Found: C, 46.87; H, 3.93; N, 2.48. IR (cm^{-1}) ν(N-H) 3445, ν(=CH) 3057, ν(CH_2) 2921_{asym}, 2855_{sym}, ν(C-H) 1439_{bend}, ν(Ar-C=C) 1630, ν(N-C) 1481. ^{1}H NMR ($CDCl_3$, ppm) δ 9.45 (s, NH); 4.65, 4.50 (d, C(1)H, H'); 4.15 (m, C(2)H, H'); 2.35, 2.17 (m, C(3)H); 1.83, 1.30 (m, C(4)H); 6.65-8.30 (m, 28H, C_6H_5). ^{13}C NMR ($CDCl_3$, ppm) δ 45.22 C(1), 62.85 C(2), 29.40 C(3), 23.65 C(4), 128.18-162.65 C(C_6H_5). ^{31}P NMR ($CDCl_3$, ppm) δ -13.25.

$[Au_2(C_{44}H_{44}N_2P_2)(C_2H_6NCS_2)_2]$ **(15)**

This complex was synthesized with sodium dimethyldithiocarbamate monohydrate (71.6 mg, 0.5 mmol) by steps similar to **(3).** Pale yellow solid was obtained, recrystallized from acetone/dichloromethane and it was dried overnight in vacuum. Yield 0.256 g (79%). Anal. calc. for $C_{50}H_{56}Au_2N_4P_2S_4$ (1297.15 g/mol): C, 46.29; H, 4.35; N, 4.31; S, 9.88. Found: C, 46.00; H, 4.11; N, 4.09; S, 9.53. IR (cm^{-1}) ν(N-H) 3430, ν(CH) 2920; ν(CH_2) 2923_{asym}, 2855_{sym}, ν(C-H) 1445_{bend}; ν(Ar-C=C) 1632; ν(N-C) 1488; ν(C=S) 1035. ^{1}H NMR ($CDCl_3$, ppm) δ 1.75 (s, NH); 4.05, 3.85 (d, C(1)H, H'); 3.40 (m, C(2)H, H'); 2.13, 1.62 (m, C(3)H,H'); 1.26, 1.10 (m, C(4)H, H'); 4.15(s, C(6)H);6.85-7.68 (m, 28H, C_6H_5). ^{13}C NMR ($CDCl_3$, ppm) δ 49.56 C(1), 59.10 C(2), 31.58 C(3), 24.34 C(4); 206.35 (C=S); 45.15 C(6); 126.25-135.55 C(C_6H_5). ^{31}P NMR ($CDCl_3$, ppm) δ 25.56.

$[Au_2(C_{44}H_{44}N_2P_2)(C_4H_{10}NCS_2)_2]$ **(16)**

This complex was synthesized with **s**odium diethyldithiocarbamate trihydrate (112.7 mg, 0.5 mmol) by steps similar to **(3)**. An orange solid was obtained, recrystallized from acetone/dichloromethane and dried overnight in a vacuum. Yield 0.277 g, (82 %). Anal. Calc. for $C_{54}H_{64}$ $Au_2N_4P_2S_4$ (1353.25 g/mol): C, 47.92; H, 4.76; N, 4.14; S, 9.47. Found: C, 47.25; H, 4.27; N, 3.89; S, 9.01. IR (cm^{-1}) ν(N-H) 3428, ν(=CH_2) 3055; ν(CH_2) 2927_{asym}, 2855_{sym}, ν(C-H) 1475_{bend}, ν(Ar-C=C) 1613, ν(N-C) 1485, ν(C=S) 1039. ^{1}H NMR ($CDCl_3$, ppm) δ 2.55 (s, NH); 4.00, 3.79 (d, C(1)H, H'); 3.64 (m, C(2)H, H'); 2.00, 1.75 (m, C(3)H,H'); 1.59, 1.12 (m, C(4)H, H'); 4.25 (t, C(6)H); 1.25 (q, C(7)H); 6.65-7.75 (m, 28H, C_6H_5). ^{13}C NMR ($CDCl_3$, ppm) δ 51.25 C(1); 60.21 C(2); 29.95 C(3); 25.15 C(4); 206.24 (C=S); 48.51 C(6); 12.18 C(7) 127.11-143.23 C(C_6H_5). ^{31}P NMR ($CDCl_3$, ppm) δ 25.50.

$[Au_2(C_{44}H_{44}N_2P_2)(C_{14}H_{14}NCS_2)_2]$ **(17)**

This complex was synthesized with **s**odium dibenzyldithiocarbamate trihydrate (153.6 mg, 0.5 mmol) by steps similar to **(3)**. A yellow solid was obtained, recrystallized from acetone/dichloromethane and dried overnight in vacuum. Yield 0.332 g (83%). Anal. calc. for $C_{74}H_{72}$ $Au_2N_4P_2S_4$ (1601.53 g/mol): C, 55.49; H, 4. 53; N, 3.49; S, 8.00. Found: C, 55.03; H, 4.11; N, 2.99; S, 7.69. IR (cm^{-1}) ν(N-H) 3438, ν(=CH_2) 3057, ν(CH_2) 2925, 2851_{sym}; ν(C-H) 1473_{bend}, ν(Ar-C=C) 1635, ν(N-C) 1403, ν(C=S) 1019. ^{1}H NMR ($CDCl_3$, ppm) δ 2.52 (s, NH); 4.50, 4.35 (d, C(1)H, H'); 4.12 (m, C(2)H, H'); 2.61, 1.79 (m, C(3)H,H'); 1.55, 1.26 (m, C(4)H); 5.14, 5.07 (d, C(6)H,H'); 7.11-7.71 (m, 38H, C_6H_5). ^{13}C NMR ($CDCl_3$, ppm) δ 52.19 C(1); 62.75 C(2); 29.30 C(3); 23.81 C(4); 208.15 (C=S); 56.10 C(6); 126.95-135.75 C(C_6H_5). ^{31}P NMR ($CDCl_3$, ppm) δ 24.15.

3.3 Synthesis of gold(I) complexes with mono-phosphine and dithiocarbamate ligands

3.3.1 Chlorido(2-(diphenylphosphino)ethylamine)Au(I) with dialkyl and dibenzyl-dithiocarbamates (18-22)

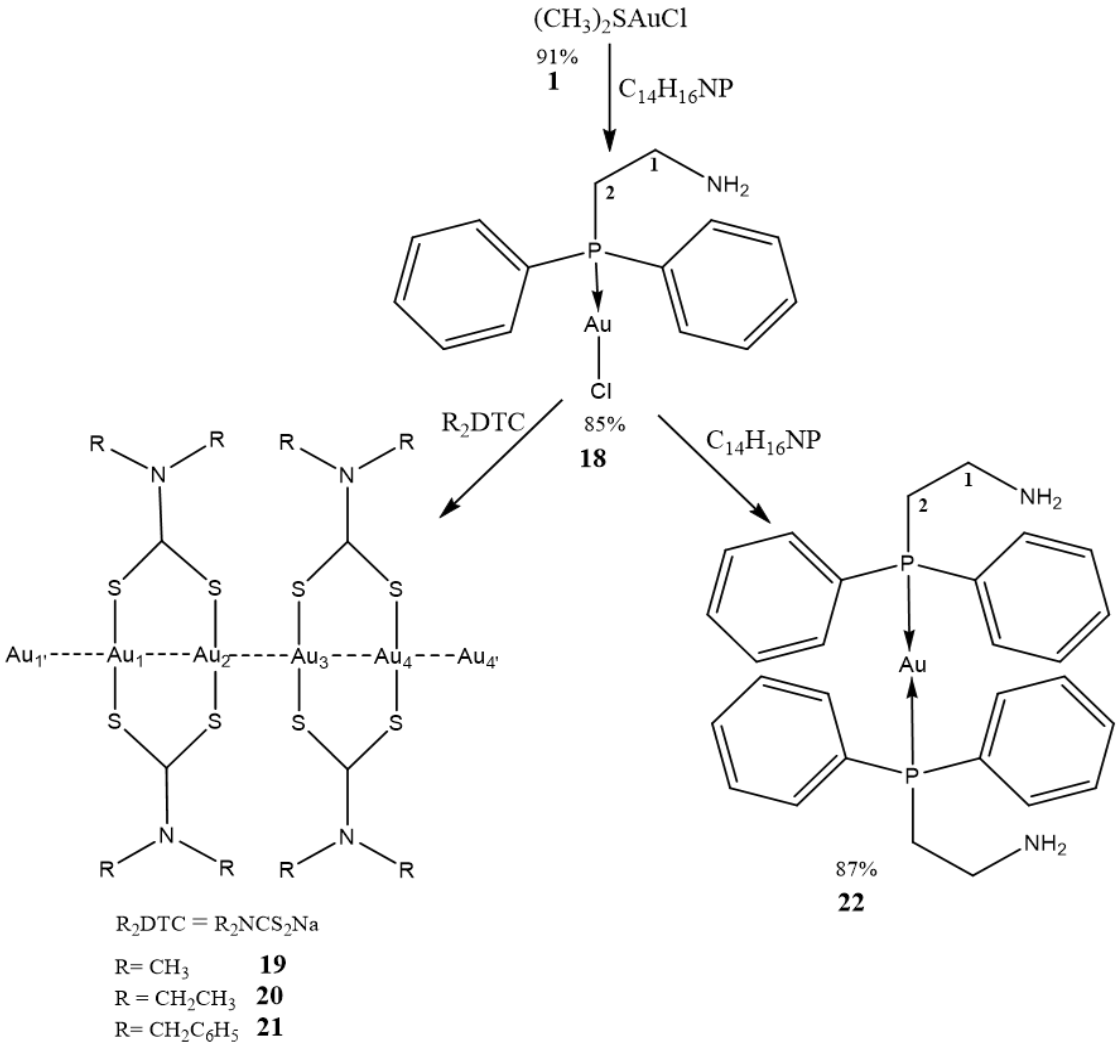

Scheme 16. *Synthesis of gold(I) polymers* ***(19-21)*** *and gold(I) monophosphine complexes* ***18*** *and* ***22.***

[$C_{14}H_{16}NPAuCl$) complex **(18**)

This complex was synthesized with *2-(diphenylphosphino)ethylamine* (114.6 mg, 0.5 mmol) by a procedure similar to **(2).** The chlorido(*2-(diphenylphosphino)ethylamine*)-gold(I) was obtained as a white solid, recrystallized from acetone/dichloromethane and dried overnight in vacuum. Yield 0.196 g (85%). Anal. calc. for $C_{14}H_{16}NPAuCl$ (461.68 g/mol): C, 36.42; H, 3.39; N, 3.03. Found: C, 35.90; H, 2.84; N, 3.36. IR (cm^{-1}) ν(N-H) 3431, 3354; ν(CH_2) 2917_{asym}, 2857_{sym}, ν(C-H) 1310_{bend}; ν(Ar-C=C) 1603; ν(N-C) 1432. ^{1}H NMR ($CDCl_3$, ppm) δ 4.03 (s, NH); 3.31, 3.17 (m, C(1)H, H'); 2.97, 2.73 (m, C(2)H, H'); 7.45-7.65 (m, 10H, C_5H_5). ^{13}C NMR ($CDCl_3$, ppm) δ 37.65 C(1), 31.50 C(2), 129.28-133.26 C(C_5H_5). ^{31}P NMR ($CDCl_3$, ppm) δ 21.39.

$[Au_2(C_2H_6NCS_2)_2]_n$ polymer **(19)**

Intermediate **(18)**, (231 mg, 0.5 mmol) in 10 mL of dichloromethane was added to sodium dimethyldithiocarbamate monohydrate (74.5 mg, 0.52 mmol) in 10 mL of ethanol at room temperature with continuous stirring for 6h. A colorless solid (*2-(diphenylphosphino)-ethylamine*) that formed was filtered off, and the clear pale yellow solution was stored for low evaporation. A yellow solid was obtained. IR (cm^{-1}) ν(C-H) 2990, ν(C-H) 1375_{bend}; ν(N-C) 1483; ν(C=S) 1100, 993. ^{1}H NMR ($CDCl_3$, ppm) δ 3.55 (s, 6H, CH_3). ^{13}C NMR ($CDCl_3$, ppm) δ 196.12-N$\underline{C}S_2$(1), 46.64 C(2).

$[Au_2(C_4H_{10}NCS_2)_2]_n$ polymer **(20)**

This polymer was synthesized with **s**odium diethyldithiocarbamate trihydrate (117.2 mg, 0.52 mmol) by a procedure similar to **(18).** After 3 days, needle-like orange crystals were

obtained. A suitable crystal was selected for X-ray diffraction analysis. IR (cm^{-1}) ν(C-H) 2970, ν(C-H) 1377_{bend}; ν(-CH_2) 2925_{asym}, 2856_{sym}; ν(-CH_2)$_{bend}$ 1264; ν(N-C) 1480; ν(C=S) 1098, 1067. ^{1}H NMR ($CDCl_3$, ppm) δ3.92 (t, 6H, CH_3), (t, 4H, C$\underline{H_2}$$CH_3$). ^{13}C NMR ($CDCl_3$, ppm) δ 205.58 -N$\underline{C}S_2$ (1), 49.35 C(2), 12.20 C(3).

$[Au_2(C_{14}H_{14}NCS_2)_2]_n$ polymer **(21)**

This polymer was synthesized with sodium dibenzyldithiocarbamate trihydrate (159.7mg, 0.52 mmol) by a procedure similar to **(18).** A yellow solid was obtained. IR (cm^{-1}) ν(CH_2) 2923_{asym}, 2850_{sym}, ν(C-H) 1265_{bend}; ν(Ar-C=C) 1602; ν(N-C) 1433; ν(C=S) 1100, 1072. ^{1}H NMR ($CDCl_3$, ppm) δ 4.85, 4.78 (d, 4H, CH_2), 7.17-7.77(m, 10H, C_5H_5). ^{13}C NMR ($CDCl_3$, ppm) δ 210.80 -N$\underline{C}S_2$ (1), 54.27 C(2), 128.58-140.93 C(C_6H_5).

$[Au(C_{14}H_{16}NP)_2]Cl$ complex **(22)**

Intermediate **(18)**, (231 mg, 0.5 mmol) in 10 mL of dichloromethane was added to *2-(Diphenylphosphino)ethylamine* (114.6 mg, 0.5 mmol) in 10 mL of dichloromethane at ambient room temperature with continuous stirring for 6h. A colorless solution was filtered off and stored for slow evaporation. A colorless solid was obtained. Yield 0.3g (87%). Anal. calc. for $[Au(C_{28}H_{32}NP)_2]Cl$ (690.68 g/mol): C, 48.67; H, 4.67; N, 4.05. Found: C, 47.89; H, 5.52; N, 4.04. IR (cm^{-1}) ν(N-H) 3421, 3332; ν(CH_2) 2909_{asym}, 2852_{sym}, ν(C-H) 1275_{bend}; ν(Ar-C=C) 1566; ν(N-C) 1496. ^{1}H NMR ($CDCl_3$, ppm) δ 4.04, 3.13 (s, 2H, NH); 3.02, 2.85 (m, C(1)$\underline{H}$, $\underline{H}$'); 2.56, 1.26 (m, C(2)$\underline{H}$, $\underline{H}$'); 7.33-7.74 (m, 20H, C_5H_5). ^{13}C NMR ($CDCl_3$, ppm) δ 36.63 C(1), 28.57 C(2), 129.17-133.08 C(C_6H_5). ^{31}P NMR ($CDCl_3$, ppm) δ 26.55.

3.3.2 Chlorido((1R,2R)-2-(diphenylphosphino)-2,3-dihydro-1H-inden-1-amine)Au(I) with dialkyl and dibenzyl-dithiocarbamate complexes (23-26)

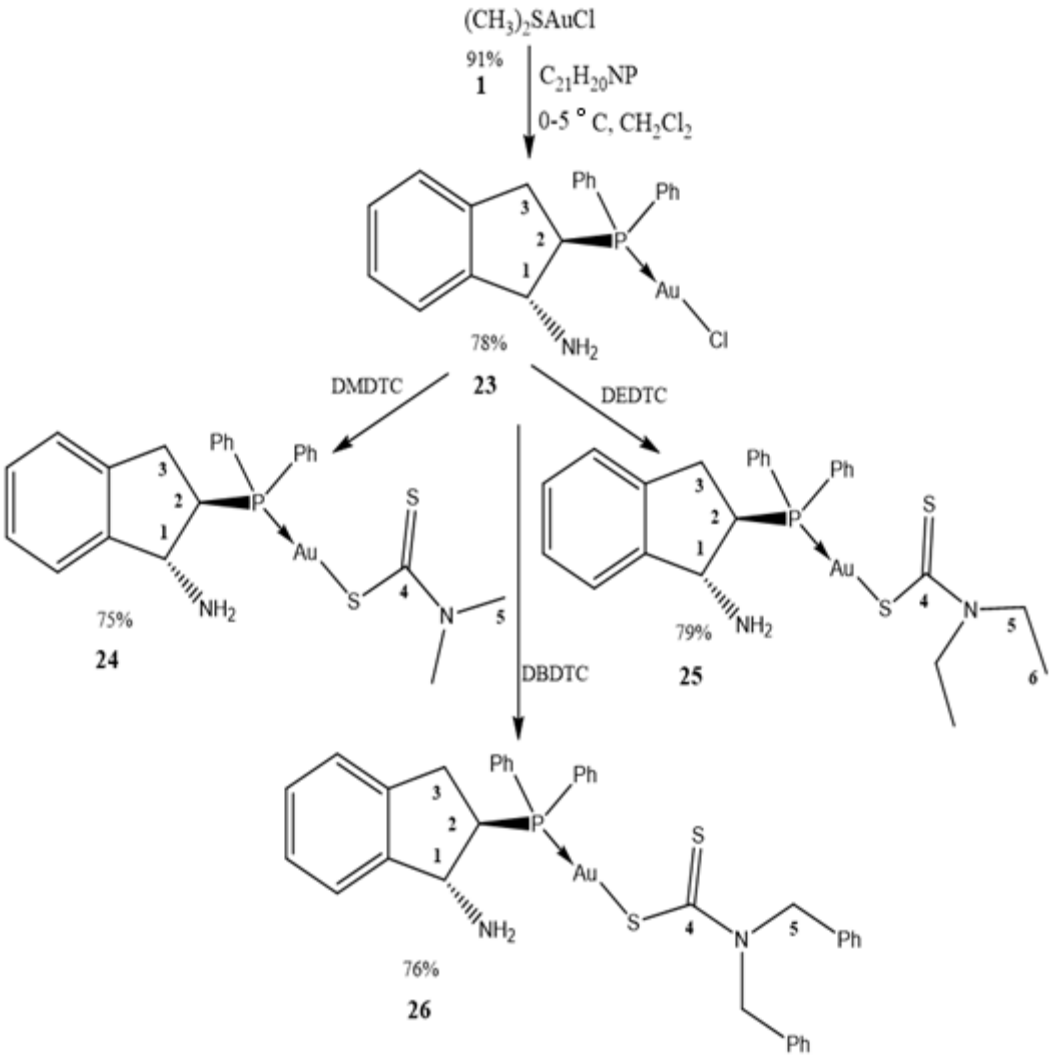

Scheme 17*. Synthesis of gold(I) mono-phosphine complexes* ***(23-26).***

[Au($C_{21}H_{20}NP$)Cl] complex **(23**)

This complex was synthesized with *(1R,2R)-2-(diphenylphosphino)-2,3-dihydro -1H-inden-1-amine)*(158.7mg, 0.5 mmol) by a procedure similar to **(2)**. A white solid was obtained, it was recrystallized from acetone/dichloromethane and dried overnight in a vacuum. Yield 0.451g (78%). Anal. calc. for $C_{21}H_{20}NPAuCl$ (549.78 g/mol): C, 45.78; H,

3.66; N, 2.54. Found: C, 45.27; H, 3.13; N, 2.18. IR (cm^{-1}) ν(N-H) 3461, 3334; ν(CH_2) 2935 $_{asym}$, 2850$_{sym}$, ν(C-H) 1280$_{bend}$, ν(Ar-C=C) 1628, ν(C-N) 1475. ^{1}H NMR ($CDCl_3$, ppm) δ1.56 (s, NH), 4.20 (d, C(1)H); 2.17 (m, C(2)H); 3.33, 2.75 (m, C(3)H,H'), 7.20-7.89 (m, 14H, C_6H_5). ^{13}C NMR ($CDCl_3$, ppm) δ 56.5 C(1), 46.7 C(2), 30.8 C(3), 126.3-139.8 C(C_6H_5). ^{31}P NMR ($CDCl_3$, ppm) δ 36.18.

[Au($C_{21}H_{20}NP$)($C_2H_6NCS_2$] **(24)**

This complex was synthesized with **s**odium dimethyldithiocarbamate monohydrate (71.6 mg, 0.5 mmol) by a procedure similar to **(3)**. Pale yellow solid was obtained, recrystallized from acetone/dichloromethane and dried overnight in a vacuum. Yield 0.238 g (75%). Anal. calc. for $C_{24}H_{26}AuN_2PS_2$= 634.55 g/mol: C, 45.78; H, 4.12; N, 4.41; S, 10.10. Found: C, 45.37; H, 4.55; N, 3.89; S, 9.83. IR (cm^{-1}) ν(N-H) 3447, 3342; ν(CH_2) 2927$_{asym}$, 2851$_{sym}$, ν(C-H) 1244$_{bend}$, ν(Ar-C=C) 1615, ν(C-N) 1486, ν(C=S) 1099,1134. ^{1}H NMR ($CDCl_3$, ppm) δ 1.63 (s, NH), 4.48 (d, C(1)H); 2.16 (m, C(2)H); 3.43, 3.17 (m, C(3)H,H'), 3.40 (s, C(4)H), 7.40-8.57 (m, 14H, C_6H_5). ^{13}C NMR ($CDCl_3$, ppm) δ 56.9 C(1), 32.5 C(2), 29.7 C(3), 184.0 C=S(4), 34.7 C(5), 125-140 C(C_6H_5). ^{31}P NMR ($CDCl_3$, ppm) δ 33.67.

[Au($C_{21}H_{20}NP$)($C_4H_{10}NCS_2$)] **(25)**

This complex was synthesized with **s**odium diethyldithiocarbamate trihydrate (112.7 mg, 0.5 mmol) by a procedure similar to **(3)**. An orange solid was obtained, recrystallized from acetone/dichloromethane and dried overnight in vacuum. Yield 0.262 g (79%). Anal. calc. for $C_{26}H_{30}AuN_2PS_2$ (662.60 g/mol): C, 47.13; H, 4.56; N, 4.23; S, 9.68. Found: C, 45.37;

H, 4.10; N, 3.87; S, 9.13. IR (cm^{-1}) ν(N-H) 3417, 3321; ν(CH_2) 2926_{asym}, 2865_{sym}, ν(C-H) 1264_{bend}, ν(Ar-C=C) 1610, ν(C-N) 1492, ν(C=S) 984,1068. ^{1}H NMR ($CDCl_3$, ppm) δ 4.05 (s, NH), 4.47 (d, C(1)H); 2.15 (m, C(2)H), 3.92 (t, C(3)H,H'), 3.55 (q,C(4)H), 1.32 (t,C(5)H), 7.42-7.75 (m, 14H, C_6H_5). ^{13}C NMR ($CDCl_3$, ppm) δ 54.5 C(1), 33.4 C(2), 29.6 C(3), 48.3 C(4), 203.6 C=S(5), 12 C(6), 126.4 -135.5 C(C_6H_5). ^{31}P NMR ($CDCl_3$, ppm) δ 30.5.

[Au($C_{21}H_{20}NP$)($C_{14}H_{14}NCS_2$)] **(26)**

This complex was synthesized with **s**odium dibenzyldithiocarbamate trihydrate (153.6 mg, 0.5 mmol) by a procedure similar to **(3)**. An orange solid was obtained, recrystallized from acetone/dichloromethane and dried overnight in vacuum. Yield 0.262g (79%). Anal. calc. for $C_{35}H_{34}AuN_2PS_2$ (774.73 g/mol): C, 54.96; H, 4.44; N, 3.56; S, 8.15. Found: C, 54.37; H, 4.11; N, 3.17; S, 7.83. IR (cm^{-1}) ν(N-H) 3406, 3319; ν(CH_2) 2921_{asym}, 2851_{sym}, ν(C-H) 1224_{bend}, ν(Ar-C=C), ν(C-N) 1492, ν(C=S) 973,1099. ^{1}H NMR ($CDCl_3$, ppm) δ 1.7 (s, NH), 4.46 (d, C(1)H); 2.14 (m, C(2)H), 4.62 (t, C(3)H,H'); 4.82, 4.69 (d, C(4)H), 7.38-7.80 (m, 24H, C_6H_5). ^{13}C NMR ($CDCl_3$, ppm) δ 53.6 C(1), 34.5 C(2), 29.7 C(3), 199.5 C=S(4), 54.3 C(5), 125.4-134.5 C(C_6H_5). ^{31}P NMR ($CDCl_3$, ppm) δ 28.66.

3.3.3 Chlorido(1R,2R)-2-(diphenylphosphino)-1-aminocyclohexane)Au(I) with dialkyl and dibenzyl-dithiocarbamates complexes (27-30)

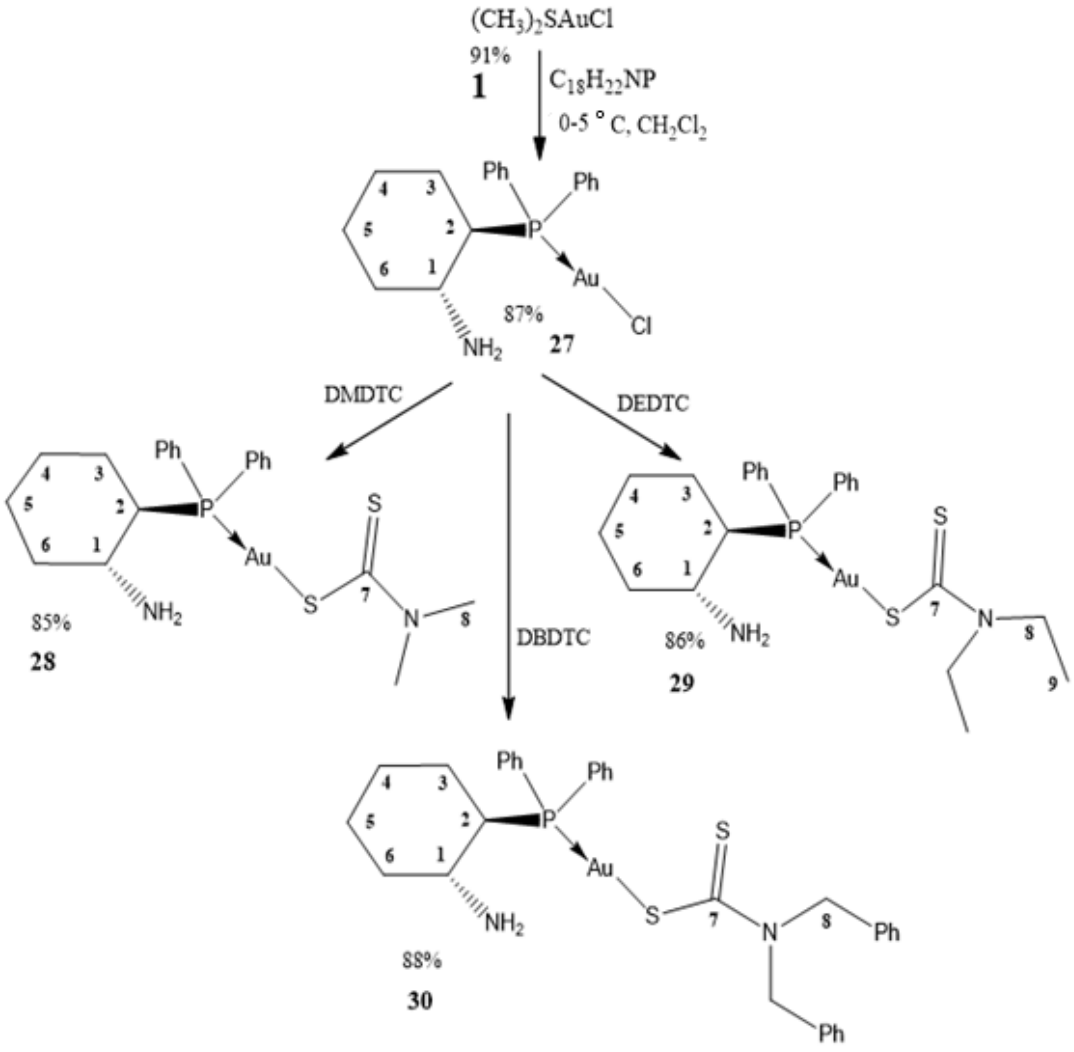

Scheme 18. *Synthesis of gold(I) mono-phosphine complexes* ***(27-30).***

[($C_{18}H_{22}NP$)AuCl] complex **(27)**

This complex was synthesized with (1*R*,*2R)-2-(diphenylphosphino)-1-aminocyclohexane* (142 mg, 0.5 mmol) by a procedure similar to **(2)**. A colorless solid was obtained, recrystallized from acetone/dichloromethane and dried overnight in vacuum. A suitable

crystal was chosen for X-ray diffraction analysis. Yield 0.224 g (87%). Anal. calc. for $C_{18}H_{22}NPAuCl$ (515.77 g/mol): C, 41.92; H, 4.30; N, 2.72. Found: C, 39.97; H, 3.55; N, 2.34. IR (cm^{-1}) ν(N-H) 3461, 33324; ν(CH_2) 2935_{asym}, 2850_{sym}, ν(C-H) 1315_{bend}, ν(Ar-C=C) 1572. ^{1}H NMR ($CDCl_3$, ppm) δ 1.97 (s, NH), 3.15 (m, C(1)H), 2.54 (m, C(2)H), 1.22 (m, C(3)H), 1.42 (m, C(4)H), 1.33 (m, C(5)H), 1.74 (m, C(6)H), 7.47-7.94 (m, 10H, C_6H_5). ^{13}C NMR ($CDCl_3$, ppm) δ 56.01 C(1), 43.54 C(2), 24.73 C(3), 28.10 C(4), 25.65 C(5), 37.65 C(6), 128.96 -134.84 C(C_6H_5). ^{31}P NMR ($CDCl_3$, ppm) δ 41.84.

[Au($C_{18}H_{22}NP$)($C_2H_6NCS_2$)] **(28)**

This complex was synthesized with **s**odium dimethyldithiocarbamate monohydrate (72 mg, 0.5 mmol) by a procedure similar to **(3)**. A yellow solid was obtained, recrystallized from acetone/dichloromethane and dried overnight in a vacuum. Yield 0.255 g (85%). Anal. calc. for $C_{22}H_{18}NPAuC_2H_6NS_2$ (600.53 g/mol): C, 42.00; H, 4.69; N, 4.66; S, 10.67. Found: C, 41.64; H, 4.77; N, 4.40; S, 10.40. IR (cm^{-1}) ν(N-H) 3461, 3334; ν(CH_2) 2927_{asym}, 2851_{sym}, ν(C-H) 1246_{bend}, ν(Ar-C=C) 1615, ν(C-N) 1486, ν$(C=S)_2$ 1134, 1099. ^{1}H NMR ($CDCl_3$, ppm) δ 1.92 (s, NH), 3.38 (m, C(1)H), 3.35 (m, C(2)H), 3.48 (m, C(3)H),1.87 (m, C(4)H),1.45 (m, C(5)H),1.29 (m, C(6)H), 3.52 (m, C(6)H),7.47-8.06 (m,10H, C_6H_5). ^{13}C NMR ($CDCl_3$, ppm) δ 54.55 C(1), 45.29 C(2), 24.04 C(3), 30.92 C(4), 25.18 C(5), 40.96 C(6), 207.51 C=S(7), 50.53 C(8), 128.97-134.05 C(C_6H_5). ^{31}P NMR ($CDCl_3$, ppm) δ 41.68.

$[Au(C_{18}H_{22}NP)(C_4H_{10}NCS_2]$ **(29)**

This complex was synthesized with **s**odium diethyldithiocarbamate trihydrate (133 mg, 0.5 mmol) by a procedure similar to **(3)**. An orange solid was obtained, recrystallized from acetone/dichloromethane and dried overnight in vacuum. Yield 0.270 g (86%). Anal. calc. for $C_{18}H_{22}NPAuC_4H_{10}NCS_2$ (600.53 g/mol): C, 42.00; H, 4.69; N, 4.66; S, 10.67. Found: C, 41.64; H, 4.77; N, 4.40; S, 10.40. IR (cm^{-1}) ν(N-H) 3461, 3334; ν(CH_2) 2927_{asym}, 2851_{sym}, ν(C-H) 1264_{bend}, ν(Ar-C=C) 1610, ν(C-N) 1496, ν$(C=S)_2$ 1068, 984. ^{1}H NMR ($CDCl_3$, ppm) δ1.93 (s, NH), 3.46 (m, C(1)H), 2.32 (m, C(2)H), 2.93 (m, C(3)H), 1.83 (m, C(4)H), 1.41 (m, C(5)H), 1.35 (m, C(6)H), 3.54 (s, C(8)H), 1.33 (s, C(9)H) 7.46-8.12 (m, 10H, C_6H_5). ^{13}C NMR ($CDCl_3$, ppm) δ 54.87 C(1), 44.12 C(2), 24.15 C(3), 29.65 C(4), 25.11 C(5), 39.55 C(6), 204.16 C=S(7), 52.25 C(8), 12.1 C(9), 128.38-134.65 C(C_6H_5). ^{31}P NMR ($CDCl_3$, ppm) δ 40.15.

$[Au(C_{18}H_{22}NP)(C_{14}H_{14}NCS_2)]$ **(30)**

This complex was synthesized with **s**odium dibenzyldithiocarbamate trihydrate (154 mg, 0.5 mmol) by a procedure similar to **(3)**. A yellow solid was obtained, recrystallized from acetone/dichloromethane and dried overnight in vacuum. Yield 0.326 g (88%). Anal. calc. for $C_{18}H_{22}AuC_{14}H_{14}NCS_2$ (600.53 g/mol): C, 51.88; H, 4.89; N, 3.78; S, 8.65. Found: C, 51.24; H, 4.25; N, 3.81; S, 8.06. IR (cm^{-1}) ν(N-H) 3461, 3334; ν(CH_2) 2923_{asym}, 2852_{sym}, ν(C-H) 1210_{bend}, ν(Ar-C=C) 1600, ν(C-N) 1437, ν$(C=S)_2$ 1099, 973. ^{1}H NMR ($CDCl_3$, ppm) δ 1.7 (s, NH), 3.88 (m, C(1)H), 2.02 (m, C(2)H), 3.25 (m, C(3)H), 1.84 (m, C(4)H), 1.46 (m, C(5)H), 0.88 (m, C(6)H), 5.11, 4.71 (d, C(7)H), 7.48-8.11 (m, 10H, C_6H_5). ^{13}C NMR ($CDCl_3$, ppm) δ 55.88 C(1), 43.65 C(2), 24.45 C(3), 27.89 C(4), 25.74 C(5), 37.06

C(6), 210.17 C=S(7), 58.40 C(8), 127.82-135.92 C(C_6H_5). ^{31}P NMR ($CDCl_3$, ppm) δ 39.18.

3.3.4 Chlorido(2-(di-*i*-propylphosphino)ethylamine)Au(I) with dialkyl and dibenzyldithiocarbamates complexes (31-34)

[Au(C_8H_{20}NP)Cl] complex **(31**)

This complex was synthesized with *2-(di-i-propylphosphino)ethylamine* (81 mg, 0.5 mmol) by steps similar to **(2)**. A white solid was obtained and it was recrystallized from acetone/dichloromethane and dried overnight in vacuum. Yield 0.138 g (70%). Anal. calc. for $C_8H_{20}AuClNP$ = 393.64 g/mol: C, 24.40; H, 5.12; N, 3.55. Found: C, 23.97; H, 5.00; N, 3.15. IR (cm^{-1}) ν(N-H) 3443, 3325; ν(CH_2) 2937_{asym}, 2853_{sym}, ν(C-H) 1375_{bend}, ν(C-N) 1485. ^{1}H NMR ($CDCl_3$, ppm) δ 1.52 (s, NH), 2.73 (m, C(1)H), 2.78 (m, C(2)H), 1.75 (m, C(3)H), 1.11 (d, C(4)H). ^{13}C NMR ($CDCl_3$, ppm) δ 61.4 C(1), 35.51 C(2), 24.64 C(3), 18.87 C(4). ^{31}P NMR ($CDCl_3$, ppm) δ 25.54.

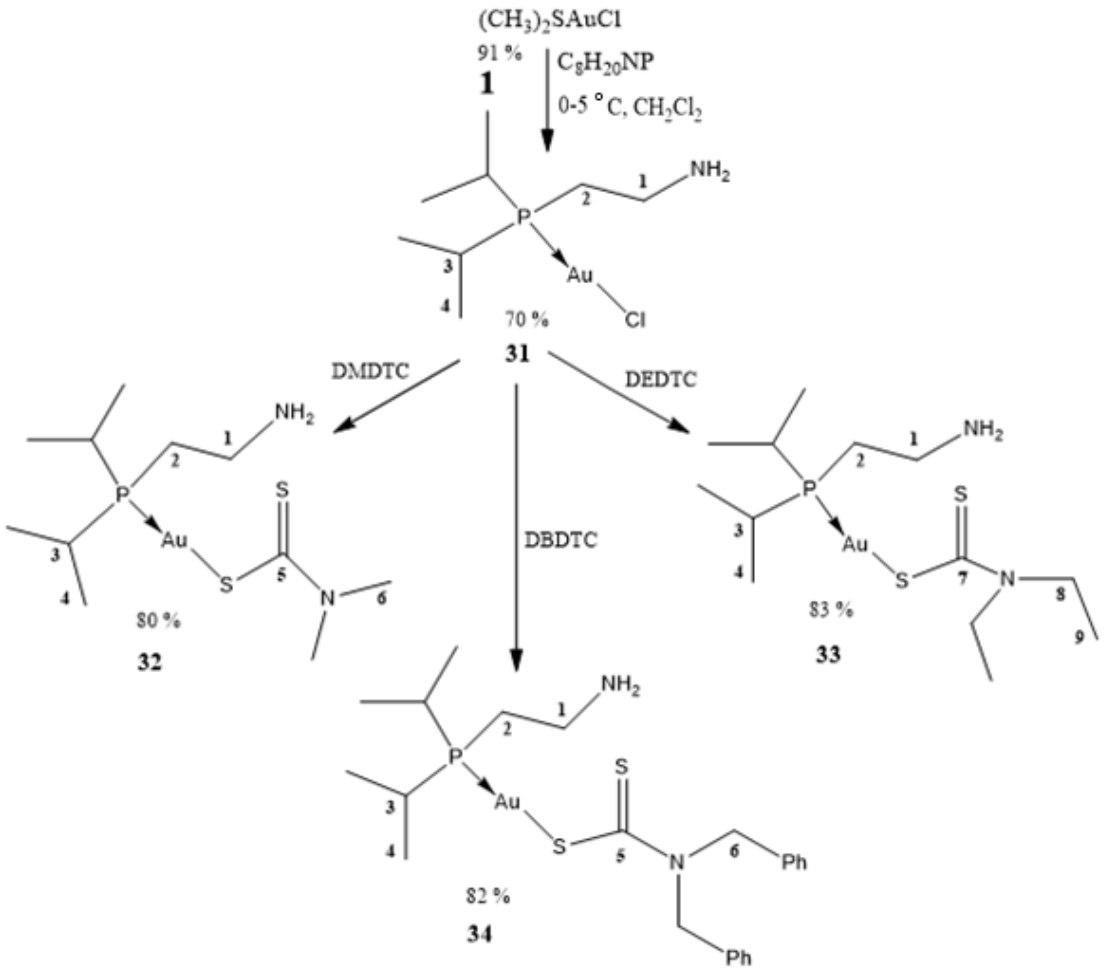

Scheme 19. *Synthesis of gold(I) mono-phosphine complexes* ***(31-34).***

$[Au(C_8H_{20}NP)(C_2H_6NCS_2]$ **(32)**

This complex was synthesized with **s**odium dimethyldithiocarbamate monohydrate (72 mg, 0.5 mmol) by steps similar to **(3)**. A yellow solid was obtained, recrystallized from acetone/dichloromethane and dried overnight in vacuum. Yield 0.191 g (80%). Anal. calc. for $C_8H_{20}NPAuC_2H_6NCS_2$ (478.41 g/mol): C, 27.61; H, 5.47; N, 5.85; S, 13.40. Found: C, 27.04; H, 4.97; N, 5.30; S, 12.80. IR (cm^{-1}) ν(N-H) 3451, 3343; ν(CH_2) 2928_{asym}, 2849_{sym}, ν(C-H) 1286_{bend}, ν(C-N) 1496, ν(C=S) 1034, 998. ^{1}H NMR ($CDCl_3$, ppm) δ 1.72 (s, NH),

2.85 (m, C(1)H), 2.97 (m, C(2)H), 1.87 (m, C(3)H), 1.21 (m, C(4)H), 3.53 (s, C(6)H). ^{13}C NMR ($CDCl_3$, ppm) δ 60.3 C(1), 34.2 C(2), 24.1 C(3), 19.3 C(4), 193.9 C=S(5), 55.5 C(6). ^{31}P NMR ($CDCl_3$, ppm) δ 47.72.

[Au($C_8H_{20}NP$)($C_4H_{10}NCS_2$] **(33)**

This complex was synthesized with **s**odium diethyldithiocarbamate trihydrate (113 mg, 0.5 mmol) by steps similar to **(3)**. A yellow solid was obtained, it was recrystallized from acetone/dichloromethane and dried overnight in vacuum. Yield 0.191 g (80%). Anal. calc. for $C_8H_{20}AuC_4H_{10}NCS_2$ (506.46 g/mol): C, 30.82; H, 5.97; N, 5.53; S, 12.66. Found: C, 30.24; H, 5.37; N, 5.30; S, 12.18. IR (cm^{-1}) ν(N-H) 3451, 3345; ν(CH_2) 2931_{asym}, 2852_{sym}, ν(C-H) 1283_{bend}, ν(C-N) 1486, ν(C=S) 1024, 996. ^{1}H NMR ($CDCl_3$, ppm) δ 1.82 (s, NH), 2.81 (m, C(1)H), 2.93 (m, C(2)H), 1.86 (m, C(3)H), 1.22 (m, C(4)H), 3.55 (s, C(6)H). ^{13}C NMR ($CDCl_3$, ppm) δ 59.53 C(1), 33.7 C(2), 23.7 C(3), 20.1 C(4), 203.7 C=S(5), 48.5 C(6), 12.1 C(7). ^{31}P NMR ($CDCl_3$, ppm) δ 43.25.

[Au($C_{18}H_{22}NP$)($C_{14}H_{14}NCS_2$)] **(34)**

This complex was synthesized with **s**odium dibenzyldithiocarbamate trihydrate (154 mg, 0.5 mmol) steps similar to **(3)**. A yellow solid was obtained, recrystallized from acetone/dichloromethane and dried overnight in vacuum. Yield 0. 254 g (82%). Anal. calc. for $C_8H_{22}NPAuC_{14}H_{14}NCS_2$ (618.59 g/mol): C, 42.71; H, 5.54; N, 5.52; S, 10.36. Found: C, 42.24; H, 5.23; N, 4.98; S, 10.06. IR (cm^{-1}) ν(N-H) 3441, 3336; ν(CH_2) 2929_{asym}, 2851_{sym}, ν(C-H) 1370_{bend}, ν(Ar-C=C) 1588, ν(C-N) 1477, ν(C=S) 1059, 993. ^{1}H NMR ($CDCl_3$, ppm) δ 1.83 (s, NH), 2.88 (m, C(1)H), 2.98 (m, C(2)H), 1.85 (m, C(3)H), 1.14 (m,

C(4)H), 5.03, 4.75. (d, C(6)H), 7.43-7.78 (m, 10H, C_6H_5). ^{13}C NMR ($CDCl_3$, ppm) δ 58.6 C(1), 35.3 C(2), 23.7 C(3), 20.1 C(4), 207.5 C=S(7), 54.5 C(8), 128.12-142.67 C(C_6H_5). ^{31}P NMR ($CDCl_3$, ppm) δ 46.6.

3.3.5 Gold(I) with mixed tri(o-methoxyphenyl)phosphine and triphenylphosphine complexes (35-37).

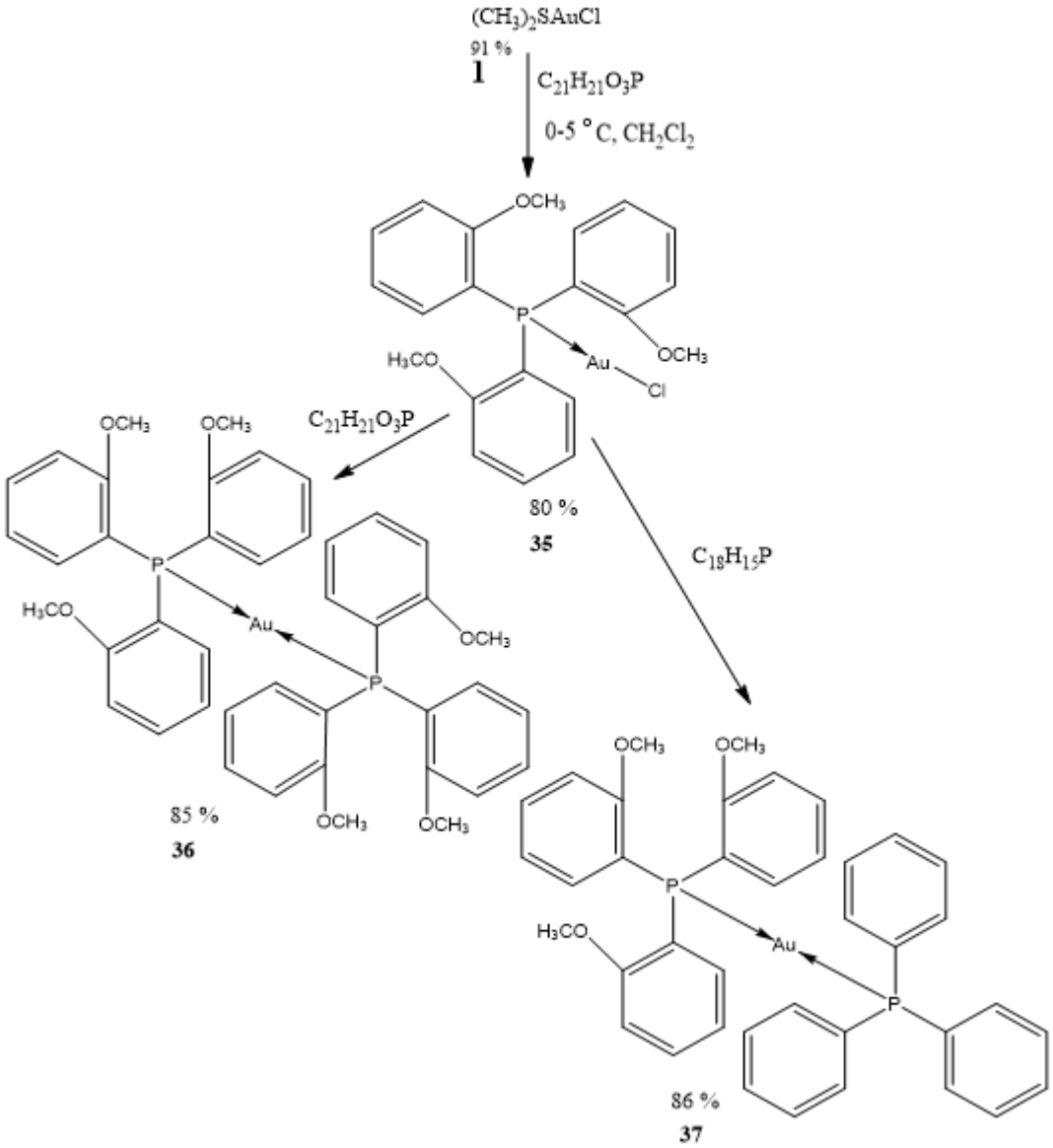

Scheme 20**. Synthesis of gold(I)-phosphine complexes **(35-37).

[$Au(C_{21}H_{21}O_3P)Cl$] **(35)**

This complex was synthesized with *tri(o-methoxy- phenyl)phosphine* (176 mg, 0.5 mmol) by a procedure similar to **(2).** A colorless solid was obtained, recrystallized from acetone/dichloromethane and dried overnight in vacuum. Yield 0.234 g (80%). Anal. calc. for $C_{21}H_{21}AuClO_3P$= 584.78 g/ mol: C, 43.13; H, 3.61. Found: C, 42.94; H, 3.11. IR (cm^{-1}) $\nu(CH_2)$ 2932_{asym}, 2855_{sym}, ν(C-H) 1370_{bend}, ν(Ar-C=C) 1623. ^{1}H NMR ($CDCl_3$, ppm) δ 3.58 (s, C(1)H), 6.73-7.35 (m, 12H, C_6H_5). ^{13}C NMR ($CDCl_3$, ppm) δ 55.56 C(1), 121.87-160.45 C(C_6H_5). ^{31}P NMR ($CDCl_3$, ppm) δ 36.18.

[$Au(C_{21}H_{21}O_3P)_2$]Cl **(36)**

This complex was synthesized with *tri(o-methoxyphenyl)phosphine* (131 mg, 0.5 mmol) following a procedure similar to **(22).** A colorless solid was obtained, recrystallized from acetone/dichloromethane and dried overnight in vacuum. Yield 0.398 g (85%). Anal. calc. for $C_{42}H_{42}O_6P_2AuCl$ (937.15 g/ mol): C, 53.82; H, 4.51. Found: C, 53.34; H, 5.10. IR (cm^{-1}) $\nu(CH_2)$ 2935_{asym}, 2853_{sym}, ν(C-H) 1360_{bend}, ν(Ar-C=C) 1589. ^{1}H NMR ($CDCl_3$, ppm) δ 3.45 (s, C(1)H), 6.95-7.56 (m, 24H, C_6H_5). ^{13}C NMR ($CDCl_3$, ppm) δ 55.77 C(1), 111.62-160.95 C(C_6H_5). ^{31}P NMR ($CDCl_3$, ppm) δ 4.92.

[$Au(C_{39}H_{36}O_3P_2)$]Cl **(37)**

This complex was synthesized with *triphenylphosphine* (176 mg, 0.5 mmol) and *tri(o-methoxyphenyl)phosphine* (131 mg, 0.5 mmol) by a procedure similar to **(22).** A colorless solid was obtained, recrystallized from acetone/dichloromethane and dried overnight on vacuum. Yield 0.364 g (86%). Anal. calc. for $C_{39}H_{36}O_3P_2AuCl$ (847.07 g/

mol): C, 55.29; H, 4.28. Found: C, 54.84; H, 4.11. IR (cm^{-1}) ν(CH_2) 2937_{asym}, 2856_{sym}, ν(C-H) 1365_{bend}, ν(Ar-C=C) 1585. ^{1}H NMR ($CDCl_3$, ppm) δ 3.56 (s, C(1)H), 7.00-7.76 (m, 27H, C_6H_5). ^{13}C NMR ($CDCl_3$, ppm) δ 55.79 C(1), 111.62-160.98 C(C_6H_5). ^{31}P NMR ($CDCl_3$, ppm) δ 12.57, 29.61.

3.4. Single crystal structure determination

Suitable crystals of complex **(27)** were obtained as colorless rods from dichloromethane/ ethanol. The X-ray data were collected at 173K (-100°C) on a STOE IPSD 2 Image Plate Diffraction System [127] connected with a two-circle goniometer and using MoKα graphite monochromator (λ= 0.71073 Å). The structure was solved by SHELXS-2014 program [128]. The refinement and further calculations were carried out with SHELXL-2014 [128].

The water H atoms were located in a difference Fourier map and refined with distance restraint of O-H = 0.84(2) Å and with $U_{iso}(H) = 1.5U_{eq}(O)$. It was not possible to locate both H atoms on water molecules O7W and O8W. The non-hydrogen atoms were refined using least-squares matrix on F^2. A semi-empirical absorption correction was applied using the MUL scan ABS routine in PLATON [129]. The crystal structure and crystal packing were drawn using Mercury software [130]. The symmetry of crystal data and structure refinement is demonstrated in Table 3.23.

3.5 MTT assay for in vitro cytotoxicity of gold(I) complexes

Gold(I) complexes **(2-17)**, **(19-22)**, **(24-26)** and **(36, 37)** were tested for their *in vitro* cytotoxic effects against MCF7 (human breast cancer), HCT15 (human colon

adenocarcinoma) and A549 (human lung carcinoma) cell lines as previously reported method [131]. The cells were seeded at 3 x 10^3 cells/well in 100 μL of DMEM containing 10% fetal bovine serum (FBS) in a 96-well tissue culture plate and incubated for 72 h at 37 ^oC, 5% CO_2 and 90% relative humidity in a CO_2 incubator. After incubation, 100 μL of 50, 25 and 12.5 μM solutions of cisplatin, gold(I) complexes **(2-17)**, **(19-22), (23-26)** and **(36, 37)** prepared in Dulbecco's Modified Eagle's Medium (DMEM), was added to the cells and the cultures were incubated for 24 h. The medium in the wells was casted off and 100 μL of DMEM containing MTT (0.5 mg/ml) was added to the wells, with subsequent incubation in the CO_2 incubator at 37 ^{o} C in the dark for 4 h. After incubation, purple-colored formazan produced by the cells appeared as dark crystals in the bottom of the wells. The culture medium was carefully removed from each well to prevent disruption of the monolayer and 100 μL of dimethyl sulfoxide (DMSO) was added in each well. The solution in the wells was thoroughly mixed to dissolve the formazan crystals which produce a purple solution. The absorbance of the 96 well-plates was measured at 570 nm with Labsystems Multiskan EX ELISA reader against a reagent blank. The experimental results are calculated as micro-molar concentration of 50% cell growth inhibition (IC_{50}) of each drug. The MTT assay was carried out in three independent experiments, each in triplicate.

3.6 Results and Discussion

3.6.1 Gold(I) complexes with mixed bis-phosphine and dithiocarbamates ligands (2-17)

3.6.1.1 Spectroscopic analysis

The synthesized gold(I) complexes with mixed bis-phosphine dithiocarbamate ligands **(2-17)** are shown in (Schemes 12, 13, 14 and 15) were characterized by ^{1}H, ^{13}C and ^{31}P NMR, mid/far FT-IR spectroscopy, elemental analysis and melting point. The FT-IR data of free ligands and complexes **(2-17)** are summarized in Table 3.1**.**

The spectra present the characteristic ν(C—N) and ν(C—S) absorbance bands. The region around 1500 cm^{-1} is associated with a thioureido ion ($RN^{+}=CS_2$) intermediate between the C-N single bond (1250-1360 cm^{-1}) and the C=N double bond (1640-1690 cm^{-1}) in the dithiocarbamate complexes. The strong ν(C—N) absorbance bands of the complexes **(2-17)** were assigned in the range (1403-1480) cm^{-1}, suggesting partial double bond character due to a partially delocalized electron density [132-134].

Table 3-1. Mid FT-IR frequencies (cm^{-1}) for free ligands and complexes (**2-17**)

Ligand/ Complex	Stretch NH						Stretch C—N	Stretch C=S
DMDTC	-	2924	1360	-	-	-	1488	926
DETDC	-	2925	1358	-	1397	-	1445	986
DBDTC	-	-	-	2922	1347	1600	1467	985
2	3442	-	-	2923, 2854	1436	1633	1478	-
3	3434	-	1372	2923, 2852	1435	1629	1478	1099
4	3424	2923	1355	2925, 2853	1435	1587	1480	1099
5	3418	2920	-	2923, 2853	1443	1639	1203	1099
6	3429	-	-	2936, 2852	1315	1625	1435	1104
7	3420	2920	1374	2931, 2851	1242	1629	1490	1108
8	3425	2970	1355	2930, 2825	1265	1624	1480	1103
9	3425	2970	1355	2929, 2825	1365	1224	1480	1103
10	3434	-	-	2934, 2847	-	-	1446	1000
11	3420	2920	1374	2928, 2845	1242	-	1490	1108
12	3436	2934	1342	2929, 2847	1273	-	1446	1118
13	3425	2970	1355	2925, 2825	1256	-	1480	1103
14	3445	-	-	2921, 2855	1439	1630	1481	-
15	3430	2920	-	2923, 2855	1445	1632	1488	1035
16	3428	-	-	2927, 2855	1475	1613	1485	1039
17	3438	3172	1106	2925, 2851	1473	1635	1403	1019

The ν(C—H) sp^3 stretching band was observed at 2924 and 2925 cm^{-1} for free methyl and ethyl dithiocarbamate ligand, respectively, and after coordination, it was observed at 2934 and 2970 cm^{-1}. The ν(C=S) stretching band for free ligand was observed at 926-986 cm^{-1}, and after coordination it was observed at 1099-1118 cm^{-1}. The ν(C=C) band observed in the region 1587–1635 cm^{-1} of these complexes**,** which were assigned to the presence of aromatic ring.

The comparison of ^{1}H NMR spectra between free dithiocarbamate ligand and their complexes **(2-17)** showed significant shifts that indicate complexation of dithiocarbamate, as shown in Table 3.2.

The ^{13}C NMR chemical shifts (Table 3.3) for these complexes showed significant shift to higher fields with respect to free dithiocarbamate ligands. For example, C=S chemical shifts for dimethyldithiocarbamate, diethyldithiocarbamate or dibenzyldithiocarbamate were observed in the range 206-213 ppm compared to their gold(I) complexes, with a range of 198-210 ppm due to back donation from metal to ligand. In addition, ^{31}P NMR chemical shifts for gold(I) complexes showed significant shift to lower field at (23.00 to 39.20 ppm), relatively to their precursors (**2**, **6**, **10** and **14**) with a range (-11.26 to 21.90 ppm) as shown in Table 3.3.

Table 3.2. ^{1}H NMR chemical shifts for free ligands and complexes (**2-17**) in $CDCl_3$ along with DMDTC, DEDTC and DBDTC in D_2O

Ligand/ cCmplex	1H, 1H’	2H	3H, 3H′	4H,4H′	6H	7H, 7H′	NH	Aromatic-Hs
DMDTC	-	-	-	-	3.35 s	-		
DEDTC	-	-	-	-	3.93 q	1.13 t	-	-
DBDTC					5.31, 4.77 d			
2	4.79, 3.84 d	4.11 m	2.31, 2.14 m	1.85, 1.32 m	-	-	1.60	8.25 m-6.77m
3	4.00, 3.81 d	3.46 m	2.13, 1.62 m	1.26, 1.10 m	4.35 s	-	1.61, 1.08	7.58m -6.80 m
4	4.07,3.89 d	3.74m	2.08, 1.78 m	1.49, 1.02 m	4.19 q	1.30 t	2.35, 1.02	8.03m-6.74m
5	4.90,4.45d	4.22 m	2.81, 2.19 m	1.59, 1.19 m	5.24, 5.07d	-	2.62, 2.16	7.91m-6.81m
6	3.67,3.17m	2.81, 2.16m	-	-	-	-	10.10	7.70m -7.42m
7	3.92,3.12m	2.99, 2.10 m	-	-	3.56 s	-	9.45	7.75m-7.50 m
8	3.92, 3.12m	2.56, 2.43m	-	-	3.55 q	1.26 t	9.45	7.75m-7.28m
9	3.64, 3.19m	2.56, 2.18m	-	-	5.08, 4.47d	-	9.03	7.76m-7.30m
10	3.79, 3.65m	2.51, 2.18m	3.47 m	1.90 m	-	-	1.76	-
11	3.88, 3.74m	3.35, 2.64	3.48 m	1.87	4.17 s	-	1.65	-
12	3.88, 3.02m	2.02 m	3.25 m	1.84 m	3.46 q	1.30 t	1.70	-
13	3.07m	2.02 m	3.14 m	1.84 m	5.24, 4.45 d	-	1.67	7.34 m- 7.28 m
14	4.65, 4.04d	4.15 m	2.35, 2.17 m	1.83, 1.30 m	-	-	9.45	8.30 m-6.65 m
15	4.04, 3.85d	3.40 m	2.13, 1.62 m	1.26, 1.10 m	4.15 s	-	1.75	7.68 -6.85 m
16	4.00, 3.79 m	3.64 m	2.00, 1.75 m	1.59, 1.12 m	4.24 q	1.25 t	2.55	7.75 m-6.65 m
17	4.50,4.35	4.12 m	2.61, 1.79 m	1.55, 1.26 m	5.14, 5.07 d	-	2.52	7.71 m-7.11 m

Table 3.3. ^{13}C and ^{31}P NMR chemical shifts for free ligands and complexes (**2-17**) in $CDCl_3$ along with DMTC, DETC and DBTC in D_2O.

Ligand/ complex	C1	C2	C3	C4	C5	C6	C7	C8	C9	Aromatic Cs	^{31}P
DMDTC	-	-	-	-	-	-	208.3	45.7	-	-	-
DEDTC	-	-	-	-	-	-	206.4	49.5	12.1	-	-
DBDTC	-	-	-	-	-	-	213.1	56.9	-	-	-
2	46.2	63.9, 59.1	29.7, 29.4	23.6, 23.0	-	-	-	-	-	-	-11.29
3	49.7	49.1	31.5, 30.9	24.8, 22.6	-	-	207.4	45.4	-	134.7-127.2	29.11
4	50.8	61.2	30.9	24.9	-	-	205.7	49.3	12.3	145.0-126.7	26.80
5	51.2	64.0	29.4	24.0	-	-	198.5	56.1	-	136.7-127.9	23.00
6	44.0	25.2	-	-	-	-	-	-	-	133.5-127.0	21.90
7	43.8	22.7	-	-	-	-	201.5	45.7	-	132.7-124.6	27.50
8	42.3	27.4	-	-	-	-	200.1	52.3	11.3	133.4-129.0	29.49
9	44.1	25.8	-	-	-	-	209.6	58.7	-	135.7-127.8	24.68
10	46.2	30.0	34.5	29.2	26.5	25.5	-	-	-	-	-11.26
11	45.1	30.1	34.8	29.8	26.2	25.8	202.6	45.2	-	-	38.36
12	47.0	32.0	34.5	28.4	26.6	25.7	205.9	49.0	12.0	-	39.18
13	47.3	29.5	34.5	28.5	26.6	25.7	210.1	55.8	-	135.9-127.8	39.20
14	45.2	62.8	29.4	23.7	-	-	-	-	-	162.6-128.2	-13.25
15	49.6	59.1	31.6	24.3	-	-	206.4	45.2	-	135.6-126.2	25.56
16	51.3	60.2	30.0	25.2	-	-	206.2	48.5	12.2	143.2-127.1	25.50
17	52.2	62.8	29.3	23.8	-	-	208.2	56.1	-	135.8-127.0	24.15

3.6.1.2 *In vitro* cytotoxic activities for gold(I) bisphosphine complexes (2-17)

In the present study, the synthesized gold(I) bis-phosphine complexes **(2, 5, 6, 9, 10, 13, 17)** compared to *cisplatin* (standard classical anticancer drug) were tested *in vitro* cytotoxicity against A549, MCF7 and HCT15 human cancer cell lines using an MTT assay.

The study of the dose-dependent inhibition of cell proliferation was obtained by increasing *cisplatin* and complex **(2-17)** concentrations against a fixed number of three human cancer cell lines as shown in Figures 3.1-3.3. IC_{50} values were obtained from the plot of the cisplatin and gold(I) complexes **(2-17)** concentration against the percentage of cell viability as shown in Table 3.4. For the A549 cell line, the complexes (**2, 6**) exhibited IC_{50} values 42 ± 0.5 and 43 ± 0.3 μM, respectively, similar to cisplatin (42 ± 2 μM). These data clearly show that the complexes **(2-17)** inhibit cell proliferation and have potency levels similar to cisplatin, suggesting that the presence of the P-Au-S moiety enhanced the activity of these complexes [135]. For HCT15 and MCF7 cell lines, all complexes showed moderate to higher IC_{50} values with respect to cisplatin.

Table 3.4. IC_{50} values (μM) of gold(I) complexes (**2-17**) against HCT15, A549 and HeLa cancer cell lines.

Complex	HCT15	A549	MCF7
Cisplatin	32 ± 2	42 ± 2	23 ± 4
2	76 ± 0.5	42 ± 0.5	82 ± 2
5	53 ± 3	291 ± 5	116 ± 3
6	46 ± 1	43 ± 0.3	36 ± 2
9	44 ± 3	206 ± 2	121 ± 3
10	58 ± 2	74 ± 1	53 ± 1
13	51 ± 3	280 ± 4	133 ± 2
17	51 ± 1	379 ± 8	142 ± 4

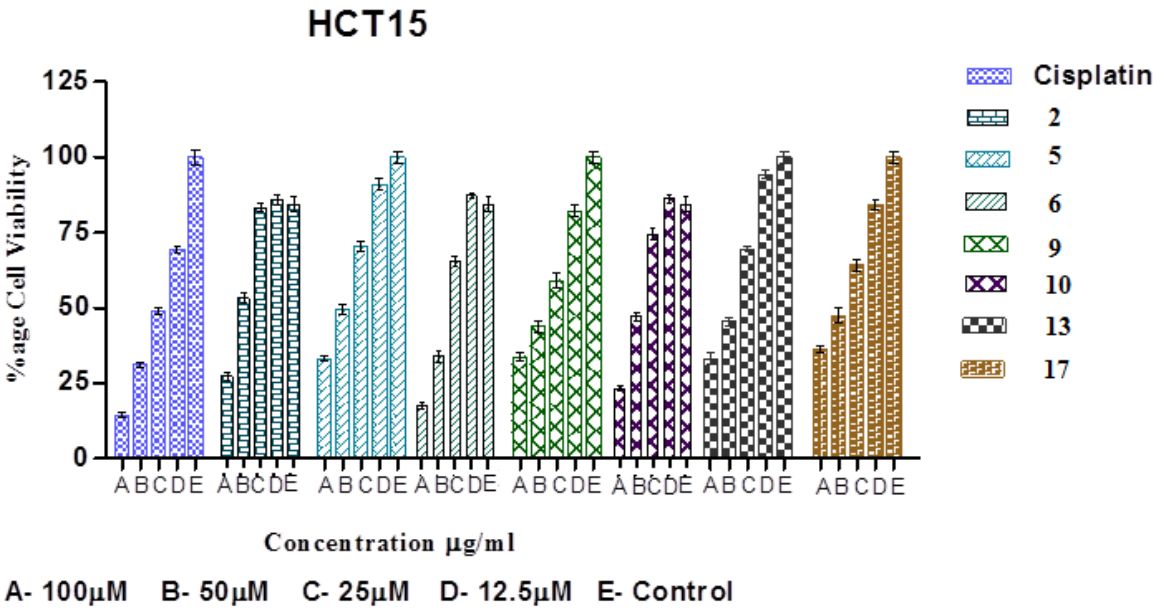

Figure 3.1. *Graph of cytotoxic effect of series concentrations of complexes (**2, 5, 6, 9, 10, 13**, and **17**) on cell viability of HCT15 cell line.*

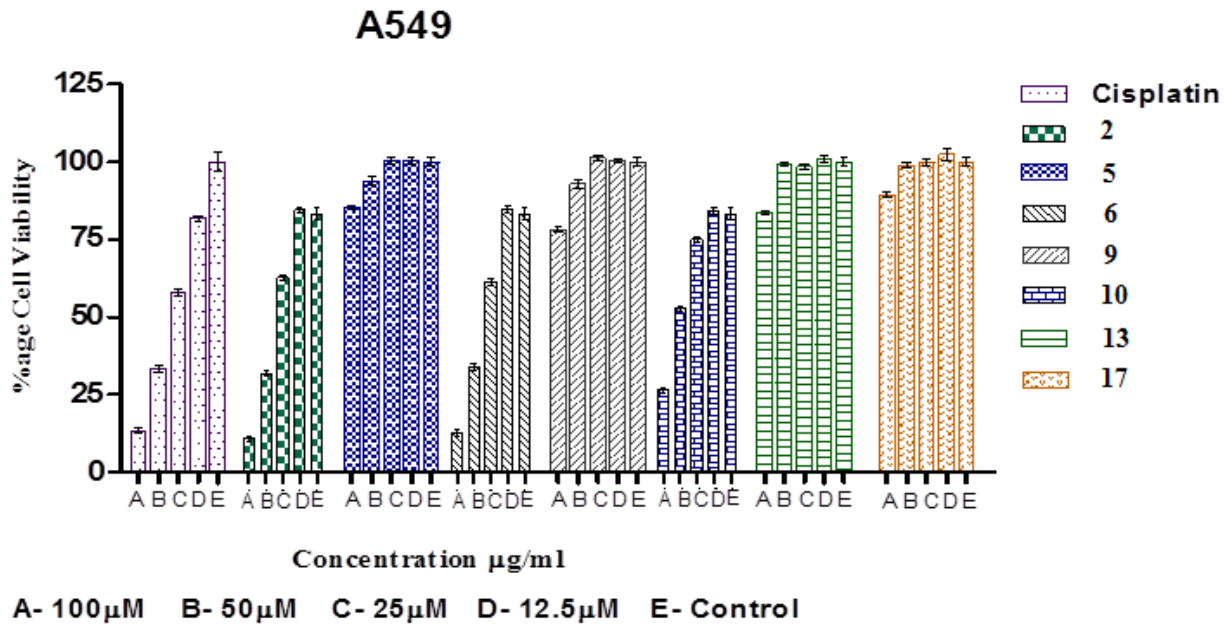

Figure 3.2. *Graph of cytotoxic effect of series concentrations of complexes (**2, 5, 6, 9, 10, 13**, and **17**) on cell viability of A549 cell line.*

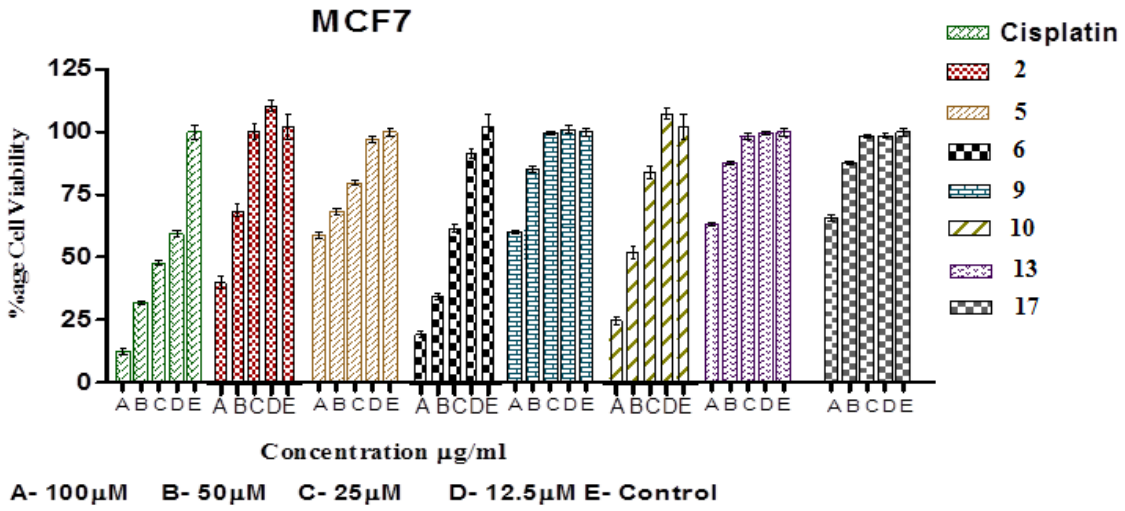

Figure 3.3. *Graph of cytotoxic effect of series concentrations of complexes (**2, 5, 6, 9, 10**, **13**, and **17**) on cell viability of MCF7 cell line.*

3.6.2 Gold(I) complexes with mixed mono-phosphine and dithiocarbamate ligands (18-22), (23-26), (27-30) and (31-34)

3.6.2.1 Spectroscopic analysis

The synthesized of complexes **(18-22),** (**23-26**), (**27-30**) and (**31-34**) are shown in (Schemes 16, 17, 18 and 19) and were characterized by ^{1}H, ^{13}C and ^{31}P NMR and mid FT-IR spectroscopy, elemental analyses and single crystal X-ray diffraction analysis.

The FT-IR spectra for free ligands and their complexes **(18-22),** (**23-26**), (**27-30**) and (**31-34**) are summarized in Tables 3.5-3.6, 3.8 and 3.10. The formation of the complexes was confirmed by the presence of the ν(C—N) and ν(C—S) absorbance bands. The region around 1500 cm^{-1} is associated with thioureido ion ($RN^{+}=CS_2$) between the C—N single bond (1250-1360 cm^{-1}) and the C=N double bond (1640-1690 cm^{-1}) in the dithiocarbamate complexes [136, 132]. The strong ν(C—N) absorbance bands of the complexes **(19, 24, 28** and **32-34)** were assigned in range of (1499-1433 cm^{-1}), suggesting partial double bond character due to a partially delocalized electron density [136].

For the (CS_2) stretching, two bands were observed for the complexes **(19, 24, 28** and **32-34)** in the range of (1134, 1099 cm^{-1}) to (1098, 973 cm^{-1}) with medium intensity. The presence of these two bands confirmed $(CS_2)_{as}$ and $(CS_2)_{s}$ of the dithiocarbamate ligand having bidentate nature [137-138].

The bands showed in the region of 1533 to1629 cm^{-1}, which were assigned to ν(C=C) of the aromatic ring [134].

In Far IR spectra, two bands of Au—Cl are observed at 220 and 250 cm^{-1} for intermediates **23** and **27** respectively, while they not for their complexes (**24-26**) and (**28-30**) and new

bands are observed in the range of 272 and 278 cm^{-1} attributed Au─S band as shown in Tables 3.7 and 3.9.

Table 3.5. Mid FT-IR frequencies (cm^{-1}) for free ligands and complexes (**18-22**).

Free ligand/ Complex	**Stretch NH**					**Stretch N─C**	**Stretch C=S**
DMDTC	-	2924	1360	-	-	1488	926
DEDTC	-	2925	1358	2979	1379	1466	986
DBDTC	-	-	-	2922	1347	1445	985
18	3431,3354	-	-	2927,2857	1310	1432	-
19	-	-	-	2990	1485	1483	1100,993
20	-	2970	1377	2926,2856	1264	1480	1098,1067
21	-	2923	-	2923,2850	1265	1433	1100,1072
22	3421,3332	-	-	2909,2852	1275	1496	-

Table 3.6. Mid FT-IR frequencies (cm^{-1}) for free ligands and complexes (**23-26**).

Free ligand/ Complex	**Stretch NH**						**Stretch N─C**	**Stretch C=S**
DMDTC	-	2924	1360	-	-	-	1488	926
DEDTC	-	-	-	2979	1379	-	1466	986
DBDTC	-	-	-	2922	1347	1600	1445	985
23	3461,3334	2993	1315	2916, 2850	1280	1628	-	-
24	3447,3342	2940	1376	2918, 2842	1244	1575	1499	1050,993
25	3417,3321	2968	1346	2926, 2852	1264	1629	1492	1068,997
26	3404,3319	3028	1349	2921,2851	1224	1533	1433	1026,991

Table 3.7. Far FT-IR frequencies (cm^{-1}) of complexes (**23-26**).

Complex	**Au─Cl**	**Au─P**	**Au─S**
23	220	301	-
24	-	311	277
25	-	310	275
26	-	311	274

Table 3.8. Mid FT-IR frequencies (cm^{-1}) for free ligands and complexes (**27-30**).

Free ligand/ Complex	**Stretch NH**					**Stretch N—C**	**Stretch C=S**
DMDTC	-	2924	1360	-	-	1488	926
DEDTC	-	2925	1358	2979	1379	1466	986
DBDTC	-	-	-	2922	1347	1445	985
27	3451,3360	-	-	2935,2850	-	1475	-
28	3441,3340	2940	1372	2927,2852	1246	1487	1134,1099
29	3414,3322	2969	1345	2923,2849	1264	1492	1068, 984
30	3411,3317	2967	1351	2923,2850	1210	1437	1099, 973

Table 3.9. Far FT-IR frequencies (cm^{-1}) of complexes (**27-30**).

Complex	**Au—Cl**	**Au—P**	**Au—S**
27	250.	298	-
28	-	304	278
29	-	302	276
30	-	306	272

Table 3.10. Mid FT-IR frequencies (cm^{-1}) for free ligands and complexes (**31-34**).

Free ligand/ Complex	**Stretch NH**					**Stretch N—C**	**Stretch C=S**
DMDTC	-	2924	1360	-	-	1488	926
DEDTC	-	2925	1358	2979	1379	1446	986
DBDTC	-	-	-	2922	1347	1445	985
31	3443,3325	2945	1365	2937,2851	1375	1485	-
32	3451,3343	2940	1372	2928,2849	1286	1496	1099, 973
33	3451,3345	2959	1345	2931,2852	1283	1486	1034, 998
34	3441,3336	2964	1353	2929,2851	1370	1477	1059, 993

The comparison of the ^{1}H NMR spectra between free dithiocarbamate ligands and their gold(I) complexes **(18-34)** showed significant shifts that indicated complexation of dithiocarbamate, as shown in Tables 3.11-3.14.

Table 3.11. ^{1}H NMR chemical shifts (ppm) for free ligands and gold(I) complexes (**18-22**) in $CDCl_3$.

Free ligand/ Complex	**1H, 1H'**	**2H, 2H'**	**4H**	**5H**	**NH**	**Aromatic-Hs**
DMDTC	-	-	-	-		
DEDTC	-	-	-	-	-	-
DBDTC						7.39 m-7.24 m
L0	2.78, 2.77m	2.19,2.16m	-	-	1.30	7.40 m-7.25m
18	3.31, 3.17 m	2.97, 2.73	-	-	4.03	7.56m -7.45 m
19	-	-	3.55 s	-	-	-
20	-	-	3.92 q	1.32 t	-	-
21	-	-	4.85,4.78	-	-	7.77m -7.23 m
22	3.02,2.85m	2.56, 1.26 m	-	-	4.04,3.12	7.70m-7.36 d

Table 3.12. ^{1}H NMR chemical shifts (ppm) for free ligands and gold(I) complexes (**23-26**) in $CDCl_3$.

Free ligand/ Complex	**1H**	**2H**	**3H, 3H'**	**4H**	**5H**	**NH**	**Aromatic-Hs**
DMDTC	-	-	-	3.35 s	-	-	-
DEDTC	-	-	-	3.93 q	1.13 t	-	-
DBDTC	-	-	-	5.31,4.77d	-	-	7.39 m-7.24 m
L1	4.20 d	2.17 m	3.12, 2.96 m	-	-	2.00	7.79m-7.49m
23	4.65 d	2.71 m	3.33, 2.75 m		-	1.56	7.89 m -7.20 m
24	4.48 d	2.16 m	3.43, 3.17m	3.40 s	-	1.63	8.57m- 7.70 m
25	4.47 d	2.15 m	3.92, 2.19 m	3.55 q	1.32 t	4.05	7.75m-7.42 m
26	4.46 d	2.14 m	4.26 t	4.82,4.69d	-	1.70	7.87m -7.41 m

Table 3.13. ^{1}H NMR chemical shifts (ppm) for free ligands and gold(I) complexes (**27-30**) in $CDCl_3$.

Free ligand/ Complex	1H	2H	3H	7H	8H	NH	Aromatic-Hs
DMDTC	-	-	-	3.35 s	-	-	-
DEDTC	-	-	-	3.93 q	1.13 t	-	-
DBDTC	-	-	-	5.31, 4.77 d	-	-	7.39 m-7.24 m
L2	2.63 m	2.16 m	1.23 m	-	-	1.97	7.79m-7.49m
27	3.15 m	2.54 m	1.22 m	-	-	1.92	7.89 m -7.20 m
28	3.38 m	3.35 m	3.48 m	3.52 s	-	1.93	8.06m- 7.47 m
29	3.41 m	3.37 m	3.49 m	4.11 q	1.31 t	1.95	7.95m-7.41 m
30	3.88 m	2.02 m	3.25 m	5.11, 4.71 d	-	1.70	8.11m -7.48 m

Table 3.14. ^{1}H NMR chemical shifts (ppm) for free ligands and gold(I) complexes (**31-34**) in $CDCl_3$.

Free ligand/ Complex	1H	2H	3H	6H	7H	NH	Aromatic-Hs
DMDTC	-	-	-	3.35 s	-		
DEDTC	-	-	-	3.93 q	1.13 t	-	-
DBDTC	-	-	-	5.31, 4.77d	-	-	7.39 m-7.24m
31	2.73 m	2.78 m	1.75 m	-	-	1.52	-
32	2.85 m	2.97 m	1.85 m	3.53 s	-	1.72	-
33	2.81 m	2.93 m	1.86 m	3.55 s	1.21 t	1.82	-
34	2.88 m	2.98 m	1.85 m	5.03, 4.75d	-	1.83	7.78m-7.35 m

The ^{13}C NMR chemical shifts for the complexes (**18-34**) showed significant shifts to up fields with respect to free dithiocarbamate ligands. For instance, C=S chemical shifts for dimethyldithiocarbamate, diethyldithiocarbamate and dibenzyldthiocarbamate were observed in the range 206—213 ppm compared to their coordinated complexes in the range 184—210 ppm. ^{31}P NMR chemical shifts for precursors **18, 31** and ligands **L1, L2**, respectively, compared to their dithiocarbamate complexes showed significant shifts

downfield, due to back donation from filled d-orbitals of gold atom to empty π* of S─C bond of dithiocarbamate moiety as shown in Tables 3.15-3.18.

The crystal structure of the gold(I) polymer (**19**) $[Au_2(C_4H_{10}NCS_2)_2]_n$. xCH_2Cl_2 has been recently published [139].

Table 3.15. ^{13}C and ^{31}P NMR chemical shifts (ppm) for free ligands and gold(I) complexes (**18-22**) in $CDCl_3$.

Free ligand/ Complex	**C1**	**C2**	**C=S**	**C4**	**C5**	**Aromatic-Cs**	**^{31}P**
DMDTC	-	-	208.3	45.7	-	-	-
DEDTC	-	-	206.4	49.5	12.1	-	-
DBDTC	-	-	213.1	56.9	-	137.2- 127.7	-
18	37.6	31.5	-	-	-	138.4-128.0	-23.46
19	-	-	196.1	46.6	-	- -	-
20	-	-	205.7	49.4	12.2	-	-
21	-	-	210.8	54.3	-	-	-
22	36.6	28.6	-	-	-	133.1-129.2	26.55

Table 3.16. ^{13}C and ^{31}P NMR chemical shifts (ppm) for free ligands and gold(I) complexes (**23-26**) in $CDCl_3$.

Free ligand/ Complex	**C1**	**C2**	**C3**	**C=S**	**C5**	**C6**	**Aromatic-Cs**	**^{31}P**
DMDTC	-	-	-	208.3	45.6	-	-	-
DEDTC	-	-	-	206.4	49.5	12.1	-	-
DBDTC	-	-	-	213.1	56.9	-	137.2-127.5	-
L1	57.4	47.5	31.9	-	-	-	140.0-124.1	-8.75
23	56.5	46.7	30.8	-	-	-	139.9-126.3	36.18
24	56.9	32.6	29.7	184.0	34.7	-	140.9-125.0	36.67
25	54.5	33.4	29.6	203.6	48.3	12.2	135.3-126.4	35.55
26	53.6	34.5	29.7	199.5	54.3	-	134.5-125.4	28.66

Table 3.17. ^{13}C and ^{31}P NMR chemical shifts (ppm) for free ligands and gold(I) complexes (**27-30**) in $CDCl_3$.

Free ligand/ complex	**C1**	**C2**	**C3**	**C4**	**C5**	**C=S**	**C9**	**C10**	**Aromatic Cs**	**^{31}P**
DMDTC	-	-	-	-	-	208.3	45.7	-	-	-
DEDTC	-	-	-	-	-	206.4	49.5	12.1	-	-
DBDTC	-	-	-	-	-	213.1	56.9	-	137.2-127.5	-
L2	52.3	43.3	24.5	26.7	25.9	-	-	-	134.3-129.0	-9.80
27	56.1	43.5	24.7	28.1	25.7	-	-	-	134.3-128.9	41.81
28	54.5	43.5	24.0	30.0	25.2	207.5	50.5	-	134.0-128.9	41.68
29	54.9	44.1	24.2	29.6	25.1	204.2	52.3	12.3	134.7-128.4	40.15
30	55.9	43.7	24.5	27.9	25.7	210.2	58.4	-	135.9-127.8	39.18

Table 3.18. ^{13}C and ^{31}P NMR chemical shifts (ppm) for free ligands and gold(I) complexes (**31-34**) in $CDCl_3$.

Free ligand/ Complex	**C1**	**C2**	**C3**	**C4**	**C=S**	**C6**	**C7**	**Aromatic Cs**	**^{31}P**
DMDTC	-	-	-	-	208.3	45.7		-	-
DEDTC	-	-	-	-	206.4	49.5	12.1	-	-
DBDTC	-	-	-	-	213.1	56.9	-	137.2-127.5	-
31	61.4	35.5	24.6	18.9	-	-	-	-	25.5
32	60.3	32.4	24.1	19.3	207.5	55.5	-	-	47.72
33	59.5	33.7	23.7	20.1	203.7	48.5	12.3	-	43.25
34	58.6	35.3	23.7	20.1	207.5	54.5	-	142.7-128.5	46.61

3.6.2.2 Gold(I) phosphine complexes (35-37)

The synthesized of complexes **(35-37)** are shown in (Scheme 20) and were characterized by ^{1}H, ^{13}C and ^{31}P NMR and mid FT-IR spectroscopy, elemental analyses.

The ν(C—H) sp^2 bending of precursor **35** was observed at 1370 cm^{-1} which is shifted to lower region in complexes **36** and **37** at 1360 and 1365 cm^{-1}, respectively. The ν(C=C) stretching appears at 1623 cm^{-1} in precursor **35**, whereas for **36- 37** it is observed at 1589 and 1585 cm^{-1}, respectively, as shown in Table 3.19.

^{1}H NMR spectra shows a significant shift for precursor **35** with respect to complexes **36-37** Table 3.20. ^{31}P NMR resonance of complexes **36-37** observed at 4.96 and (12.57, 29.61) ppm were shifted upfield with respect to precursor **35 (**36.18 ppm**)** due to back donation from gold center atom to empty π* of P—C bond as illustrated in Table 3.21.

Table 3.19. Mid FT-IR frequencies (cm^{-1}) for complexes (**35-37**).

Complex		**Bend (CH_2)**	**Stretch Ar(C=C)**
35	2932, 2855	1370	1623
36	2935, 2853	1360	1589
37	2937, 2865	1365	1585

Table 3.20. ^{1}H NMR chemical shifts (ppm) of gold(I) complexes (**35-37**) in $CDCl_3$.

Complex	**1H**	**Aromatic-Hs**
35	3.58 s	7.35 m - 6.73 m
36	3.45 s	7.56 m- 6.95 m
37	3.56 s	7.76 m- 7.00 m

Table 3.21. ^{13}C and ^{31}P NMR chemical shifts (ppm) gold(I) complexes (**35-37**) in $CDCl_3$.

Complex	**C1**	**Aromatic-Cs**	**^{31}P**
35	55.6	160.5 - 121.9	36.18
36	55.8	161.0 - 111.6	4.92
37	55.8	161.0 - 111.6	12.57, 29.61

3.6.3 Single crystal X-ray structure of complex 27

The molecular structure of complex *[Au($C_{18}H_{22}NP$)Cl]* (**27**) is depicted in Figures 3.4- and 3.5. Selected bond lengths and bond angles for complex **27** are shown in Table 3.22 and structure refinement & the crystal data are given in Table 3.23. The coordination geometry around the gold central atom is close to linearity, with (P1—Au—Cl1) 176.8 (1)º. The Au1—P1 and Au1—Cl1 bond lengths are 2.24 (2) and 2.28 (3) Å, respectively. The bond lengths and bond angles are similar to that reported for similar compounds [140-141]. .

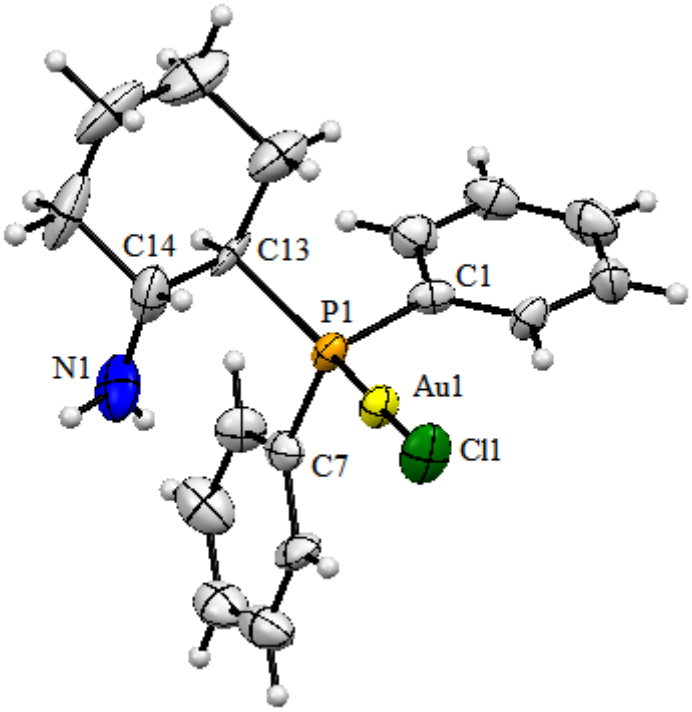

Figure 3.4. *Molecular structure of complex* ***27****, with partial labelling atoms and 50% probability ellipsoids.*

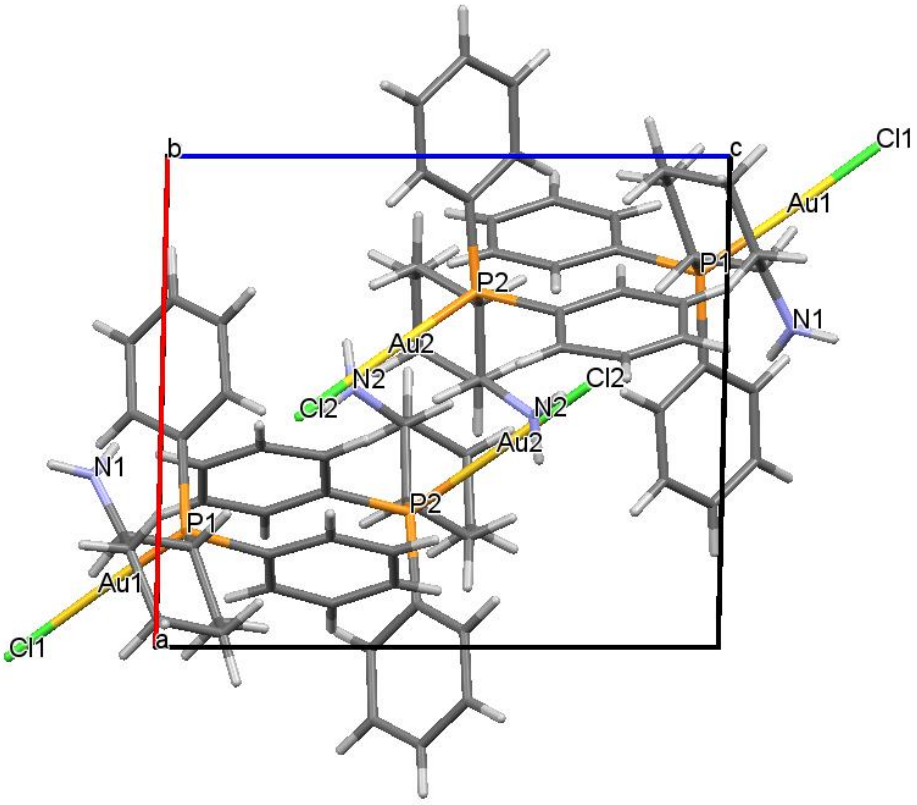

Figure 3.5. *Crystal packing of complex 27 viewed along b-axis*

Table 2.22. Selected bond lengths and bond angles for complex **27**.

Bond Length (Å)		**Bond Angles (°)**	
$Au_1—Cl_1$	2.28 (3)	P1—Au1—Cl1	176.81 (1)
$Au_1—P_1$	2.24 (2)	Au1—P1—C1	113.12 (3)
$P_1—C_1$	1.82 (1)	Au1—P1—C7	114.83 (3)
$P_1—C_7$	1.84 (9)	Au1—P1—C13	110.64 (3)
$P_1—C_{13}$	1.86 (9)	C1—P1—C7	102.15 (4)
$C_{14}—N_1$	1.36 (1)	C1—P1—C13	106.76 (4)
		C7—P1—C13	108.95 (4)
		C13—C14—N1	114.15 (9)

Table 3.23. Summary of crystal data and details of the structure refinement for complex **27**.

Complex	**Experimental details**
Crystal data	
Empirical formula	$C_{18}H_{22}AuClNP$
Formula weight	515.76 g/mol
Wavelength/Å	0.71073
Temperature/K	173
Crystal symmetry	Monoclinic
Space group	P 2_1
Cell lengths (Å)	**a**=9.5364(5) **b**=17.3845(11) **c**=10.9433(5)
Cell Angles (°)	**α**=90, **β**=91.417(4), **γ** =90
*D*x	1.889 Mg/ m^{-3}
μ	8.34 mm^{-1}
Radiation type	MoK\α
Cell volume ($Å^3$)	1813.69 (17)
Z	4
Data collection	
Radiation source	Fine-focus sealed tube
Radiation monochromator	Plane graphite
$(\sin\theta/\lambda)_{max}$ ($Å^{-1}$)	0.609
Refinement	
$R[F^2 > 2\sigma(F^2)]$, $wR(F^2)$, S	0.025, 0.054, 0.88
$\Delta\rho_{max}$	1.18 e $Å^{-3}$
$\Delta\rho_{min}$	−1.01 e $Å^{-3}$
H-atom treatment:	H atoms treated by a mixture of independent and constrained refinement

3.6.4 *In vitro* cytotoxic activities of gold(I) monophosphine complexes (18-22, 35 and 37)

In the present study, the precursors (**18**, **35**), gold(I) polymers **(19-21)** and complexes (**22**, **37)** were tested for *in vitro* cytotoxicity against A549, MCF7 and HCT15 human cancer cell lines using an MTT assay and compared to that of *cisplatin*.

The dose-dependent inhibition of cell proliferation was obtained by specific increase of complex concentrations against a fixed number of three human cancer cell lines Figures (3.6-3.8). IC_{50} values were obtained from the plot of the complex concentration against

the percentage of cell viability (Table 3.24). For the A549 cell line, the IC_{50} values for polymers **(20, 21)** and complex **(22)** were 20 ± 1, 29 ± 2, 34 ± 1 μM, respectively, compared to *cisplatin* at 42 ± 2 μM. These data clearly show that polymers **(20, 21)** and complex **(22)** have inhibition of cell proliferation and potency levels one to two times better than that exhibited by *cisplatin*, suggesting the presence of the labile dithiocarbamate in (**20**, **21**) and two phosphine ligands around gold ion in complex **22** enhanced the activity of these complexes [135]. Polymer **(20)** was the most active among the series, exhibiting IC_{50} =20 ± 1 μM due to the labile diethyldithiocarbamate ligand bonded to the gold(I) center. Gold(I) polymer **(20)** and complexes **(22, 37)** showed moderate IC_{50} values with respect to cisplatin and the other gold(I) dithiocarbamate complexes reported for their activity against HCT15 cell line [126]. For the MCF7 cell line, all complexes exhibited higher IC_{50} values than the standard *cisplatin* IC_{50} values.

Table 3.24. IC_{50} values (μM) of gold(I) complexes (**18-22, 35** and **37**) against HCT15, A549 and HeLa cancer cell lines.

Complex	HCT15	A549	MCF7
Cisplatin	32 ± 2	42 ± 2	23 ± 4
18	51 ± 1	54 ± 1	38 ± 1
19	257 ± 4	304 ± 6	139 ± 5
20	39 ± 2	20 ± 1	49 ± 2
21	69 ± 3	29 ± 2	76 ± 3
22	34 ± 2	34 ± 1	52 ± 2
35	92 ± 2	97 ± 1	95 ± 3
37	37 ± 1	49 ± 1	48 ± 2

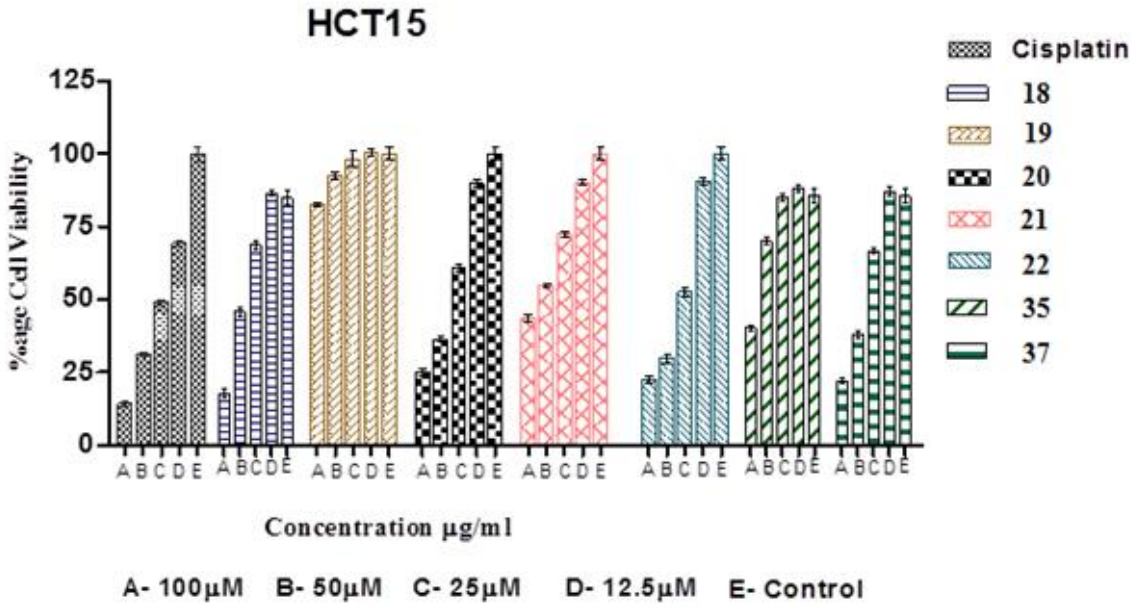

Figure 3.6. *Cytotoxic effects of various concentrations of complexes (**18-22, 35** and **37**) on the cellular viability of the HCT15 cell line.*

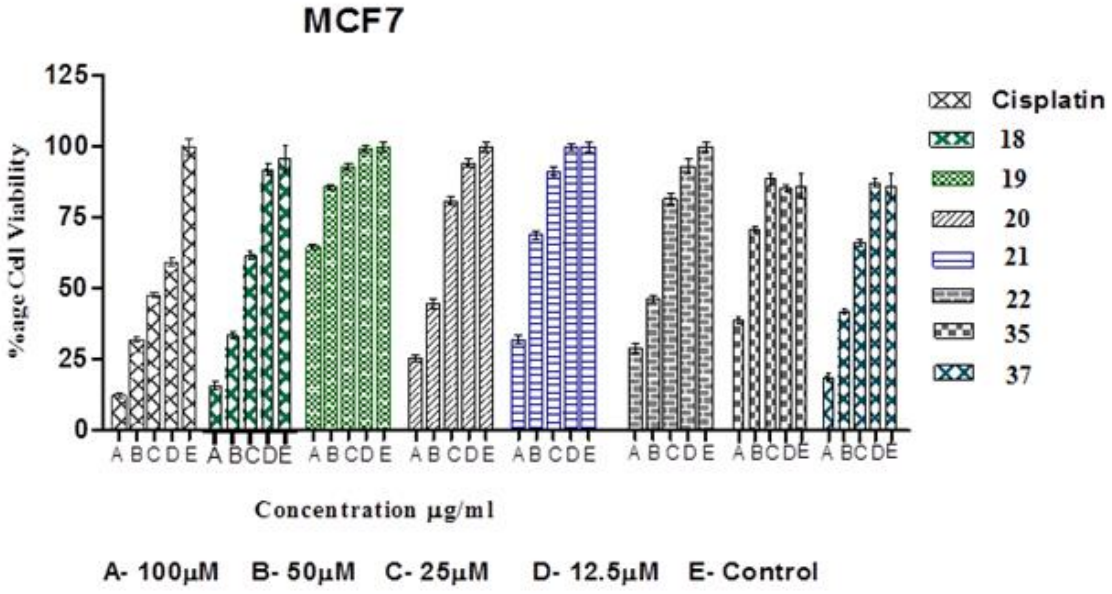

Figure 3.7*. Cytotoxic effects of various concentrations of complexes (**18-22, 35**and **37**) on the cellular viability of the MCF7 cell line.*

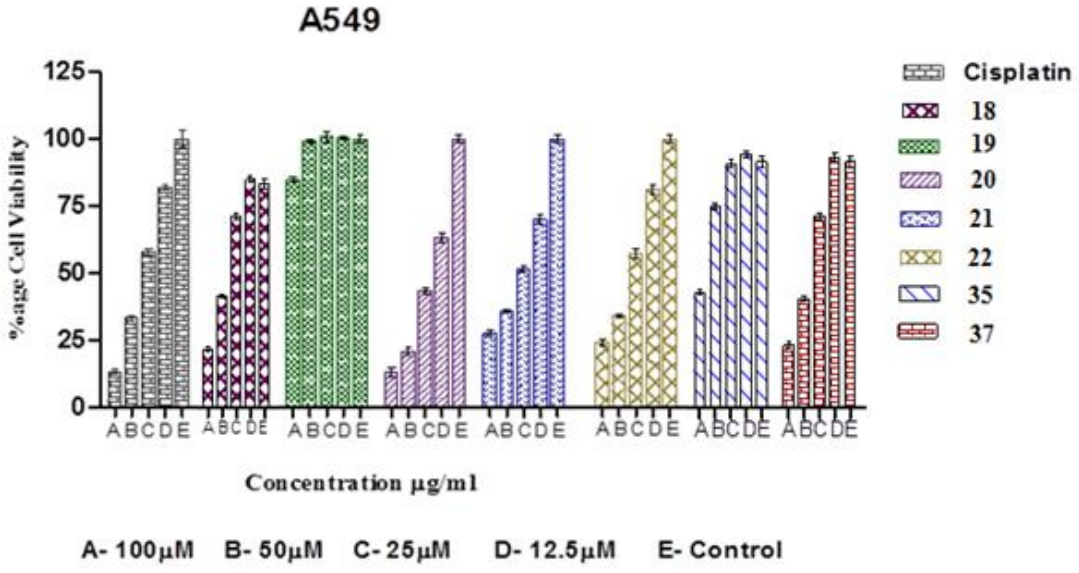

Figure 3.8*. Cytotoxic effects of various concentrations of complexes (**18-22, 35** and **37**) on the cellular viability of the A549 cell line.*

CHAPTER 4

SYNTHESIS, CHARACTERIZATION AND *IN VITRO* CYTOTOXIC EVALUATION OF GOLD(I) CARBENE COMPLEXES WITH SELONE LIGANDS

4.1 Introduction

Gold complexes bearing N-Heterocyclic carbene (HNC) ligands have gained much attention due to their important applications in medicine, catalysis, anticancer and antimicrobial activity [142-145]. Since these ligands were first synthesized by Arduengo, a number of NHCs metal complexes are extensively used for catalysis, biochemistry and anticancer treatments [146-149]. NHC ligands form stable complexes with metal ions via σ-donation stronger than π-back donation [150].

Selenocysteine is the active side of selenoenzymes such as glutathione peroxidase (GPx), which is used to protect different organisms from damage due to catalytic cycle to reduce harmful peroxidase [151-153]. Spectroscopic properties of selenocyanide ligand with some transitional metals have been investigated [154]. The interaction of Au(III) compound with two equivalents of this ligand resulted in reduction of Au(III) to Au(I). In addition, Brendenkamp et al. studied the reactivity of N-selenocarbamyl benzamidin with

Ni(II), Pd(II) and Au(III) compounds [155]. A number of seleno-metal compounds were reported as potentially a promising new class of drugs for instance, gold antimalarial drug [156], Cd/Hg antibacterial [157,117], ruthenium antitumor agent [158] and Pt(II) /Pd(II) anticancer agents [159].

4.2. Experimental Section

4.2.1 Materials and Instrumentation

All chemicals and solvents are analytical grade, they were used without further purification. $AgPF_6$, selenourea, N,N-dimethylthiourea, 1,3-bis(2,6-di-isopropylphenyl)-imidazol-2-ylidenegold(I)chloride [Au(Ipr)Cl], and all organic solvents were purchased from Sigma -Aldrich St. Louis, Missouri United States and Stream Chemicals, Massachusetts, United States. ImSe, Diaz-Se, Diap-Se and their derivatives were synthesized according to methods in the literature [160-161].

^{1}H, ^{13}C NMR and FTIR spectroscopy along with elemental analysis instruments were mentioned previously in section 3.1.

^{77}Se NMR spectra were recorded on a LAMBDA 500 spectrophotometer operating at 200.0 MHz. ^{13}C (MAS) NMR results were recorded on a Bruker 400 MHz spectrometer at ambient room temperature of 25 ^{o}C. Samples were packed into 4 mm zirconium oxide rotors. Pulse delay of 7.0 s and a contact time of 5.0 ms. The magic angle spinning rates were 4 and 8 kHz. Carbon chemical shifts were measured relative to adamantane at 38.56 ppm.

4.2.2 Synthesis of gold(I) carbene complexes with selones (39-50)

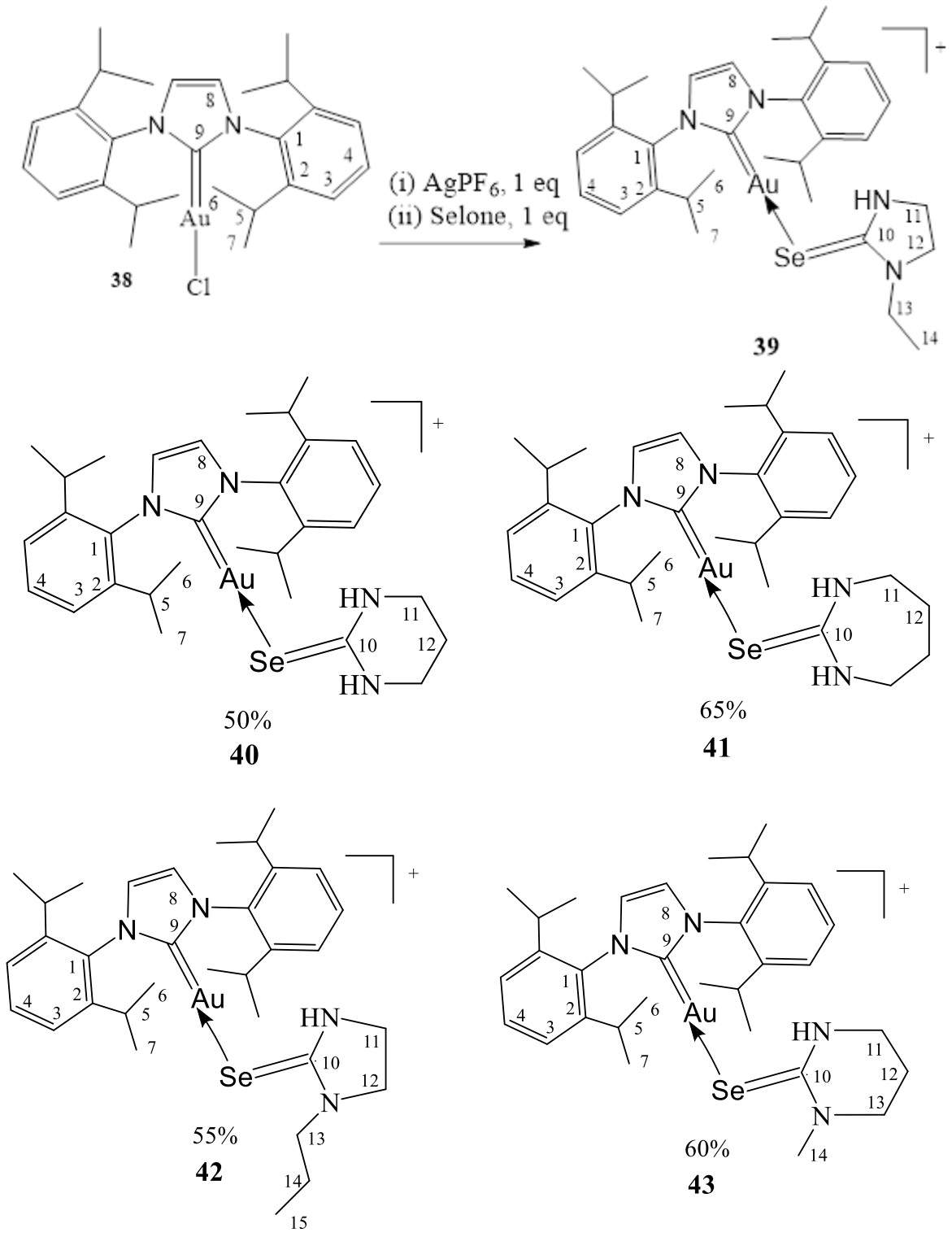

Scheme 21A. Synthesis of gold(I)-selone complexes (**39-43**).

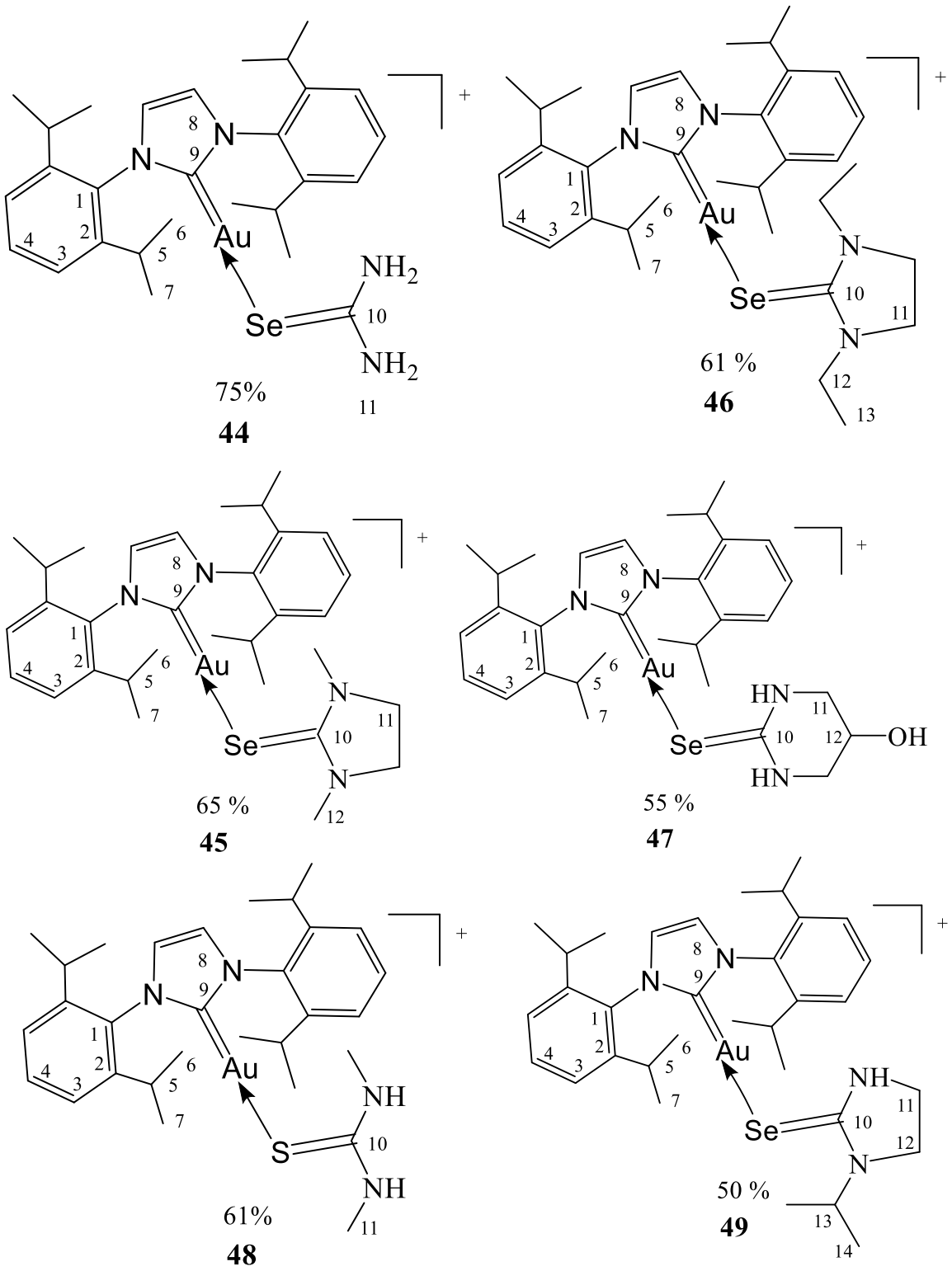

Scheme 21A. Synthesis of gold(I)-selone complexes (**44-49**).

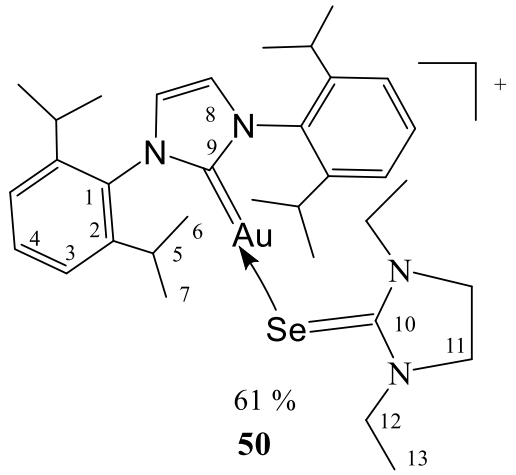

61 %

50

Scheme 21C. Synthesis of gold(I)-selone complex **50.**

$[Au(Ipr)(SeCN_2C_4H_{10})]PF_6$ (**39)**

This complex was synthesized using a modified previously reported method [138]. $AgPF_6$ (127 mg, 0.5 mmol) was dissolved in 5 mL of ethanol and added to 1,3-Bis(2,6-di-isopropylphenyl)imidazol-2- ylidenegold(I)chloride [Au(Ipr)(Cl)] (311 mg, 0.5 mmol) in 5 mL of CH_2Cl_2. Then stirred for 5 min at room temperature and filtered off. N-ethyl,-1,3-imidazolidine-2-selone (*N-EtImSe)* (88.6 mg, 0.5 mmol) was added to the filtrate, stirred for 1 hour and filtered. The formed complex was kept in undisturbed area, after three days bright gray crystals were obtained and a suitable crystal was selected for single crystal diffraction analysis. Yield 0.264 g (60%). Anal calc. for $C_{32}H_{46}AuN_4SePF_6$ (907.62 g/mol): C, 42.39; H, 5.11; N, 6.18. Found: C, 42.43; H, 5.83; N, 6.46.

[Au(Ipr)($SeCN_2C_3H_8$)]PF_6 (**40)**

This complex was synthesized with 1,3-diazinane-2-selone (DiazSe) by a procedure similar to (**39).** After four days a yellowish-white solid was obtained. The yield was 0.180 g (50%). Anal. calc. for $C_{31}H_{44}AuN_4SePF_6$ (893.60 g/mol): C, 41.71; H, 4.97; N, 6.28. Found: C, 41.92; H, 5.14; N, 6.82.

[Au(Ipr)($SeCN_2C_4H_{10}$)]PF_6 (**41)**

This complex was synthesized using 1,3-diazepine-2-selone (DiapSe) by a procedure similar to (**39**). After five days white solid was obtained. The yield was 0.275 g (65%). Anal. calc. for $C_{32}H_{46}AuN_4Se.PF_6$ (907.62 g/mol): C, 42.39; H, 5.11; N, 6.18. Found: C, 41.93; H, 5.26; N, 6.08.

[Au(Ipr)($SeCN_2C_5H_{12}$)]PF_6 (**42)**

This complex was synthesized with N-propyl-1,3-imidazolidine-2-selone (N-Pr-Imse) by a procedure similar to (**39**). After three days a gray solid was obtained. The yield was 0.240 g (55%). Anal. calc. for $C_{33}H_{48}AuN_4SePF_6$ (921.65g/mol): C, 43.05; H, 5.25; N, 6.09. Found: C, 42.57; H, 5.51; N, 5.81.

[Au(Ipr)($SeCN_2C_4H_{10}$)]PF_6 (**43)**

This complex was synthesized using N-methyl-1,3-diazinane-2-selone (N-MeDiazSe) by a procedure similar to (**39**). After four days a pale red solid was obtained. The yield was 0.274 g (60%). Anal calc. for $C_{32}H_{46}AuN_4SePF_6$ (907.63g/mol): C, 42.39; H, 5.11, N 6.18; found: C 41.98, H 5.38, N 6.16.

[Au(Ipr)($SeCN_2H_4$)]PF_6 (**44**)

This complex was synthesized with selenourea by a procedure similar to (**39**). After four days colorless crystals were obtained and a suitable crystal was selected for single crystal diffraction analysis. The yield was 0.313 g (75%). Anal. calc. for $C_{28}H_{40}AuN_4SePF_6$ (853.53 g/mol): C, 39.40; H, 4.72; N, 5.56. Found: C, 41.04; H, 5.23; N 6.04.

[Au(Ipr)($SeCN_2C_2H_6$)]PF_6 (**45**)

This complex was synthesized using 1,3-imidazolidine-2-selone by a procedure similar to (**39**). After four days a white solid was obtained. The yield was 0.248 g (56%). Anal. calc. for $C_{30}H_{42}AuN_4SePF_6$ (879.57 g/mol): C, 40.97; H, 4.81; N, 6.37. Found: C, 41.38; H, 4.64; N, 6.28.

[Au(Ipr)($SeCN_2C_4H_{10}$)]PF_6 (**46**)

This complex was synthesized using N,N′-dimethyl-1,3-imidazolidine-2-selone (N,N'-ImSe) by a procedure similar to (**39**). After four days, brick-red crystals were obtained and a suitable crystal was selected for single crystal diffraction analysis. The yield was 0.265 g (60%). Anal. calc. for $C_{32}H_{46}AuN_4SePF_6$ (907.63 g/mol): C, 42.35; H, 5.11; N, 6.17. Found: C, 42.68; H, 5.21; N 5.91.

[Au(Ipr)($SeCN_2C_3H_7(OH)$)]PF_6 (**47**)

This complex was synthesized using 5-hydroxy-1,3-diazinane-2-selone by a procedure similar to (**39**). After five days a gray solid was obtained. The yield was 0.250 g (55%).

Anal. calc. for $C_{31}H_{44}AuN_4SePF_6$ (909.60 g/mol): C, 41.67; H, 4.96; N, 6.30. Found: C, 41.60; H, 4.92; N. 5.99.

[Au(Ipr)($SCN_2C_2H_8$]PF_6 (**48)**

This complex was synthesized using N,N′-dimethyl-thiourea by a procedure similar to (**39**). After five days colorless crystals were obtained and the suitable crystal was selected for single crystal diffraction analysis. The yield was 0.245g (61%). Anal. calc. for $C_{30}H_{44}AuN_4S$. PF_6= 881.59 g/mol: C, 41.69; H 5.10; N, 6.94; S, 3.97. Found: C, 41.26; H, 5.57; N, 7.20; S, 3.66.

[Au(Ipr)($SeCN_2C_5H_{12}$]PF_6 (**49).**

This complex was synthesized with N-isopropyl-1,3-imidiazolidine-2-selone (N-isopr-ImSe) by a procedure similar to (**39**). After four days gray crystals were obtained and a suitable crystal was selected single crystal diffraction analysis. The yield was 0.220g (50%). Anal. calc. for $C_{33}H_{48}AuN_4SePF_6$ (921.65 g/mol): C, 43.00; H, 5.25; N, 6.08. Found: C, 42.93; H, 5.56; N, 6.20.

[Au(Ipr)($SeCN_2C_6H_{14}$]PF_6 (**50*)***

This complex was synthesized using N,N′-diethyl-1,3-imidiazolidine-2-selenone by a procedure similar to (**39**). After four days yellow solid was obtained. The yield was 0.284 g (61%). Anal. calc. for $C_{34}H_{50}AuN_4SePF_6$ (935.68 g/mol): C, 43.64; H, 5.39; N, 5.99. Found: C, 43.19; H, 5.71; N, 5.49.

4.3 Results and Discussion

4.3.1 Spectroscopic characterizations

The synthesized of complexes **(39-50)** are shown in (Scheme 21) and were characterized by ^{1}H, ^{13}C and ^{31}P NMR and mid FT-IR spectroscopy, elemental analyses and single crystal X-ray diffraction analysis.

FT-IR spectra for free ligands and gold(I) complexes (**39-50**) clearly show a significant shift between the ligands and their complexes (**39-50**) inconsistence with complexation as shown in Table 4.1. For instance, ν(C=Se) for free ligands is in the range of (588-636) cm^{-1}, while for the complexes (**39-50**) it is in the range (554-557) cm^{-1}. This is consistent with back donation to π* C=Se [103-105].

The stretching bands of ν(N─H) and ν(O─H) were shifted to higher frequency in complexes relative to the free ligands due to increase C-N π bond character [64].

^{1}H NMR data for the ligands and their complexes (**38-50**) are shown in Table 4.2.

^{13}C NMR chemical shift of Au=C in the precursor (**38**) was observed at 175.3 ppm and it is shifted downfield in complexes (**39-50**) in the range of (181.1-185.3) ppm. This deshielding is related to back donation from d-orbital of Au atom to π* C=Se [92]. The chemical shift of C=Se in all free ligands was observed in the range of (167.4-182.1 ppm), with an up-field shift in their complexes (**39-50**) in the range of (159.8-178.3 ppm) due to more electron shielding C=Se by back donation from d-orbital of gold atom [92,100,162]. ^{13}C NMR results of free ligands and their complexes (**38-50**) are shown in Table 4.3.

Table 4.1. Mid FT-IR frequencies (cm^{-1}) of free ligand and Au(I) complexes (**38**-**50**).

Ligand/ Complex	**Stretch NH**							**Stretch C=Se**
38	**-**	3073	1109	2960	1366	1258	1462	-
EtImSe	3198	-	-	2961	-	-	-	588 b
39	3396	3166	1114	2956	1325	1272	1441	556
DiazSe	3198	-	-	-	-	-	-	602b
40	3351	3165	1057	2957, 2867	1464	1205	1554	554
DiapSe	3224	-	-	-	-	-	-	613
41	3351	3167	1061	2962, 2867	1469	1218	1553	556
42	3400	-	-	2960, 2871	1327	1294	1467	557
43	3375	3164	1116	2958, 2872	1313	1210	1461	555
44	3468,3363	3160	1055	2960, 2873	1463	1406	1643	606
ImSe	3250	-	-	-	-	-	-	558b
45	3382	3161	1053	2960, 2872	1463	1323	1531	559
Me_2ImSe	-	-	-	-	-	-	-	636
46	3143	-	1108	2965, 2870	1413	1288	1563	556
HOdiazSe	3345	-	-	-	-	-	-	578
47	3561(OH)3370	3159	1112	2957, 2874	1464	1208	1581	555
48	3377	3162	1133	2931, 2873	1371	1371	1462	985
iPrImSe	3395	-	-	-	-	-	-	597
49	3404	3157	1060	2959, 2874	1468	1287	1529	556
Et_2IMSe	-	-	-	-	-	-	-	602, 626
50	3145	-	1118	2963, 2873	1387	1274	1468	556

Table 4.2. ^{1}H NMR chemical shifts (ppm) for free ligands and gold(I) complexes (**38-50**) in $CDCl_3$.

Ligand/ complex	3H	4H	5H	6H	7H	8H	9H	10H	11H	12H	13H	NH
38	7.39 d	7.55 t	2.46 m	1.33 d	1.21 d	7.98 s					-	-
EtImSe							3.62 m	3.69 m	3.72 m	1.21 m	-	6.95
39	7.36 d	7.61 t	2.54 m	1.31 d	1.26 d	7.33 s	3.46 m	3.54 m	3.76 m	1.15 m	-	5.35
DiazSe	-	-	-		-	-	3.31 t	1.98 p				1.71
40	7.37 d	7.58 t	2.56 m	1.33 d	1.23 d	7.50 s	3.14 t	1.85 t	-	-	-	2.93
DiapSe							3.28 t	1.81 t	-	-	-	7.19
41	7.36 d	7.57 t	2.54 m	1.31 d	1.24 d	7.30 s	3.22 d	1.77 d	-	-	-	1.61
Pr ImSe	-	-	-	-	-	-	3.67 t	3.63 t	3.60 p	1.65 p	0.96 t	6.70
42	7.38 d	7.62 t	2.55 m	1.31 d	1.26 d	7.37 s	3.76 t	3.48 t	3.28 t	1.56 d	0.86 t	4.62
MeDiazSe							3.48 s	3.37 t	3.24 m	2.06 p	-	2.15
43	7.37 d	7.59 t	2.54 m	1.31 d	1.26 d	7.35 s	3.15 s	3.36 t	2.99 m	1.96 p	-	1.77
USe										-		2.01
44	7.36 d	7.57 t	2.56 m	1.32 d	1.26 d	6.91 s	-	-	-	-	-	3.48
ImSe											-	8.35
45	7.39 d	7.57 t	2.56 m	1.33 d	1.28 d	7.65 s	3.60			-	-	3.15
Me_2ImSe							3.48 s	2.91 s		-	-	-
46	7.35 d	7.59 t	2.51 m	1.26 d	1.25 d	7.30 s	3.66 s	2.85 s			-	-
HODiazSe							3.17 dd	4.08 m			-	2.50
47	7.37 d	7.59 t	2.58 m	1.32 d	1.27 d	7.73 s	3.11 dd	4.01 m	-	-	-	2.15
Me_2Tu										-		6.62
48	7.36 d	7.57 t	2.52 m	1.30 d	1.26 d	7.27 s	-	-	-	-	-	1.72
iPrImSe							3.53 t	3.57 t	4.85 p	1.18 d	-	6.63
49	7.39 d	7.63 t	2.54 m	1.32 d	1.26 d	7.36 s	3.48 t	3.69 t	4.16 p	1.15 d	-	4.75
Et_2ImSe							3.56 d	3.77 m	1.19dd	-	-	-
50	7.41d	7.61 t	2.51 m	1.31 d	1.25 d	7.31 s	3.49 d	3.75 m	1.23dd	-	-	-

^{13}C (MAS) solid state NMR for all complexes showed significant downfield shits (6-11 ppm) for all carbon bonded to gold atom (Au=C) and up-field shift (~8 ppm) for all carbon bonding to selenium atom (C=Se). This attributed to back donation from gold to Se atom and indicating all complexes formed through binding to the selenium atom of the ligand. These phenomena were also observed in sulfur gold(I) complexes [102]. For all complexes, solid and liquid state chemical shift were consistent indicating the stability of the synthesized complexes in solid and liquid states. ^{13}C (MAS) NMR Chemical shifts of complexes (**38-50**) are given in Table 4.4.

^{77}Se NMR chemical shift in all complexes is more shielded than that of free ligands. This phenomenon is attributed to (Au→Se=C) back bonding and the transferred electron density of N→C resulting a partial double character in C—N bond which confirms the coordination is done through binding to the selenium atom [105]. ^{77}Se NMR studies showed that DiapSe and DiazSe and their derivatives ligate more strongly than ImSe along with their derivatives. The selenol form be as a higher contribution for DaipSe and DaizSe relatively to ImSe due to ring strain hindering the rehybridization of N culminating in DaipSe as shown in Table 4.5. A linear correlation between ^{13}C NMR chemical shifts of ^{13}C=Se and ^{77}Se NMR chemical shift of complexes (**40**,**41, 43-45** and **49**) due to decrease ring constrain is shown in Figure 4.1.

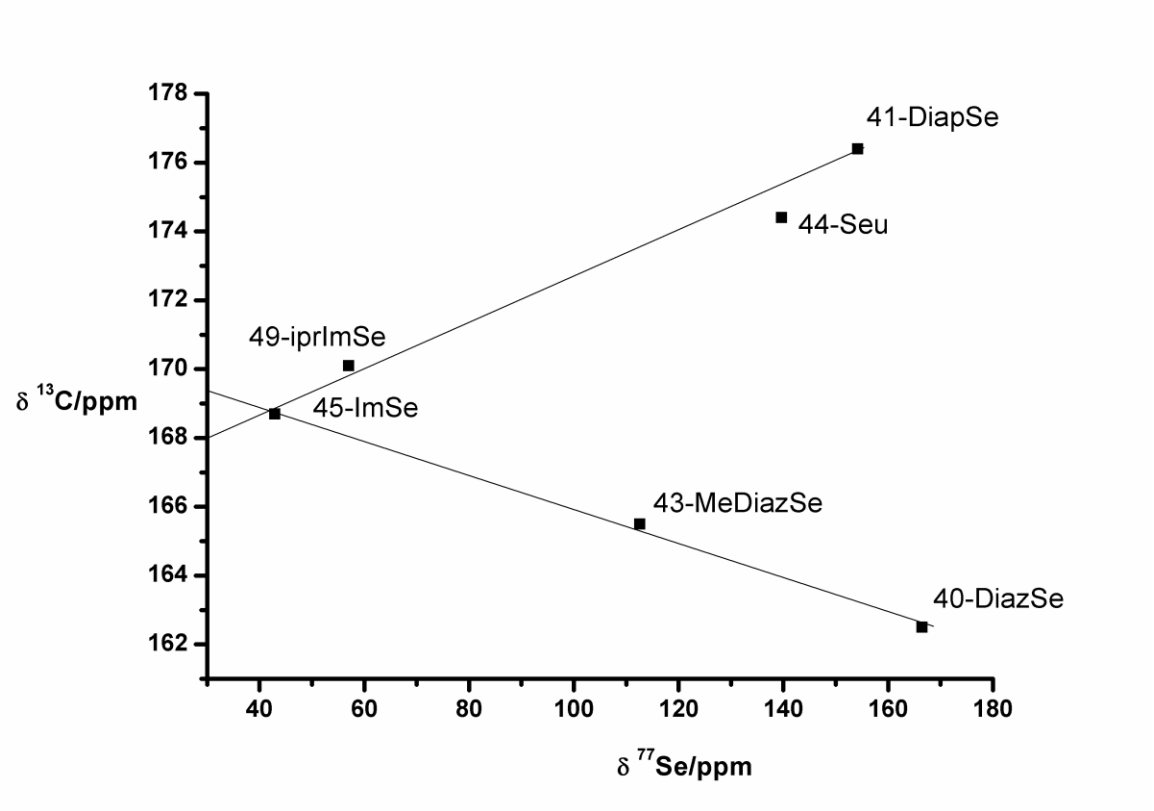

Figure 4.1. *Plot of ^{13}C=Se NMR chemical shift against observed ^{77}Se chemical shifts for complexes (**40**, **41**, **43-45**, and **49**).*

Table 4.3. ^{13}C NMR chemical shifts (ppm) for free ligands and gold(I) complexes (**38-50**) in $CDCl_3$.

Ligand/ complex	C1	C2	C3	C4	C5	C6	C7	C8	Au=C	C=Se	C11	C12	C13	C14	C15
38	145.5	130.7	133.9	123.0	28.8	24.5	24.0	124.2	175.3	-	-	-	-	-	-
EtImSe	-	-	-	-	-	-	-	-	-	178.7	43.3	47.9	42.5	12.1	-
39	145.9	131.3	133.5	123.9	28.8	24.5	23.9	124.4	182.0	171.8	43.9	49.0	43.4	12.0	-
DiazSe	-	-	-	-	-	-	-	-	-	171.0	40.8	18.9	-	-	-
40	145.7	130.8	133.4	123.8	28.6	24.3	23.7	124.1	183.2	162.5	40.8	18.1	-	-	-
DiapSe	-	-	-	-	-	-	-	-	-				-	-	-
41	145.8	131.0	133.4	123.7	28.8	24.6	23.9	124.4	183.2	174.4	46.8	25.8	-	-	-
PrImSe	-	-	-	-	-	-	-	-	-	179.6	42.6	48.6	50.2	20.4	11.0
42	146.0	131.2	133.5	123.9	28.8	24.5	23.9	124.4	182.4	170.5	43.6	49.7	50.7	20.2	10.9
MeDiazSe										173.3	44.9	20.5	47.9	40.4	-
43	145.8	131.3	133.3	123.9	28.8	24.6	23.9	124.4	183.1	165.5	44.6	19.8	49.5	41.2	-
Selenourea	-	-	-	-	-	-	-	-	-	182.2	-	-	-	-	-
44	145.8	131.6	133.9	123.5	28.8	24.5	23.8	124.2	185.3	173.2	-	-	-	-	-
ImSe	-	-	-	-	-	-	-	-	-	175.8	43.7	-	-	-	-
45	145.1	130.0	132.7	123.2	27.8	23.5	23.0	123.4	181.6	168.7	44.8	-	-	-	-
Me_2ImSe	-	-	-	-	-	-	-	-	-	181.2	36.7	49.1	-	-	-
46	141.7	131.2	133.5	123.7	28.8	24.4	23.9	123.7	181.2	170.4	36.5	49.9	-	-	-
HO-DiazSe	-	-	-	-	-	-	-	-	-	167.4	45.1	56.2	-	-	-
47	145.5	130.5	133.3	123.9	28.4	24.1	23.6	124.3	182.7	159.8	46.8	56.6	-	-	-
Me_2Tu	-	-	-	-	-	-	-	-	-	182.3	30.8	-	-	-	-
48	145.9	131.1	133.3	124.0	28.8	24.5	23.9	124.4	181.1	176.4	32.3	-	-	-	-
iPr-ImSe	-	-	-	-	-	-	-	-	-	178.4	42.6	42.9	48.9	19.4	-
49	146.0	131.3	133.4	123.9	28.8	24.5	23.9	124.5	182.5	170.1	43.5	44.1	50.5	19.5	-
Et_2ImSe	-	-	-	-	-	-	-	-	-	179.3	43.9	46.1	12.0	-	-
50	145.6	131.1	133.5	123.9	28.8	24.5	23.8	124.4	182.2	178.3	44.2	47.0	12.0	-	-

Table 4.4. ^{13}C (MAS) Solid State NMR chemical shifts (ppm) for gold(I) complexes (**38-50**).

Ligand/ complex	C1	C2	C3	C4	C5	C6	C7	C8	Au=C	C=Se	C11	C12	C13	C15
38	145.5	130.7	133.9	123.0	28.7	24.4	24.0	124.2	175.3	-	-	-	-	-
39	144.8	131.4	133.1	122.1	28.0	24.1	22.1	125.1	184.6	169.5	-	48.6	43.7	-
40	146.9	133.0	134.8	123.6	28.6	24.4	23.7	124.6	186.6	165.5	42.4	19.4	-	-
41	146.7	133.2	134.6	123.6	27.6	24.9	24.1	126.0	186.4	172.9	49.7	26.0	-	-
42	147.4	131.8	134.4	123.8	30.3	25.5	23.5	124.7	188.5	171.5	45.2	50br	-	12.6
43	144.5	-	132.4br	121.7	28.0	25.8	23.4	124.6	183.1	165.5	44.6	19.8	49.9	-
44	147.0	134.1	133.5	123.6	29.4	26.9	24.3	126.9	186.7	165.1	-	-	-	-
45	145.1	130.0	132.7	123.2	27.8	23.5	23.0	123.4	181.6	168.7	44.9	-	-	-
46	144.9	132.6 br	135.2	-	28.0	25.3	22.7	124.0br	181.2	164.4	38.5	50.8	-	-
47	145.0	131.3	132.9	-	28.1	24.1	22.2	124.0 br	186.0	164.7	46.6	57.0	-	-
48	143.9	-	133.2 br	123.2	27.8	24.7	23.3	125.1	183.7	171.8	31.3	-	-	-
49	146	131.3	133.4	123.9	28.8	24.5	23.9	124.5	182.5	170.1	43.5	44.1	50.5	-
50	146.6	131.7	133.5	124.7	30.1	24.8	23.1	126.8	186.3	166.6	45.2	67.3	13.3	-

Table 4.5. ^{77}Se NMR chemical shifts (ppm) for gold(I) complexes (**39-50**) in $CDCl_3$.

Compound	**^{77} Se δ(ppm)**	Δ
EtImSe	80.89	5.53
39	75.36	
DiazSe	199.93	33.46
40	166.47	
DiapSe	292.00	134.26
41	139.74	
PrImSe	85.50	6.10
42	79.40	
MeDiazSe	193.60	80.96
43	112.64	
Selenourea	200.70	46.53
44	154.17	
ImSe	73.53	30.45
45	42.78	
Me_2ImSe	101.00	12.56
46	88.44	
HO-DiazSe	208.00	45.27
47	168.73	
iPrImSe	69.29	12.34
49	56.92	
Et_2ImSe	114.10	12.67
50	101.43	

Δ= **δ** free ligand ─ **δ** complex

4.3.2 Single crystal X-ray structure determination

X-ray data of **39**, **44**, **46**, **48** and **49** were collected on a Stoe Mark IPD-2 System [163] with a two-circle goniometer and using MoK_{α} graphite monochromator. The distance between the imaging plate and the sample was 100 mm. Structures were solved using the program SHELXS-97 [164]. The non-H atoms were refined using least-squares matrix on F^2. Crystal data and refinement details for complexes 39 and 49 are given in Table 4.8. The structures of these complexes were drawn using the programs PLATON and MERCURY [130].

The molecular structure of complex $[Au(Ipr)(SeCN_2C_4H_{10})]^+$ (**39**) is depicted in Figure 4.2. Selected bond lengths and angles are given in Table 4.6. The coordination geometry around the gold ion is close to linearity, with (C—Au—Se) 176.8(7)º. The Au—C and Au—Se bond lengths are 2.40(4) and 2.00(2) Å, respectively. The bond lengths and bond angle are similar to those reported for other compounds [165].

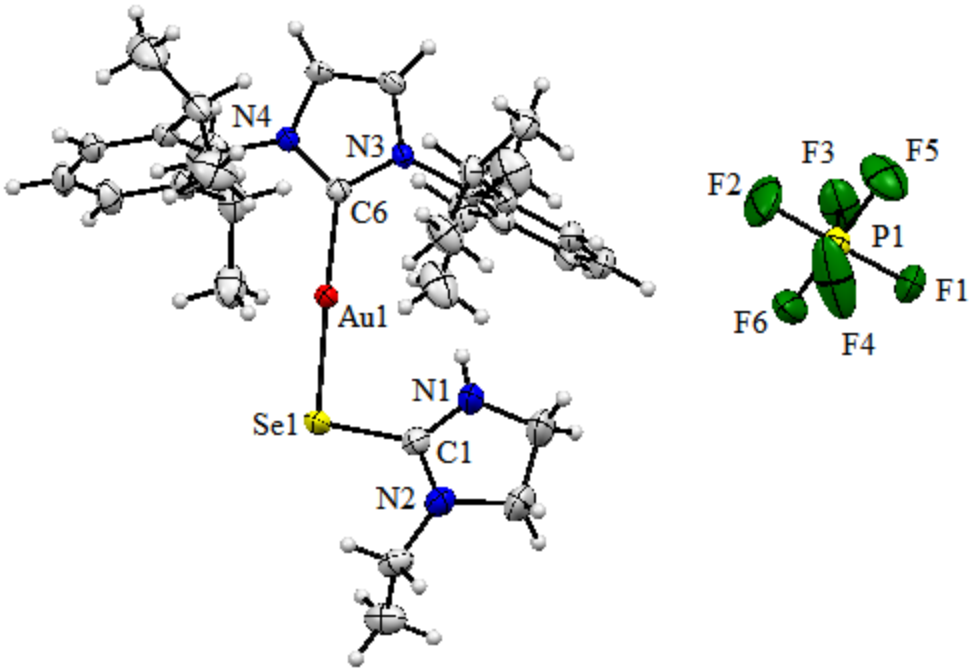

Figure 4.2. *Molecular structure of complex 39, with partial labelling atoms and 50% probability ellipsoids.*

Table 4.6. Selected bond lengths and bond angles for complex **39**.

Bond Length (Å)		**Bond Angles (°)**	
Au_1—Se_1	2.40 (4)	Se1—Au1—C6	176.8 (7)
Au_1—C_6	2.00 (2)	Au1—Se1—C1	98.62 (8)
Se_1—C_1	1.86 (3)	C1—N1—C2	112.1 (3)
N_1—C_1	1.32 (4)	C1—N1—C3	110.9 (2)
N_2—C_2	1.45 (5)	Se1—C1— N2	126.4 (2)
N_3—C_6	1.33 (3)	Se1—C1—N2	122.7 (2)
N_4—C_6	1.35 (3)	Au1—C6—N3	129.9 (2)
		Au1—C6—N4	124.6 (2)
		N3—C6—N4	105.5 (2)

The molecular structures of complexes **44**, **46** and **48** are shown in Figures 4.3, 4.4 and 4.5 respectively.

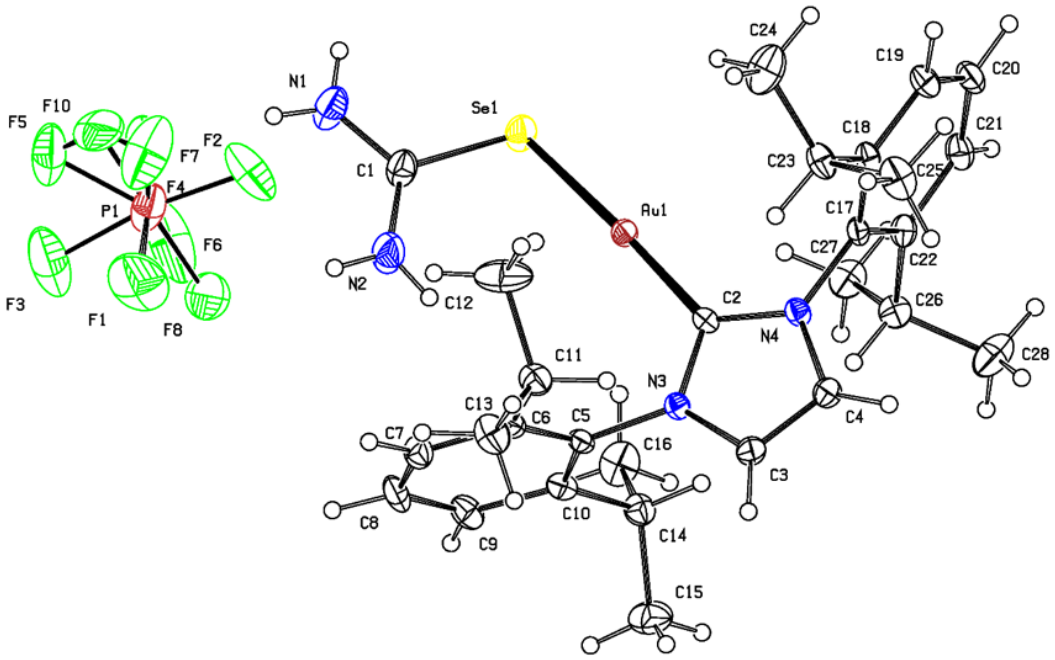

Figure 4.3. *Molecular structure of complex [Au(Ipr)(SeCN$_2$H$_4$)]PF$_6$ (44), with partial labelling atoms and 50% probability ellipsoids.*

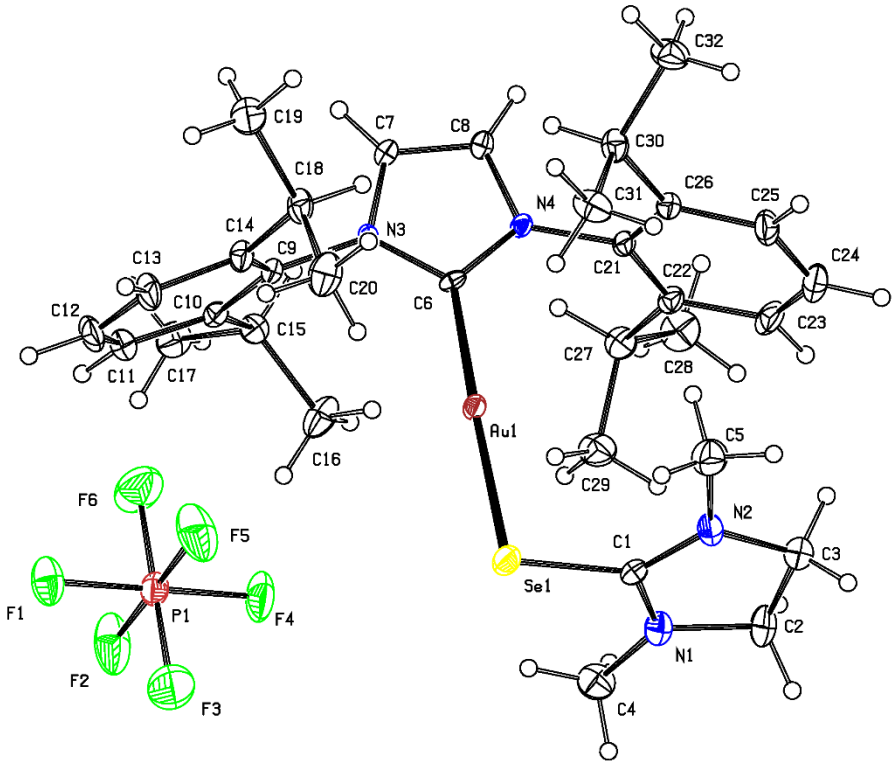

***Figure 4.4**. Molecular structure of complex [Au(Ipr)(SeCN$_2$C$_4$H$_{10}$)]PF$_6$ (46), with partial labelling atoms and 50% probability ellipsoids.*

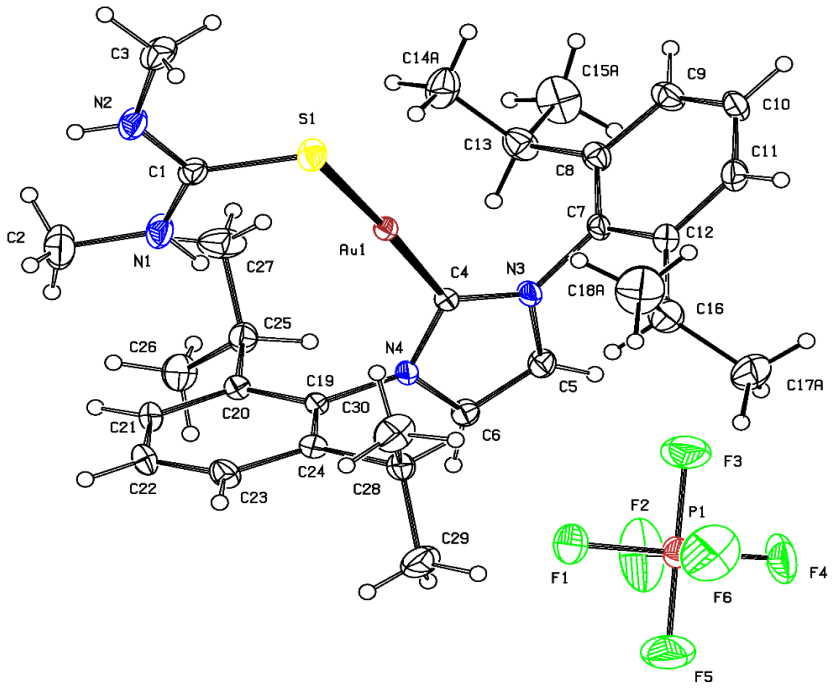

Figure 4.5. *Molecular structure of complex [Au(Ipr)(SCN$_2$C$_2$H$_8$]PF$_6$ (48), with partial labelling atoms and 50% probability ellipsoids.*

The molecular structure of complex *[Au(Ipr)(SeCN$_2$C$_5$H$_{12}$]PF$_6$* (**49**) is shown in Figure 4.6. Selected bond lengths and angles are illustrated in Table 4.7. The geometry of the coordination around gold ion formed by carbon of NHC ligand and Selenium ligand, is close to linearity, with (C—Au—Se) angle of 177.1(5)º. The Au—C and Au—Se bond lengths are 2.11(2) and 2.38(3) Å, respectively. The bond lengths and bond angles are similar to those reported for other compounds [166].

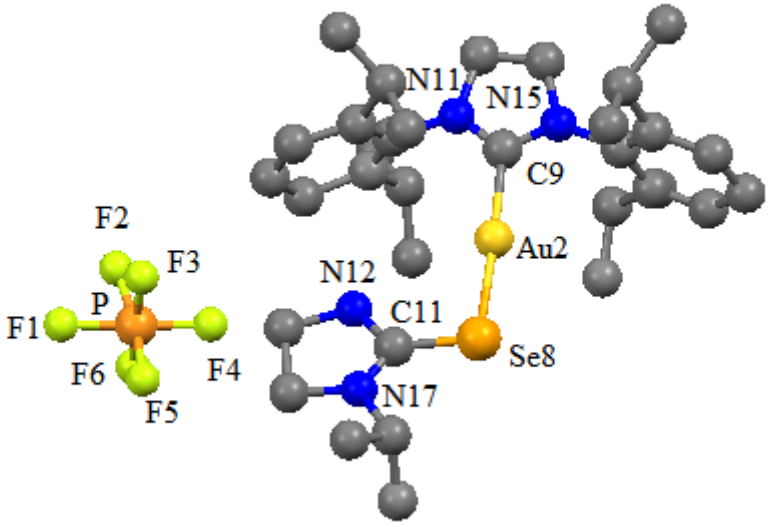

Figure 4.6. *Molecular structure of complex 49, with partial labelling atoms and 50% probability ellipsoids. The hydrogen atoms have been omitted for clarity.*

Table 4.7. Selected bond lengths and bond angles for complex **49**.

Bond Length (Å)		**Bond Angles (°)**	
Au2—Se8	2.38 (3)	Se8—Au2—C9	177.1 (5)
Au2—C9	2.11 (2)	Au2—Se8—C11	102.1 (6)
Se8—C11	1.80 (2)	Au2—C9—N11	123.0 (1)
C9—N11	1.24 (3)	Au2—C9—N15	122.0 (1)
C9—N15	1.31 (2)	N11—C9—N15	115.0 (2)
N12—C11	1.40 (3)	Se8—C11—N12	123.0 (1)
N17—C11	1.33 (3)	Se8—C11—N17	123.0 (2)

Table 4.8. Summary of crystal data and details of the structure refinement for complexes (**39** and **49**).

Complex	**39**	**49**
Empirical formula	C_{32} H_{46} Au F_6N_4PSe	C_{33} H_{48} AuF_6N_4PSe
Formula weight	907.62	921.65
Crystal symmetry	Monoclinic	Triclinic
Space group	P 21/c	P 1
Crystal color	Colorless	Colorless
Crystal size / mm	0.4x 0.31 x 0.13	Not given
Wavelength/Å	0.71073	0.71073
Temperature/K	173(2)	293
a (Å)	13.3698 (6)	9.9945 (6)
b (Å)	17.3635 (5)	13.7841 (8)
c (Å)	16.0631 (6)	14.1416 (8)
α (°)	90	100.394 (5)
β (°)	102.411	98.683 (5)
γ (°)	90	95.727 (5)
Cell volume ($Å^3$)	3641.8 (2)	1890.31 (19)
D_x	1.686 Mg m^{-3}	1.686 Mg m^{-3}
μ	5.14 mm^{-1}	4.96 mm^{-1}
Radiation type	Mo *K*α	Mo *K*α
Z	4	1
Diffractometer	STOE IPDS 2	STOE IPDS 2
Absorption correction	Multi-scan (MULABS in *PLATON; Spek, (2009*)	Multi-scan (MULABS in *PLATON,(2009)*
Radiation source	Plane graphite	Plane graphite
$R[F^2 > 2\sigma(F^2)]$, $wR(F^2)$, S	0.018, 0.043, 1.01	0.36, 0.087, 0.96
$\Delta\rho_{max}$	0.68 e $Å^{-3}$	4.29 e $Å^{-3}$
$\Delta\rho_{min}$	−0.58 0 e $Å^{-3}$	−3.25 e $Å^{-3}$
H-atom treatment:	Treated by a mixture of independent and constrained refinement	Treated by a mixture of independent and constrained refinement

4.3.3 In vitro cytotoxic activities of gold(I) complexes (38-50)

Gold(I) complexes labeled **(38-50)** were tested for *in vitro* cytotoxicity against A549 (human lung carcinoma), MCF7 (human breast adenocarcinoma) and HCT15 human cancer cell lines (human colon cancer) using MTT assay and compared with *cisplatin* (standard anticancer drug). IC_{50} values (μM) of complexes **(38-50)** against HCT15, A549 and MCF7 cancer cell lines are shown in Table 4.9.

The dose-dependent inhibition of cell proliferation was obtained by specific increase *of cisplatin* and complexes **(38-50)** concentrations against a fixed number of three human cancer cell lines Figures 4.7(a, b and c)- 4.9(a, b and c). IC_{50} values were obtained from the curve of the concentration of *cisplatin*, and complexes **(38-50)** against percentage of cell viability. For HCT15 cell line, the IC_{50} values for complexes **(38-50)** are in the range of (54 ± 1─ 51 ± 2 μM), respectively, compared to *cisplatin* 32 ± 2 μM. The data showed the complex **48** (28 ± 2 μM) has inhibition of cell proliferation and potency levels batter than that exhibited by *cisplatin* (32. ± 2 μM), suggesting S containing ligand is more labile than Se containing ligand and enhanced the cytotoxic activity of this complex Au(Ipr)($SCN_2C_2H_8$]PF_6. The complex **45** (33 ± 1 μM) has similar IC_{50} value to *cisplatin.* However, for A549 and MCF7 cell lines, complexes **(38-50)** exhibited moderate to higher IC_{50} values with respect to *cisplatin*.

Table 4.9. IC_{50} values (μM) of gold(I) complexes (**38-50**) against HCT15, A549 and MCF7 cancer cell lines.

Complex	HCT15	A549	MCF7
Cisplatin	32 ± 2	42 ± 2	23 ± 4
38	54 ± 1	62 ± 2	60 ± 2
39	45 ± 1	56 ± 1	42 ± 1
40	70 ± 1	77 ± 1	67 ± 1
41	69 ± 1	81 ± 1	45 ± 1
42	62 ± 1	75 ± 1	53 ± 1
43	43 ± 1	54 ± 1	62 ± 2
44	76 ± 2	82 ± 1	75 ± 3
45	33 ± 1	47 ± 1	43 ± 2
46	42 ± 1	58 ± 1	51 ± 1
47	72 ± 2	76 ± 1	58 ± 1
48	28 ± 2	44 ± 1	39 ± 1
49	44 ± 2	49 ± 1	49 ± 1
50	51 ± 2	71 ± 1	51 ± 1

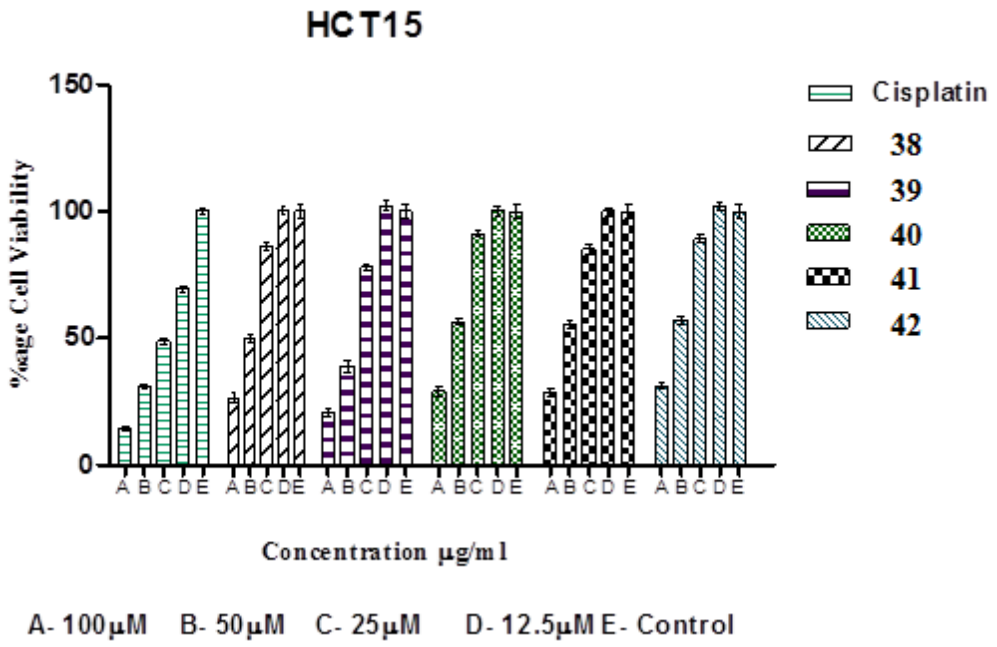

***Figure 4.7a**. Graph of cytotoxic effect of series complexes (**38-42**) concentrations on cell viability of HCT15 cell line.*

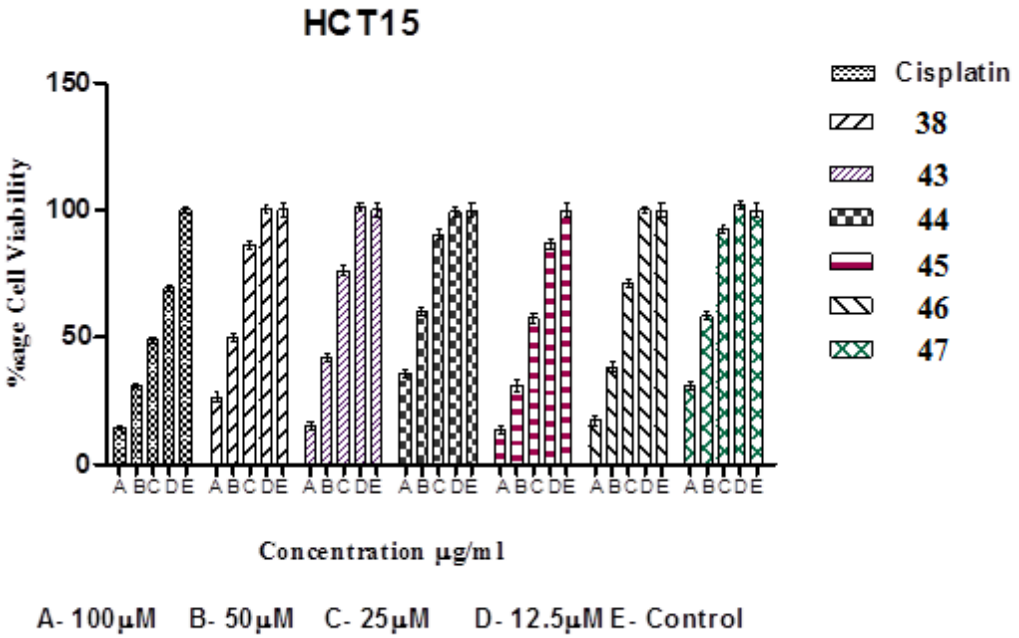

***Figure 4.7b**. Graph of cytotoxic effect of concentrations complexes (**38, 43-47**) on cell viability of HCT15 cell line.*

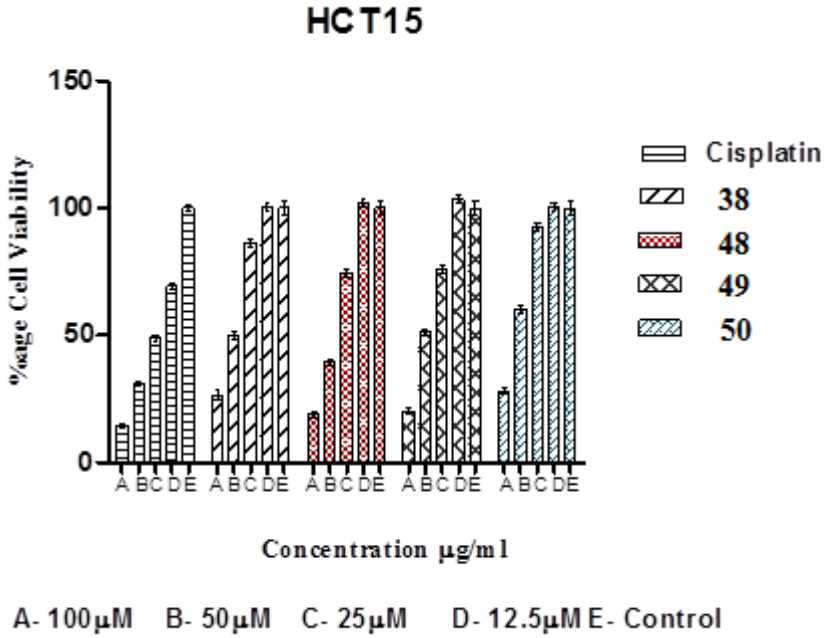

***Figure 4.7c.** Graph of cytotoxic effect of concentrations of complexes (**38, 48-50**) on cell viability of HCT15 cell line.*

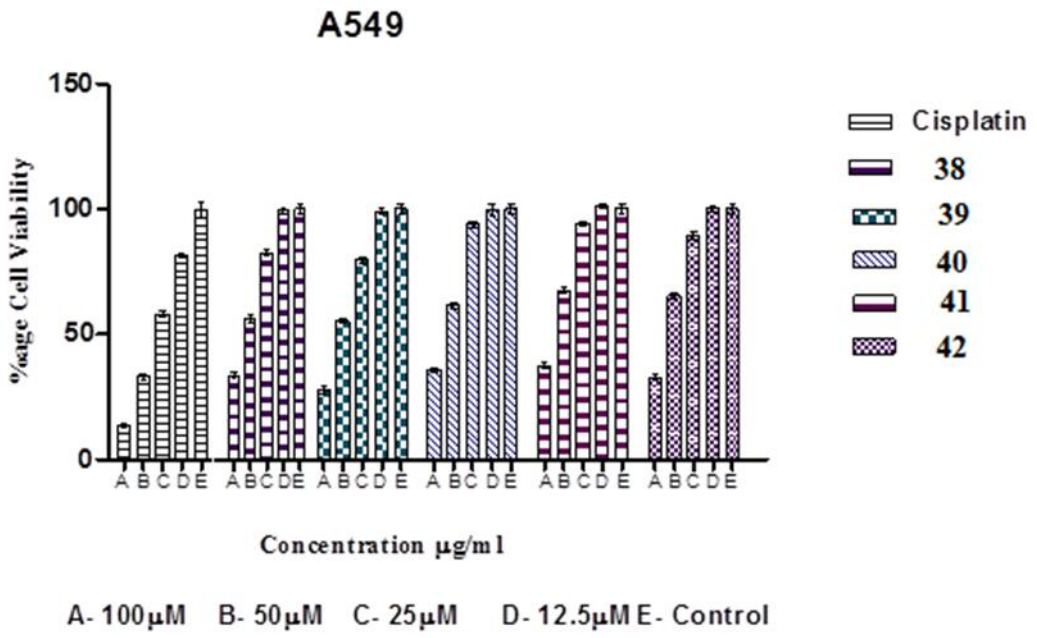

***Figure 4.8a**. Graph of cytotoxic effect of concentrations of complexes (38-42) on cell viability of A549 cell line.*

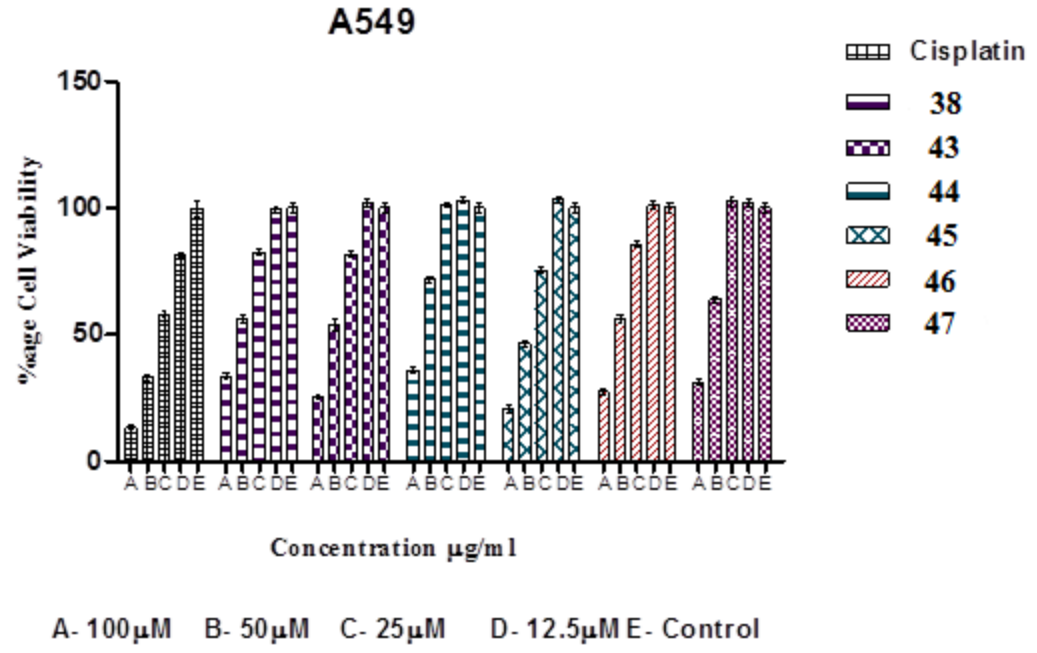

***Figure 4.8b**. Graph of cytotoxic effect of concentrations of complexes (38, 43-47) on cell viability of A549 cell line.*

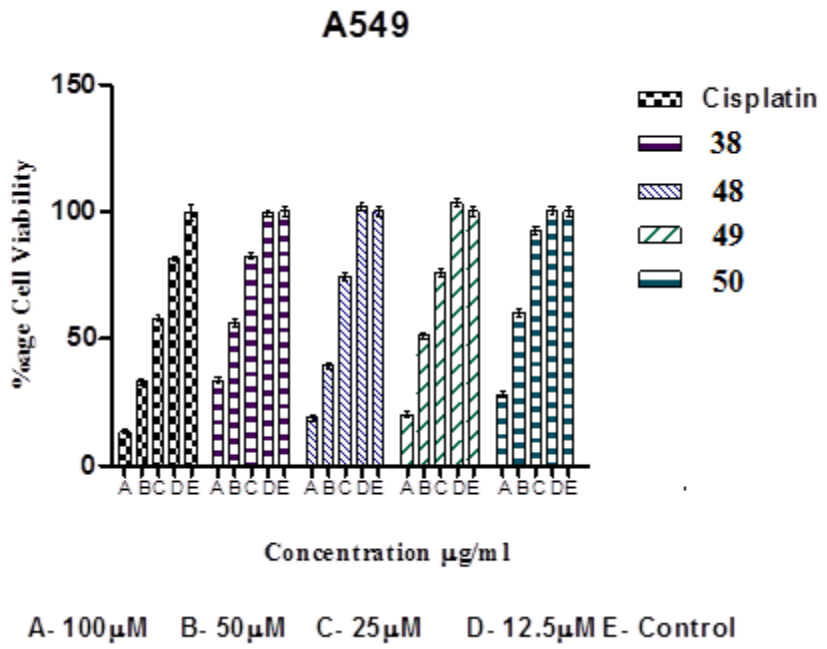

***Figure 4.8c**. Graph of cytotoxic effect of concentrations of complexes (**38, 48-50**) on cell viability of A549 cell line.*

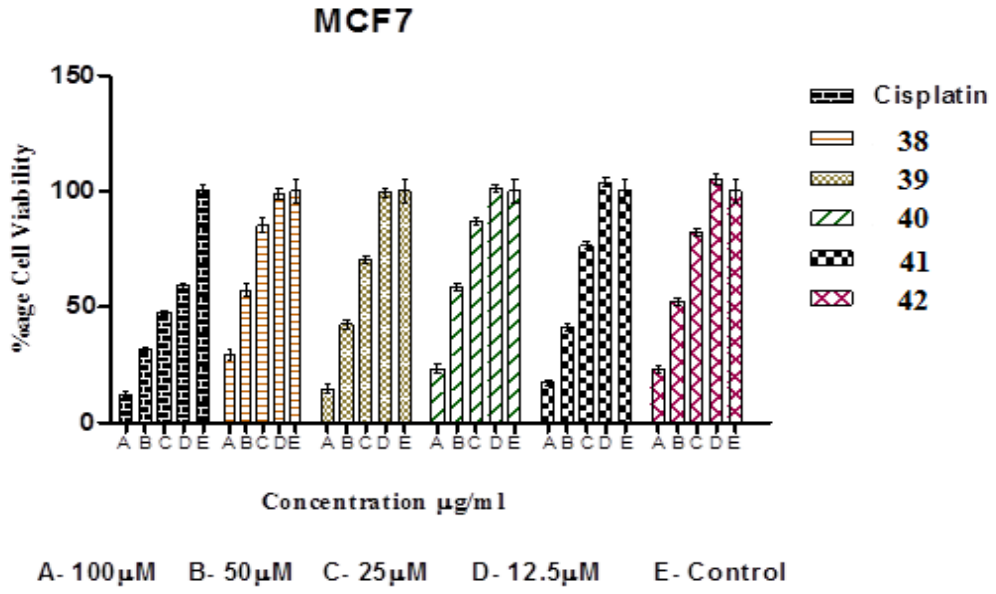

***Figure 4.9a**. Graph of cytotoxic effect of concentrations of complexes (38-42) on cell viability of MCF7 cell line.*

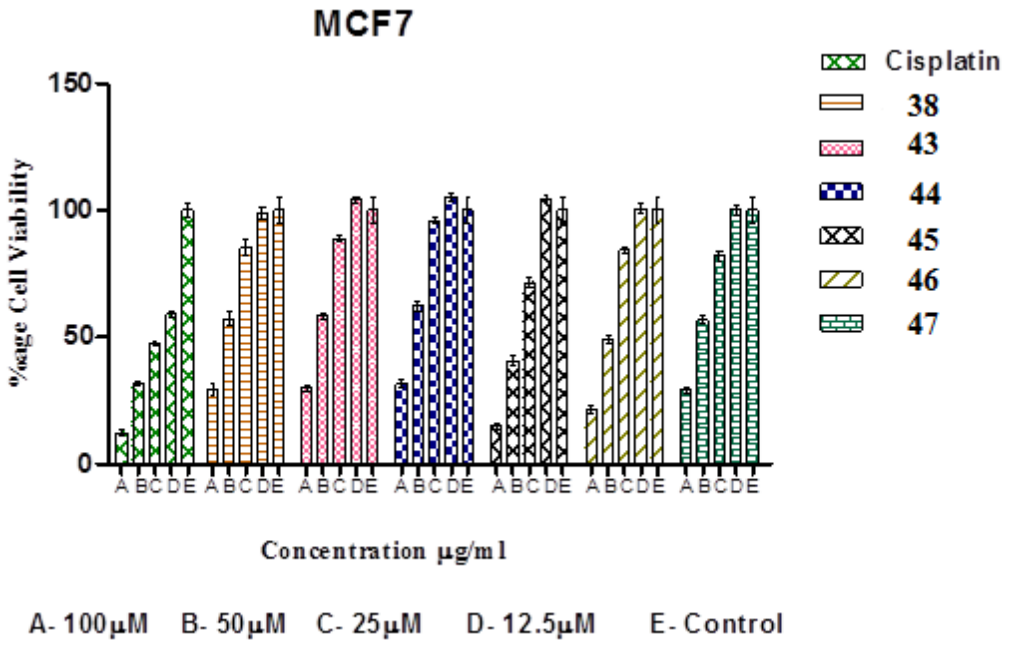

***Figure 4.9b**. Graph of cytotoxic effect of concentrations of complexes (38, 43-47) on cell viability of MCF7 cell line.*

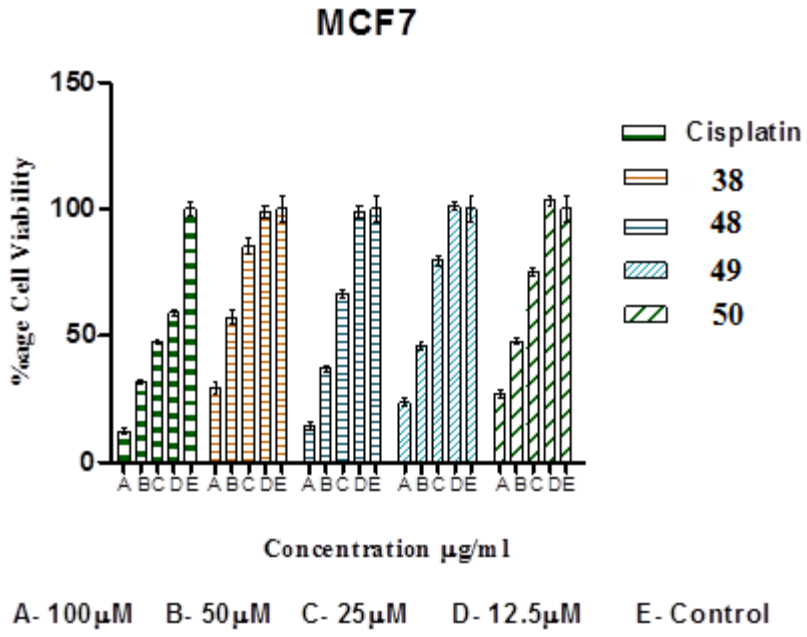

***Figure 4.9c**. Graph of cytotoxic effect of concentrations of complexes (38, 48-50) on cell viability of MCF7 cell line.*

CHAPTER 5

SYNTHESIS AND CHARACTERIZATION OF (TRI-TERT-BUTYLPHOSPHINO)GOLD(I)THIONE COMPLEXES

5.1 Introduction

Auranofin is a linear Au(I) complex of triethyl phosphine and tetracetylthiogulcose ligands, which has been used as anti-arthritis drug. Later in 1980s it was investigated clinically as anticancer drug in mice [166]. A series of analogues, mainly Au(I) phosphine complexes showed promising in vitro and in vivo anticancer tests [167-169]. Recently, studies on gold complexes with phosphine and sulfur donor ligands in cancer chemotherapy are growing rapidly. Some water soluble gold(I) phosphine derivatives have tested against *in vitro* and *in vivo* against colon cancer [170]. Zou et al. reviewed the biochemistry of Au(I) and Au(III) complexes and demonstrated their mechanism of action [124].

5.2 Experimental Section

5.2.1 Materials and instrumentation

All solvents were of analytical grade, used without further purification. Ethanol, diethyl ether, dichloromethane, acetone, were purchased from Fluka AG (St. Gallen, Switzerland). Chloro(tri-tert-butylphosphine)gold(I) complex from Stream Chemicals Inc. (Newburyport, Massachusetts. United States). $AgPF_6$ was purchased from Sigma-Aldrich, United States. 1,3-diazinane-2-thione (Diaz), N-hydroxyethyl, 1,3-imidazolidine-2-thione (2-EtOH-Imt), 1,3-diazepine-2-thione (Diap) and N-ethyl-1,3-diazinane-2-thione (N-Et-Diaz) were prepared as reported [171]. ^{1}H, ^{13}C, ^{31}P NMR, FT-IR spectroscopy and elemental analyses were described in section 3.1.

5.2.2 Synthesis of (tri-tert-butylphosphino)gold(I) thione complexes (52-55)

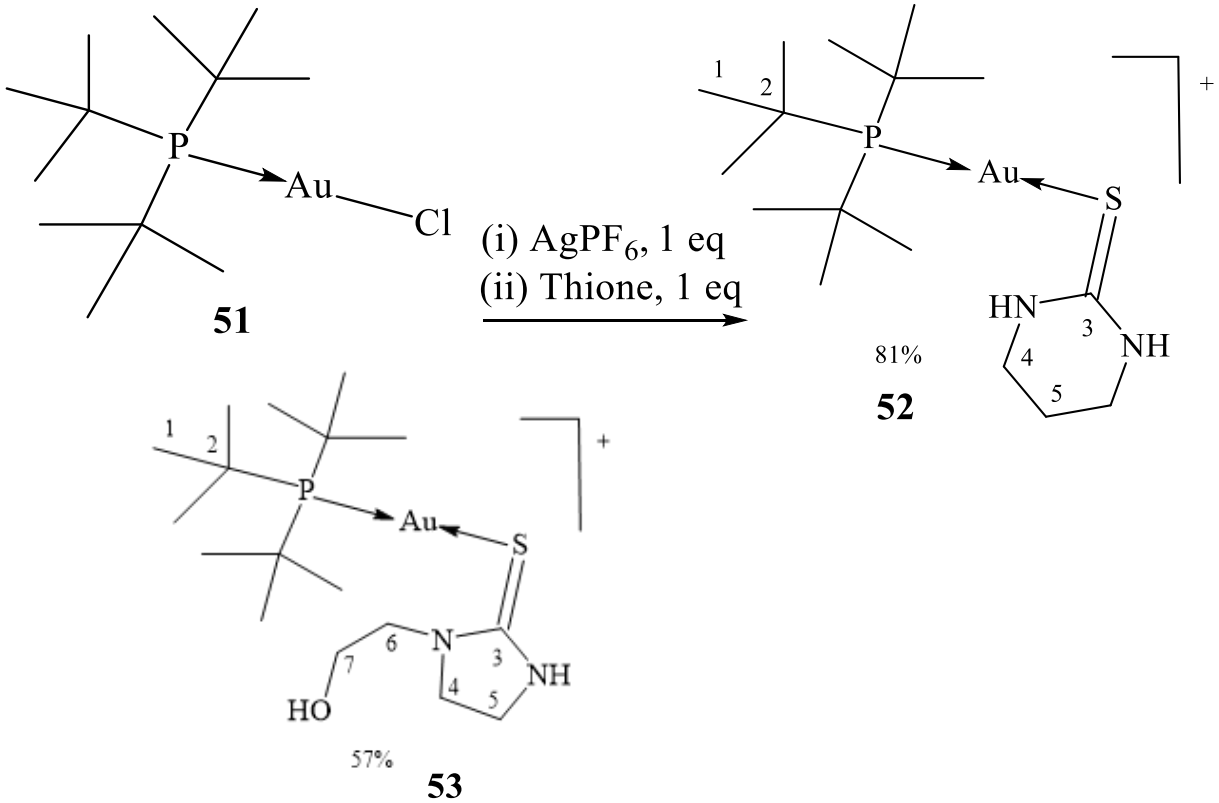

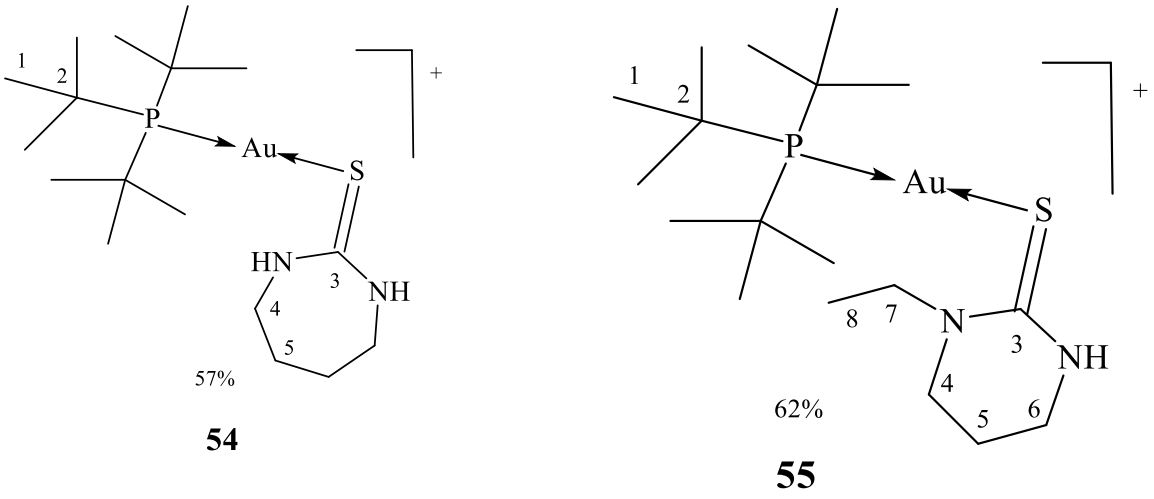

Scheme 22. *Synthesis of (tri-tert-butylphosphino)gold(I) with thione complexes (**52-55**).*

$[Au\{P(t\text{-}Bu)_3\}(SN_2C_3H_6)]PF_6$ (**52**)

$AgPF_6$ (0.127 g, 0.500 mmol) was dissolved in 7 mL of ethanol and then added to a solution of $(t\text{-}Bu)_3PAuCl$ (0.217 g, 0.500 mmol) in acetone (7 mL). The resulting mixture was stirred at ambient temperature for 30 mins. and filtered off. 1, 3-diazinane-2-thione (0.058 g, 0.50 mmol) was then added to the filtrate, the mixture was stirred for 2 hours, filtered and stored in undisturbed area. After four days bright yellowish-white crystals were obtained and a suitable crystal was selected for single crystal diffraction analysis. Yield 0.268 g (81%). Anal. calc. for $C_{16}H_{35}AuN_2P_2SF_6$ (660.43 g/mol): C, 29.09; H, 5.34; N, 4.24; S 4.85. Found: C, 31.26; H, 3.99; N 3.01; S 3.03.

$[Au\{P(t\text{-}Bu)_3\}(SN_2C_5H_9\text{-}OH)]PF_6$ **(53)**

Complex **53** was prepared using N-hydroxyethyl-1,3-imidazolidine-2-thione (0.073 g, 0.50 mmol) by a procedure similar to **(52)**. After three days a colorless solid was obtained.

Yield 0.213 g (62%). Anal. calc. for $C_{17}H_{37}AuN_2OP_2SF_6$ (690.46 g/mol): C, 29.57; H, 5.40; N, 4.05; S, 4.64. Found: C, 30.39; H, 4.52; N, 4.13; S, 4.55.

$[Au\{P(t\text{-}Bu)_3\}(SN_2C_5H_{10}]PF_6$ **(54)**

Complex **54** was prepared using 1,3-diazepine-2-thione (0.065 g, 0.50 mmol) by a procedure similar to **(52)**. After three days the colorless crystals were obtained. A suitable crystal was selected for single crystal diffraction analysis. Yield 0.192 g (57%). Anal. Calc. for $C_{17}H_{37}AuN_2P2SF_6$ (674.46 g/mol): C, 30.27; H, 5.52; N, 4.15; S, 4.75. Found: C, 30.91; H, 4.16; N, 4.70; S, 4.94.

$[Au\{P(t\text{-}Bu)_3\}(SN_2C_5H_{10}]PF_6$ **(55)**

Complex **55** was prepared using N-ethyl-1,3-diazinane-2-thione (0.072 g, 0.50 mmol) by a procedure similar to **(52)**. After three days the yellow crystals were obtained. A suitable crystal was selected for X-ray diffraction analysis. Yield 0.213 g, (62 %). Anal. Calc. for $C_{18}H_{39}AuN_2P_2SF_6$ (688.49 g/mol): C, 31.40; H, 5.70; N, 4.06; S, 4.65. Found: C, 31.52; H, 4.24; N, 4.57; S, 4.97.

5.3 Results and discussion

5.3.1 Spectroscopic characterization

The synthesized chloro(tri-tert-butylphosphino)gold(I) with thione complexes **(52-55)** are shown in (Scheme 22) and were characterized by ^{1}H, ^{13}C and ^{31}P NMR and mid FT-IR spectroscopy, elemental analyses and single crystal X-ray diffraction analysis. The mid

FT-IR spectroscopy data of free ligands and complexes **(52-55)** are summarized in Table 5.1**.**

The formation of complexes (**52-55**) was confirmed by the significant shift in frequencies of free ligands to their complexes. For instance, ν(C=S) band in free ligands is in the range of (1001-1191 cm^{-1}), however for complexes (**52-55**) it is in the range of (830-875 cm^{-1}) due to C=S weaken upon coordination [133]. In the complexes (**52-55**) the strong ν(C—N=S) absorbance bands were assigned in the range (1443-1480) cm^{-1} due to increasing double character in C—N bond.

Table 5.1. Mid FT-IR frequencies (cm^{-1}) of free ligand and (tri-tert-butylphosphino)gol(I) thione complexes (**52-55**).

Ligand/ Complex	**Stretch NH/OH**					**Stretch N—C**	**Stretch C=S**
Diaz	-	-	-	2924	1360	1488	1066
2EtOHImt	-	2979	1379	2925	1358	1466	1065
Diap	-	-	-	2922	1347	1445	1001
EtDiaz	-	-	-	2935	1315	1448	1191
52	3402 (NH)	3000	1370	2954, 2870	1319	1480	875
53	3600 (OH)	2999	1368	2953, 2895	1328	1476	830
54	3379 (NH)	3005	1370	2952, 2861	1223	1480	846
55	3409 (NH)	2952	1375	2904, 2870	1258	1443	852

The comparison of the ^{1}H NMR spectra of free thione ligands and their complexes **(52-55)** showed significant shifts that indicate complexation. For example, ^{1}H NMR data for the complex **52** display a doublet at 1.48 ppm, triplet at 3.23 ppm, and triplet at 1.77 ppm while t-Bu_3PAuCl shows a doublet at 1.51 ppm as shown in Table 5.2.

Table 5.2. ^{1}H NMR chemical shifts (ppm) for free ligands and (tri-tert-butylphosphino) gold(I) thione complexes (51-55) in DMSO.

Ligand/ complex	1H	4H	5H	6H	7H	8H	NH	OH
t-Bu$_3$PAuCl	1.51 d	-	-	-	-	-	-	-
Diaz	-	3.07 t	1.70 m	-	-	-	7.76	-
52	1.48 d	3.23 t	1.77 m	-	-	-	8.93	-
2-EtOHImt	-	3.48 t	3.67 t	3.52 t	3.37 t	-	7.93	4.75
53	1.48 d	3.52 t	3.89 t	3.62 t	3.45 t	-	8.95	4.98
Diap	-	-	-	-	-	-	-	-
54	1.48 d	3.48 t	1.85 m	-	-	-	7.20	-
EtDiaz	-	3.05 t	1.80 m	3.26 t	3.71 q	1.04 t	7.71	-
55	1.47 d	3.21 t	1.86 m	3.44 t	3.77 q	1.17 t	8.97	-

The chemical shifts of ^{13}C and ^{31}P NMR for free ligand and their Au(I) compounds (**51-55**) are shown in Table 5.3.

^{13}C NMR spectra support the proposed structure of the synthesized complexes. The C=S resonance shifted to upfield in all complexes by 4-7 ppm most likely due to back donation from gold ion to the π* C=S [171-172]. The C4 (C—N) resonance was shifted downfield in all complexes relatively to the free ligand likely due to the increase of sp2 character of nitrogen upon coordination.

^{31}P NMR spectra are in agreement with ^{1}H and ^{13}C NMR results. The ^{31}P resonance appears at -10.69 ppm for t-Bu$_3$PAuCl, thus being shifted downfield upon coordination in all complexes. A linear correlation between ^{31}P NMR chemical shift and ^{13}C=S NMR chemical shifts due to increase ring constrain of complexes (**52-55**) is shown in Figure 5.1.

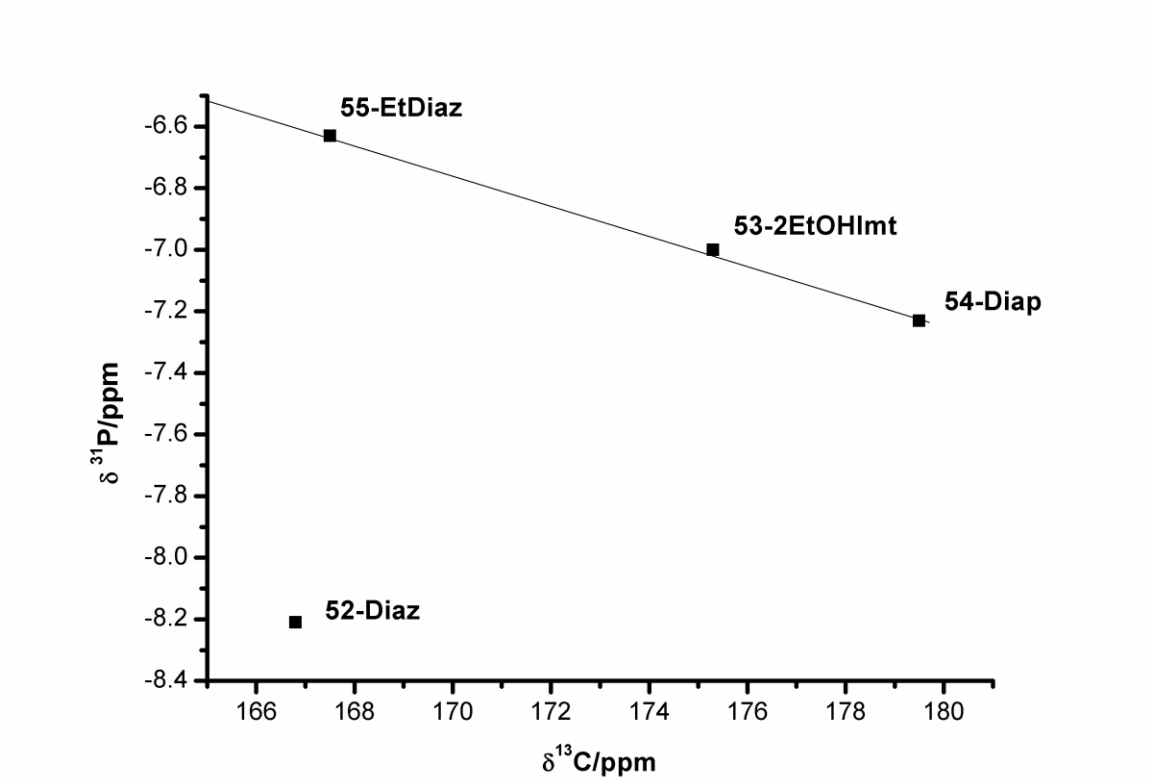

Figure 5.1. *Plot of ^{31}P NMR cemical shift against observed ^{13}C=S NMR chemical shift for complexes (**52-55**).*

Table 5.3. ^{13}C and ^{31}P NMR chemical shifts (ppm) for free ligands and (tri-tert-butylphosphino)gold(I) thione complexes (**51-55**) in DMSO.

Ligand/ complex	C1	C2	C=S	C4	C5	C6	C7	C8	^{31}P
t-Bu$_3$PAuCl	32.2	39.5	-	-	-	-	-	-	-10.69
Diaz	-	-	173.9	40.1	18.6	-	-	-	-
52	31.8	40.9	166.8	41.2	18.4	-	-	-	-8.21
2-EtOHImt	-	-	182.4	40.9	48.5	49.1	58.8	-	-
53	32.2	40.4	175.3	42.5	49.8	50.3	58.5	-	-7.0
Diap	-	-	183.9	45.9	26.9	-	-	-	-
54	32.3	39.7	179.5	46.5	26.1	-	-	-	-7.23
EtDiaz	-	-	175.9	40.2	20.9	45.0	47.6	12.1	-
55	32.2	40.4	167.5	40.7	20.2	46.6	49.4	12.9	-6.63

5.3.2 Signal crystal X-ray structure determination

The structures of complexes **54** and **55** were determined at 173 K (–100 °C) using a STOE IPDS 2 with a two-circle goniometer and MoK_{α} graphite monochromator [127]. Diffraction data collected using a detector image plate (34 diameter) and sealed X-ray tube diffraction source 12 x 0.4 mm long fine-focus. The structures were solved using the programs SHEXLX97, SHELXS-2014 [173]. The non-hydrogen atoms were refined using least-squares matrix on F^2. The structure of complex **54** and **55** were drawn using the programs PLATON and MERCURY [174]. A summary of crystal data and refinement details for complexes **54** and **55** are given in Table 5.6.

The molecular structure and crystal backing of compound *[Au{P(t-Bu)$_3$}(SN$_2$C$_5$H$_{10}$]PF$_6$* (**54**) are shown in Figures 5.2 and 5.3 respectively. The selected bond lengths and bond angles for complex **54** is shown in Table 5.4.

The coordination geometry around gold ion with is close to linearity, with (P1—Au—S1) 178.1(7)º. The Au1—P1 and Au1—S1 bond lengths are 2.23(2) and 2.27(2) Å, respectively. The bond lengths and bond angle are similar to those reported for other compounds [126, 175].

The molecular structure and crystal packing of complex *[Au{P(t-Bu)$_3$}(SN$_2$C$_5$H$_{10}$]PF$_6$* (**55**) are shown in Figures 5.4 and 5.5 respectively. The selected bond lengths and bond angles for complex 54 are shown in Table 5.5.

The coordination geometry around gold ion is close to linearity, with (P1—Au—S1) 178.0(5)º. The Au1—P1 and Au1—S1 bond lengths are 2.32(1) and 2.29(1)Å,

respectively. These bond lengths and bond angle are similar to those reported for analogous compounds [140-141].

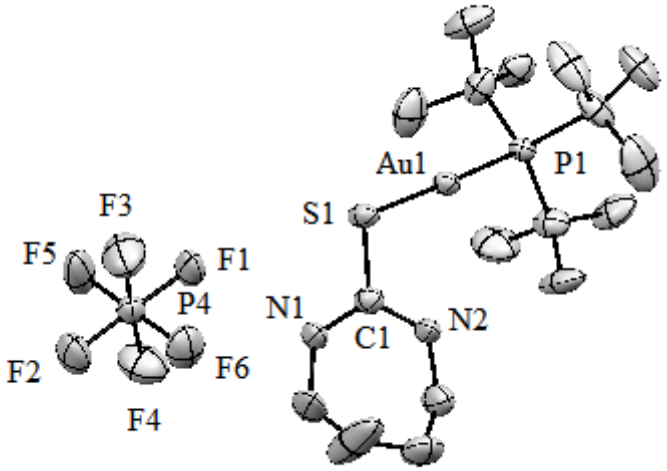

Figure 5.2. *Molecular structure of complex* ***54****, with partial labelling atoms and 50% probability ellipsoids. The hydrogen atoms have been omitted for clarity.*

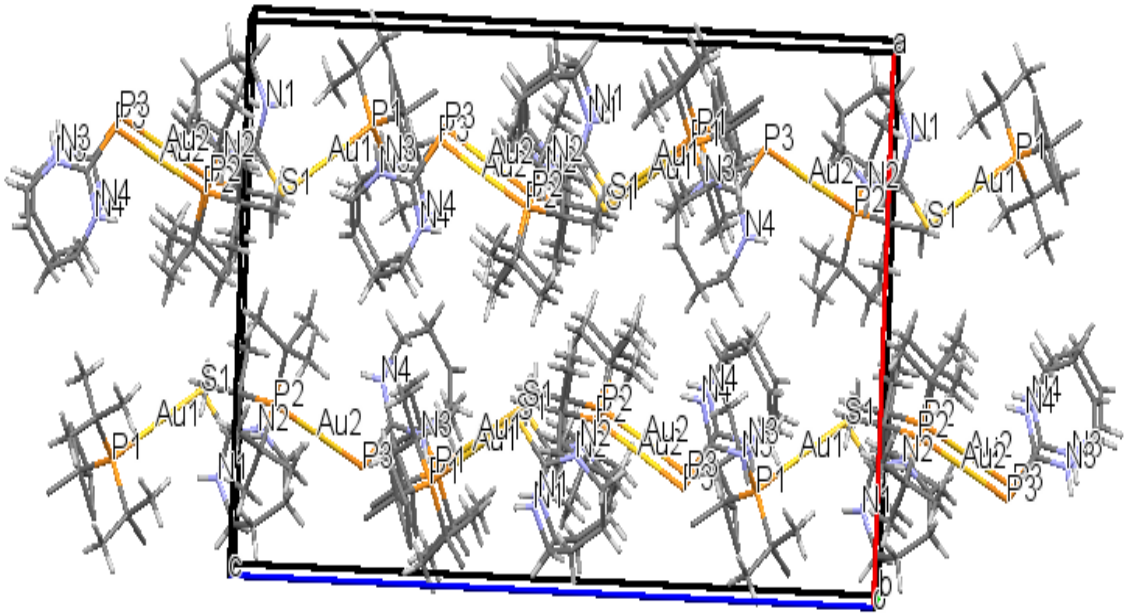

Figure 5. 3. *Crystal packing of complex* ***54*** *viewed along b-axis.*

Table 5.4. Selected bond lengths and bond angles for complex **54**.

Bond Length (Å)		**Bond Angles (°)**	
Au1—S1	2.32 (2)	S1—Au1—P1	178.1 (7)
Au1—P1	2.27 (2)	Au1—S1—C1	100.8 (2)
S1—C1	1.74 (7)	S1—C1—N1	119.6 (5)
N1—C1	1.32 (8)	S1—C1—N2	117.1 (5)
N2—C1	1.31 (3)	N1—C1—N2	123.3 (6)

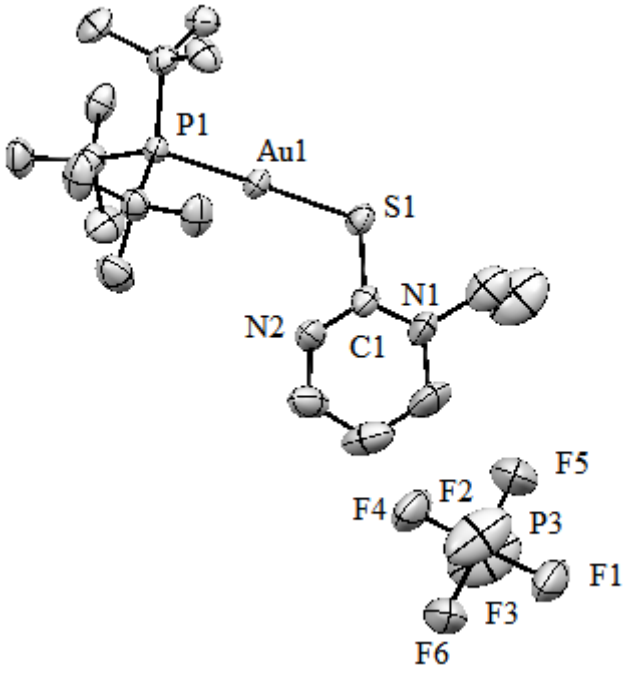

***Figure 5.4**. Molecular structure of complex **55**, with partial atom labelling atoms and 50% probability ellipsoids. Hydrogen atoms have been omitted for clarity.*

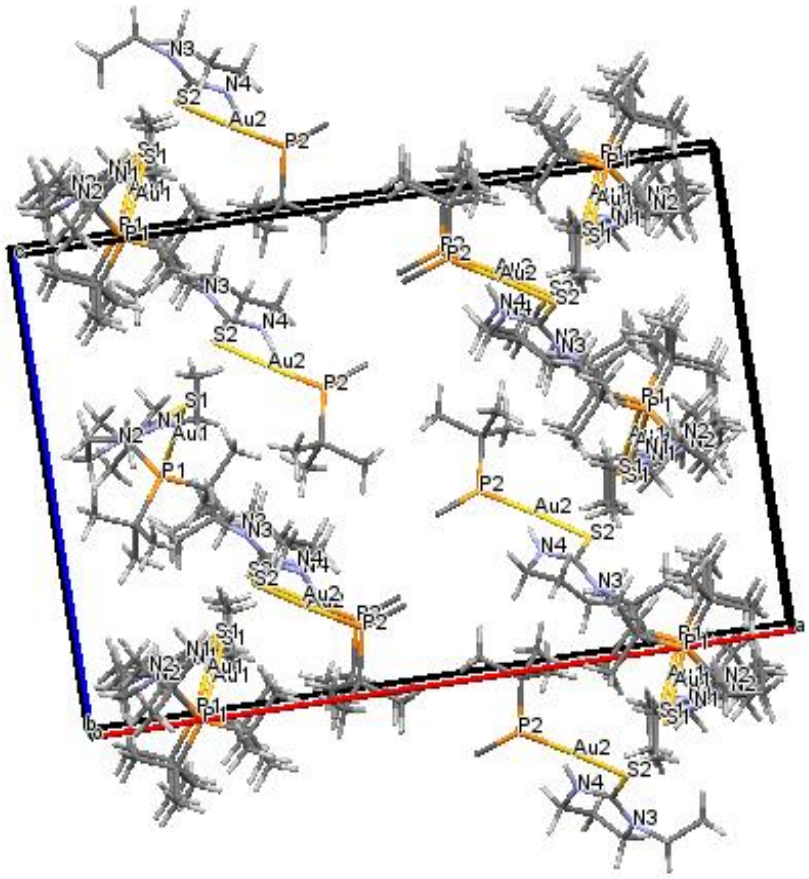

Figure 5.5. *Crystal packing of complex 55 viewed along b-axis.*

Table 5.5. Selected bond lengths and bond angles for complex **55**.

Bond Length (Å)		**Bond Angles (°)**	
Au1—S1	2.32 (1)	S1—Au1—P1	178.0 (5)
Au1—P1	2.29 (1)	Au1—S1—C1	103.8 (2)
S1—C1	1.74 (5)	S1—C1—N1	121.0 (4)
N1—C1	1.31 (7)	S1—C1—N2	120.3 (4)
N2—C1	1.32 (9)	N1—C1—N2	118.6 (5)

Table 5.6. Summary of crystal data and details of the structure refinement for complexes (**54** and **55**).

Complex	**54**	**55**
Crystal data		
Empirical formula	C_{17} H_{37} $AuF_6N_2P_2S$	C_{18} H_{39} $AuF_6N_2P_2S$
Formula weight	674.46 g/ mol	688.49 g/mol
Crystal symmetry	Monoclinic	Monoclinic
Space group	P 21/c	P 21/c
Crystal color	Colorless	Colorless
Crystal description	-	Block
Crystal size / mm	-	0.40 x 0.33 x 0.19
Wavelength/Å	0.71073	0.71073
Temperature/K	293(2)	233(2)
Cell length **a** (Å)	16.053(4)	24.9014(16)
Cell length **b** (Å)	11.756(3)	13.0453(5)
Cell length **c** (Å)	26.392(4)	16.0089(9)
Cell angles **α** (°)	90	90
Cell angles **β** (°)	90	90
Cell angles **γ** (°)	90.97	90.764 (5)
D_x	1.686 Mg m^{-3}	1.686 Mg m^{-3}
μ	6.16 mm^{-1}	5.92 mm^{-1}
Radiation type	Mo *K*α	Mo *K*α
Cell volume ($Å^3$)	4979.96(3)	5197.9 (5)
Z	-	8
Data collection		
Diffractometer	STOE IPDS 2	STOE IPDS 2
Absorption correction	-	Multi-scan (MULABS in PLATON; 2009
Radiation source	Plane graphite	Fine-focus sealed tube
Refinement		
$R[F^2>2\sigma(F^2)]$,$wR(F^2)$,S	-	0.36, 0.087, 0.96
$\Delta\rho_{max}$	1.01 e $Å^{-3}$	1.14 e $Å^{-3}$
$\Delta\rho_{min}$	−1.50 e $Å^{-3}$	−1.38 e $Å^{-3}$
H-atom treatment	Treated by a mixture of independent and constrained refinement.	Treated by a mixture of independent and constrained refinement.

CHAPTER 6

SYNTHESIS AND CHARACTERIZATION OF GOLD(I) CARBENE COMPLEXES WITH MONO AND BIS-PHOSPHINE LIGANDS

6.1 Introduction

N-heterocyclic carbene (NHC) is versatile ligand with unique properties. Their metal complexes have potential applications in the field of medicinal inorganic chemistry and industry are currently a focus of the interest [119-121, 176]. Horvath et al. prepared a series of gold(I) N-heterocyclic carbene complexes with bisphosphine ligands and evaluated for their *in vitro* and *in vivo* anticancer activity [177].

6.2 Experimental Section

6.2.1 Materails and Instrumentation

All solvents were of analytical grade and used without further purification. Ethanol, diethyl ether, dichloromethane, acetone, were purchased from Fluka AG (St. Gallen, Switzerland). 1,3-Bis(2,6-di isopropylphenyl)imidazol-2-ylidenechloridogold(I) [Au(Ipr)Cl], Bis(2-cyanoethyl)phenylphosphine, (1R,2R)-2-(diphenylphosphino)-1

-aminocyclohexane, (1R, 2R)-2-(diphenylphosphino)-1,2-diphenylethylamine, (R)-2-(diphenylphosphino)-1-phenylethylamine, (R)-1-(diphenylphosphino)-2-amino-3, 3-dimethylbutane, tricyclohexylphosphine, 3-(diphenylphosphino)propylamine, 1,3-bis(Diphenylphosphino)propane, 1,2-bis(Diphenylphosphino)ethane and bis[2-(Dicyclohexyl(phosphino)ethyl]amine were purchased from Stream Chemicals Inc. (Newburyport, Massachusetts. United States). $AgPF_6$ was purchased from Sigma-Aldrich, United States. ^{1}H, ^{13}C, ^{31}P NMR, FT-IR spectroscopy and elemental analysis were described in section 3.1.

6.2.2 Synthesis of gold(I) N-heterocyclic carbene with mono and bis-phosphine complexes (56-65)

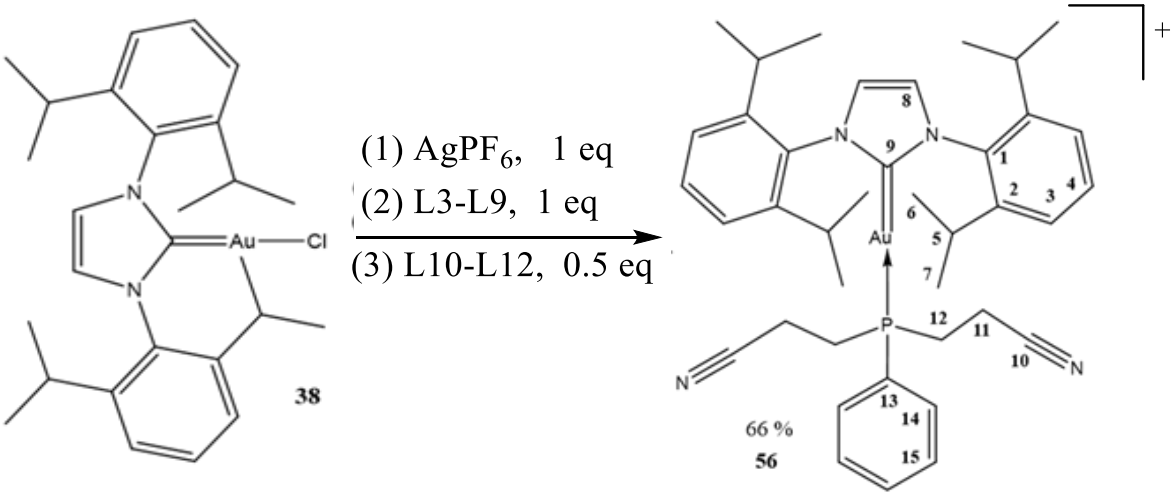

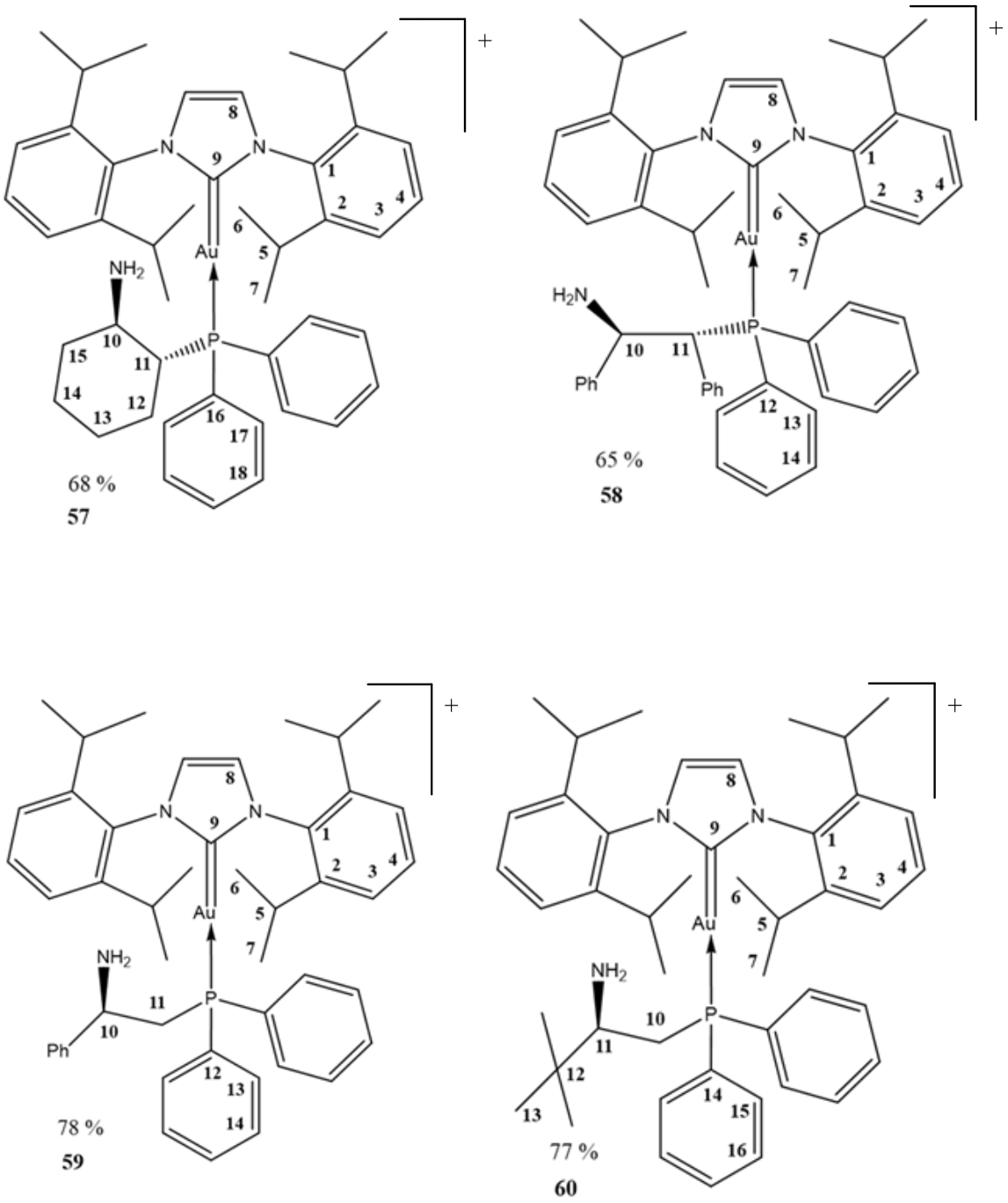

Scheme 23. Synthesis of gold(I)-carbene with mono and bis-phosphine complexes **(56-65).**

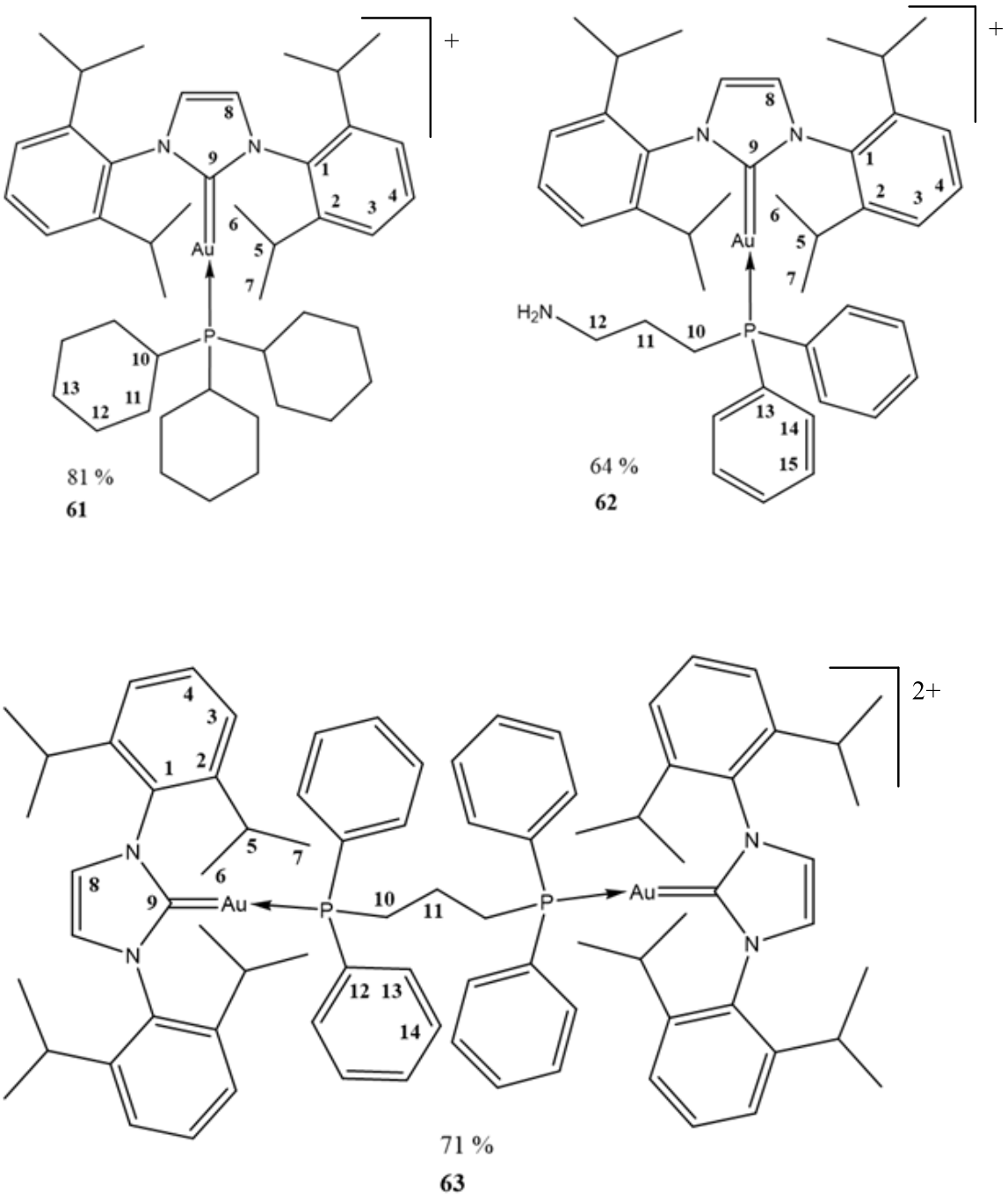

Scheme 23. Synthesis of gold(I)-carbene with mono and bis-phosphine complexes **(56-65).**

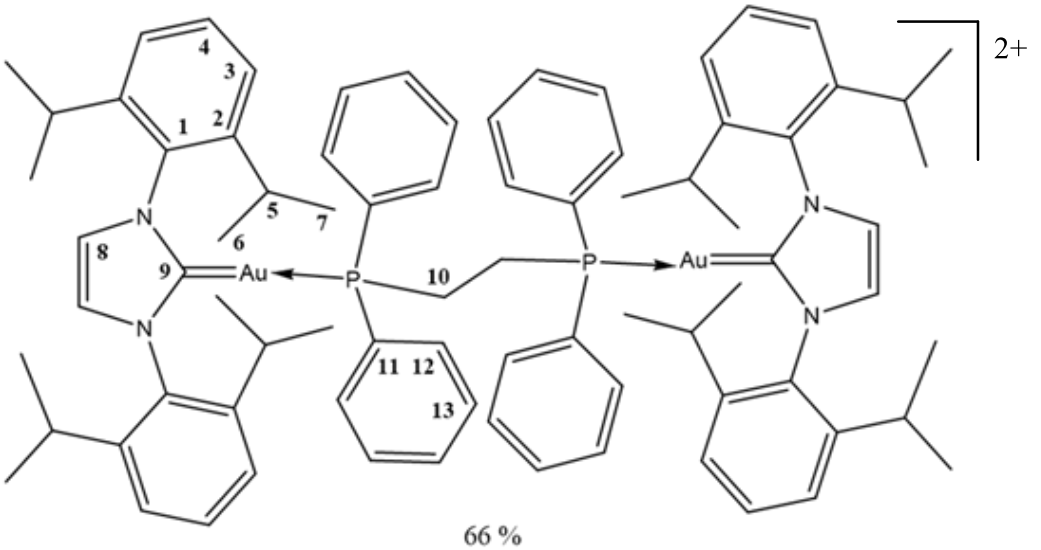

66 %

64

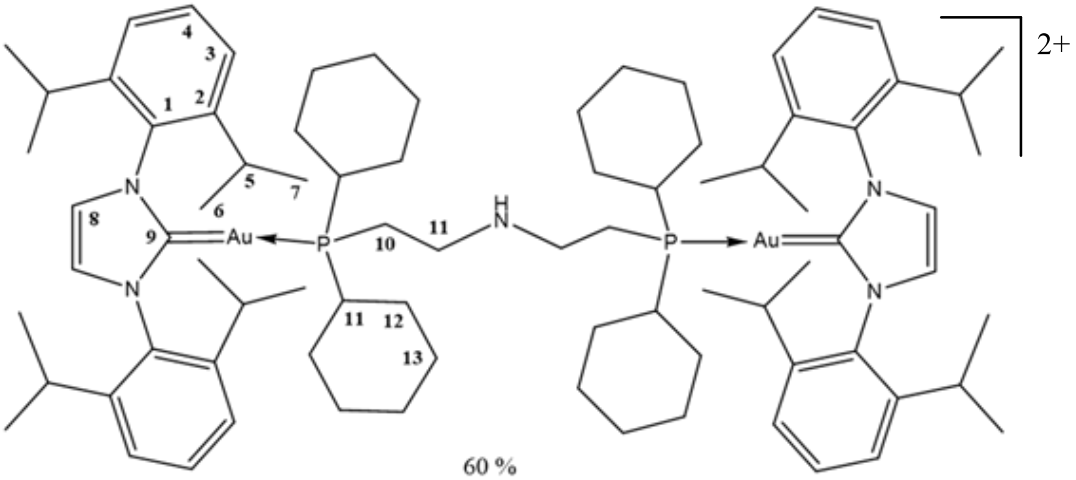

60 %

65

Scheme 23. Synthesis of gold(I)-carbene with mono and bis-phosphine complexes **(56-65).**

[Au(Ipr)($C_{12}H_{13}N_2P$)]PF_6 **(56)**

$AgPF_6$ (0.127 g, 0.500 mmol) was dissolved in 5 mL of ethanol was added to a solution of 1,3-Bis(2,6-diisopropylphenyl)imidazol-2-ylidenechloridogold(I) [Au(Ipr)Cl] (0.311 g, 0.500 mmol) in acetone (5 mL). The resulting mixture was stirred at ambient temperature for 10 min and then the mixture was filtered off. Bis(2-cyanoethyl) phenylphosphine (0.108 g, 0.500 mmol) was added to the filtrate, stirred for 30 min, filtered and stored in undisturbed area. After five days colorless crystals were obtained and a suitable crystal was selected for X-ray diffraction analysis. Yield 0.313 g (66%). Anal. calc. for $C_{39}H_{49}AuN_4P_2F_6$ (946.75 g/mol): C, 49.42; H, 5.31; N, 5.91. Found: C, 55.28; H, 5.31; N, 6.73.

[Au(Ipr)($C_{18}H_{22}NP$)]PF_6 **(57)**

Complex **57** was prepared using (1R,2R)-2-(diphenylphosphino)-1-aminocyclohexane (0.142 g, 0.500 mmol) following a procedure similar to **(56)**. After three days a colorless solid was obtained. Yield 0.344 g (68%). Anal. calc. for $C_{45}H_{59}AuN_3P_2F_6$= (1014.87 g/mol): C, 49.42; H, 5.31; N, 4.14. Found: C, 53.61; H, 6.06; N, 4.15

[Au(Ipr)($C_{26}H_{24}NP$)]PF_6 **(58)**

Complex **58** was prepared using (1R,2R)-2-(diphenylphosphino)-1,2-diphenylethylamine (0.159 g, 0.500 mmol) following a procedure similar to **(56)**. After five days a yellow solid was obtained. Yield 0.363 g (65%). Anal. calc. for $C_{53}H_{61}AuN_3P_2F_6$ (1112.98 g/mol): C, 57.19; H, 5.52; N, 3.77. Found: C, 56.08; H, 5.93; N, 3.79.

[Au(Ipr)($C_{20}H_{20}NP$)]PF_6 **(59)**

Complex **59** was prepared using (R)-2-(diphenylphosphino)-1-phenylethylamine (0.153 g, 0.500 mmol) following steps similar to **(56)**. After five days a yellow solid was obtained. Yield 0.402 g (78%). Anal. calc. for $C_{53}H_{61}AuN_3P_2F_6$ (1036.88 g/mol): C, 54.44; H, 5.54; N, 4.05. Found: C, 53.47; H, 5.93; N, 3.99.

[Au(Ipr)($C_{18}H_{24}NP$)]PF_6 **(60)**

Complex **60** was prepared using (R)-1-(diphenylphosphino)-2-amino-3,3-dimethylbutane (0.143 g, 0.500 mmol) following a procedure similar to **(56)**. After four days a colorless solid was obtained. Yield 0.357 g (77%). Anal. calc. for $C_{39}H_{49}AuN_3P_2F_6$ (932.73 g/mol): C, 50.22; H, 5.29; N, 4.50. Found: C, 45.96; H, 5.80; N, 3.72.

[Au(Ipr)($C_{18}H_{33}P$)]PF_6 **(61)**

Complex **61** was prepared using tricyclohexyl-phosphine (0.140 g, 0.50 mmol) by a procedure similar to **(56)**. After five days colorless solid was obtained. Yield 0.411 g (81%). Anal. calc. for $C_{45}H_{69}AuN_2P_2F_6$ (1010.95 g/mol): C, 53.46; H, 6.87; N, 2.77. Found: C, 56.42; H, 8.34; N, 3.02

[Au(Ipr)($C_{15}H_{18}NP$)]PF_6 **(62)**

Complex **62** was prepared using 3-(diphenyl- phosphino)propylamine (0.122 g, 0.5 mmol) following a procedure similar to **(56)**. After three days a colorless solid was obtained. Yield 0.310 g (64%). Anal. calc. for $C_{42}H_{54}AuN_3P_2F_6$ (973.80 g/mol): C, 51.80; H, 5.58; N, 4.31. Found: C, 52.68; H, 6.48; N, 4.54.

$[(Au(Ipr))_2(C_{27}H_{26}P_2)](PF_6)_2$ **(63)**

$AgPF_6$ (0.127 g, 0.500 mmol) was dissolved in 5 mL of ethanol and the solution was added to a solution of 1,3-Bis(2,6-di-isopropylphenyl)imidazol-2-ylidenegoldchlorido(I) [Au(Ipr)Cl] (0.311 g, 0.500 mmol) in dichlormethane 5 mL. The resultant mixture was stirred at ambient temperature for 10 min and then filtered off. 1,3-Bis(Diphenyl-phosphino)propane (0.103 g, 0.250 mmol) in dichloromethane 5 mL was added to the filtrate. The mixture stirred for 30 min, filtered and the filtrate stored in a undisturbed area. After five days the colorless crystals were obtained and a suitable crystal was selected for X-ray diffraction analysis. Yield 0.332 g, (71%). Anal. Calc. for $C_{81}H_{98}Au_2N_4P_4F_{12}$ (1873.48 g/mol): C, 51.92; H, 5.27; N, 2.99. Found: C, 44.85; H, 5.04; N, 3.02.

$[(Au(Ipr))_2(C_{26}H_{24}P_2)](PF_6)_2$ **(64)**

Complex **64** was prepared using 1,2-Bis(Diphenylphosphino)ethane (0.100 g, 0.250 mmol) by a procedure similar to **(63)**. After five days a colorless solid was obtained. Yield 0.308 g, (66 %). Anal. Calc. for $C_{80}H_{96}Au_2N_4P_4F_{12}$ (1873.48 g/mol): C, 51.67; H, 5.20; N, 3.01. Found: C, 56.42; H, 6.22; N, 3.32.

$[(Au(Ipr))_2(C_{28}H_{24}P_2)](PF_6)_2$ **(65)**

Complex **65** was prepared using Bis[2-(Dicyclohexylphosphino)ethyl]amine (0.117 g, 0.250 mmol) by a procedure similar to **(63)**. After five days the colorless crystals were obtained and a suitable crystal was selected for X-ray diffraction analysis. Yield 0.290 g

(60%). Anal. calc. for $C_{82}H_{125}Au_2N_5P_4F_{12}$ (1926.71 g/mol): C, 51.11; H, 6.53; N, 3.63. Found: C, 50.68; H, 6.52; N, 3.45.

6.3 Results and Discussion

6.3.1 Spectroscopic Characterization

The ligands (**L3-L12**) and their gold(I) complexes (**56-65**) were synthesized (Scheme 23) and were characterized using by ^{1}H, ^{13}C and ^{31}P NMR and mid FT-IR spectroscopy, elemental analyses and single crystal X-ray diffraction analysis.

The FT-IR frequencies for free ligand and their complexes (**56-65**) are shown in Table 6.1. FT-IR spectra showed weak absorbance in the region of (3049-3078 cm^{-1}) assigned to benzene ring =C—H stretching for the free ligands and precursor **38**. This absorbance was shifted to higher frequency in the range (3120 -3175 cm^{-1}) in all complexes. The ν(C≡N) band for free ligand **L2** appears at 2250 cm^{-1} and for it is complex **56** was shifted lower frequency at 2242 cm^{-1} this significant shift support complexation.

Table 6.1. Mid FT-IR frequencies (cm^{-1}) of gold(I) with mixed carbene and phosphine complexes (**56-65**).

Compound	Stretch NH	Stretch =C—H						Stretch C≡N
38	-	3037	1109	2960	1366	1258	1462	-
L3	-	3073	1095	2933, 2911	1327	1426	-	2250
56	-	3120	1108	2956, 2874	1327	1256	1467	2242
L4	3334, 3259	3074	1099	2916, 2844	1327	1230	1478	-
57	3433, 3358	3170	1103	2963, 2867	1328	1215	1466	-
L5	3371, 3302	3063	1071	2903, 2854	1314	1238	1484	-
58	3288, 3275	3171	1118	2960, 2869	1329	1214	1469	-
L6	3376, 3350	3055	1066	2939, 2838	1399	1271	1485	-
59	3400, 3392	3168	1104	2962, 2869	1329	1214	1467	-
L7	3381, 3301	3055	1084	2955, 2867	1363	1184	1479	-
60	3292, 3285	3172	1105	2958, 2870	1329	1217	1472	-
L8	-	-	-	2932, 2849	-	-	1444	-
61	-	3167	1119	2927, 2853	1328	1272	1452	-
L9	3367, 3292	3052	1095	2929, 2854	1306	1434	1586	-
62	3392, 3326	3148	1103	2962, 2870	1329	1215	1497	-
L10	-	3050	-	2920, 2850	1370	-	1455	-
63	-	3175	1105	2962, 2870	1329	1215	1469	-
L11	-	3049	-	2923, 2853	1365	-	1452	-
64	-	3172	1106	2963, 2870	1329	1216	1467	-
L12	3285	-	-	2934, 2841	1324	1256	1442	-
65	3333	3172	1117	2920, 2852	1329	1215	1469	-

The ^{1}H NMR chemical shifts of free ligands and their complexes (**56-65**) are given in Table 6.2. ^{1}H NMR data showed significant shift in carbene moiety between precursor **38** and their complexes (**56-65**). ^{1}H NMR chemical shift of NH in free ligands (**L2-L5** and **L7**) was observed in the range (1.09-2.02 ppm) and shifted downfield for their complexes (**57-60** and **62**) in range (1.17-2.21 ppm). For all free ligands, ^{1}H MNR data of H─C─P moiety observed downfield to their complexes due to back donation from gold ion to π* P─C bond.

^{13}C NMR chemical shifts for free ligands and their complexes are summarized in Table 6.3. ^{13}C NMR chemical shift (C=Au) for precursor **38** was observed at 175.3 ppm. whereas, for their complexes was shifted downfield in the range (187.9-207.2 ppm) likely due to weaker back bonding from gold ion to π* P─C bond.

.

Table 6.2. ^{1}H NMR chemical shifts (ppm) for free ligands and gold(I) complexes (**56-65**) in $CDCl_3$.

Ligand/ complex	3H	4H	5H	6H	7H	8H	9H	10H	11H	12H	13H	NH
38	7.39 d	7.55 t	2.46 m	1.33 d	1.21 d	7.98 s	-	-	-	-	-	-
L3	-	-	-	-	-	-	2.36 t	2.10 t	7.53 dd	7.45dd	-	-
56	7.36 d	7.61 t	2.54 m	1.13 d	1.26 d	7.33 s	2.43 t	2.15 t	7.55 dd	7.51 dd	-	-
L4	-	-	-	-	-	-	2.59 m	1.69 m	2.06, 1.21 m	1.95 m	0.87 m	2.02
57	7.35 d	7.55 t	2.63 m	1.33 d	1.24 d	7.50 s	3.08 m	1.64 m	2.51, 1.24 m	2.09 m	1.00 m	2.12
L5	-	-	-	-	-	-	4.41 d	4.40 dd	7.82 m	7.14 m	7.44m	1.8
58	6.67 d	6.88 t	2.60 m	1.31 d	1.32 d	5.60 s	4.24 d	3.70 dd	7.92 m	6.95 m	7.75 m	2.17
L6	-	-	-	-	-	-	3.99 d	2.73,183 d	7.41 m	7.11 m	-	1.99
59	6.62 d	6.87 t	2.59 m	1.31 d	1.27 d	5.31 s	3.72 d	2.70, 240 d	7.54 m	7.08 m	-	2.16
L7	-	-	-	-	-	-	2.90 dd	2.40,1.83 d	7.78 m	7.34 m	0.94 m	2.14
60	6.81 d	6.91 t	2.87 m	1.35 d	1.27 d	5.79 s	3.09 s	2.47,1.87 d	7.68 m	7.53 m	0.71 m	2.18
L8	-	-	-	-	-	-	1.66	1.89, 1.22	1.80, 138	1.73, 1.58	-	-
61	7.34 d	7.49 t	2.46 m	1.25 d	1.20 d	5.24 s	1.41	1.76, 0.89	1.65, 1.04	1.60, 1.18	-	-
L9	-	-	-	-	-	-	1.50 m	1.99 p	2.69 t	7.25 m	7.35 t	1.09
62	7.50 d	7.59 t	2.33 m	1.24 d	1.20 d	7.13 s	1.27 m	1.92 p	2.54 t	7.33 m	7.41 t	1.17
L10	-	-	-	-	-	-	1.62 t	2.36 t	7.30 m	7.36 m	-	-
63	7.39 d	7.64 t	2.49 m	1.17 d	0.91 d	8.20 s	1.21 t	2.20 t	6.96 m	7.59 m	-	-
L11	-	-	-	-	-	-	2.10 t	7.30 m	7.32 m	-	-	-
64	7.32 d	7.54 t	2.41 m	1.19 d	1.01 d	7.76 s	1.79 t	6.74 m	7.47 m	-	-	-
L12	-	-	-	-	-	-	3.94, 378 m	2.97,2.14 m	3.18 m	1.76 m	1.56 m	-
65	7.29 d	7.49 t	2.46 m	1.23 d	1.21 d	7.42 s	3.68 m	2.23 m	2. 35 m	1.69 m	1.49 m	-

Table 6.3. ^{13}C NMR chemical shifts (ppm) for free ligands and gold(I) complexes (**56-65**) in $CDCl_3$.

Ligand/ complex	C1	C2	C3	C5	C6	C8	Au=C	C10	C11	C12	C13	C14	C15	C16	C17	C18
38	145.5	130.7	133.9	28.8	24.5	124.2	175.3	-		-		-	-	-	-	-
L3								119.1	14.1	23.9	133.2	132.6	129.2	-	-	-
56	144.5	130.1	132.4	27.7	23.5	124.1	187.9	110.8	11.9	21.4	131.9	128.6	128.5	-	-	-
L4								52.5	43.8	24.8	27.3	26.2	36.6	135.6	132.3	128.3
57	145.9	131.0	133.5	28.4	24.9	124.1	190.3	56.5	42.4	24.4	28.8	25.2	38.8	134.1	132.7	129.3
L5								58.8	53.4	143.6	137.6	136.9	133.7	128.7	127.6	126.2
58	145.3	131.7	132.9	28.7	24.4	124.5	207.2	60.7	52.7	146.0	134.9	133.5	133.2	128.6	127.2	125.1
L6								53.7	39.4	145.6	138.4	132.9	128.7	126.2	-	-
59	145.9	131.1	133.0	28.7	24.6	124.6	189.1	45.1	37.0	143.8	133.6	132.2	127.9	126.1	-	-
L7								32.3	57.4	34.6	25.7	139.6	133.4	128.8	-	-
60	145.5	131.1	133.3	28.8	24.6	124.6	188.6	32.9	59.5	36.0	25.6	133.2	130.7	128.8	-	-
L8								31.0	35.5	27.6	26.5	-	-	-	-	-
61	145.7	130.9	133.4	28.8	24.5	124.7	193.1	32.8	34.4	26.7	25.5	-	-	-	-	-
L9								25.2	30.0	43.3	138.6	132.4	128.3	-	-	-
62	145.9	131.2	133.3	28.9	24.7	125.0	190.6	24.5	28.5	41.9	132.8	129.4	128.8	-	-	-
L10								29.6	22.4	138.6	132.7	128.4	-	-	-	-
63	145.2	130.9	132.5	28.8	23.5	125.6	188.9	26.4	19.1	132.9	129.5	127.7	-	-	-	-
L11								23.7	137.9	132.6	128.3	-	-	-	-	-
64	145.2	130.8	132.2	28.3	24.3	125.2	188.7	22.8	132.7	129.5	126.0	-	-	-	-	-
L12	-	-	-	-	-	-	-	46.9 30.0	30.2 32.9	33.0 28.8	28.9 27.1	27.2	26.3	-	-	-
65	145.7	131.0	133.2	29.5	24.4	124.5	193.1	47.0	29.5 33.0	26.4 28.6	25.4 26.3	-	-	-	-	-

^{31}P NMR chemical shifts (ppm) for free ligands and gold(I) complexes (**56-65**) are given in Table 6.4. The resonance values for free ligands are in the range (-25.14─ -9.22 ppm), whereas those of their complexes were observed downfield in the range (30.26─46.46 ppm) due to back donation from gold ion to π* P─C bond. Expect for **L8** appearing at 9.33 ppm and complex **61** observed upfield at -44.54.

Table 6.4. ^{31}P NMR chemical shifts (ppm) for free ligands and gold(I) complexes (**56-65**) in $CDCl_3$.

Compound	^{31} P δ(ppm)
38	-
L3	-25.14
56	34.30
L4	-09.22
57	46.46
L5	-10.65
58	33.64
L6	-23.59
59	30.26
L7	-21.24
60	32.53
L8	09.33
61	-44.54
L9	-17.80
62	34.47
L10	-19.08
63	31.88
L11	-14.26
64	35.55
L12	-10.41
65	41.79

6.3.2 Signal crystal X-ray structure

The structure of complexes **56**, **61**, **63** and **65** were determined using STOE IPDS 2 system at 203-293K with a two-circle goniometer and MoK_{α} graphite monochromatic radiation[127]. Structures were solved using the program SHELXS-97 [178-180]. The non-hydrogen atoms were refined using least-squares matrix on F^2. The molecular structures of complexes are consistent with spectroscopic data and are illustrated in Figures (6.1─6.4). The coordination geometry around gold(I) ion is distorted from linearity with angle (C─Au─P) of 177.0(4)º, 179.9(3)º, (173.1(6) and 174.4(6)º [181]. The bond lengths and bond angles for complexes **56, 61** and **63** are illustrated in Tables 6.5, 6.7 and 6.9. Summary of crystal data and details of the structure refinement for complex (**56**, **63** and **65)** are shown in Tables 6.6, 6.8 and 6.10.

The pronounced distortion in compound **63** (173.1(6). The C─Au and Au─P bond lengths (Å) are 2.052(14); 2.022 (11); 2.060(2) and 2.261(5); 2.295(3); 2.280(6) are similar to those reported [182].

The hydrogen-bond (Å) for complex **61** is found to be PF_6----H─CCl_3 between (F1) of counter ion (PF_6^-) and hydrogen of ($CHCl_3$) as solvent. The hydrogen bond length (Å) and bond angle (º) are H----F1 2.25(5) and C─H----F1 is 170º, rrespectively.

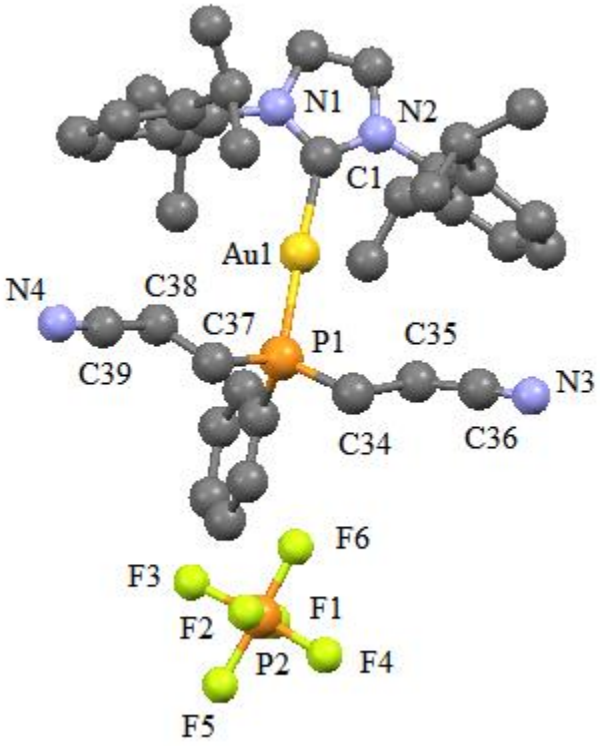

Figure 6.1. *Molecular structure of complex 56, with partial labelling atoms and 50% probability ellipsoids. Hydrogen atoms have been omitted for clarity.*

Table 6.5. Selected bond lengths and bond angles for complex **56**.

Bond Length (Å)		**Bond Angles (°)**	
P1—Au1	2.261 (5)	C1—Au1—P1	177.0 (4)
C1—Au1	2.052 (14)	C28—P1—Au1	115.0 (5)
C1—N1	1.285 (17)	C34—P1—Au1	112.0 (6)
C2—N2	1.353 (17)	C37—P1—Au1	112.4 (6)
C28—P1	1.834 (15)	N2—C1—Au1	126.5 (9)
C34—P1	1.827 (15)	N1—C1—Au1	127.0 (11)
C37—P1	1.837 (15)	N1—C1—N2	106.4 (12)

Table 6.6. Summary of crystal data and details of the structure refinement for complex **56.**

Complex 56	**Experimental details**
Crystal data	
Empirical formula	$C_{39}H_{49}AuN_4P_2F_6$
Formula weight	946.75
Wavelength/Å	0.71073
Temperature/K	293(2)
Crystal symmetry	Monoclinic
Crystal color	colorless
Space group	*Cc*
Cell lengths (Å)	**a**=17.053 (1), **b**=17.959 (2), **c**= 13.483 (1)
Cell Angles (°)	**α**= 90.000, **β**= 91.026 (7), **γ**= 90.000
D_x	1.392 Mg m^{-3}
μ	3.64 mm^{-1}
Radiation type	Mo *K*α
Cell volume ($Å^3$)	4128.6 (6)
Z	4
Data collection	
Diffractometer	*STOE IPDS 2*
Absorpance correction	Not given
Radiation source	fine-focus sealed tube
Radiation monochromator	plane graphite
$(\sin\theta/\lambda)_{max}$ ($Å^{-1}$)	0.686
Refinement	
$R[F^2 > 2\sigma(F^2)]$, $wR(F^2)$, S	0.061, 0.173, 1.09
$\Delta\rho_{max}$	4.01 e $Å^{-3}$
$\Delta\rho_{min}$	−1.63 e $Å^{-3}$
H-atom treatment	H atoms treated by a mixture of independent and constrained refinement

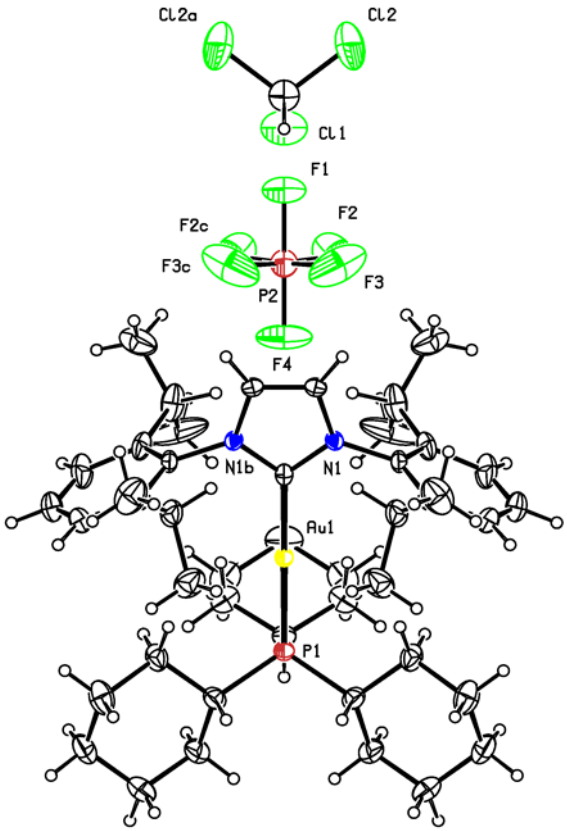

***Figure 6.2**. Molecular structure of complex 61, with partial labelling atom and 50% probability ellipsoids.*

Table 6.7. Selected bond lengths and bond angles for complex **61**.

Bond Length (Å)		**Bond Angles (°)**	
P1—Au1	2.295 (3)	C1—Au1—P1	179.9 (3)
C1—Au1	2.022 (11)	C15—P1—Au1	110.7 (3)
N1—C1	1.355 (8)	C21—P1—Au1	110.1 (3)
P1—C15	1.386 (7)	N1—Au1—C1	128.2 (4)
P1—C21	1.387 (9)		

Table 6.8. Summary of crystal data and details of the structure refinement for complex **61**.

Complex 61	**Experimental details**
Crystal data	
Empirical formula	$C_{46}H_{70}AuCl_3N_2P_2F_6$
Formula weight	1130.29
Wavelength/Å	0.71073
Temperature/K	203
Crystal symmetry	Orthorhombic
Crystal color	Plate, colorless
Crystal size/ mm	0.40 x 0.22 x 0.03
Space group	$Cmc2_1$
Cell lengths (Å**)**	**a**=17.2904 (7), **b**=18.2392 (11), **c**= 16.1154 (7)
Cell Angles (°)	**α**= 90.000 (5), **β**= 90.000 (5), **γ**= 90.000 (5)
D_x	1.477 Mg m^{-3}
μ	3.17 mm^{-1}
Radiation type	Mo *K*α
Cell volume ($Å^3$)	5082.2(4)
Z	4
Data collection	
Diffractometer	*STOE IPDS 2*
Absorpance correction	Multi-scan (*MULABS*; Spek, 2009)
Radiation source	fine-focus sealed tube
Radiation monochromator	plane graphite
T_{min}, T_{max}	0.746, 1.000
$(\sin\theta/\lambda)_{max}$ ($Å^{-1}$)	0.622
Refinement	
$R[F^2 > 2\sigma(F^2)]$, $wR(F^2)$, S	0.024, 0.047, 0.90
$\Delta\rho_{max}$	0.95 e $Å^{-3}$
$\Delta\rho_{min}$	−0.61 e $Å^{-3}$
H-atom treatment	H atoms treated by a mixture of independent and constrained refinement

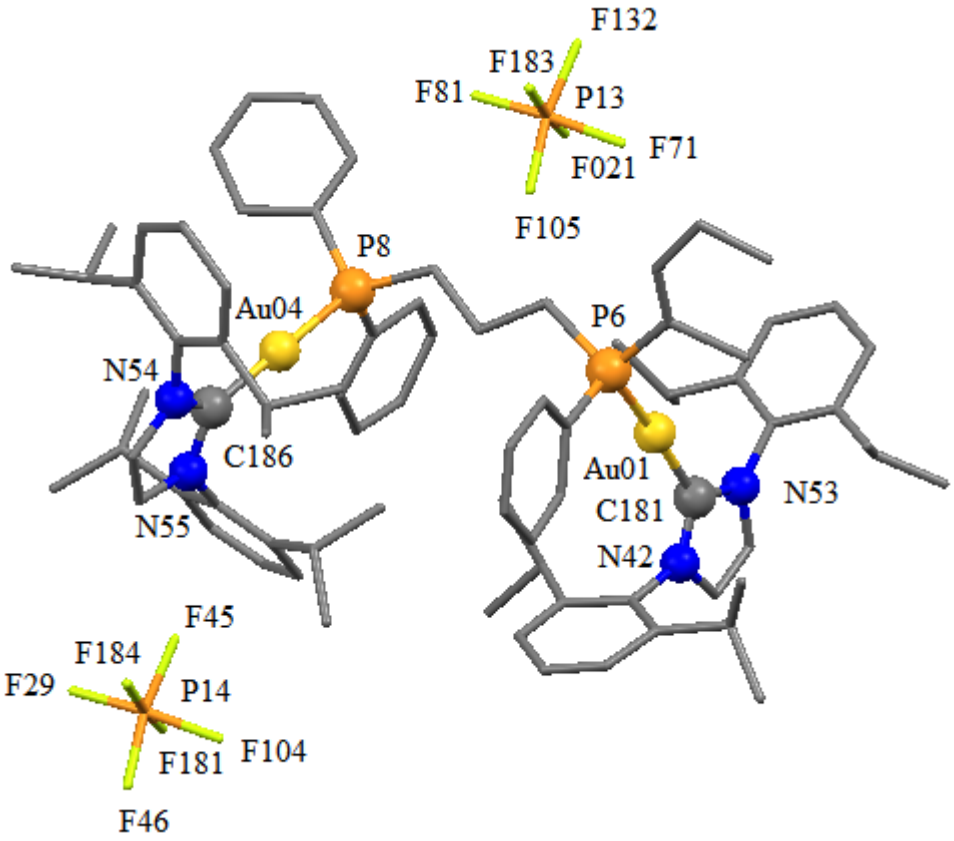

Figure 6.3. *Molecular structure of binuclear complex 63, with partial labelling atoms and 50% probability ellipsoids. Hydrogen atoms have been omitted for clarity.*

Table 6.9. Selected bond lengths and bond angles for complex **63**.

Bond Length (Å)		**Bond Angles (°)**	
Au01—P6	2.28 (6)	P6—Au01—C181	174.4 (6)
Au01—C181	2.06 (2)	P8—Au04—C186	173.1 (6)
Au04—P8	2.27 (7)	Au01—C181—N42	122.0 (2)
Au08—C186	1.97 (2)	Au01—C181—N53	130.0 (2)
N42—C181	1.32 (3)	N42—C181—N53	107.0 (2)
N53—C181	1.31 (3)	Au04—C186—N54	134.0 (2)
N54—C186	1.37 (3)	Au04—C186—N55	124.0 (2)
N55—C186	1.42 (3)	N54—C186—N55	102.0 (2)

Table 6.10. Summary of crystal data and details of the structure refinement for complex **63**.

Complex 63	**Experimental details**
Crystal data	
Empirical formula	$C_{81}H_{98}$ $Au_2F_{12}N_4P_4$
Formula weight	1873.48
Wavelength/Å	0.71073
Temperature/K	293(2)
Crystal symmetry	monoclinic
Space group	P 21/c
Cell lengths (Å)	**a**=18.819 (5), **b**=22.480 (5), **c**= 42.175 (5)
Cell Angles (°)	**α**= 90.000 (5), **β**= 94.936 (5), **γ**= 90.000 (5)
D_x	1.686 Mg m^{-3}
μ	385.24 mm^{-1}
Radiation type	Mo *K*α
Cell volume ($Å^3$)	17776(7)
Z	4
Data collection	
Radiation source	fine-focus sealed tube
Radiation monochromator	graphite
T_{min}, T_{max}	0.39, 1.000
$(\sin\theta/\lambda)_{max}$ ($Å^{-1}$)	0.577
Refinement	
$R[F^2 > 2\sigma(F^2)]$, $wR(F^2)$, S	0.164, 0.429, 2.47
$\Delta\rho_{max}$	10.15 e $Å^{-3}$
$\Delta\rho_{min}$	−7.65 e $Å^{-3}$
H-atom treatment	H atoms treated by a mixture of independent and constrained refinement

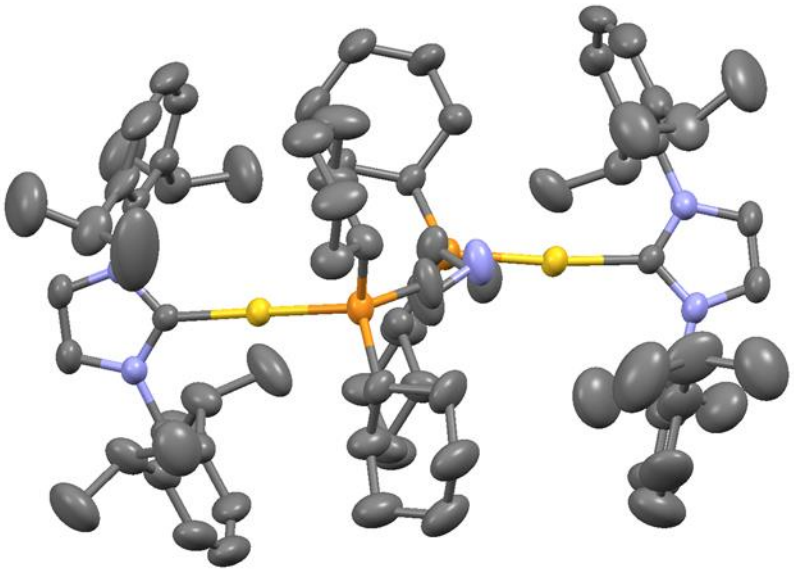

Figure 6.4. *Molecular structure of binuclear complex 65, with 50% probability ellipsoids. Hydrogen atoms have been omitted for clarity.*

CHAPTER 7

SPECTROSCOPIC STUDIES OF INTERACTIONS OF THE POTENTIAL ANTICANCER AGENTS [Au(*cis*-DACH)Cl_2]Cl AND [Au(*cis*-DACH)$_2$]Cl_3 WITH BIOLOGICALLY RELEVENT THIONES

7.1 Introduction.

The study of metallo-drugs, containing sulfur donor ligands, with interesting physical, chemical, biological and pharmacological properties have attracted attention [183-184]. Among these, gold complexes are a new class of metal-based drugs with promising potential antitumor properties [23]. Notably, a number of gold(I) and gold(III) complexes are reported to possess cytotoxic effects against selected human cancer cell lines [185], gold(I)-thiolates as anti-arthritic [186-187] and antitumor drugs [8,138,188]. In contrast, the pharmacological behavior of gold(III) derivatives containing thiols and thiones is unclear and is an underdeveloped field in modern inorganic chemistry [133]. These compounds have the ability to form uranophilic bond [49-50]. Gold(III) is isoelectronic

and square planar structure similar to Pt(II), and the interaction of their complexes with thiols and thiones have been widely reported [189].

Ghosh et al. studied kinetics of the interaction of Pd(II) imidazole derivative and 2-aminopyrimidine and they concluded their study with a proposed mechanism [190]. Moreover, the kinetic and mechanistic studies were carried out for the interaction of *cis*-$[Pt(en)(H_2O)_2](ClO_4)_2$ and *cis*-$[Pt(dmen)(H_2O)_2](ClO_4)_2$, where en = ethylenediamine and dmen = *N*,*N*-dimethyl-ethylenediamine, with glycine under pseudo fist-order conditions as a function of temperature, pH and ligand concentration [191]. Ray et al. evaluated activation parameters of kinetics for the substitution reactions of *cis*$[Pt(cis\text{-}DACH)(H_2O)_2]^{2+}$, DACH=1,2-diaminocyclohexane, with dipeptides containing glycine, glutathione and penicillamine under pseudo first-order conditions dependent on pH, ligand [192].

The oxidation of thiols and thioether groups that are part of amino acids, via metal ions, has been investigated for decades due to their important role in function and structure of proteins [193]. The interaction of $[Au(CN)_4]^-$, $[Au(terpy)Cl]^{2+}$, $[Au(bpma)Cl]^{2+}$, $[Au(dien)Cl]^{2+}$ and $[AuCl_4]^-$, where terpy =2,2', 6',2''-terpyridine, bpma = bis(pyridyl methyl)amine, dien = diethylene-triamine, with the biologically relevant thiols and thioether, such as L-Cysteine, glutathione and L-methionine, has been studied [106,194]. These studies were conducted by cyclic voltammetry (CV), ESI-MS, ^1H NMR and UV-Vis spectroscopy. In addition, researchers extensively studied kinetics and mechanism of redox reactions of Au(I) and Au(III) complexes to investigate their ligand exchange reactions and metabolism [195-196]. The kinetics of the formation and equilibrium hydrolysis of $[AuBr_4]^-$ and $[AuCl_4]^-$ have been studied and found to follow

a two-term rate law [197]. The study showed that their hydrolysis are faster than the analogous Pt(II) complexes.

The preparation and characterization of new gold(III) compounds with DACH was reported [198], the effect of stereochemistry of DACH on tumor activity, and the *cis*-DACH isomer showed the highest activity against human cancer cell lines such as prostate cancer (PC-3) and gastric carcinoma (SGC-7901). We report the interaction of [Au(*cis*-DACH)Cl_2]Cl and [Au(*cis*-DACH)$_2$]Cl_3 with enriched thiourea (Tu) and 1,3-diazinane-2-thione (DIAZ) by ^{1}H, ^{13}C and ^{15}N NMR spectroscopy, UV-Vis spectroscopy, and electrochemistry. We also present the kinetics of these interactions.

7.2 Experimental Section

7.2.1 Materials and Instrumentation

$NaAuCl_4.2H_2O$ and *cis*-DACH were purchased from Sigma-Aldrich, USA; absolute EtOH from Merck, D_2O from Alfa-Aesar, and thiourea from Cambridge Isotope Lab. Inc. DIAZ was prepared as described [171]. Deionized water with a resistivity of 18.6 MΩ cm^{-1} was used to prepare all solutions. It was obtained directly from a PURELABs Ultra Laboratory Water Purification System.

7.2.2 Spectroscopic techniques

^{1}H NMR spectra were recorded on a JEOL-LA 500 MHz NMR spectrophotometer. The spectral conditions were: 32k data point, 3.2 s acquisition time, and 5.75 μs pulse width. ^{13}C NMR measurements were recorded at 125.65 MHz with ^{1}H broadband decoupling. The spectral conditions were: 32k point data, 1s acquisition time, 2.5s pulse delay, and

5.12 μs pulse width. ^{15}N NMR spectra were recorded at 50.53 MHz with benzamide as external reference (932.56 ppm) relative to internal reference NH_4NO_3 (375.11 ppm). All spectra were recorded at 297 K in D_2O using tetramethylsilane (TMS) as internal standard.

7.2.3 Electrochemical technique

A CHI660 potentiostat was used for all square wave stripping voltammetric (SWSV) measurements. The electrochemical cell contained a glassy carbon electrode (GCE; 3.0 mm diameter, Model CHI104, CH Instruments, Austin, TX) as a working electrode, Ag/AgCl (sat. KCl) reference electrode (Model CHI111, CH Instruments, Austin, TX), and a platinum wire counter-electrode were inserted into a 2-mL glass cell through holes in its Teflon cover. Prior to each SWSV measurement, the GCE was polished with 3.0 and 0.05 μm alumina slurries and washed with double-distilled water. Each SWSV measurement was performed at room temperature in a quiescent 0.2 M KCl aqueous solution, and with an initial potential of 0.0V and final potential of +1.6V.

7.2.4 Synthesis of [Au(cis-DACH)Cl_2]Cl

[Au(*cis*-DACH)Cl_2]Cl was synthesized as described in the literature [199]. λ_{max} = 305 nm. ^1H NMR, ppm, δ: 3.59 m, 2.02 m, 1.76 m, 1.47 m, and 1.29 m. ^{13}C NMR, ppm, δ: 63.3, 26.8, and 21.4. Anal. Found (calculated) for $C_6H_{14}AuCl_3N_2$ (417.51 g/mol): C, 17.22 (17.26); H, 3.38 (3.35); N, 6.67 (6.71).

7.2.5 Synthesis of [Au(cis-DACH)$_2$]Cl_3

[Au(*cis*-DACH)$_2$]Cl$_3$ was synthesized as described in the literature [199]. λ_{max} = 344 nm. ^{1}H NMR, ppm, δ: 3.58 m, 1.94 m, 1.74 m, 1.54 m, 1.38 m. ^{13}C NMR, ppm, δ: 61.7, 61.6, 26.3, 26.1 and 20.6. Anal. Found (calculated) for $C_{12}H_{28}AuCl_3N_4$ (531.70 g/mol): C, 27.02 (27.11); H, 5.28 (5.31); N, 10.61 (10.54).

7.2.6 Kinetic Measurements

The kinetic measurements were carried out on a Cary 100 UV-Vis spectrophotometer (Agilent Technologies) connected with a Cary temperature controller (accuracy = ± 0.1 °C). The working wavelengths were determined over the wavelength range (200 -500 nm) (Fig. 7.11). The reactions were started by mixing the complex in 30 mM KCl solution and ligand solutions in equal volumes directly in a vial kept inside the instrument. The kinetic measurements were made under pseudo first-order conditions, where concentration of the complex is 0.2 mM with excess ligands (2-10 mM). The reactions were carried out at different temperatures of 288.2, 298.2 and 310.2 K. The pseudo firs-order rate constant k_{obsd} was calculated as an average value of seven independent kinetic runs. All calculations were maintained using Microsoft Excel, Origin 8.

7.3 Results and Discussion

7.3.1 Interaction of [Au(*cis*-DACH)Cl$_2$]Cl and [Au(*cis*-DACH)$_2$]Cl$_3$ with enriched Tu and DIAZ

Interactions of [Au(*cis*-DACH)Cl$_2$]Cl and [Au(*cis*-DACH)$_2$]Cl$_3$ with enriched 10 % Tu (^{13}C,^{15}N) and DIAZ were carried out in D_2O using different concentrations of Tu and

DIAZ. The reaction products were monitored by ^{1}H, ^{13}C and ^{15}N NMR, UV-Vis spectroscopy and electrochemistry. The interaction of [Au(*cis*-DACH)Cl_2]Cl and [Au(*cis*-DACH)$_2$]Cl_3 with Tu was monitored by ^{13}C NMR as shown in (Fig. 7.1). Fig. 7.1a shows the ^{13}C NMR spectrum of 1 mg Tu (^{13}C enriched), and Fig. 1b shows the ^{13}C NMR spectrum of the oxidation reaction of Tu by H_2O_2, which resulted in the formation of urea $(NH_2)_2CO$ and Tu dioxide, $(NH_2)_2CO_2S$ [200-201]. When enriched Tu (0.25 eq.) was added to 1 eq. of [Au(*cis*-DACH)Cl_2]Cl, their solution changed to yellow colour (Fig. 7.1A-c) and the ^{13}C NMR peak of enriched Tu was observed up-field at 179.68 ppm due to complexation, similar to previous observations [96]. Whereas, no peak was observed for [Au(*cis*-DACH)$_2$]Cl_3 at the same conditions. Figure 7.1A-d shows the formation of [Au(*cis*-DACH)Tu_2]$^{3+}$ at 164.59 ppm, which is consistent with Fig. 7.1B-c of [Au(*cis*-DACH)$_2$]Cl_3 at the same mole ratio (1: 0.5). Upon addition of enriched Tu to the solutions complex: Tu (1:1) and (1:4) of [Au(*cis*-DACH)Cl_2]Cl and [Au(*cis*-DACH)$_2$]Cl_3 respectively, a colourless solution was observed with yellow precipitation due to the reduction of Au(III) to Au(I) [202], as shown in Fig.7.1(A-e), Fig. 7.1(A-f) and Fig. 7.1(B-d). The signal at 164.59 ppm remained constant and two new intense signals at 182.04 ppm and 184.87 ppm, which appeared as triple due to ^{15}N coupling [203-204]. The ^{13}C NMR chemical shifts of different species in the interaction progress are shown in Table 7.1.

Table 7.1. ^{1}H, ^{13}C NMR chemical shifts of the free ligand enriched (Tu), the [Au(cis-DACH)Cl_2]Cl (A) and [Au(cis-DACH)$_2$]Cl_3 (B) complexes in D_2O.

Ligand/ complex	**^{1}H, ^{13}C(δ in ppm)**																	
	C=S (C1)		**C2,C3**		**C4,C7**		**C5,C6**		**2H, 3H**		**4H, 7H eq**		**4H, 7H ex**		**5H, 6Heq**		**5H, 6H ex**	
	A	**B**	**A**	**B**	**A**	**B**	**A**	**B**	**A**	**B**	**A**	**B**	**A**	**B**	**A**	**B**	**A**	**B**
Tu	185.6	-	-	-	-	-	-	-	-	-	-	-	-	-	-	-	-	-
Tu + H_2O_2	169.5	164.5	158.5	-	-	-	-	-	-	-	-	-	-	-	-	-	-	-
(1: 0)	- -	- -	63.3 -	61.7 61.6	26.7 -	26.3 26.1	21.4 -	20.6 -	3.59 m	3.58 m	2.02 m	1.94 m	1.76 m	1.74 m	1.47 m	1.54 m	1.29 m	1.38 m
(1: 0.25)	179.9 -	- -	63.3, 51.4	- -	26.7, 27.2	- -	21.4	- -	3.67 m	- -	2.01 m	- -	1.89 m	-	1.59 m	-	1.49 m	-
(1: 0.5)	164.5 -	173.5 -	51.5 -	50.1 -	27.1, 26.1	26.4 -	21.7 20.5	20.8 -	3.72 m	3.68 m	1.92 m	-	1.73 m	1.80 m	1.60 m	1.55 m	1.32 m	1.49 m
(1: 1)	164.5 182.0	166.2 -	51.3 -	50.6 -	27.0 -	26.4 -	21.6 -	20.8 -	3.70 m	3.68 m	1.91 m	-	1.74 m	1.80 m	1.60 m	1.56 m	1.34 m	1.47 m
(1: 4)	164.5 184.8 174.5 157.5	181.7	51.4	50.7	27.1	26.5	21.7	20.9	3.70 m	3.65 m	1.92 m	-	1.73 m	1.77 m	1.60 m	1.52 m	1.34 m	1.47 m

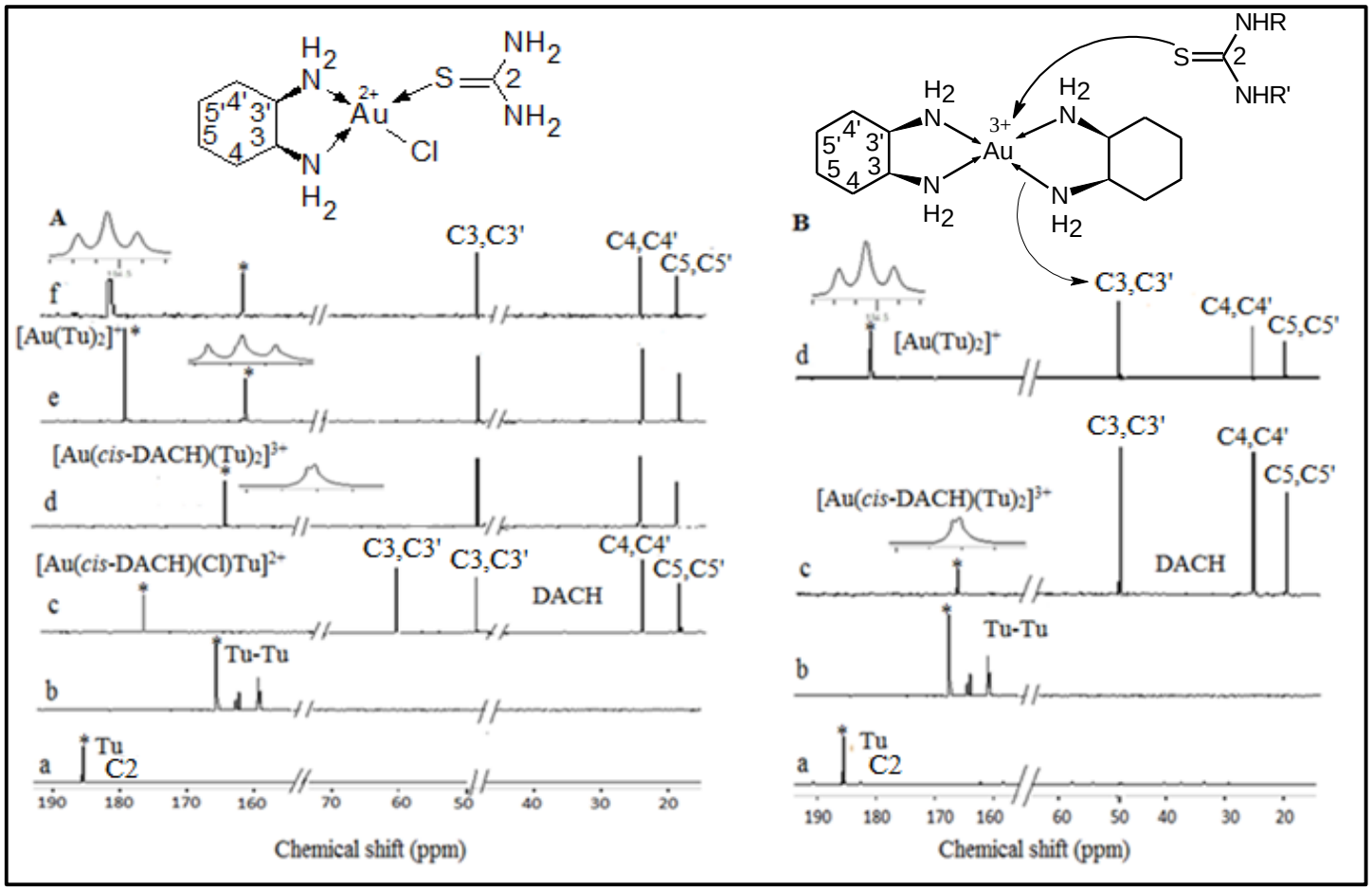

Figure 7.1. *(A) ^{13}C NMR spectra for: free Tu (a), oxidation of Tu by H_2O_2 (b), the reaction of [Au(cis-DACH)Cl_2]Cl and Tu, 1:0.25 (c), at 1:0.5 (d), at 1:1 (e), and at 1: 4 (f). (B) ^{13}C NMR spectra for: free Tu (a), oxidation of Tu by H_2O_2 (b), the react of [Au(cis-DACH)$_2$]Cl_3 with Tu at 1:1(**c**), and at 1:4 (**d**). All spectra were recorded in D_2O.*

^{15}N NMR spectrum of the reaction of enriched Tu (^{13}C, ^{15}N) with [Au(*cis*-DACH)Cl_2]Cl (Fig. 7.2-A) shows a peak for free Tu at 583.26 ppm. An up-field shift to 409.17 ppm and 244.55 ppm at complex: Tu (1:1) and (1:2) mole ratio, respectively, indicates consecutive replacement of chloride. At complex: Tu (1:4 eq.), [Au(*cis*-DACH)Cl_2]Cl was reduced to colourless $[Au(Tu)_2]^+$, which was confirmed by a peak at 538.07 ppm [101]. Similarly, the reaction of the same ligand with [Au(*cis*-DACH)$_2$]Cl_3 showed three peaks: 403.56 ppm at (1:1), as well as 277.15 ppm and 538.58 ppm at (1:2), which are indicative for the presence of $[Au(cis\text{-}DACH)_2Tu]^{3+}$, $[Au(cis\text{-}DACH)(Tu)_2]^{3+}$ and $[Au(Tu)_2]^+$, respectively (Fig. 7.2 B).

The substitution reaction of [Au(*cis*-DACH)Cl_2]Cl and Tu was studied by UV-Vis spectroscopy in aqueous solution containing 30 mM KCl at pH 3.5. Two bands at 390 nm and 249 nm, assigned to $[Au(cis\text{-}DACH)(Tu)Cl]^{2+}$ and $[Au(cis\text{-}DACH)(Tu)_2]^{3+}$, respectively, were observed, which are attributed to charge transfer from metal to ligand (M→Tu). The bands at 237 nm and 230 nm represent a redox reaction, assigned to $[Au(Tu)_2]^+$ Fig. 7.3 [101].

We then studied the interaction of [Au(*cis*-DACH)Cl_2]Cl and [Au(*cis*-DACH)$_2$]Cl_3 with Tu in aqueous solution containing 0.2 M KCl by square wave stripping voltammetry. Well-defined SWSV peaks are obtained at +0.82V and +1.35V (vs. Ag/AgCl) for 0.48 mM [Au(*cis*-DACH)Cl_2]Cl and [Au(*cis*-DACH)$_2$]Cl_3, respectively (Fig. 7.4 and Fig. 7.5). The obtained peak disappeared with the subsequent additions of Tu as in Fig. 7.4 (c-g) and Fig. 7.4 (c-h). The electrochemical results are in agreement with the ^{1}H, ^{13}C and ^{15}N NMR, and UV-Vis spectroscopy and confirmed the suggested mechanism (scheme 23).

Fig. 7.6 shows SWSV voltammetry for different concentrations of Tu itself in 0.2 M KCl solution.

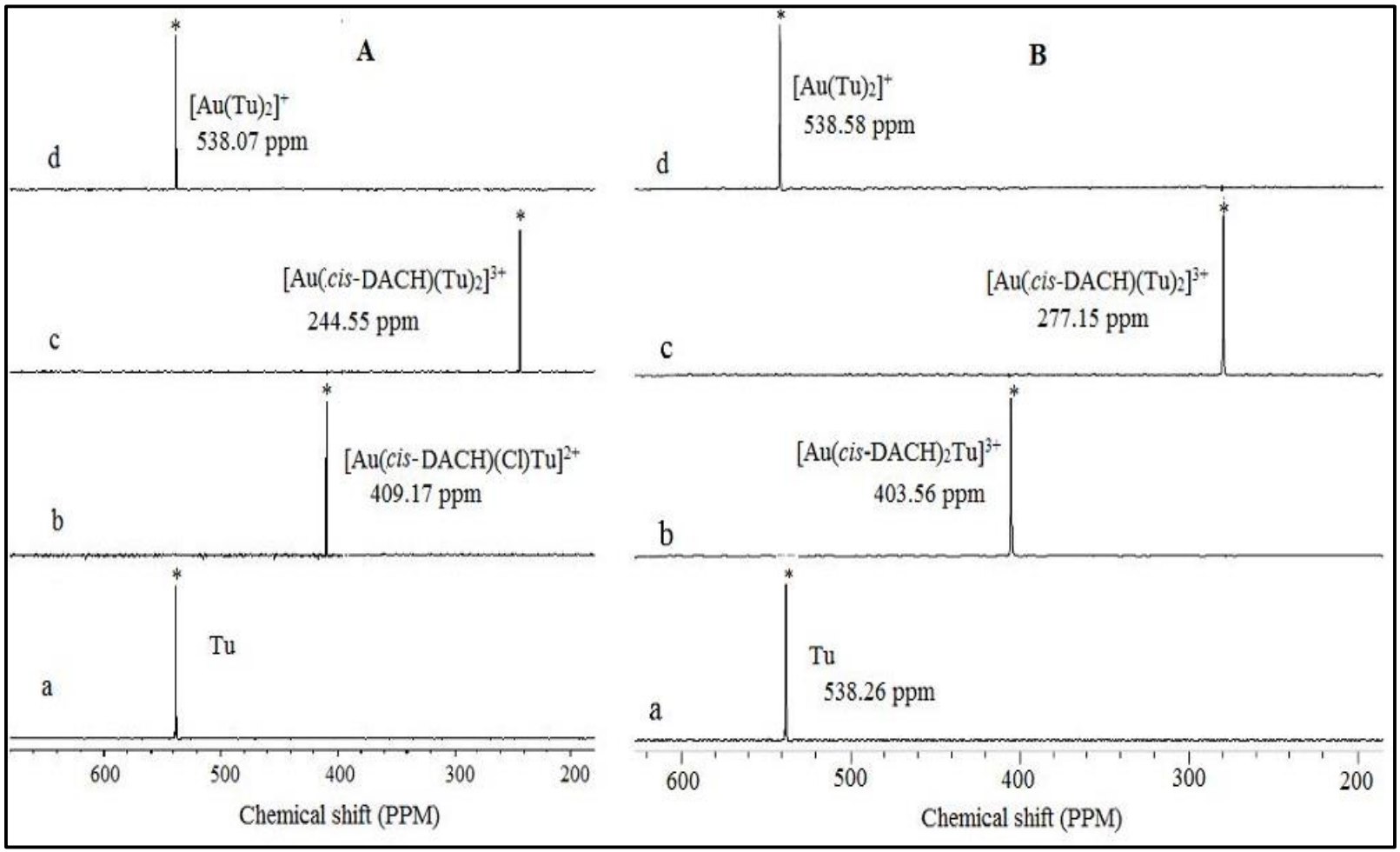

Figure 7.2. *(**A**). ^{15}N NMR spectra of free Tu (**a**), after the reaction with [Au(cis-DACH)Cl_2]Cl at (1:1) (**b**), at (1:2) (**c**) and at (1: 4) (**d**) (**B**). ^{15}N NMR spectra of free Tu (**a**), after the reaction with [Au(cis-DACH)$_2$]Cl_3 at (1:1) (**b**), at (1: 2) (**c**) and at (1:4) (**d**) in D_2O.*

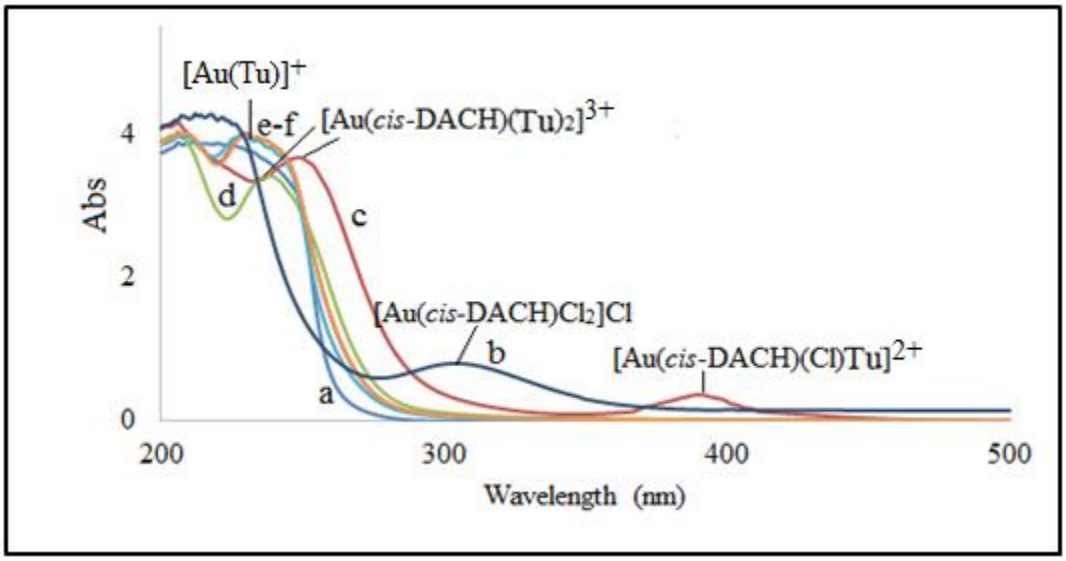

Figure 7.3. *UV-Vis spectra for: ree Tu (0.1 mM) (**a**), after reaction with [Au(cis-DACH)Cl$_2$]Cl (0.1 mM) (**b**), complex: Tu, 1:0.5 (**c**), (1:1) (**d**), (1:2) (**e**) and at (1:4) (**f**) in aqueous solutions containing 30 mM KCl at pH 3.5.*

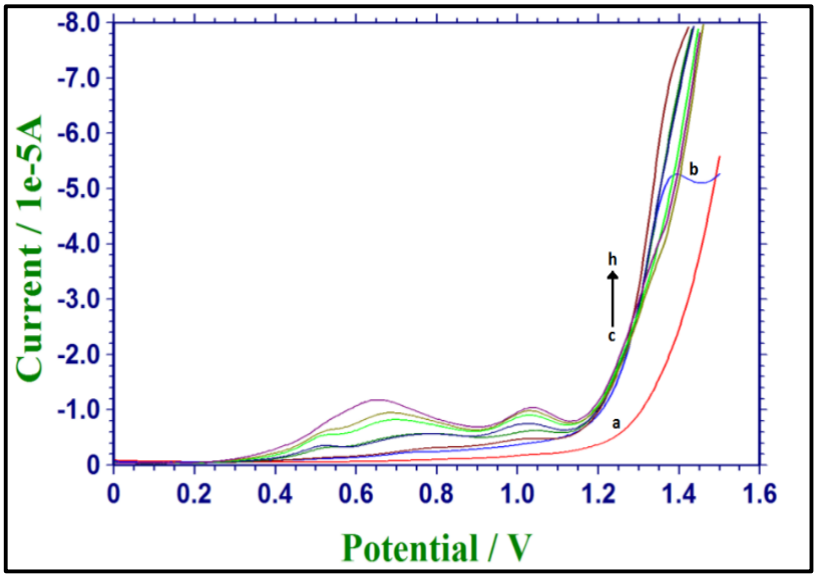

Figure 7.4. *SWSV of ree (a) and presence (b) of 0.48 mM of [Au(cis-DACH)Cl$_2$]Cl in 0.2 M KCl solution. Subsequent additions of 0.24 mM Tu (c-g). Working conditions of the pulse width (increment), 4 mV; pulse height (amplitude), 25 mV; frequency, 15Hz.*

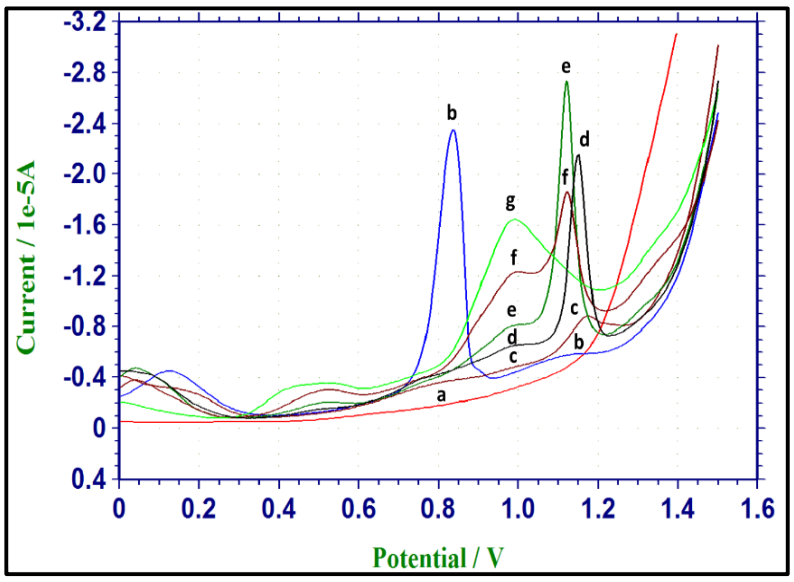

***Figure 7.5**. SWSV of free (a) and presence (b) of 0.48 mM of [Au(cis-DACH)$_2$]Cl$_3$ in 0.2 M KCl solution. Subsequent additions of 0.24 mM Tu (c-h). Working condition of the pulse width (increment), 4 mV; pulse height (amplitude), 25 mV; frequency, 15 Hz.*

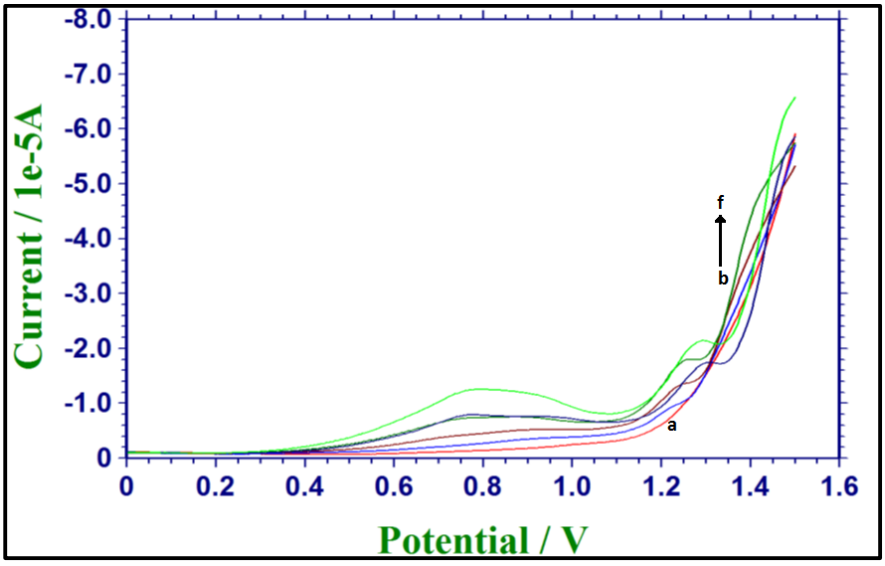

***Figure 7.6.** SWSV of free (**a**) and presence (**b**) of 0.24 mM of Tu in 0.2 M KCl solution. Subsequent additions of 0.48 mM Tu (**b-f**) at pH 3.5. Working condition of the pulse width (increment), 4 mV; pulse height (amplitude), 25 mV; frequency 15 Hz and in aqueous solution.*

We also monitored the interaction of [Au(*cis*-DACH)Cl_2]Cl and [Au(*cis*-DACH)$_2$]Cl_3 with DIAZ by ^{13}C NMR in D_2O, as shown in Fig. 7.7. Fig. 7.7a shows the ^{13}C NMR spectrum of 5 mM of DIAZ, and Fig. 7.7b shows the ^{13}C NMR spectrum of oxidation of DIAZ ($RN_2C=S$) with H_2O_2, which produces RN_2CSSCN_2R. Reaction of both complexes with equimolar of DIAZ resulted in an up-field shift to 164.82 ppm in the ^{13}C NMR (Fig. 7.7 A-c and Fig. 7.7 B-c. Their solutions changed from yellow to orange after 1 hr, and later turned to colourless with white precipitation due to initial reduction of Au(III) to Au(I) and then oxidation of DIAZ to $(DIAZ)_2$ [147, 205]. When [Au(*cis*-DACH)Cl_2]Cl and [Au(*cis*-DACH)$_2$]Cl_3 reacted with 2 eq. of DIAZ (Fig. 7.7A-d and Fig. 7.7B-d, the chemical shift of (C=S) of DIAZ shifted down-field to 169.55 ppm, and the solutions changed to pale yellow with yellow precipitation. At higher concentration of DIAZ (4 eq.), the ^{13}C chemical shift of (C=S) shifted down-field to 172.32 ppm and 171.61 ppm, respectively, (Fig. 7.7A-c and Fig. 7.7B-c) in agreement with that reported [99]. The proof of total reduction of Au(III) specie to Au(I) is confirmed by disappearance of the solution color with yellowish white precipitation.

The evidence for the coordination sulphur of the thione ligand is provided by ^{13}C NMR spectroscopy. The chemical shifts of the complexes are provided in Table 7.2.

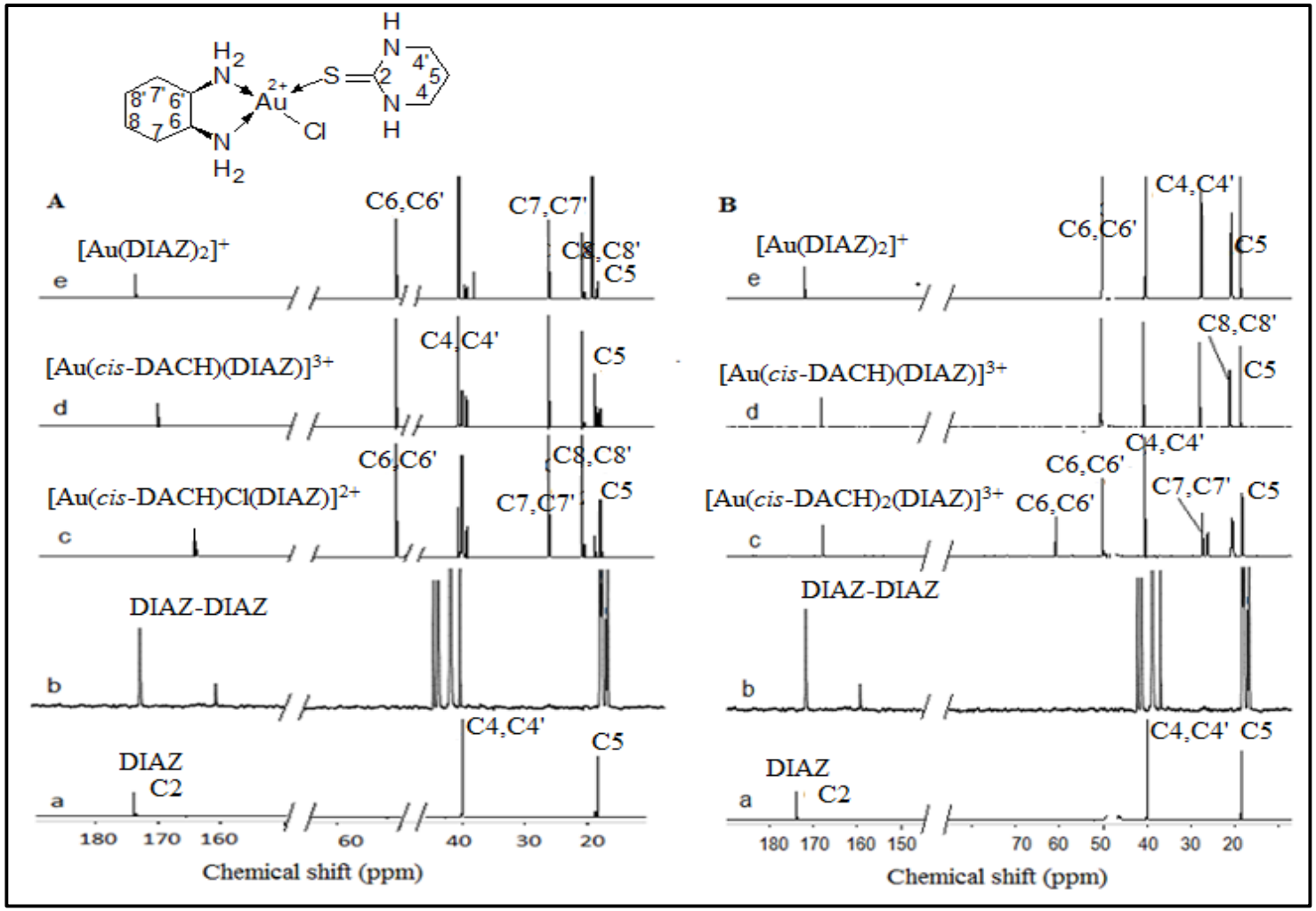

*Figure 7.7. (A) ^{13}C NMR spectra for: free DIAZ (a), oxidation of DIAZ by H_2O_2 (b), reaction of [Au(cis-DACH)Cl_2]Cl and DIAZ at (1:1)(c), at (1:2) (d) and at (1:4) (e); (B) ^{13}C NMR spectra for: free DIAZ (a), oxidation of DIAZ by H_2O_2 (b), reaction [Au(cis-DACH)$_2$]Cl_3 and DIAZ at (1:1) (**c**), at (1:2) (**d**) and at (1:4) (**e**) in D_2O.*

Table 7.2. ^{13}C NMR chemical shifts of the free ligand (DIAZ) and the [Au(cis-DACH)Cl_2]Cl(A) and [Au(cis-DACH)$_2$]Cl_3 (B) complexes in D_2O.

Ligand/ Complex	**C=S (C2)**		**C4,C6**		**C5**		**C7,C8**		**C9, C12**		**C10, C11**	
	A	**B**	**A**	**B**	**A**	**B**	**A**	**B**	**A**	**B**	**A**	**B**
Diaz	176.6	-	41.3	-	20.3	-	-	-	-	-	-	-
Diaz + H_2O_2	171.5	-	42.2, 41.6 40.0, 39.8	-	18.8, 18.6 18.5, 17.5	-	-	-	-	-	-	-
[1: 0]	- -	- -	-	-	-	-	63.3 -	61.7, 61.6	26.7 -	26.3, 26.1	21.4	21.6
[1: 1]	169.5 -	167.5	41.7, 41.6	40.2	19.7	18.1	51.4	60.6, 49.9	27.1	27.1, 25.9	21.7	20.5
[1: 2]	-	167.8	40.2	40.5	18.7	18.5	-	50.3	-	27.7	-	20.9, 20.1
[1: 4]	174.5	171.6	41.6, 40.7 40.1, 39.0	-	20.1, 19.1 19.6, 18.8	18.4	51.4	49.9	27.1	27.4	21.7	20.5

The ^{13}C chemical shift of C=S (C2) shifted up-field by 2.1-11.8 ppm in all of the complexes according to reduction of double bond character in (C=S) thione group. (C4,C4') and C(5) are shifted downfield by 0.44-0.88 ppm due to the increase in double bond character of C=N group [61]. The substitution reaction of [Au(*cis*-DACH)Cl_2]Cl and DIAZ was studied by UV-Vis spectroscopy. It was carried out in aqueous solution containing 30 mM KCl at pH 3.5. Fig. 7.8 shows the UV-Vis spectra of the substitution reaction followed by redox reaction. Two bands at 235 nm and 245 nm correspond to the products substitution reaction referred to [Au(*cis*-DACH)Cl(DIAZ)]$^{2+}$ and [Au(*cis*-DACH)(DIAZ)$_2$]$^{3+}$, respectively. They are due to back bonding from metal to ligand (M→DIAZ). The band at 207 nm represents redox reaction product [Au(DIAZ)$_2$]$^{+}$, which is due to reductive elimination through trans-effect [147].

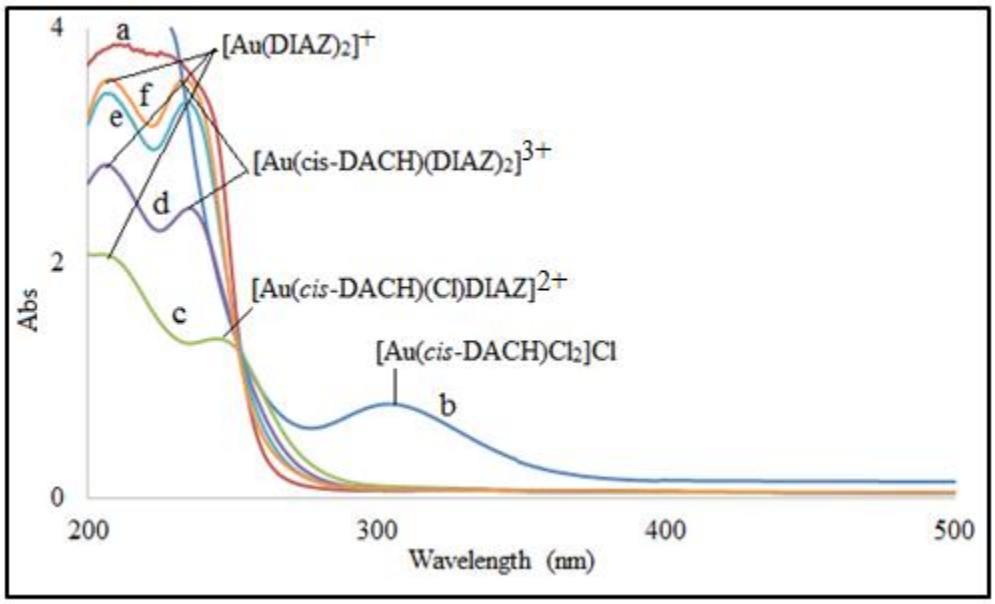

Figure 7.8. *UV-Vis spectra for: free DIAZ (0.1 mM) (**a**), [Au(cis-DACH)Cl2]Cl (0.1 mM) (**b**), reaction of [Au(cis-DACH)Cl2]Cl and DIAZ 1:0.5 (**c**), 1: 1 (**d**), 1:2 (e), and 1:4 (f). All reactions were performed in aqueous solution containing 30 mM KCl at pH 3.5.*

We then studied the interaction of [Au(*cis*-DACH)Cl_2]Cl and [Au(*cis*-DACH)$_2$]Cl_3 with DIAZ in aqueous solutions containing 0.2 M KCl by square wave stripping voltammetry. A well-defined SWSV peak is obtained at +0.82V (vs. Ag/AgCl) for 0.48 mM [Au(*cis*-DACH)Cl_2]Cl (Fig. 7.9). Whereas for [Au(*cis*-DACH)$_2$]Cl_3 is obtained at +1.35V (Fig. 7.10). The obtained peak disappeared with the subsequent additions of DIAZ [Fig. 7.9(c-h).

Fig. 7.11 includes different concentrations of DIAZ itself in the presence of 0.2 M KCl solution.

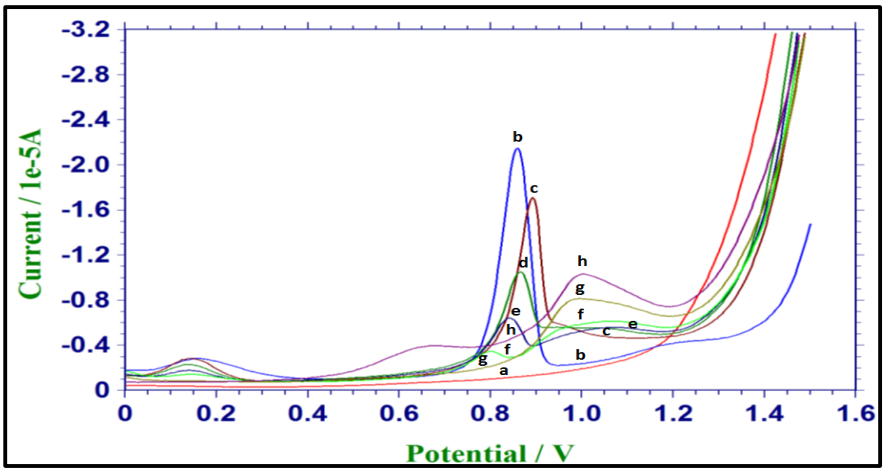

Figure 7.9. *SWSV of free (a) and presence (b) of 0.48 mM of [Au(cis-DACH)Cl_2]Cl in 0.2 M KCl solution. Subsequent additions of 0.24 mM of DIAZ (c-h). Working conditions of the pulse width (increment), 4 mV, pulse height (amplitude), 25 mV, frequency, 15*

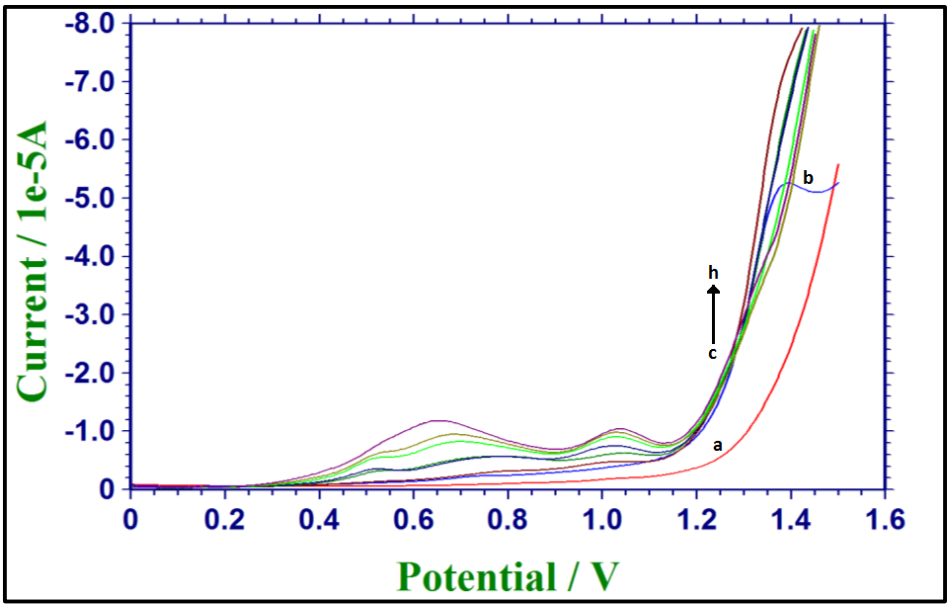

Figure 7.10. *SWSV of free (a) and presence (b) of 0.48 mM of [Au(cis-DACH)$_2$]Cl$_3$ in 0.2 M KCl solution. Subsequent additions of 0.24 mM DIAZ (c-h) at pH 3.5. Working condition of the pulse width (increment), 4 mV; pulse height (amplitude), 25 mV; frequency, 15Hz in aqoueous solution.*

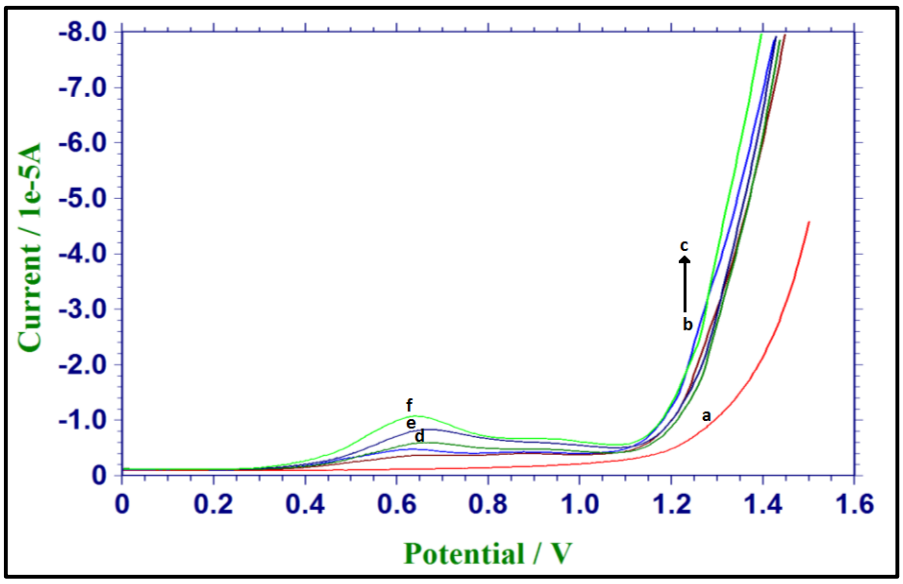

Figure 7.11. *SWSV of free (a) and presence (b) of 0.24 mM of DIAZ in 0.2 M KCl solution. Subsequent additions of 0.48 mM DIAZ (b-f) at pH 3.5. Working condition of the pulse width (increment), 4 mV; pulse height (amplitude), 25 mV; frequency, 15 Hz in aqueous solution.*

7.3.2 Kinetic Data

The kinetics of substitution reactions of [Au(*cis*-DACH)Cl_2]Cl and [Au(*cis*-DACH)$_2$]Cl_3 with Tu and DIAZ were studied by following the change of absorbance at selected λ_{max}. Pseudo first-order reaction conditions were employed for all kinetic runs at pH 3.5 using excess thione ligands with concentration of 2-10 mM. The reactions were carried out in the presence of 30 mM KCl to prevent the complex hydrolysis. All kinetic data are summarized in (Tables 7.3-7.6).

Plots of $\ln(A_\infty - A_t)$ *versus* time, at constant temperature, pH 3.5 and fixed concentration of complex (0.2 mM) with excess Tu or DIAZ, were observed as nonlinear as shown in Fig. 7.12. The nonlinear plots, initially curved and subsequently plateaued (Figs.7.14-7.16), support that the interactions proceeded through two consecutive steps, as shown in Scheme 24.

$$(A_\infty - A_t) - a_2 \exp(-k_{obsd2}\, t) = a_1 \exp(-k_{obsd1}\, t) \qquad (1)$$

$$\Delta = \quad a_1 \exp(-k_{obsd1}\, t) \qquad (2)$$

Where, a_1 and a_2 are constants that are dependent on the rate constants and extinction coefficient (ε), and Δ values are the difference of $\ln(A_\infty - A_t)$ values between the observed and extrapolated part of the linear portion of the plot of $\ln(A_\infty - A_t)$ versus time (t). The values of $(A_\infty - A_t) - a_2 \exp(-k_{obsd2}\, t)$ are obtained from the difference of X-Y values at different time (Fig. 7.12) when time is 0-10 seconds (A_∞ is the absorbance after reaction completion and A_t is absorbance at time t).

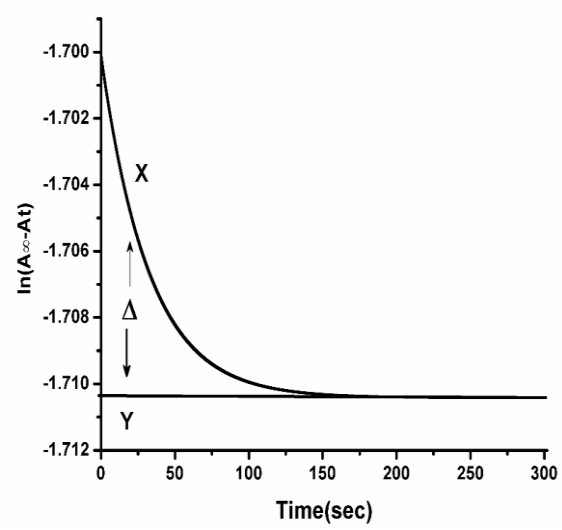

Figure 7.12. *Kinetic plot of ln(A_∞-At) versus time (sec); [Au(cis-DACH)Cl_2]Cl= 2.0 × 10^{-4} M;[DIAZ]= 5.0×10^{-3} M; in aqeous solutions containging 30 mM KCl, at pH 3.5 and 15 °C.*

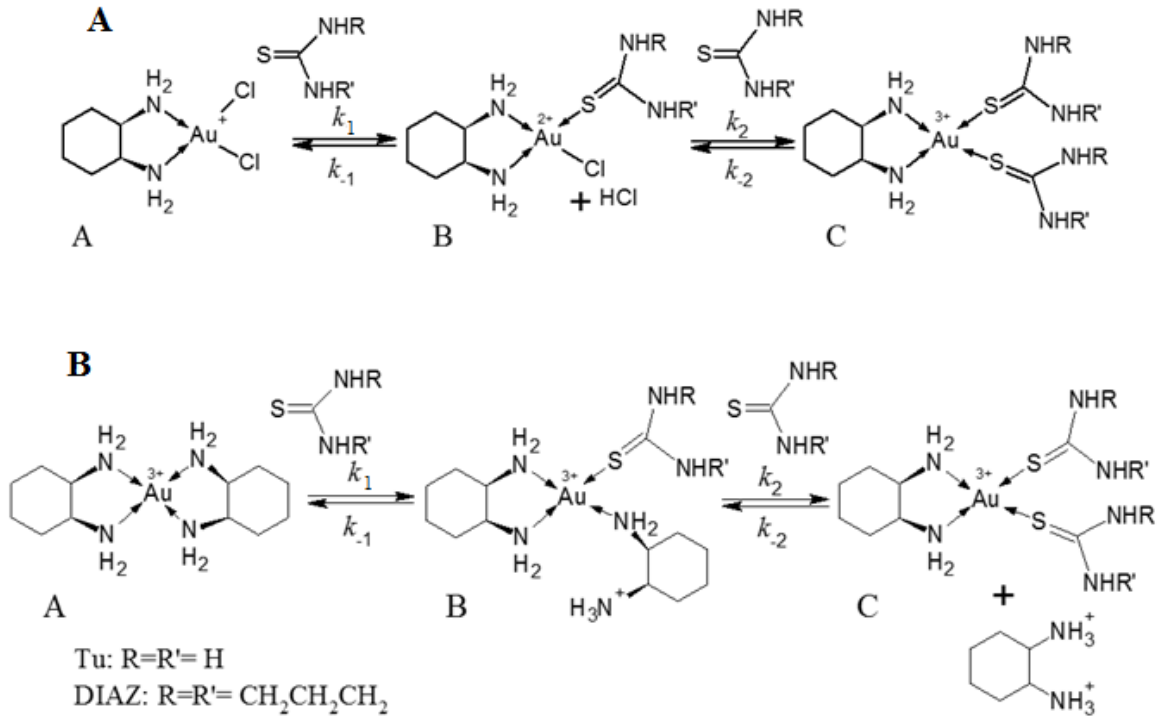

Scheme 24: *Proposed reaction pathways for the substitution reaction of:* ***(A)*** *[Au(cis-DACH)Cl_2]Cl,* ***(B)*** *[Au(cis-DACH)$_2$]$^{3+}$ with Tu and DIAZ in aqueous solution at pH 3.5*

Table 7.3. Observed pseudo first-order rate constants as a function of nucleophile concentration and temperature for the substitution reaction between $[Au(cis\text{-}DACH)Cl_2]^+$ and Tu, in aqueous solution containing 30 mM KCl at pH 3.5.

λ/nm	T/K	[Tu] /M	k_{obsd1}/s^{-1}	k_{obsd2}/s^{-1}
237	288.1	0.002	0.617	0.0325
		0.003	0.685	0.0376
		0.004	0.746	0.0427
		0.005	0.806	0.0482
		0.006	0.856	0.0536
		0.008	0.935	0.0633
		0.010	1.019	0.0688
	298.0	0.002	0.715	0.0396
		0.003	0.795	0.0464
		0.004	0.858	0.0525
		0.005	0.947	0.0564
		0.006	0.997	0.0624
		0.008	1.183	0.0726
		0.010	1.288	0.0792
	310.0	0.002	0.998	0.0426
		0.003	1.095	0.0485
		0.004	1.249	0.0589
		0.005	1.365	0.0652
		0.006	1.462	0.0712
		0.008	1.75	0.0824
		0.010	1.952	0.0892

Table 7.4. Observed pseudo first-order rate constants as a function of nucleophile concentration and temperature for the substitution reaction between $[Au(cis\text{-}DACH)_2]^{3+}$ and Tu, in aqueous solution containing 30 mM KCl at pH 3.5.

λ/nm	T/K	[Tu] /M	k_{obsd1} /s^{-1}	k_{obsd2} /s^{-1}
245	288.1	0.002	0.652	0.0302
		0.003	0.695	0.0333
		0.004	0.722	0.0391
		0.005	0.762	0.0420
		0.006	0.815	0.0468
		0.008	0.881	0.0535
		0.010	0.995	0.0586
	298.0	0.002	0.666	0.0345
		0.003	0.698	0.0384
		0.004	0.753	0.0428
		0.005	0.796	0.0502
		0.006	0.884	0.0543
		0.008	0.996	0.0626
		0.010	1.098	0.0687
	310.0	0.002	0.679	0.0386
		0.003	0.729	0.0429
		0.004	0.829	0.0514
		0.005	0.886	0.0569
		0.006	0.967	0.0625
		0.008	1.084	0.0703
		0.010	1.185	0.0786

Table 7.5. Observed pseudo first-order rate constants as a function of nucleophile concentration and temperature for the substitution reaction between $[Au(cis\text{-}DACH)Cl_2]^+$ and DIAZ in aqueous solution containing 30 mM KCl at pH 3.5.

λ/nm	T/K	[Tu] /M	k_{obsd1}/s^{-1}	k_{obsd2}/s^{-1}
249	288.2	0.002	0.536	0.0259
		0.003	0.596	0.0285
		0.004	0.619	0.031
		0.005	0.632	0.0325
		0.006	0.663	0.0343
		0.008	0.699	0.0392
		0.010	0.749	0.0466
	298.2	0.002	0.722	0.0335
		0.003	0.761	0.0367
		0.004	0.802	0.0406
		0.005	0.834	0.0435
		0.006	0.866	0.0466
		0.008	0.922	0.0529
		0.010	0.976	0.0572
	310.2	0.002	0.749	0.0372
		0.003	0.799	0.0423
		0.004	0.847	0.0473
		0.005	0.886	0.0514
		0.006	0.933	0.0554
		0.008	0.998	0.0621
		0.010	1.142	0.0673

Table 7.6. Observed pseudo first-order rate constants as a function of nucleophile concentration and temperature for the substitution reaction between $[Au(cis\text{-}DACH)_2]^{3+}$ and DIAZ in aqueous solution containing 30 mM KCl at pH 3.5.

λ/nm	T/K	[Tu] /M	k_{obsd1}/s^{-1}	k_{obsd2}/s^{-1}
251	288.2	0.002	0.536	0.0198
		0.003	0.566	0.0212
		0.004	0.589	0.0232
		0.005	0.612	0.0255
		0.006	0.633	0.0272
		0.008	0.679	0.0322
		0.010	0.709	0.0342
	298.2	0.002	0.588	0.0202
		0.003	0.627	0.0234
		0.004	0.656	0.0266
		0.005	0.673	0.0298
		0.006	0.708	0.0323
		0.008	0.754	0.0372
		0.010	0.798	0.0418
	310.2	0.002	0.686	0.0356
		0.003	0.748	0.0409
		0.004	0.776	0.0444
		0.005	0.829	0.0471
		0.006	0.88	0.0511
		0.008	0.942	0.0569
		0.010	1.019	0.0625

Evaluation of the rate constant k_1

The rate constant of the first step (A→B in Scheme 24) is dependent on the thione concentration, which is consistent with previous reports [61,192]. At constant temperature, the rate constant ($k_{obsd}1$) for reaction of Tu or DIAZ with [Au(*cis*-DACH)Cl_2]Cl and [Au(*cis*-DACH)$_2$]Cl_3 were obtained from the slopes of the plots of lnΔ *versus* time as illustrated in Figures (7.17-7.20).

Typical calculations were made for each thione at concentrations of 2 -10 mM, 0.2 mM of [Au(*cis*-DACH)Cl_2]$^+$ or [Au(*cis*-DACH)$_2$]$^{3+}$, pH 3.5, in aqueous solutions containing 30 mM KCl and at different temperatures of 288.2, 298.2 and 310.2 K. $k_{obsd}1$ values were calculated by the Weyh and Hamm method [206].

A plot of $k_{obsd}1$ *versus* thione concentration gives a straight line with an intercept = k_{-1} and a slope = k_1. As illustrated in Eq. 3,

$$k_{obsd1} = k_1[\text{thione}] + k_{-1}[Cl^-] \qquad (3)$$

Evaluation of the rate constant k_2

The second step (B→C in Scheme 24) is a slower process than the first one due to competition between the second thione and the solvent. Kinetics showed that this step is independent on ligand concentration. The k_{obsd2} values were calculated from the slopes of the linear portion of the plots of ln(A_∞ -A_t) *versus* time.

A plot of $k_{obsd}2$ *versus* thione concentration gave a straight line with an intercept = k_{-2} and a slope = k_2 as illustrated in Eq. 4.

$$k_{obsd}2 = k_2[\text{thione}] + k_{-2}[Cl^-] \qquad (4)$$

Plots of pseudo first-order rate constants as a function of thione concentration at different temperatures for the substitution reactions of [Au(*cis*-DACH)Cl_2]Cl or

[Au(*cis*-DACH)$_2$]Cl$_3$ with Tu and DIAZ are shown in Figs. (7.21-7.24). The rate constants (k_1 *and* k_2) are summarized in Table 7.7.

Evaluation of activation parameters

The activation parameters ($\Delta H^{\#}$, $\Delta S^{\#}$) for the reaction of [Au(*cis*-DACH)Cl$_2$]Cl or [Au(*cis*-DACH)$_2$]Cl$_3$ with Tu and DIAZ were evaluated using Eyring plots. The Eyring plots for these substitution reactions at various temperatures are shown in Figures. (7.25-7.31). $\Delta H^{\#}$ and $\Delta S^{\#}$ values are summarized in Table 7.7. Enthalpies of activation are comparable to Ag-Cl and Ag-S bond energies and are consistent with previous studies [106]. Entropies of activations are all highly negatives, which support that all steps follow associative mechanisms. This is expected, at least for the Au(III) complexes. These d^8 Au(III) complexes are expected to show similar behavior to square planar Pt(II) complexes [2007-209].

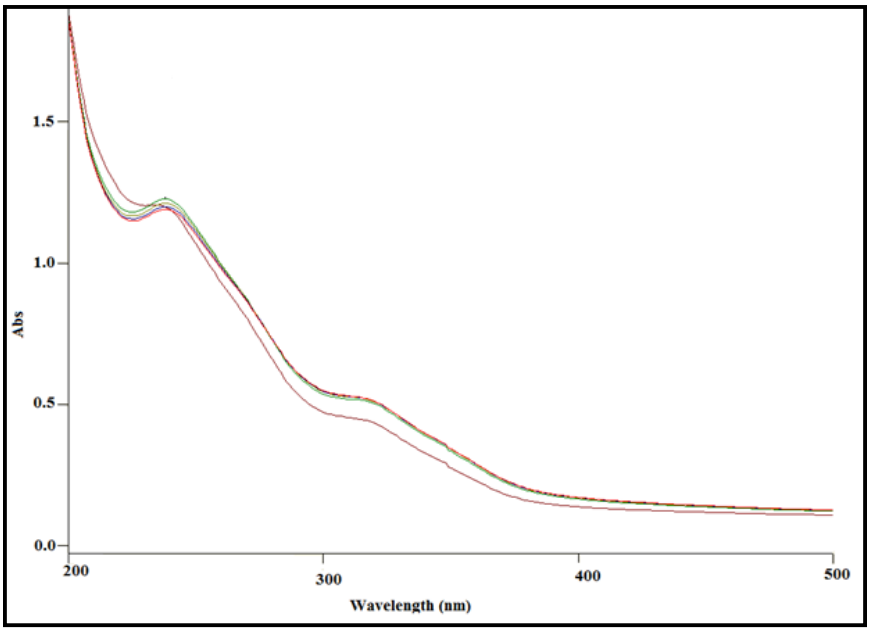

Figure 7.13*. UV-Vis spectra for the substitution reaction between [Au(cis-DACH)Cl$_2$]$^+$ (2.0 ×10^{-4} M) with Tu (2.0 ×10^{-4} M), in aqueous solution containing 30 mM KCl, pH 3.5 at 298 K.*

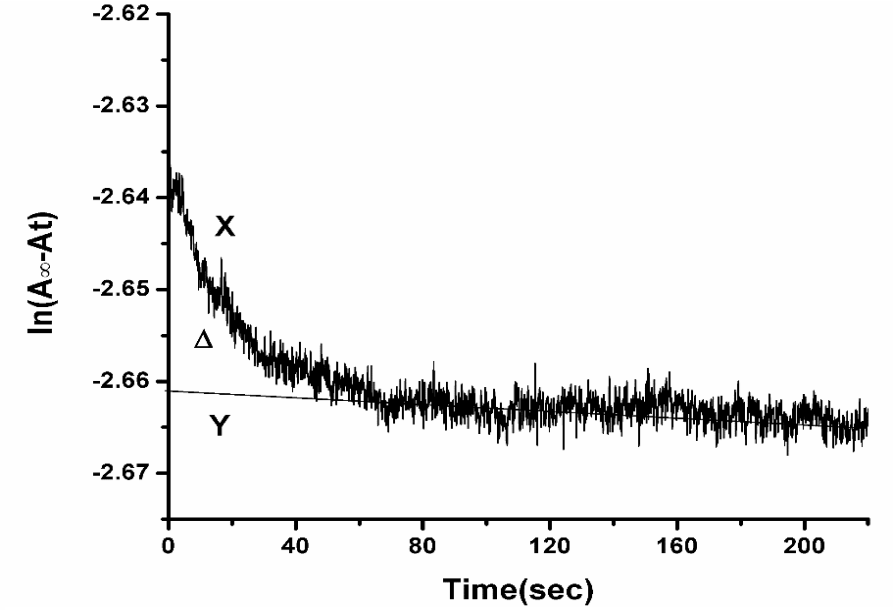

***Figure 7.14**. A typical kinetic trace for the substitution reaction between $[Au(cis\text{-}DACH)Cl_2]^+$ (10.0×10^{-4} M) and Tu (2.0×10^{-3} M), in aqueous solution containing 30 mM KCl, pH 3.5 with wavelength 237nm and at 310 K.*

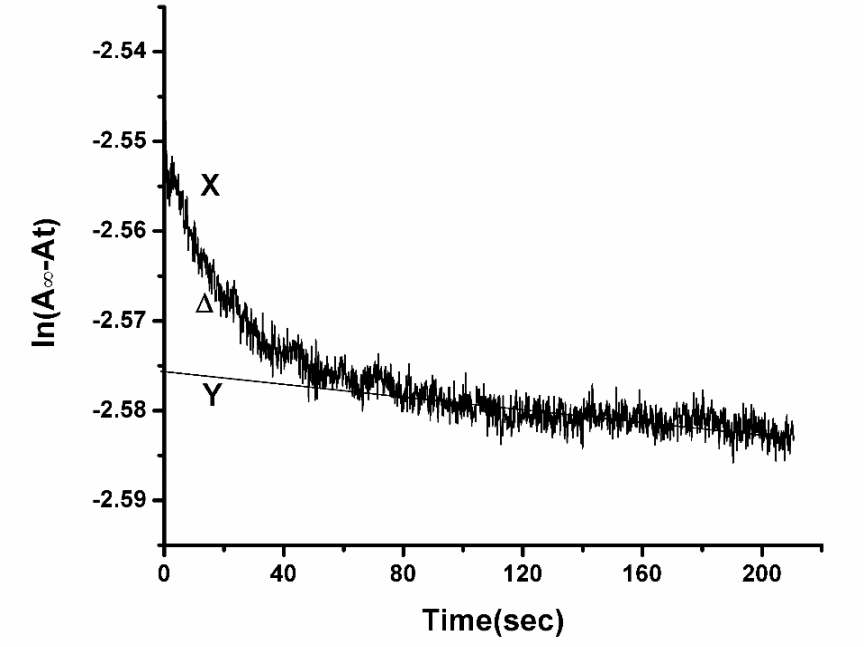

***Figure 7.15**. A typical Kinetic trace for the substitution reaction between $[Au(cis\text{-}DACH)_2]^{3+}$ (2.0×10^{-4} M) and Tu (2.0×10^{-3} M), in aqueous solution containing 30 mM KCl, at pH 3.5, wavelength 245 nm and at 288 K.*

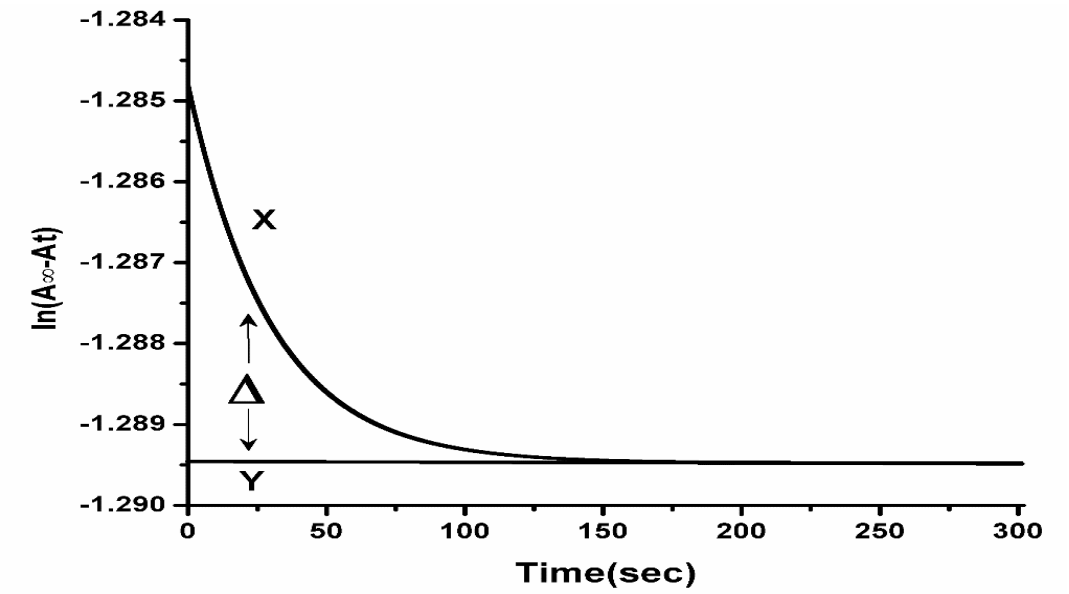

Figure 7.16. *A typical kinetic trace for the substitution reaction between* $[Au(cis\text{-}DACH)_2]^{3+}$ *(2.0 × 10*$^{-4}$ *M) and DIAZ (6.0×10*$^{-3}$ *M), in aqueous solution containing 30 mM KCl, at pH 3.5, wavelength 251 nm and 288 K.*

Table 7.7 shows that the rate constant for the reaction of the two complexes with DIAZ and Tu. The reactivity of these thione ligands are shown to be slower than that for cyanide. It is also much faster than other nucleophiles as in these order: L-Histidine > guanosine-5'-monophosphate> inosine-5'-monophosphate> inosine towards the [Au(*cis*-DACH)Cl_2]Cl complex [62].

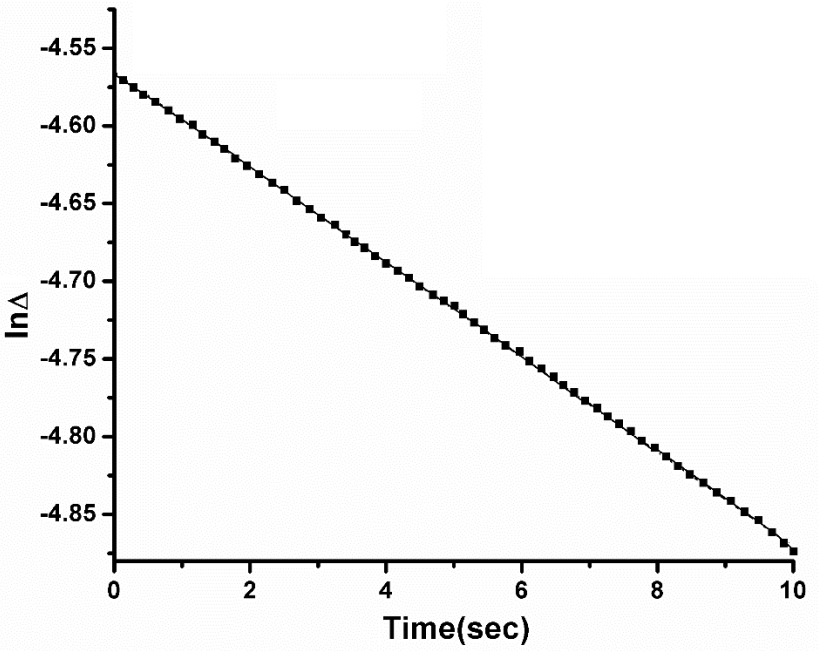

Figure 7.17. *A typical Kinetic plot of lnΔ versus time (sec); [Au(cis-DACH)Cl$_2$]Cl= 2.0 × 10^{-4}M; [DIAZ]= 5.0 × 10^{-3}M; in the presence of 30 mM KCl, at pH 3.5 and 288 K.*

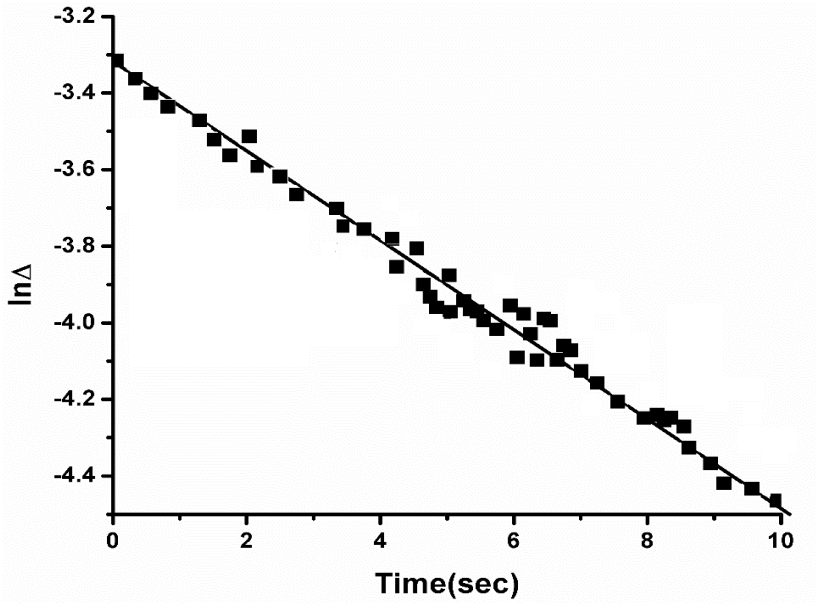

Figure 7.18*. A typical Kinetic trace of the plot lnΔ versus time (sec) for the substitution reaction between [Au(cis-DACH)Cl$_2$]$^+$ (10.0 x 10^{-4} M) and Tu = 2.0×10^{-3} M, in aqueous solution containing 30 mM KCl, at pH 3.5, wavelength 237 nm and at 310 K.*

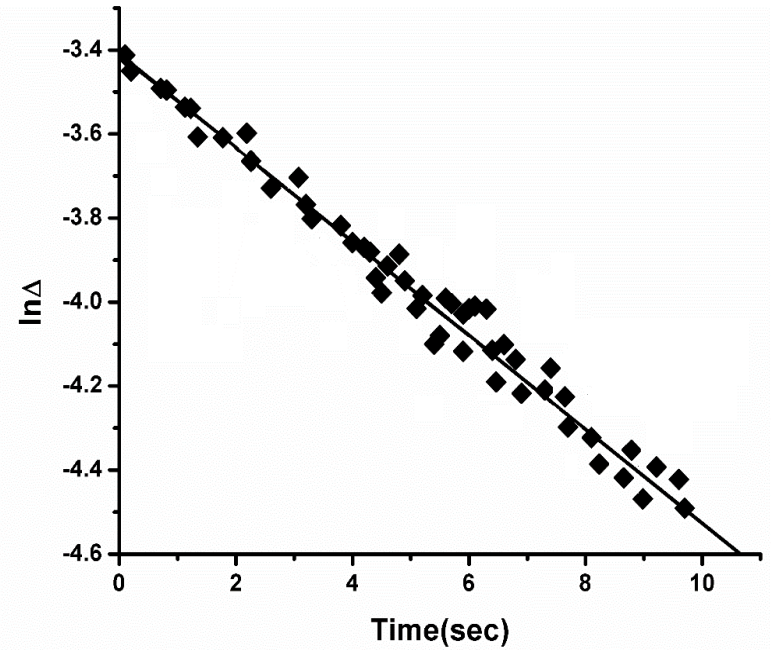

Figure 7.19. *A typical Kinetic trace of the plot lnΔ versus time (sec) for the substitution reaction between* $[Au(cis\text{-}DACH)_2]^{3+}$ *(*2.0×10^{-4}*M) and Tu (*2.0×10^{-3}*M), in aqueous solution containing 30 mM KCl, at pH 3.5, wavelength 245 nm and at 288 K.*

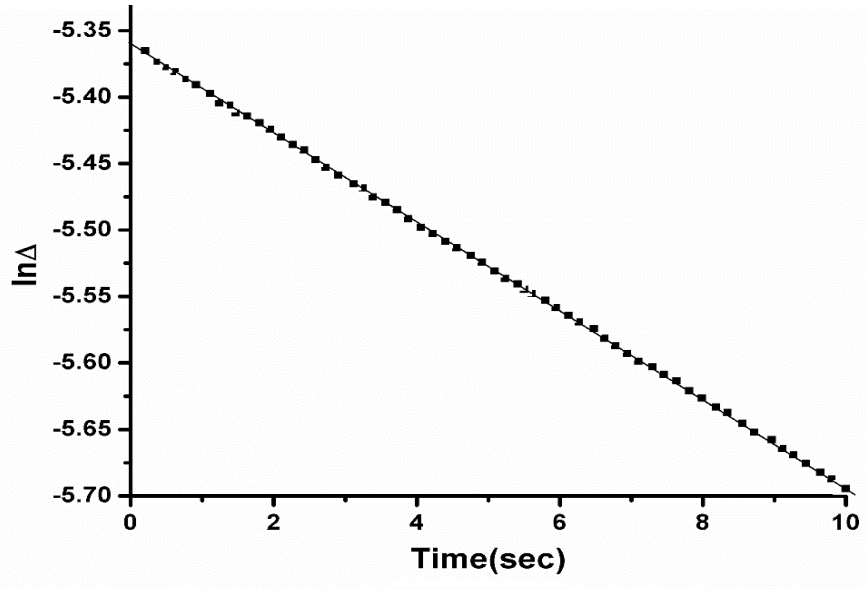

Figure 7.20. *A typical kinetic trace of the plot lnΔ versus time (sec) for the substitution reaction between* $[Au(cis\text{-}DACH)_2]^{+3}$*(*$2.0\times10^{-4}$ *M) and DIAZ (*6.0×10^{-3} *M), in aqueous solution containing 30 mM KCl, at pH 3.5, wavelength 251 nm and 288 K.*

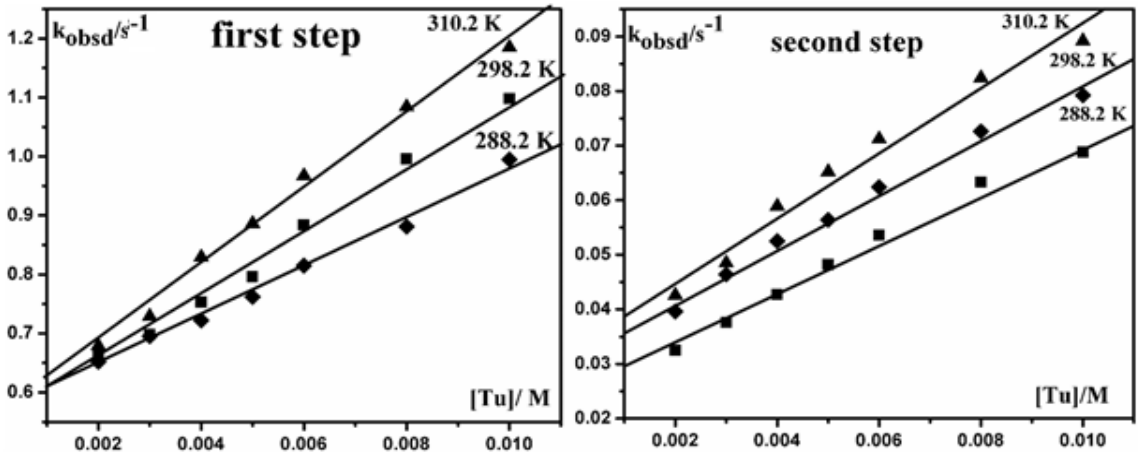

Figure 7.21. *Plot of pseudo first-order rate constants for the first ($k_{obsd}1$) and second ($k_{obsd}2$) steps as a function of nucleophilic concentration and temperature of the substitution reaction between $[Au(cis\text{-}DACH)Cl_2]^+$ and Tu in aqueous solution containing 30 mM KCl.*

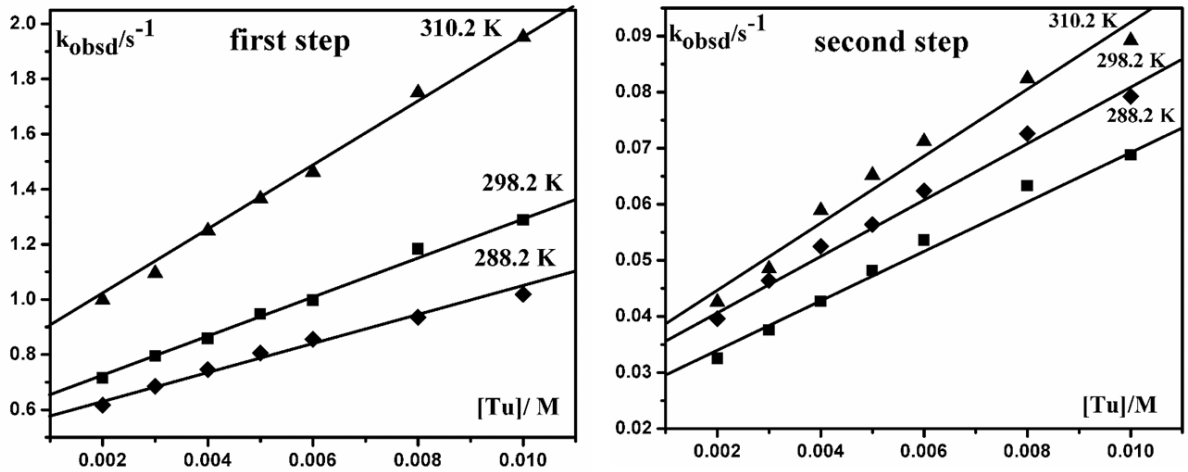

Figure 7.22. *Plot of pseudo first-order rate constants for the first ($k_{obsd}1$) and second ($k_{obsd}2$) steps as a function of nucleophilic concentration and temperature of the substitution reaction between $[Au(cis\text{-}DACH)_2]^{3+}$ and Tu in aqueous solution containing 30 mM KCl*

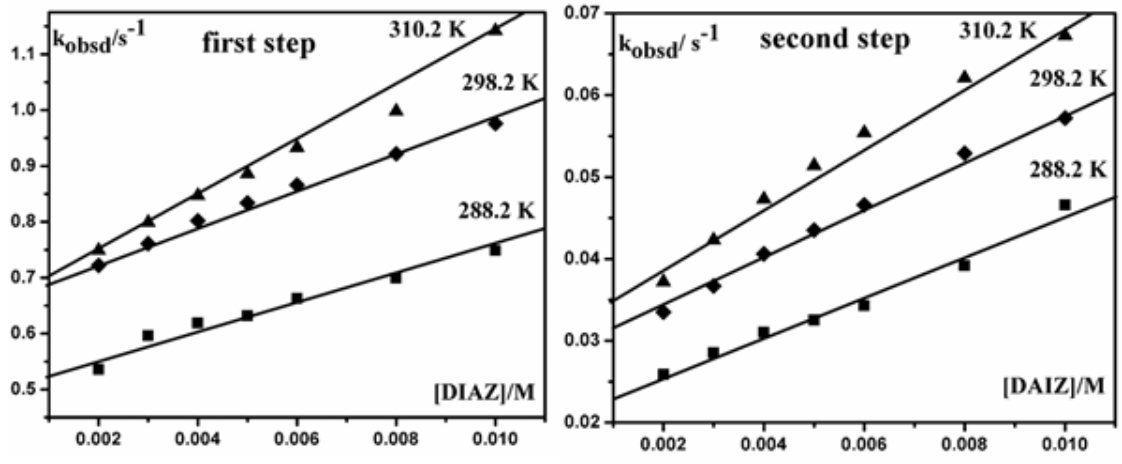

Figure 23. *Plot of pseudo first-order rate constants for the first ($k_{obsd}1$) and second ($k_{obsd}2$) steps as a function of nucleophilic concentration and temperature of the substitution reaction between $[Au(cis\text{-}DACH)Cl_2]^+$ and DIAZ in aqueous solution containing 30 mM KCl.*

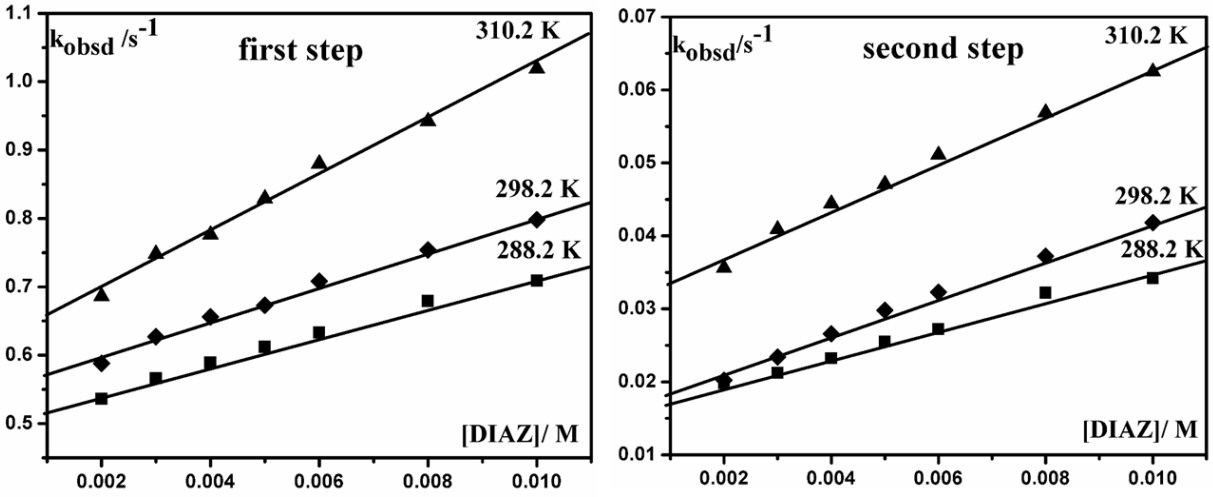

Figure 24*. Plot of pseudo first-order rate constants for the first ($k_{obsd}1$) and second ($k_{obsd}2$) steps as a function of nucleophilic concentration and temperature of the substitution reaction between $[Au(cis\text{-}DACH)_2]^{3+}$ and DIAZ in aqueous solution containing 30 mM KCl.*

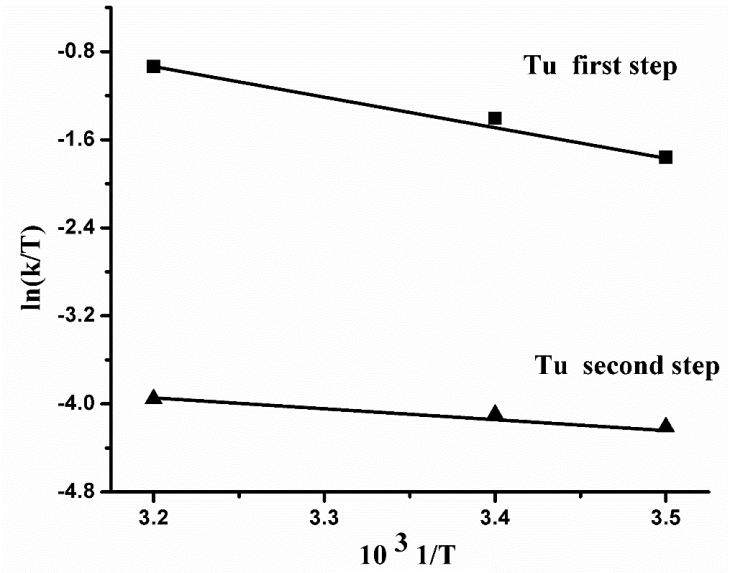

Figure 7.25. *Eyring plots for forward substitution reactions of $[Au(cis\text{-}DACH)Cl_2]^+$ with Tu for the first ($k_{obsd}1$) and second ($k_{obsd}2$) step in aqueous solution containing 30 mM KCl at pH 3.5.*

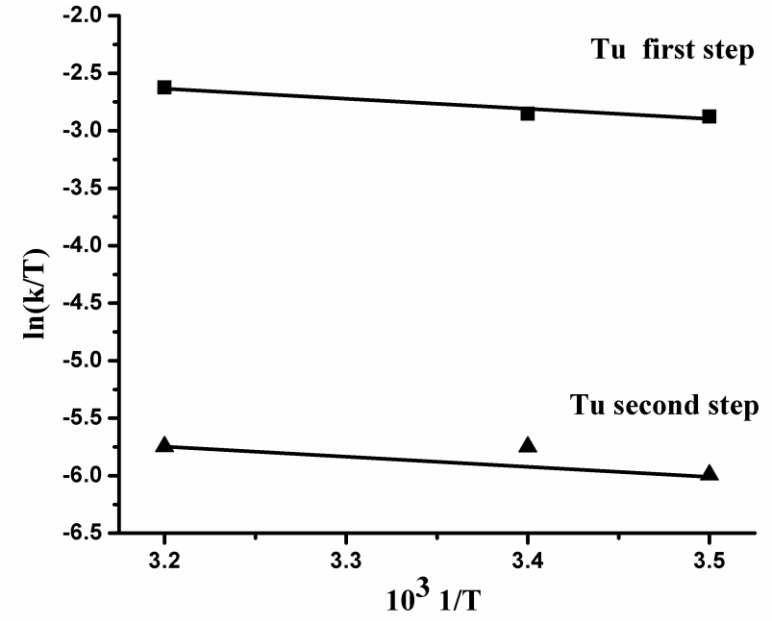

Figure 7.26. *Eyring plots for the reverse substitution reactions of $[Au(cis\text{-}DACH)Cl_2]^+$ with Tu for the first ($k_{obsd}1$) and second ($k_{obsd}2$) step in aqueous solution containing 30 mM KCl at pH 3.5.*

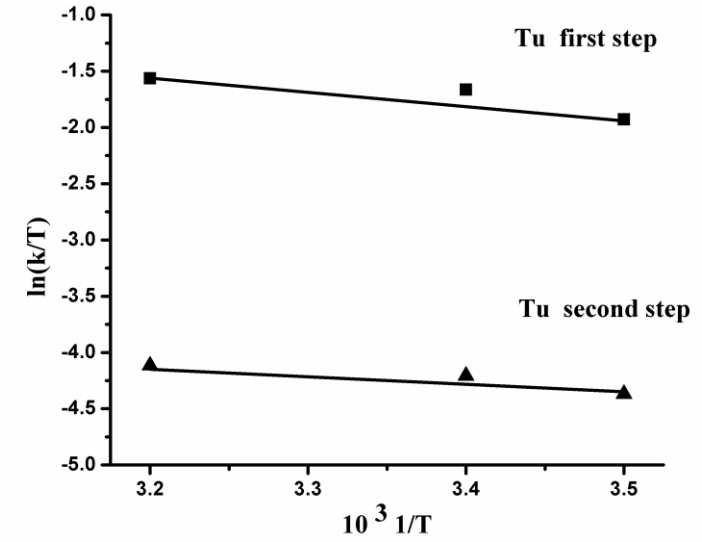

***Figure 7.27**. Eyring plots for the forward substitution reactions of $[Au(cis\text{-}DACH)_2]^{3+}$ with Tu for the first ($k_{obsd}1$) and second ($k_{obsd}2$) step in aqueous solution containing 30 mM KCl at pH 3.5*

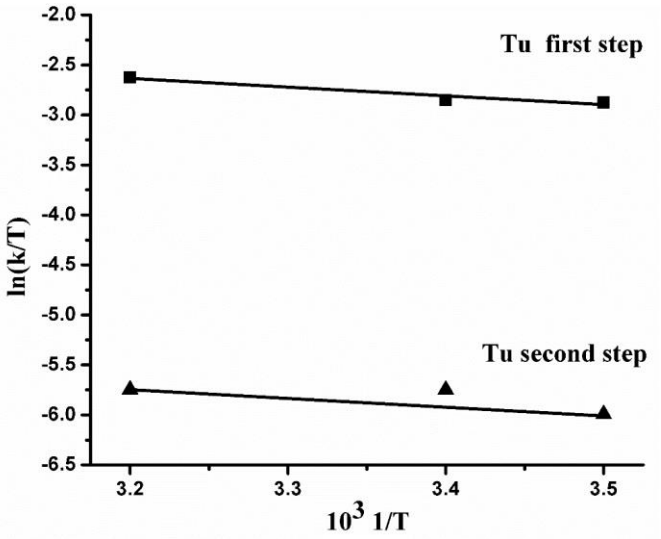

***Figure 28**. Eyring plots for the reverse substitution reactions of $[Au(cis\text{-}DACH)_2]^{3+}$ with Tu for the first ($k_{obsd}1$) and second ($k_{obsd}2$) step in aqueous solution containing 30 mM KCl at pH 3.5.*

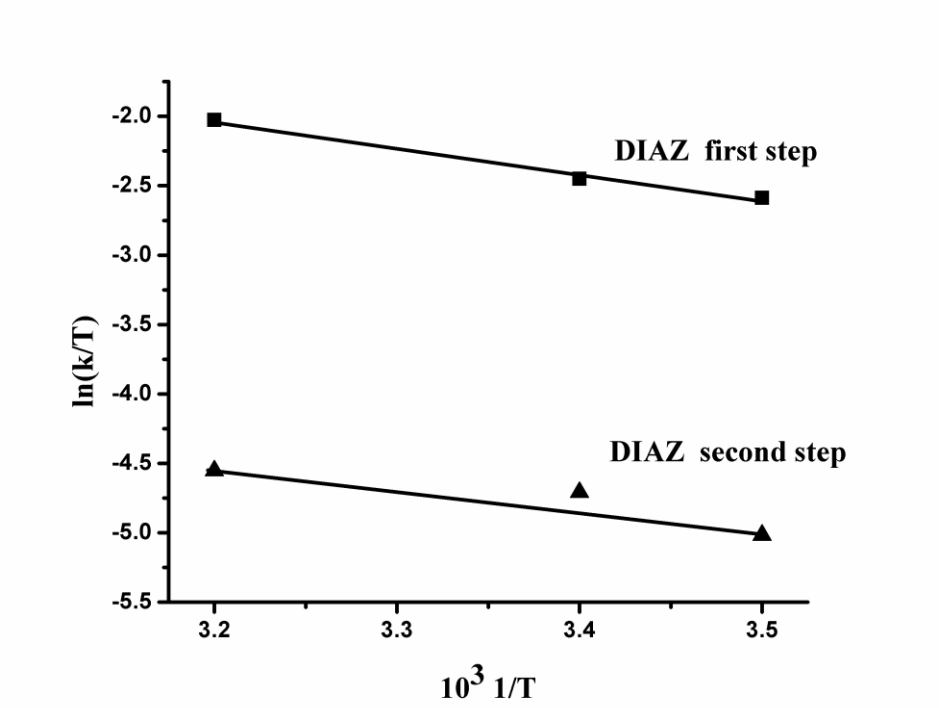

Figure 7.29. *Eyring plots for the forward substitution reactions of $[Au(cis\text{-}DACH)Cl_2]^+$ with DIAZ for the first ($k_{obsd}1$) and second ($k_{obsd}2$) step in aqueous solution containing 30 mM KCl at pH 3.5.*

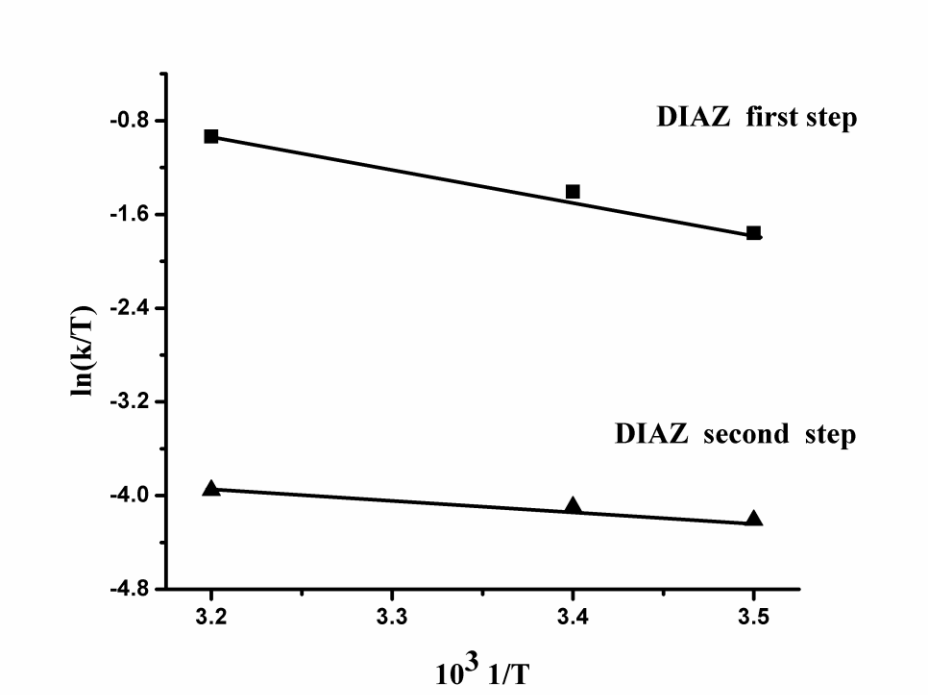

Figure 7.30. *Eyring plots for the forward substitution reactions of $[Au(cis\text{-}DACH)_2]^{3+}$ with DIAZ for the first ($k_{obsd}1$) and second ($k_{obsd}2$) step in aqueous solution containing 30 mM KCl at pH 3.5***.**

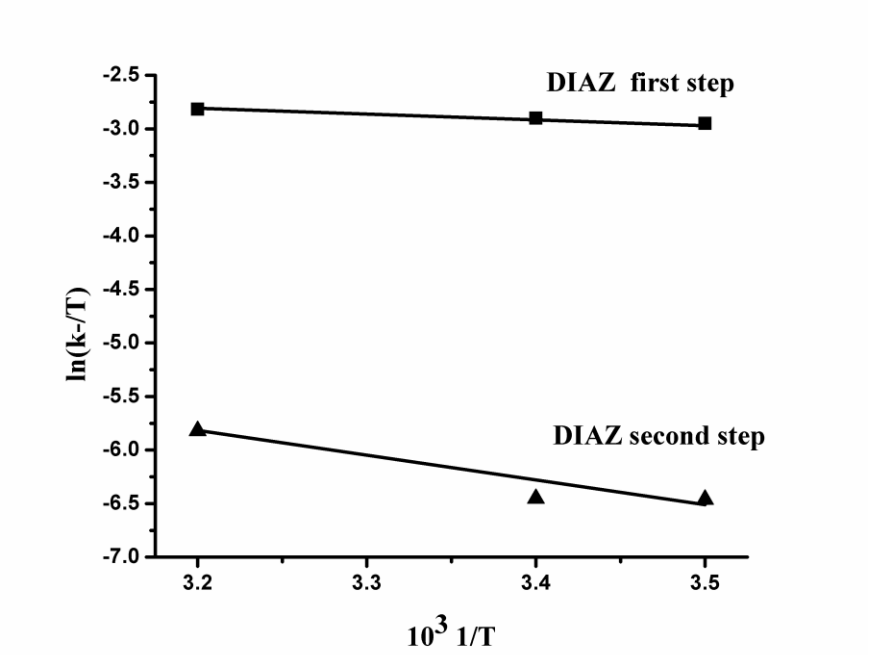

Figure 7.31. *Eyring plots for the reverse substitution reactions of* $[Au(cis\text{-}DACH)_2]^{3+}$ *with DIAZ for the first* ($k_{obsd}1$) *and second* ($k_{obsd}2$) *step in aqueous solution containing 30 mM KCl at pH 3.5.*

Table 7.7. Rate constants for the substitution reactions of [Au(cis-DACH)Cl_2]Cl and [Au(cis-DACH)$_2$]Cl_3 with Tu

[Au(*cis*-DACH)Cl_2]$^+$						
First step	k_1/M^{-1} s^{-1}	$\Delta H_1^{\neq}$/kJmol^{-1}	$\Delta S_1^{\neq}$/J$K^{-1}mol^{-1}$	k_{-1}/M^{-1} s^{-1}	$\Delta H_{-1}^{\neq}$/kJmol^{-1}	$\Delta S_{-1}^{\neq}$/J$K^{-1}mol^{-1}$
Tu	73.0 ± 3	22.4 ± 2.5	-133 ± 8	17.2 ± 0.3	7.4 ± 2.0	-196 ± 6.0
Diaz	31.5 ± 1.2	16 ± 1	-164.3 ± 3.3	10.1 ± 0.2	-	-
Second step	k_2/M^{-1} s^{-1}	$\Delta H_2^{\neq}$/kJmol^{-1}	$\Delta S_2^{\neq}$/J$K^{-1}mol^{-1}$	k_{-2}/M^{-1} s^{-1}	$\Delta H_{-2}^{\neq}$/kJmol^{-1}	$\Delta S_{-2}^{\neq}$/J$K^{-1}mol^{-1}$
Tu	5 ± 0.2	7 ± 0.8	-208 ± 3	0.95 ± 0.4	6 ± 0.6	-227 ±7
Diaz	3.0 ± 0.1	9.4 ± 1.4	-204 ± 5	0.84 ± 0.2	9 ± 2	-218 ±16
[Au(*cis*-DACH)$_2$]$^{3+}$						
First step	k_1/M^{-1} s^{-1}	$\Delta H_1^{\neq}$/kJmol^{-1}	$\Delta S_1^{\neq}$/J$K^{-1}mol^{-1}$	k_{-1}/M^{-1} s^{-1}	$\Delta H_{-1}^{\neq}$/kJmol^{-1}	$\Delta S_{-1}^{\neq}$/J$K^{-1}mol^{-1}$
Tu	56 ± 2	9.2 ± 0.5	-181 ± 15	16.1 ± 0.4	-	-
Diaz	26 ± 1	16 ± 2	-164 ± 5	16.4 ± 0.2	4 ± 0.2	-209 ± 0.5
Second step	k_2/M^{-1} s^{-1}	$\Delta H_2^{\neq}$/kJmol^{-1}	$\Delta S_2^{\neq}$/J$K^{-1}mol^{-1}$	k_{-2}/M^{-1} s^{-1}	$\Delta H_{-2}^{\neq}$/kJmol^{-1}	$\Delta S_{-2}^{\neq}$/J$K^{-1}mol^{-1}$
Tu	4.4 ± 0.2	6.6 ± 0.3	-211 ± 8	0.8 ± 0.1	5 ± 0.2	-232 ± 1
Diaz	2.7 ± 0.1	12 ± 5	-197 ± 16	0.5 ± 0.1	19 ± 6	-186 ± 21

CHAPTER 8

NMR AND KINETIC STUDIES OF THE INTERACTION OF [Au(*cis*-DACH)Cl_2]Cl AND [Au(*cis*-DACH)$_2$]Cl_3 WITH POTASSIUM CYANIDE IN AQUEOUS SOLUTION

8.1 Introduction

Recently, chemical and biochemical studies of Au(III) complexes containing N-chelating ligands have been reported showing biological activity [41, 68,210-215]. In addition, a number of other Au(III) complexes with N-ligands have been developed as promising anti-cancer and showed better cytotoxic activities. Gold(III) is analogue of the antitumor agent *cis*-diaminedichloroplatinum(II) (*cisplatin*) and in *cis*-1,2-diaminocyclohexane dichlorido- platinum(II) (DACH) complexes. The new gold(III) complexes may be attractive as anticancer drugs to overcome *cisplatin* side-effects [26, 188, 216-218].

Al-Maythalony et al. investigated the interaction of Au(III)–alkyldiamine complexes with L-histidine and imidazole ligands by ^{1}H, ^{13}C NMR and UV spectrophotometry, and found that the rate of reaction is dependent on pH [101]. Zhu et al. reported the synthesis, structure and electrochemistry of Au(III) ethylenediamine complexes and their interactions with Guanosine5-phosphate [219]. Sanghvi et al. described antitumor properties of five-coordinate gold(III) complexes bearing substituted polypyridyl ligands, and found that [(sec-butyl)phen)$AuCl_3$] has more significant in vitro antitumor activity than

metallotherapeutic *cisplatin* [220]. Ahmed et al. studied histological changes in kidney and liver of rats due to exposure of $[Au(en)Cl_2]Cl$ complex [8]. Al-Jaroudi et al. described the synthesis, characterization and cytotoxicity of gold(III) complexes with the ligand 1,2-diaminocyclohexane, and showed the influence of stereochemistry on antitumor activity [198]. Monim-ul-Mehboob et al. prepared a series of Au(III)-alkanediamine complexes, with ligands ethylenediamine, propylenediamine, butylenediamine, and N-alkyl substituted ethylenediamine, those were characterized and tested against gastric, prostate and ovarian cancer cells [221].

The interaction of Au(III) with cyanide ligand has interest in therapeutic values and pharmacological activity, due to the formation of $[Au(CN)_4]^-$, which is unstable in physiological condition and produces $[Au(CN)_2]^-$. Cyanide is naturally produced in the body by oxidation of SCN^- by the enzyme myeloperoxidase (MPO) and released by phagocytic cells [50, 203, 222]. The $[Au(CN)_2]^-$ has been extensively used in the treatment of rheumatoid arthritis since 1920s, while other Au(I) complexes showed activity against malaria and HIV [52, 109].

Canumalla et al. described redox and ligand exchange reactions of potential gold(I) and gold(III)-cyanide metabolites under biomimetic conditions [195]. Yangyuoru et al. studied the reduction of auricyanide using biological ligand glutathione (GSH) as reductant through two intermediates I_{230} and I_{290} [194]. Al-Maythalony et al. described ^1H, ^{13}C NMR and UV-Vis spectroscopy studies of gold(III)-tetracyanide complex with L-cysteine, glutathione, captopril, L-methionine and DL-seleno-methioninein aqueous solution [101].

8.2 Experimental section

8.2.1 Materials and instrumentation

$NaAuCl_4.2H_2O$, *cis*-DACH ($C_6H_{14}N_2$) were purchased from Sigma-Aldrich- USA, absolute ethanol from Merck, CH_3OD and D_2O were purchased from Alfa-Aesar, KCN, 99.9% enriched $K^{13}CN$ and 99% enriched $K^{13}C^{15}N$ from Cambridge Isotope Lab. Inc. Deionized water with a resistivity of 18.6 MΩ cm^{-1} is used to prepare all solutions. The water is obtained directly from a PURELABs Ultra Laboratory Water Purification System.

Spectroscopic and electrochemical techniques, synthesis of [Au(*cis*-DACH)Cl_2]Cl and [Au(*cis*-DACH)$_2$]CL_3 were described in section 3.1.

8.2.2 Kinetic Measurements

The UV-Vis spectra of the complex and cyanide solutions were recorded over the range 200-500 nm, Fig. 8.1 (five runs) and are showing λ_{max} at 305 nm and 258 nm for [Au(*cis*-DACH)Cl_2]Cl and [Au(*cis*-DACH)$_2$]Cl_3 respectively. The reactions were started by mixing the complex and cyanide solutions in equal volumes directly in a vial kept inside the instrument. The kinetic measurements were made under pseudo-first order conditions, where concentration of the complex is 0.1 mM and for the cyanide it was in the range 2-10 and 20 mM. The reactions were followed over 10 minutes and were carried out at ambient temperature of 25 °C. The pseudo-first order rate constant k_{obsd} is calculated as an average value of eight independent kinetic runs [61]. Observed experimental data are reported in Table 8.5.

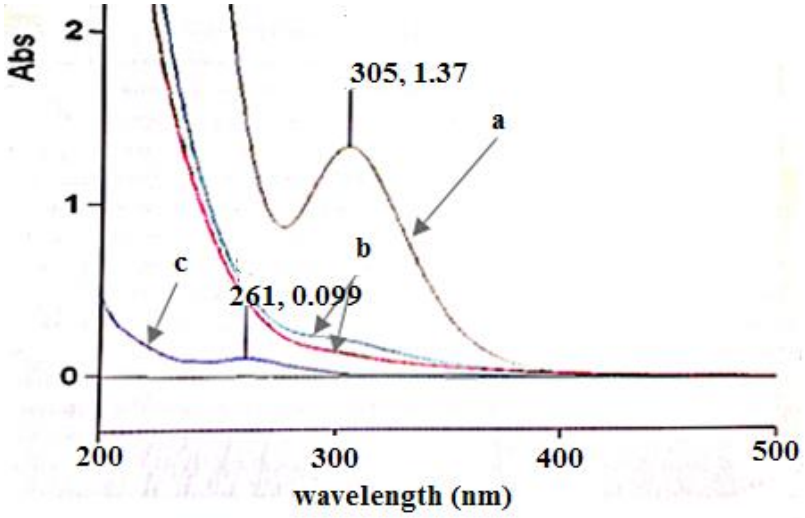

Figure 8.1. *The UV-Vis spectra for the substitution reaction of [Au(cis-DACH)Cl_2]Cl (1.0 ×10^{-4}M) (**a**) before and (**b**) after addition of cyanide (5.0 ×10^{-3}M) and (c) cyanide before reaction, the substitution reaction carried out at ambient temperature of 25°C.*

8.3 Results and Discussion

8.3.1 Interaction of [Au(*cis*-DACH)Cl_2]Cl With K^{13}CN

Interaction of [Au(*cis*-DACH)Cl_2]Cl with enriched KCN was carried out in CH_3OD by mixing the reactants at different ratios and monitored by ^{1}H, ^{13}C, ^{15}N NMR, UV-Vis spectroscopy and electrochemistry.^{1}H, ^{13}C and ^{15}N NMR chemical shifts for the species in this interaction are given in Tables (8.1-8.2, 8.4A) .

When ^{13}C NMR is used to monitor the reaction, (Fig.8.2a) shows the chemical shift of (5 mM) 20% enriched K^{13}CN at 160.48 ppm. The peak at 103 ppm in (Fig.8.2b) indicates the white precipitate [Au (^{13}CN)$_4$]$^-$. It is formed by interaction of [Au(*cis*-DACH)Cl_2]Cl with K^{13}CN at (1:0.25) ratio, and consistent with the data reported in previous studies [101,195, 223].

Table 8.1. ^{1}H NMR chemical shifts of the reaction of [Au(cis-DACH)(Cl_2]Cl complex with $K^{13}CN$ ligand in CH_3OD solution.

Specie	1H, 2H	3H, 6H eq	3H, 6H ex	4H, 5H eq	4H, 5H ex
(1: 0)	3.59 m	2.02 m	1.76 m	1.47 m	1.29 m
(1: 1)	3.56 m	2.00 m	1.75 m	1.48 m	-
(1: 2)	3.39 m	1.87 m	1.62 m	1.40 m	0.86 m
(1: 4)	3.61 m	1.76 m	1.51 m	1.32 m	0.86 m

The anionic complex, $[Au(^{13}CN)_4]^-$ is not stable and goes, through *trans*-effect, into reductive elimination to form cyanogen (NCCN), which appeared at 110.52 ppm, while Au(III) was reduced to $[Au(^{13}CN)_2]^-$, which was shifted up-field at 152-157 ppm, due to the back donation of gold to cyanide ligand [205]. The $[Au(CN)_2]^-$ complex has higher stability due to its significant covalent bond than the corresponding $[Cu(CN)_2]^-$ and $[Ag(CN)_2]^-$ described by Wang et al [224].

Figure 8.2**c** shows the ^{13}C spectrum, where the two peaks at 101.31 ppm and 96.50 ppm, indicate the rapid consecutive exchange of chloride ions by $^{13}CN^-$ ion to produce [Au(*cis*-DACH)(^{13}CN)Cl]$^-$ and [Au(*cis*-DACH)($^{13}CN)_2]^-$ respectively. The down-field shift at (1:1.5) ratio to 119.13 ppm, 120.52 ppm, and 121.34 ppm indicates the formation of $[Au(CN)_2Cl_2]^-$, $[Au(CN)_3Cl]^-$, and $[Au(^{13}CN)_2(OH)Cl]^-$ respectively. While the peak at 137 ppm indicates HCN generated by 99.9 % hydrolysis of $K^{13}CN$ [101].

Table 8.2. ^{13}C NMR chemical shifts of the $^{13}CN^-$ for different species during the reaction of [Au(cis-DACH)Cl_2]Cl complex with cyanide in CH_3OD solution.

Species	**^{13}C(δ in ppm)**	**Reference**
KCN	160 ppm	[200]
[Au(*cis*-DACH)(CN)Cl]Cl	101 ppm	This work
$[Au(CN)_4]^-$	103 ppm	[195- 200]
$[Au(CN)_2Cl_2]^-$	119 ppm	[195]
HCN	137 ppm	This work
NCCN	110 ppm	[196]
$[Au(CN)_2(OH)Cl]Cl$	121 ppm	[195]
$[Au(CN)_2(OH)_2]Cl$	120 ppm	[195]
$[Au(CN)_2]^-$	152-157 ppm	[195-200]

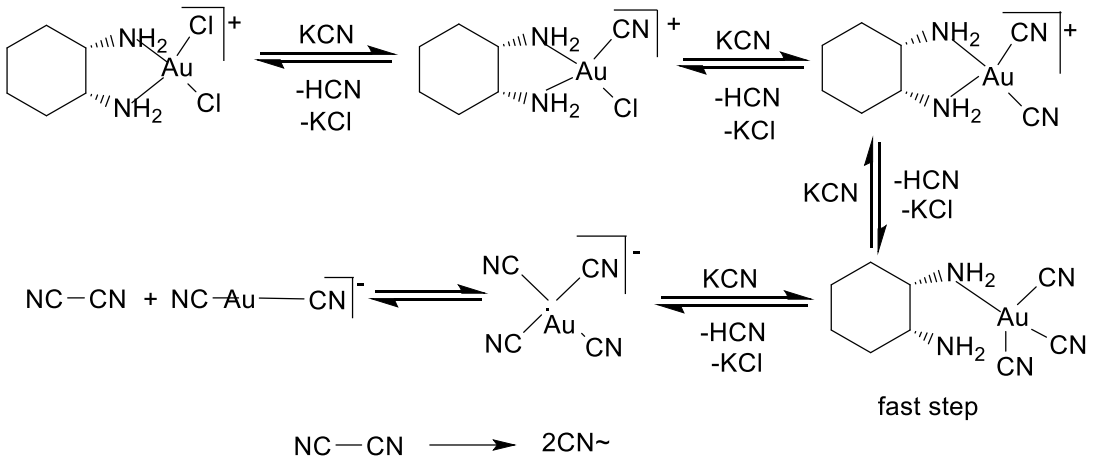

Scheme 25. *Suggested mechanism reaction of* [Au(*cis*-DACH)Cl_2]Cl *with* K^{13}CN *in the range of (1:0.25) to (1:4) ratios.*

The ^{13}C spectrum, fig.2d sheds a light on another reaction mechanism of the reduction of $[Au(^{13}CN)_4]^-$ to $[Au(^{13}CN)_2]^-$ through intermediate complexes $[Au(^{13}CN)_2Cl_2]^-$, $[Au(^{13}CN)_3Cl]^-$, and $[Au(^{13}CN)_2(OH)Cl]^-$ by displacement of cyanide by chloride through *cis* effect kinetics, unlike the behaviour of Pt(II) described by Skibsted [225].

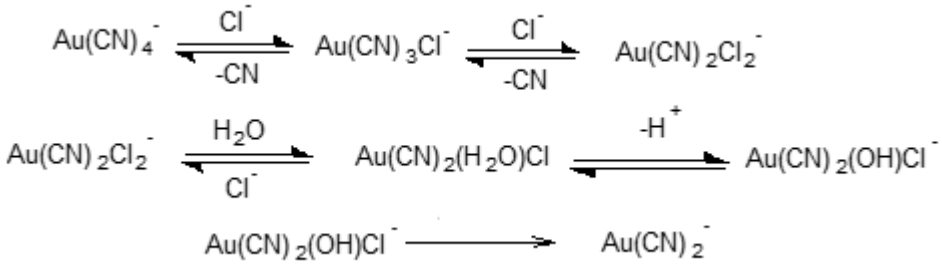

***Scheme 26**. Suggested mechanism of conversion $[Au(^{13}CN)_4]^-$ to $[Au(^{13}CN)_2]^-$.*

The above mechanism is the solvolytic pathway through reversible exchange of chloride and H_2O. For instance, H_2O is being the stronger compared to chloride and cyanide ions in spectrochemical series [226]

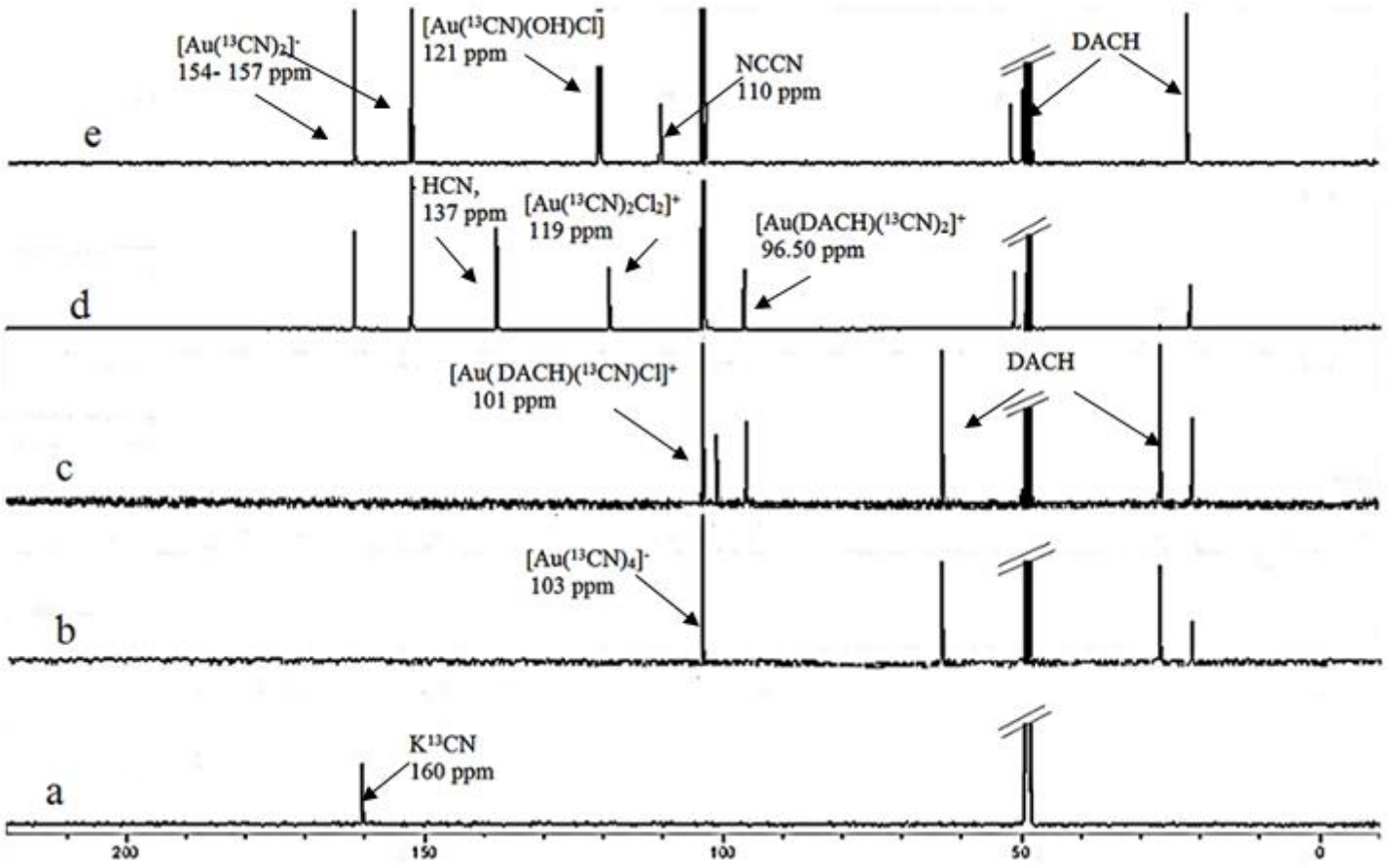

Figure 8.2. *^{13}C NMR spectra of (**a**) free $K^{13}CN$, (**b**) after reaction with [Au(cis-DACH)Cl_2]Cl at (I: 0.25) ratio, (**c**) at (1: 0.5) ratio, (**d**) at (1: 1.5) ratio and (**e**) at (1: 2) ratio, in CH_3OD.*

The CN^- ion, being the strong π-acceptor rapidly displaces DACH at (1:2) ratio as shown by the resonance of free DACH at 53.03 ppm, 31.03 ppm, 22.95 ppm (Fig.2e) [194]. Table 8.1 shows ^1H NMR chemical shifts of [Au(*cis*-DACH)Cl_2]Cl complex interacting with CN^- ligand at different ratios. (Fig. 8.3a) shows a peak at 265 ppm assigned to (5 mM) free 99.9 % enriched $K^{13}C^{15}N$. for the ration reaction (1:2) (Fig.3b) this peak shifted down-field at 281 ppm and it is assigned to $[Au(^{13}C^{15}N)_4]^-$. While at (1:4) ratio, (Fig. 8.3c) there are two resonances at 262 ppm and at 281 assigned to $[Au(^{13}C^{15}N)_2]^-$ and $[Au(^{13}C^{15}N)_4]^-$ respectively [205].

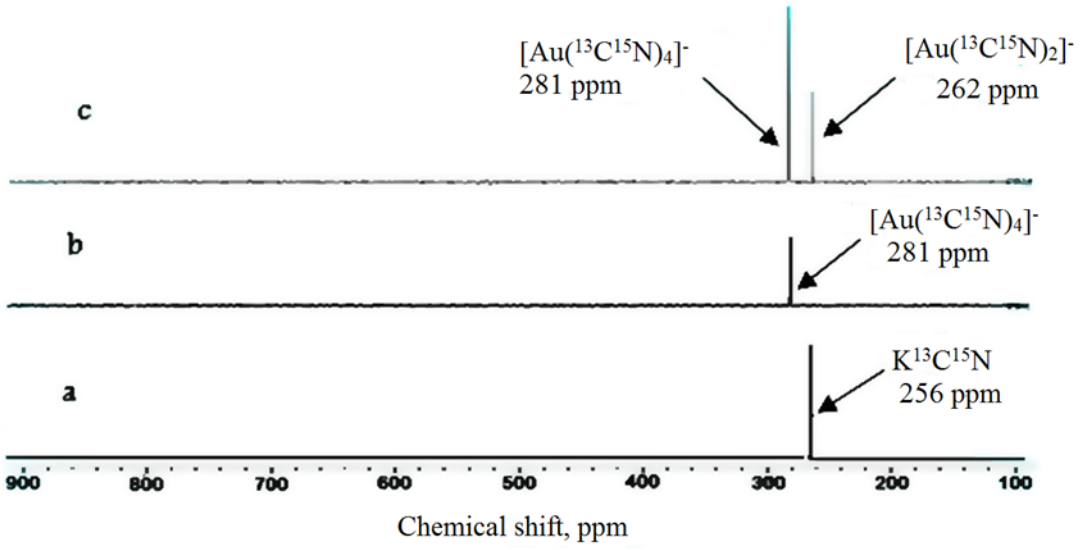

Figure 8.3. *^{15}N NMR spectra of (**a**) free $K^{13}C^{15}N$, (**b**) after reaction with [Au(cis-DACH)Cl_2]Cl at (complex: ligand) (1:2) ratio, (**c**) after reaction with [Au(cis-DACH)Cl_2]Cl at (complex: ligand) (1:4) ratio, in CH_3OD.*

Moreover, the obtained electrochemical results came in a complete agreement with ^1H, ^{13}C, and ^{15}N NMR and UV spectroscopy, and confirmed the suggested mechanism (Schemes 25 and 26). Figure 8.4 and its inset show the SWVs obtained at the GCE

(glassy carbon electrode) in a quiescent aqueous solution of 0.2 M KCl. A well-defined SWV peak (Fig. 8.4b) was obtained at +0.82V (vs. Ag/AgCl) for 1.0 mM [Au(*cis*-DACH)Cl_2]Cl. This peak showed a systematic decrease on its peak area with subsequent additions of CN^- at different equivalents (1:0.5), (1:1) and (1:1.5) (Fig. 4 c-e). At (1:2) ratio, a complete peak disappearance was observed with the appearance of a new peak shoulder around +1.4V (Fig.8.4f), which became more defined at (1:3) and (1:4) ratios. The same additions of CN^- to 0.2 M KCl solution in absence of the [Au(*cis*-DACH)Cl_2]Cl complex showed no peaks (data not shown).

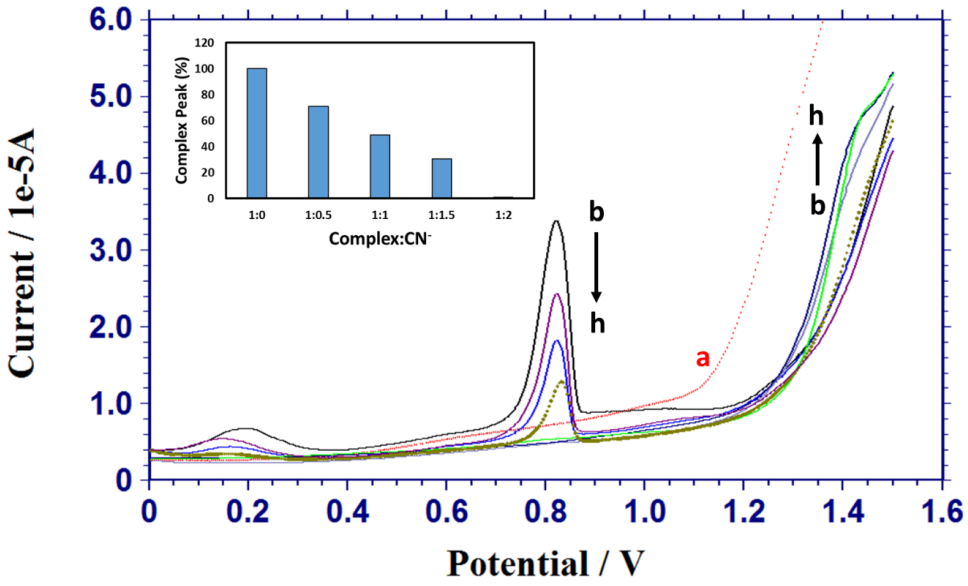

Figure 8.4*. SWVs in a 0.2 M KCl aqueous solution at a GCE in absence (a) and presence (b) of 1.0 mM [Au(cis-DACH)Cl_2]Cl, and subsequent additions of 0.5 mM (c-f) and 1.0 mM (g, h) of KCN aqueous solution. Working condition of the pulse width (increment), 4mV; pulse height (amplitude), 25 mV; frequency, 15 Hz. Inset is the corresponding histogram at different complex: CN^- ratio.*

8.3.2 Interaction of [Au(*cis*-DACH)$_2$]Cl$_3$ with K^{13}CN

Interaction of [Au(*cis*-DACH)$_2$]Cl$_3$ with 20% enriched K^{13}CN was carried out in D_2O by mixing the reactants at different mole ratios and monitored by ^1H, ^{13}C ,^{15}N NMR, UV-vis spectroscopy, and electrochemistry. The ^1H, ^{13}C and ^{15}N NMR chemical shifts for this interaction are given in Tables (8.3-8.4B). ^{13}C NMR is used to monitor the interaction, (Fig. 8.5a) shows a peak for (5 mM) 20% enriched K^{13}CN assigned at 157.4 ppm. (Fig. 8.5b) shows two new peaks up-field at 104.5 ppm and at 119.8 ppm corresponding to $[Au(^{13}CN)_4]^-$ and $[Au(CN)_2Cl_2]^-$ respectively [101,195]. When the reaction is carried out at (1:1) ratio, the peak at 119.8 ppm is shifted down-field 120.47 ppm and a new peak is observed at 154.37 ppm, assigned to $[Au(^{13}CN)_2]^-$, which is the result of reductive elimination of $[Au(^{13}CN)_4]^-$ (Fig. 8.5c) [223].

Figure 8.5d shows a peak at 110.10 ppm of cyanogen (NCCN) due to an oxidation of CN^- and reduction of Au(III) to Au(I) [101]. There is a significant down-field shift from 119.8 ppm to 122.5 ppm corresponding to very fast consecutive two cyanide ligands exchanged by H_2O due to solvolytic pathway [226].

Table 8.3. ^1H NMR chemical shifts of DACH protons for the reaction of [Au(cis-DACH)$_2$]Cl$_3$ with (K13CN) in D_2O.

Species	1H, 2H	3H, 6H eq.	3H, 6H ex.	4H, 5H eq.	4H, 5H ex.
(1:0)	3.58 m	1.94 m	1.74 m	1.56 m	1.38 m
(1:1)	3.32, 3.20 m	1.86 m	1.65 m	1.53 m	1.33 m
(1:2)	3.21, 3.06 m	1.80 m	1.62 m	1.49 m	1.26 m
(1:4)	3.75, 2.85 m	-	1.65 m	1.42 m	1.23 m

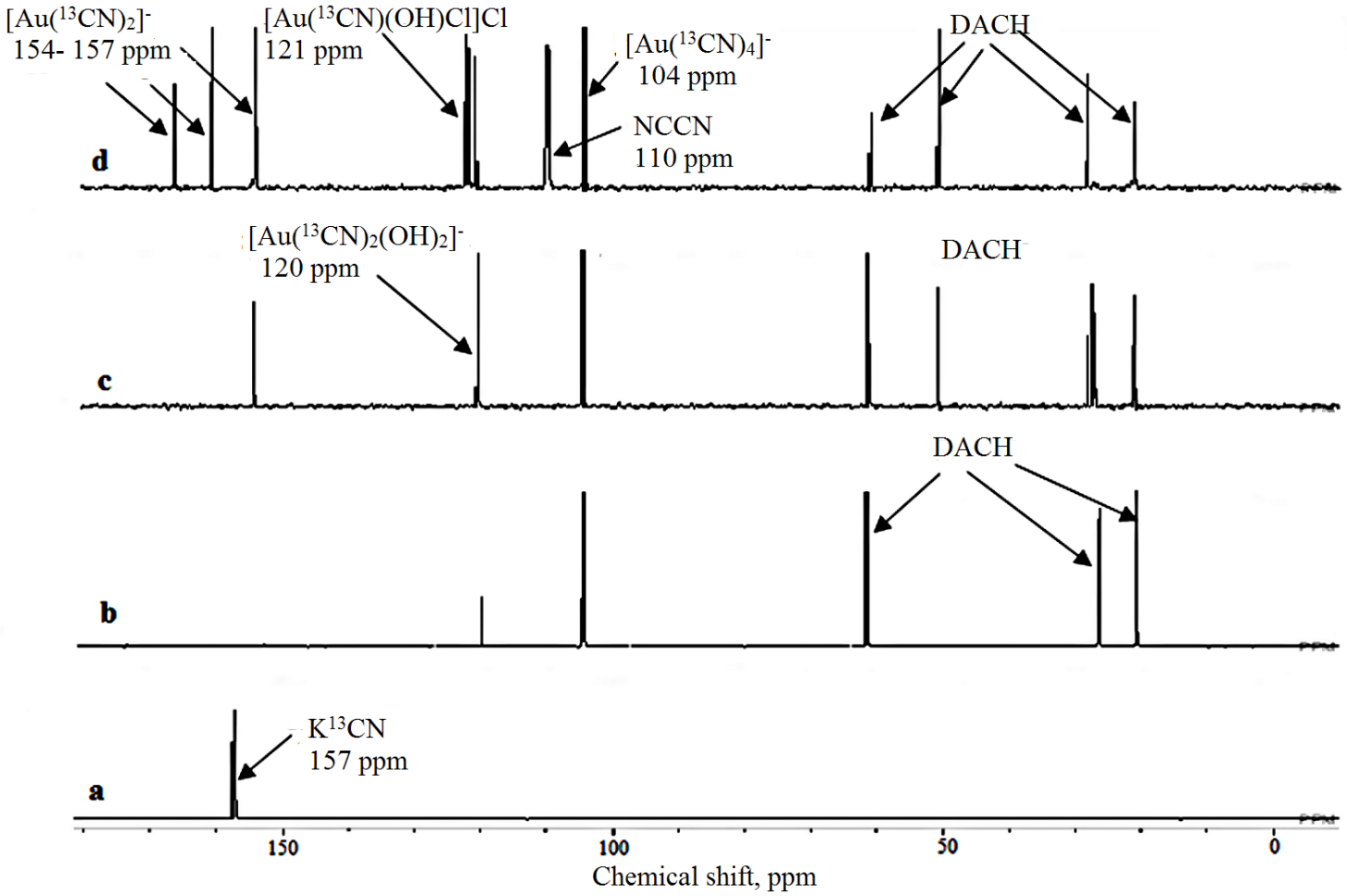

Figure 8.5. *13C NMR spectra of (a) free K13CN, (b) after reaction with [Au(cis-DACH)2]Cl3 at(I: 0.25) ratio, (c) at (1:1) ratio, (d) at (1: 2) ratio in D_2O.*

At higher concentration of $^{13}CN^-$ ion into (1:4) ratio, an up-field shift of DACH's carbons was observed, which corresponds to the displacement of DACH ligands. The peak observed at 121 ppm is an indication of H_2O being exchanged by chloride to form $[Au(CN)_2(OH)Cl]^-$ (Fig. 8.5d) [195]. Table 8.3 shows ^1H NMR chemical shifts for $[Au(cis\text{-}DACH)_2]Cl_3$ reaction with $K^{13}CN$ in the range (1:1) to (1:4) ratio.

Table 8.4(A-B). ^{15}N NMR chemical Shifts of the $^{13}C^{15}N^-$ for different species during the reactions of $[Au(cis\text{-}DACH)Cl_2]Cl$ (A) and $[Au(cis\text{-}DACH)_2]Cl_3$ (B) with $K^{13}C^{15}N$ in CH_3OD and D_2O.

Specie	**A**	**B**
$K^{13}C^{15}N$	265.03 ppm	271.82 ppm
$[Au(^{13}C^{15}N)_2]^-$	262.63 ppm	265.06 ppm
$[Au(^{13}C^{15}N)_4]^-$	281.52 ppm	275.01 ppm

The ^{15}N NMR spectrum (Fig.8.6b) shows two resonances at 275.01 ppm and 265.06 ppm assigned to $[Au(^{13}C^{15}N)_4]^-$ and $[Au(^{13}C^{15}N)_2]^-$ respectively.

Figure 8.7 shows a SWV peak for the $[Au(cis\text{-}DACH)_2]Cl_3$ at +1.35V (vs. Ag/AgCl). The peak area decreased systematically with the additions of CN^-. However, and due to the relatively high potential peak position (+1.35V), the decrease was not easy to follow, yet the trend is clear.

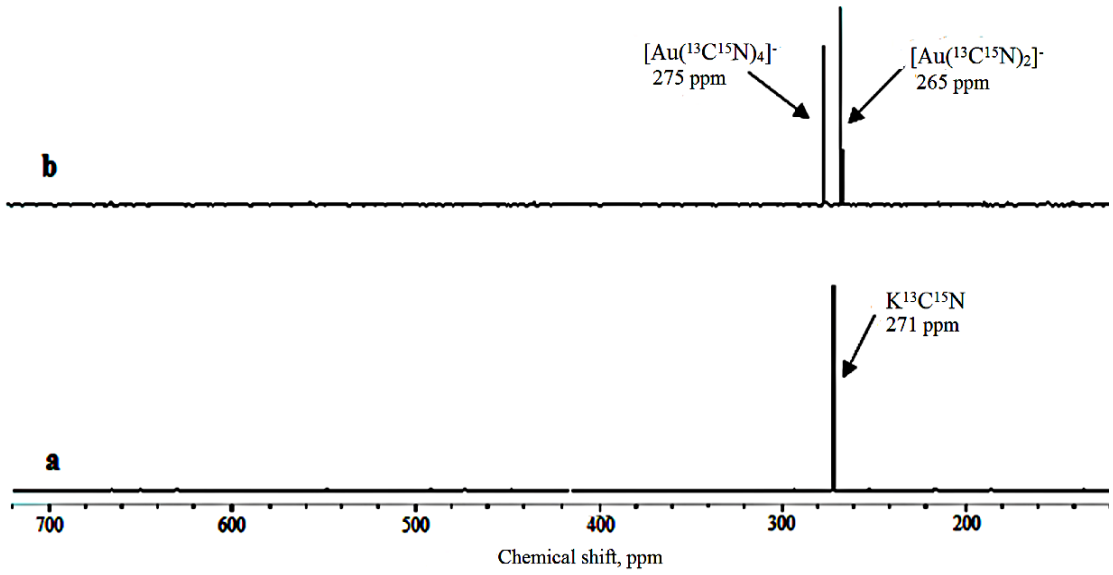

Figure 8.6. *^{15}N NMR spectra of (a) free $K^{13}C^{15}N$ and (b) after reaction with $[Au(cis\text{-}DACH)_2]Cl_3$ at (complex: ligand) (I:2) ratio in D_2O.*

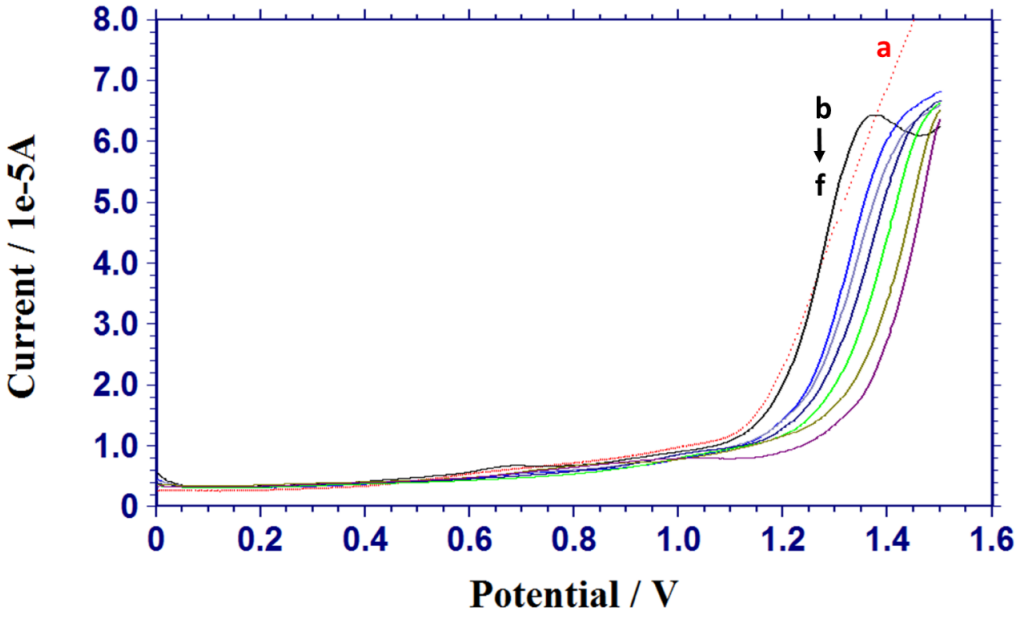

Figure 8.7. *SWVs in a 0.2 M KCl aqueous solution at a GCE in absence of complex (a) and presence (b) of 1.0 mM $[Au(cis\text{-}DACH)_2]Cl_3$, and subsequent additions of 0.5 mM (c-f) and 1.0 mM (g, h) of KCN aqueous solution. Working condition of the pulse width (increment), 4* mV; pulse height (amplitude), 25 mV; frequency, 15 Hz.

8.3.3 Kinetic Data

The substitution reactions of these square-planar gold(III) complexes [(*cis*-DACH) $AuCl_2$]Cl and [Au(*cis*-DACH)$_2$]Cl_3 with cyanide ion were investigated spectro-photometrically by the change of absorbance at the selected wavelengths as function of time under pseudo-first order conditions. The substitution reaction proceeds most likely through an associative mechanism. All reactions were studied in aqueous solution. An addition of 20 mM NaCl prevents hydrolysis of the complex. The suggested reaction mechanism of cyanide ion with [Au(*cis*- DACH)Cl_2]Cl is shown in Scheme 25. The rate constants are determined from the plot of linear dependence of k_{obsd} versus total cyanide concentration (figure 8.8A) according to equation (1). The slope of the line represents k_f, while the intercept indicates $k_b[Cl^-]$. All kinetic data are summarized in Table 8.5.

$$k_{obsd} = k_f[CN^-] + k_b[Cl^-] \quad (1)$$

The Enthalpy, Entropy and Activation energy for the reaction of [Au(*cis*-DACH)Cl_2]Cl with cyanide ion are calculated using Eyring equation (2) and Arrhenius equation (3)

$$\ln\frac{k}{T} = \frac{-\Delta H^{\ddagger}}{R}\cdot\frac{1}{T} + \ln\frac{k_B}{h} + \frac{\Delta S^{\ddagger}}{R} \quad (2)$$

$$\ln(k) = \ln(A) - \frac{E_a}{R}\frac{1}{T} \quad (3)$$

From the rate constant values, it can be clearly seen that the [Au(*cis*-DACH)Cl_2]Cl reacts much faster than [Au(*cis*-DACH)$_2$]Cl_3 complex. The difference in reactivity can be attributed most likely to the lability of chloride and the chelate of two (*cis*-DACH) ligands [223].

Table 8.5. Rate constant k, for substitution reaction of [Au(cis-DACH)Cl_2]Cl and [Au(cis-DACH)$_2$]Cl_3 with cyanide ion, in the presence of 20 mM NaCl in aqueous solution at 298 K.

λ max	**[Au(*cis*-DACH)Cl_2]Cl = 0.1 mM**						
	[CN^-]/ M	K_{obsd} / s^{-1}	k_f / $M^{-1}s^{-1}$	k_b/ $M^{-1}s^{-1}$	$\Delta H^{\neq}$/kJmol^{-1}	$\Delta S^{\neq}$/JK^{-1}mol^{-1}	E_a/kJmol^{-1}
305 nm	0.00200	0.1993	148 ± 1.00	(11 ±1)10^{-4}	39 ± 3.0	-80 ± 4.0	42± 4.0
	0.00300	0.3458					
	0.00400	0.5989					
	0.00500	0.7246					
	0.00600	0.9971					
	0.00800	1.3654					
	0.01000	1.7456					
	0.02000	2.8345					
λ max	**[Au(*cis*-DACH)$_2$]Cl_3 = 0.1 mM**						
258 nm	0.00200	0.0696	18 ±1.0	(94 ±1)10^{-4}	11 ± 2.0	-185 ± 4.0	13 ± 2.0
	0.00300	0.0797					
	0.00400	0.09478					
	0.00500	0.10739					
	0.00600	0.11663					
	0.00800	0.14978					
	0.01000	0.2552					
	0.02000	0.38307					

The reactive kinetics of the cyanide ligand is found to be much faster than the following nucleophiles: L-histidine (L-His), guanine-5′-monophosphate (5′-GMP), inosine (Ino), and inosine-5′-monophosphate (5′-IMP) towards the [Au(*cis*-DACH)Cl_2]Cl complex [61-62].

The reactivity order of these ligands toward [Au(*cis*-DACH)Cl_2]Cl complex is CN^- >>> L-His >5′-GMP > Ino > 5′-IMP as shown in (Table 8.6). it is substitution reaction and absorbance band is 305 nm as shown in Fig. 8.9.

Table 8.6. Rate constants for substitution reactions of [Au(cis-DACH)Cl_2]Cl and [Au(cis-DACH)$_2$]Cl_3 complexes with cyanide in presence of 20 mM NaCl in aqueous solution at 298K.

Specie	k_f / M^{-1} s^{-1}	K_b / M^{-1} s^{-1}	$\Delta H^{\neq}$/kJ mol^{-1}	$\Delta S^{\neq}$/$JK^{-1}mol^{-1}$	ΔE_a / kJmol^{-1}	Reference
[Au(*cis*-DCH)Cl_2]$^+$						
Cyanide	148 ± 3	(11± 1)10^{-4}	39 ± 3.0	-80 ± 4.0	42 ± 4.0	This work
L-His	75 ± 2	4.0 ± 0.1	12 ± 3	-160 ± 10	-	[171]
5′-GMP	66 ± 2	9.3 ± 0.2	10 ± 3	-180 ± 10	-	[61, 62]
5′-IMP	6. ± 0.3	0.6 ± 0.2	-	-	-	[61]
Ino	10 ± 1	0.6 ± 0.2	-	-	-	[61]
[Au(*cis*-DACH)$_2$]$^{3+}$						
Cyanide	18 ±1	(94 ± 1)10^{-4}	11 ± 2.0	-185 ± 4.0	13 ± 2.0	This work

Figure 8.10 shows UV spectra of an oxidation reduction reaction of [Au(*cis*-DACH)Cl_2]Cl with CN^- ion at (complex: ligand) (1:2) ratio. The bands observed at 204 nm and 211 nm, correspond to $[Au(CN)_2]^-$, by the back donation from d-orbital(d^8) in Au(III) ion to empty π^* -acceptor in cyanide ligand, which strengthens Au-CN and weakens Au-NR. Figure 8.11 shows an oxidation reduction reaction of

[Au(cis-DACH)Cl_2]Cl with CN^- ion at (1: 4) ratio. The bands observed at 204, 211and 240 nm assigned to $[Au(CN)_2]^-$, remains unchanged after 24 h, indicating completion of the oxidation reduction reaction [228-229]. Figure 8.12(A-B) show pseudo-first order rate constant as function of nucleophilic concentration and temperature for the reaction of [Au(*cis*-DACH)Cl_2]Cl and [Au(*cis*-DACH)$_2$]Cl_3 with cyanide ion.

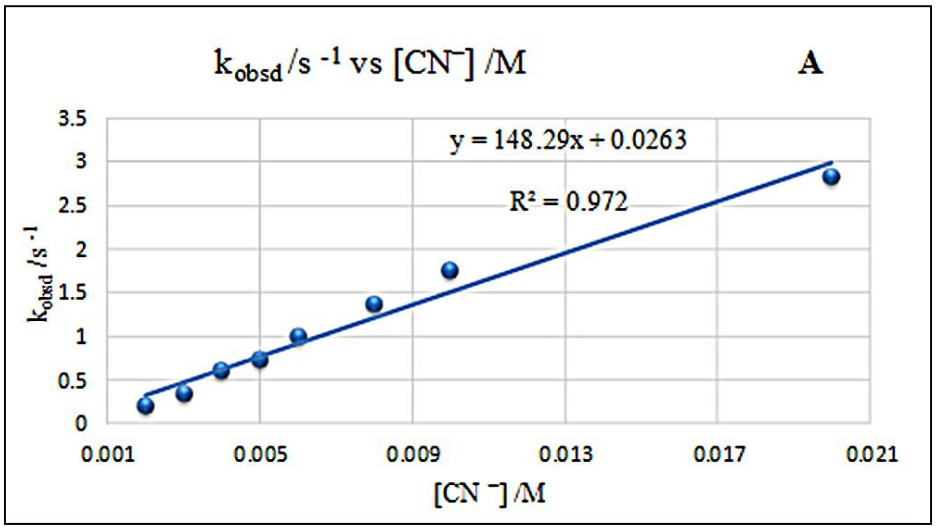

Figure 8.8A. *Plot of pseudo-first order rate constant for the reaction between [Au(cis-DACH)Cl_2]Cl with cyanide ion in aqueous solution at ambient temperature of 25 °C.*

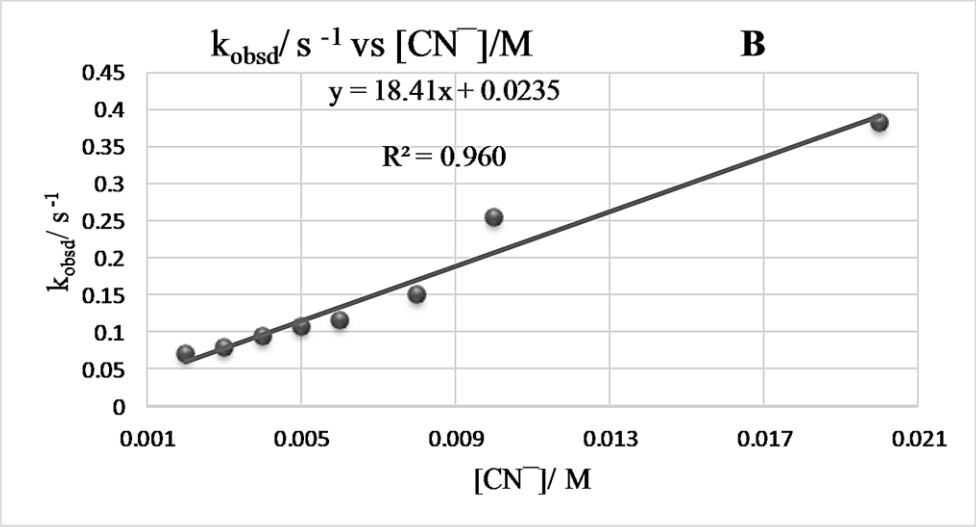

***Figure 8.8B**. Plot of pseudo-first order rate constant for the reaction between [Au(cis-DACH)$_2$]Cl$_3$ with cyanide ion in aqueous solution at ambient temperature of 25 ℃.*

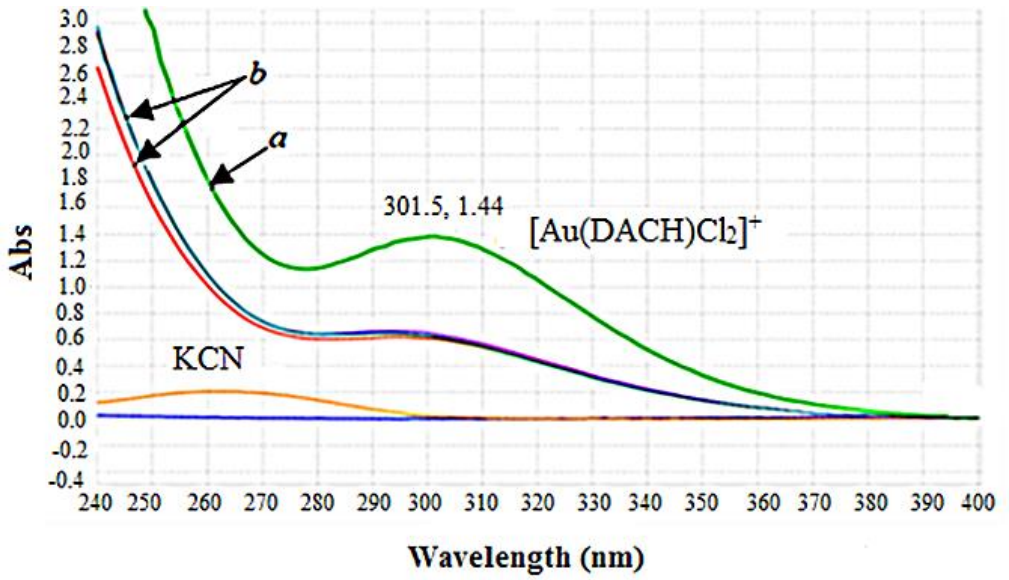

***Figure 8.9.** UV-Vis spectra for the substitution reaction of (**a**) [Au(cis-DACH)Cl$_2$]Cl (1 mM) before and (**b**) after addition of KCN(1 mM) at (complex: ligand) (1:0.5) ratio in the range 240-400 nm at ambient temperature of 25 °C.*

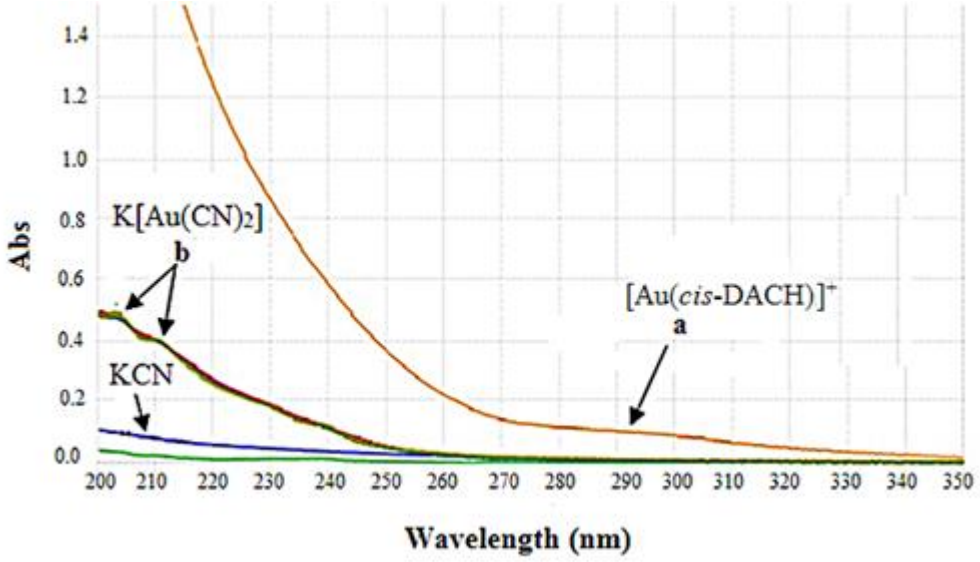

Figure 8-10. *UV-Vis spectra for an oxidation reduction reaction of (**a**) [Au(cis-DACH)Cl$_2$]Cl (0.1 mM) before and (**b**) after addition of KCN (0.1 mM) at (complex: ligand) (1:2) mole ratio in the range 200-350 nm at 25 °C.*

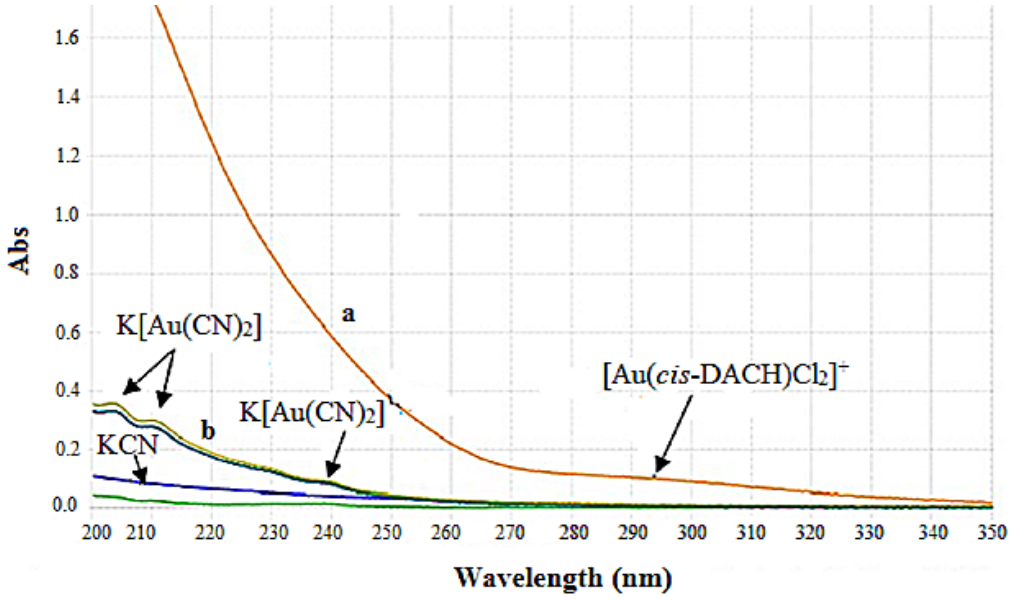

Figure 8.11. *UV-Vis spectra for an oxidation reduction reaction of (**a**) [Au(cis-DACH)Cl$_2$]Cl (0.1 mM) before and (**b**) after 30 min of addition of KCN (0.1 mM) at (complex: ligand) (1:4) mole ratio in the range 200-350 nm at 25 °C.*

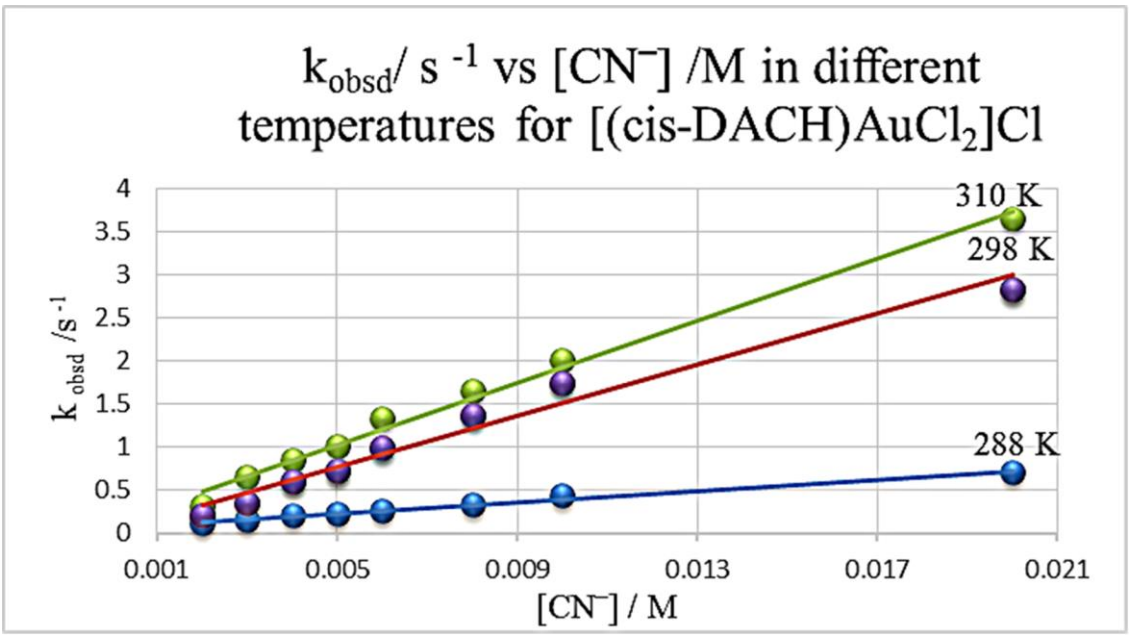

***Figure 8.12A**: Plot of pseudo first order rate constants, as function of CN^- concentration and temperature for the reaction between [Au(cis-DACH)Cl_2]Cl and cyanide ion in the presence of 20 mM NaCl in aqueous solution.*

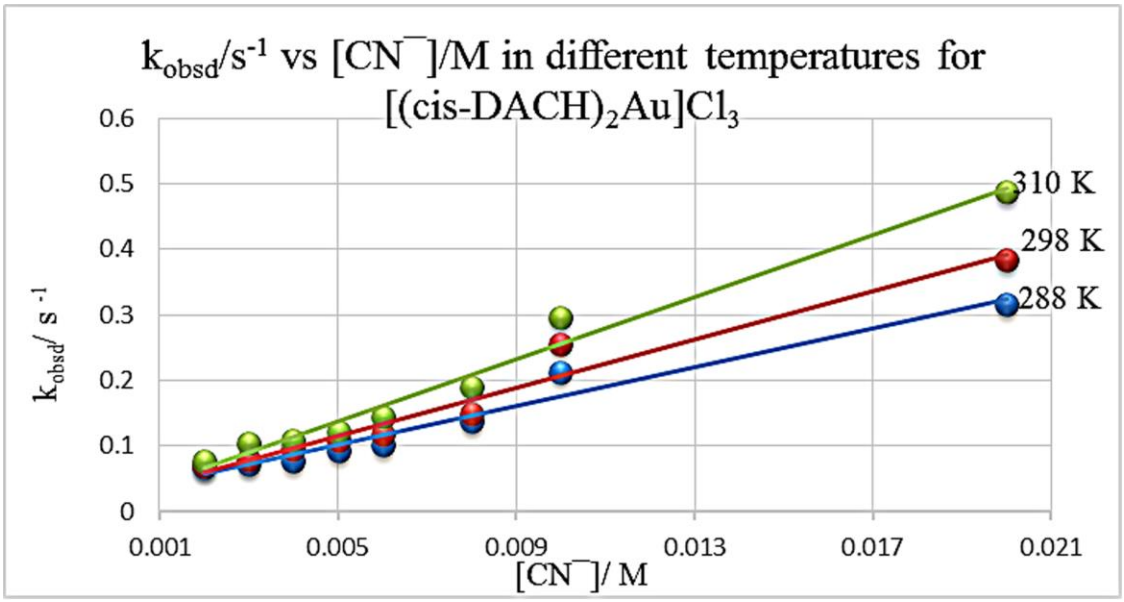

***Figure 8.12B**: Plot of pseudo first order rate constants, as function of CN^- concentration and temperature for the reaction between [Au(cis-DACH)$_2$]Cl_3 and cyanide ion in the presence of 20 mM NaCl in aqueous solution.*

CONCLUSION AND FUTURE STUDIES

Gold(I) complexes belong to an emerging class of potential anticancer agents. During the past couple of decades many gold(I) compounds with versatile structures, showing promising cytotoxic effects against selected human cancer cell lines and acceptable stability under physiological conditions have been reported. All attributes make them good candidates as antitumor drugs. Herein, we report the synthesis, and characterization of gold(I) complexes [Au(R_3P)(R_2NCS_2)] **(2-34)**;[Au(R_3P)$_2$] (**35-37**); [Au(Ipr)-(Se=CR_2)] (**38-50**); [Au(R_3P)(S=CR_2)], (**51-55**),[Au(Ipr)(R_3P)] and [Au(Ipr)$_2$(R_6P_2)] **(56-65)**. Compounds (**2-22**), (**35-37**), and (**38-50**) were tested for their an *in vitro* cytotoxicity against three human cancer cell lines; HeLa (human cervical cell line), HCT 15(human colon cell line) and A549 (human lung carcinoma). Gold(I) compounds **(20-22, 48)** exhibited better cytotoxicity in terms of IC_{50} values against A549 cell line and HCT15 than the standard anticancer chemotherapy drug (cisplatin). Whereas, the other studied gold(I) compounds showed moderate to lower *in vitro* cytotoxicity against HCT15 and HeLa cancer cell lines. The significant cytotoxicity of gold(I) compounds against A549 and HCT15 human cancer cells has made them strong candidates as potential anticancer agents for further exploration against lung and colon cancer.

The interaction of [Au(*cis*-DACH)Cl_2]Cl and [Au(*cis*-DACH)$_2$]Cl_3 with cyanide, Tu and DIAZ was studied using (^{1}H, ^{13}C and ^{15}N) NMR and square wave stripping voltammetry. contribution for DaipSe and DaizSe relatively to ImSe due to ring strain hindering the rehybridization of N culminating in DaipSe NMR studies showed that DIAZ ligates more strongly than Tu. Thiol form be as a higher contribution for DIAZ than thione relatively

to Tu (evident from the magnitude of (C=S) chemical shift). Kinetic measurements revealed that the substitutive reaction [Au(*cis*-DACH)Cl_2]Cl reacting faster than [Au(*cis*-DACH)$_2$]Cl_3. Also the trend of the rate constants for the ligands oder as following: cyanide >>> Tu > DIAZ. The negative values of $\Delta S^{\neq}$ for these reactions lend support for an associative mechanism and these results may contribute to a better understanding of biochemical mechanism of [Au(*cis*-DACH)Cl_2]Cl and [Au(*cis*-DACH)$_2$]Cl_3.

For further future studies

- ✓ *In vitro* cytotoxicity assay of the compounds (**23-34**), (**51-55**) and (**56-65**).
- ✓ *In vivo* assay for gold(I) compounds with the significant cytotoxicity to explore their mechanism of action.
- ✓ Stopped flow kinetics of [Au(*cis*-DACH)Cl_2]Cl and [Au(*cis*-DACH)$_2$]Cl_3 with biomolecules.

REFERENCES

[1] P. J. Sadler, R. E. Sue, The Chemistry of Gold Drugs, *Met. Based Drugs*, 1, 104-144, 1994.

[2] A. Laguna, *Mod. Supramol. Gold Chem. Gold-Metal Interact. Appl.*, WILEY-VCH Verlag GmbH & Co. KGaA, Weinheim, 2008.

[3] S. Komeda, M. Lutz, A. Spek, M. Chikuma, J. Reedijk, New antitumor-active azole-bridged binuclear platinum(II) complexes: Synthesis, characterization, crystal structures, and cytotoxic studies, *Inorg. Chem*, 39, 4230, 2000.

[4] E. R. T. Tiekink , Gold derivatives for treatment of cancer, *Rev. Oncol. Hematol.*, 42, 225, 2002.

[5] L. Sun, H. Chen, Z. Zhang, Q. Yang, H. Tong, A. Xu, C. Wang, Synthesis and cancer cell cytotoxicity of water-soluble gold(III) substituted tetraarylporphyrin, *J. Inorg. Biochem*, 108, 47, 2012.

[6] S. Wang, W. Shao, H. Li, C. Liu, K. Wang, J. Zhang, Synthesis, characterization and cytotoxicity of the gold(III) complexes of 4,5-dihydropyrazole-1-carbothioamide deriv-atives, *Eur. J. Med. Chem*, 46, 1914, 2011.

[7] S. Van Zutphen, J. Reedijk, Targeting platinum anti-tumour drugs: Overview of strategies employed to reduce systemic toxicity, *Coord. Chem. Rev*, 249, 2845, 2005.

[8] A. Ahmed, D. M. AlTamimi, A. A. Isab, M.Alkhawajah, M., A.Shawarby, M. A. Shawarby, Histological changes in kidney and liver of rats due to gold(III) compound $[Au(en)Cl_2]Cl$, *PLoS One*, 7, e51889, 2012.

[9] A. Casini, C. Hartinger, C. Gabbiani, E. Mini, P. J. Dyson, B. K. Keppler, L. Messori,

Gold(III) compounds as anticancer agents: Relevance of gold–protein interactions for their mechanism of action. *J. Inorg. Biochem.*, 102, 564, 2008.

[10] M. N. Kouodom, Ronconi, L. M. Celegato, C. Nardon, L. Marchiò, Q. P. Dou, Aldinucci, F. F, and D. Fregona, Toward the selective delivery of chemotherapeutics into tumor cells by targeting peptide transporters: Tailored gold-based anticancer peptidomimetics, *J. Med. Chem.*, 55, 2212, 2012.

[11] V. Milacic, D. Chen, L. Ronconi, K. R. Landis-Piwowar, D. Fregona, and Q. P. Dou, A novel anticancer Gold(III) dithiocarbamate compound inhibits the activity of a purified 20S Proteasome and 26S Proteasome in Human Breast Cancer Cell Cultures and Xenografts, *Cancer Res.*, 66, 10478, 2006

[12] L. Ronconi, C. Marzano, P. Zanello, M. Corsini, G. Miolo, C. Macca, A. Trevisan, D. Fregona, Gold(III) dithiocarbamate derivatives for the treatment of cancer: Solution chemistry, DNA binding, and hemolytic properties, *J. Med. Chem.*, 49, 1648, 2006.

[13] M. Carreira, R.Calvo-Sanjuán, M. Sanaú, X. Zhao, R. S. Magliozzo, I. Marzo, and and M. Contel, Cytotoxic hydrophilic iminophosphorane coordination compounds of d^8 metals. Studies of their interactions with DNA and HSA *J. Biochem.*, 116, 204, 2012.

[14] L. Giovagnini, L. Ronconi, D. Aldinucci, D. Lorenzon, S. Sitran, and D. Fregona, Synthesis, Characterization, and Comparative in vitro cytotoxicity studies of platinum(II), palladium(II), and gold(III) methylsarcosinedithiocarbamate complexes, *J. Med. Chem.*, 48, 1588, 2005.

[15] A. Casini, M. A. Cinellu, G. Minghetti, C. Gabbiani, M. Coronnello, E. Mini, and L.

Messori, Structural and solution chemistry, antiproliferative effects, and DNA and protein binding properties of a series of dinuclear Gold(III) compounds with bipyridyl ligands, *J. Med. Chem.*, 49, 5524, 2006.

[16] D. Aldinucci, D. Lorenzon, L. Stefani, L. Giovagnini, A. Colombatti, and D. Fregona, Antiproliferative and apoptotic effects of two new gold(III) methylsarcosine -dithiocarbamate derivatives on human acute myeloid leukemia cells in vitro, *Anti-Cancer Drug.*, 18, 323, 2007.

[17] M. Coronnello, G. Marcon, S. Carotti, B. Caciagli, E. Mini, T. Mazzei, P. Orioli, L. Messori, Cytotoxicity, DNA damage, and cell cycle perturbations induced by two representative gold(III) complexes in human leukemic cells with different cisplatin Sensitivity, *Oncol. Res.*, 12, 361, 2001.

[18] L. Ronconi, L. Giovagnini, C. Marzano, F. Bettio, R. Graziani, Pilloni, and G.D. Fregona, Gold dithiocarbamate derivatives as potential antineoplastic agents: Design, spectroscopic properties, and in vitro antitumor activity, *J. Inorg. Chem*, vol. 44, p. 1867, 2005.

[19] A. Bindoli, M. P. Rigobello, G. Scutari, C. Gabbiani, A. Casini, and L. Messori, Thio-redoxin reductase: A target for gold compounds acting as potential anticancer drugs, *Coord. Chem. Rev.*, 253, 1692, 2009.

[20] G. Marcon, S. Carotti, M. Coronnello, L. Messori, E. Mini, P. Orioli, T. Mazzei, M. A. Cinellu, and G. Minghetti, Gold(III) complexes with bipyridyl Ligands: solution chemistry, cytotoxicity, and DNA binding properties, *J. Med. Chem.*, 45. 1672, 2002.

[21] F. Abbate, P. Orioli, B. Bruni, G. Marcon, L. Messori, Crystal structure and solution chemistry of the cytotoxic complex 1,2-dichloro(o-phenanthroline)gold(III) chloride,

Inorg. Chim.Acta, 3111, 2000.

[22] T. Yang, Zhang, J. Y. Tu, C. J. Lin, Q. Liu, Z. J. Guo, Chin., *J. Inorg. Chem.*, 19, 45, 2003.

[23] S. Nobili, E. Mini, I. Landini, C. Gabbiani, A. Casini, and L. Messori, Gold compounds as anticancer agents: chemistry, cellular pharmacology, and preclinical studies, *Med. Res. Rev.*, 550, 2010.

[24] R. G. Buckley, A. M. Elsome, S. P. Fricker, G. R. Henderson., B. R. Theobald, R. V. Parish, B.P. Howe, L.R.Kelland, Antitumor properties of some 2-[(Dimethylamino) -methyl]phenylgold(III) complexes, *J. Med. Chem.*, 39, 5208, 1996.

[25] P. Ctdamai, S. C. A. Guerri, L. M. E. Mini, P. Orioli, and G.P. Speroni, Biological properties of two gold(III) complexes: $AuCl_3$ (Hpm) and $AuCl_2$ (pm), *J. Inorg. Biochem*, 66, 103-109, 1997.

[26] P.C. Hydes M. J. H. Russell., Advances in platinum cancer chemotherapy, *Cancer Metastasis Rev.*,7, 67, 1988.

[27] J. C. Dabrowiak, W. T. Bradner, Platinum Antitumor Agents, *Prog. Med. Chem.*, 24, 129, 1987.

[28] L.S. Hollis, A. R. Amundsen, E. W. Stern., Chemical and biological properties of a new series of cis-diammineplatinum(II) antitumor agents containing three nitrogen donors: cis-$[Pt(NH_3)_2(N\text{-donor})Cl]^+$, *J. Am. Chem. Soc.*, 32, 128-136, 1989.

[29] Y. Kidani, K. Inagaki, R. Saito, S. Tsukagoshi., Synthesis and antitumor activities of platinum(II) complexes of 1,2-diaminocyclohexane isomers and their related derivatives, *J. Clin. Hematol. Oncol.*, 7, 197-209, 1977.

[30] M. Gulloti, A. Pasini, R. Ugo, Filippeschi, S. L. Marmonti, F. Spreafico,

Enantiomeric cisplatin analogues: an investigation on their activity towards tumors in mice, *Inorg. Chim. Acta,* 91, 223, 1984.

[31] Y. Kidani, K. Inagaki, Iigo, M. A. Hoshi, K. Kuretani., Antitumor activity of 1,2-diaminocyclohexaneplatinum complexes against Sarcoma-180 ascites form, *J. Med. Chem.*,21, 1315-1318, 1978.

[32] M. Noji, K. Okamoto, Y. Kidani, T. Tashiro., Relation of conformation to antitumor activity of platinum(II) complexes of 1,2-cyclohexanediamine and 2-(aminomethyl) -cyclohexylamine isomers against leukemia P388. *J. Med. Chem.*, 24, 508-515, 1981.

[33] Y. Kidani, M. Noji, and and T. Tashiro, Antitumor activity of platinum(II) complexes of 1,2-diamino-cyclohexane isomers, *J. Japanese. Cancer Res.*, 71, 637, 1980.

[34] A. Pasini, A. Velcich, A. Mariani, Absence of diasteroisomeric behaviour in the interaction of chiral platinum anticancer compounds with DNA, *Chem. Biol. Interact.*, 42, 311, 1982.

[35] J. H. Burchenal, K. Kalaher, T. O'Toole, Synergistic Effects of the Combination of cis-Platinum Diamminodichioride and 2,2'-Anhydro-l -D-arabinofuranosyl-5-fluoro-cytosine in transplanted mouse leukemias1, *J. Chisholm. Cancer Res.*, 37, 3455, 1977.

[36] M. A. Bruck, R. Bau, M. Noji, K. Inagaki, Y. Kidani., The crystal structures and absolute configurations of the anti-tumor complexes Pt(oxalato) (1R,2R-cyclohexanediamine) and Pt(malonato)(1R,2R-cyclohexanediamine), *Inorg. Chim. Acta,* 92, 279, 1984.

[37] J. F. Vollano, S. Al-Baker, J. C. Dabrowiak, J. E. Schurig, Comparative antitumor studies on platinum(II) and platinum(IV) complexes containing 1,2-diamino-

cyclohexane, *J..Med. Chem.*, 30, 716, 1987.

[38] N. P. Johnson, J. L. Butour, G. Villani, F. L. Wimmer, M. Dafais, V. Pierson, V. Brabec, Metal antitumor compounds: The mechanism of action of platinum complexes, *Prog. Clin. Biochem. Med.*, 10, 1-24, 1989.

[39] M. J. Cleare, P. C. Hydes, B. W. Malerbi, D. M. Watkins, *Biochimie*, 60, 835, 1978.

[40] M. Al-Sarraf, J. Kish, J. Ensley, B. Metch, J. Rinehart, D. Schuller, C. Coltman, *Proc. Am. Soc. Clin. Oncol.,* 6, A485, 1987.

[41] I. ott., On the medicinal chemistry of gold complexes as anticancer drugs, *Coord. Chem. Rev.*, 253, 1670–1681, 2009.

[42] O. Rackham, S. J. Nichols, P. J. Leedman, A. F. Susan J. Berners-Price, A gold(I) phosphine complex selectively induces apoptosis in breast cancer cells: Implications for anticancer therapeutics targeted to mitochondria, *Biochem. Pharmacol.*, 74, 992–1002, 2007.

[43] F. Bakar, G. Caglayan, O. Mehmet, N, Feyyaz, M, Serpil P. Ismail, Gold nanoparticle-lignan complexes inhibited MCF-7 cell proliferation in vitro: A novel conjugation for cancer therapy, *Anti-Can. Agent. Med. Chem.*, 15, 336-344, 2015

[44] D. Wang, Y. Zhang, R. Cai, X. S. Beilstein, Triazole–Au(I) complex as chemo-selective catalyst in promoting propargyl ester rearrangements. *J. Org. Chem.*, 7, 1014–1020, 2011.

[45] Z. Assefa, J. M. Forward, T. A. Grant, R. J. Staples, B. E. Hanson, A. A. Mohamed, J. P. Fackler, Three-coordinate, luminescent, water-soluble gold(I) phosphine complexes: structural characterization and photoluminescence properties in aqueous solution, *J. Inorg. Chim. Acta*, 352, 31–45, 2003.

[46] M. F. Fillat, M. C. Gimeno, A. Laguna, E. Latorre , L. Ortego, M. D. Villacampa, Synthesis, structure and bactericide activity of (Aminophosphane)gold(I) thiolate complexes, *Eur. J. Inorg. Chem.*, 1487–1495, 2011.

[47] S. D. Khanye, G. S. Smit, C. Lategan P. J. Smith, J. Gut, P. J. Rosenthal, K. Chibale, Synthesis and in vitro evaluation of gold(I) thiosemicarbazone complexes for antimalarial activity, *J. Inorg. Biochem.*, 104, 1079–1083, 2010.

[48] S. Tian, F.-M. Siu, S. C. F. Kui, C.-N. Lok, C.-M. Che, Anticancer gold(I)–phosphine complexes as potent autophagy-inducing agents, *Chem. Commun.*, 47, 9318–9320, 2011

[49] G. C. Fortman, S. P. Nolan, Solution calorimetric study of ligand exchange reactions in the [Au(L)Cl] System (L= Phosphine and Phosphite), *Organometallics*, 29, 4579–4583, 2010.

[50] G. F. Shaw III, S. Schraa, E. Gleichmann, Y. P. Grover, L. Dunemann, A. Jagarlamudi, Redox chemistry and $[Au(CN)_2]^-$ in the formation of gold metabolites, *Met. Based Drugs*, 1, 351–362, 1994.

[51] S. Ahmad, A. A. Isab, ^{13}C, ^{31}P and ^{15}N NMR studies of the ligand exchange reactions of auranofin and chloro(triethylphosphine)gold(I) with thiourea, *J. Inorg. Biochem.*, 88, 44–52, 2002.

[52] A. A. Isab, S. Ahmad, Waqar Ashraf, ^{13}C-NMR studies of the binding of 1,3-diazinane-2-selenone and 1,3-diazipine-2-selenone to gold(I) drugs, *Trans. Met. Chem.*, 30, 389–392, 2005.

[53] İ. Özdemir, N. Temelli, S. Günal, S. Demir, Gold(I) complexes of *N*-Heterocyclic carbene ligands containing benzimidazole: Synthesis and antimicrobial activity,

Molecules, 15, 2203–2210, 2010.

[54] C. P. Bagowski, Y. You, H. Scheffler, D. H. Vlecken, D. J. Schmitz, I. Ott, Naphthalimide gold(I) phosphine complexes as anticancer metallodrugs, *Dalt. Trans.*, 10799–10805, 2009.

[55] R. V. Parish, B. P. Howe, J. P. Wright, J. Mack, R. G. Pritchard, Chemical and biological studies of dichloro(2-((dimethylamino)methyl)phenyl)gold(III), *Inorg Chem.*, 35, 1659, 1996.

[56] R. G. Buckley, A. M. Elsome, S. P. Fricker, G. R. Henderson, B. R. Theobald, R. V. Parish, B. P. Howe, R. J. Kelland, Correlation of anti-HIV potency with lipophilicity in a series of cosalane analogs having normal alkenyl and phosphodiester chains as cholestane replacements, *Med. Chem.*, 39, 5208, 1996.

[57] R. Bhattacharya, P. Mukherjee, Biological properties of "naked" metal nanoparticles, *Adv. Drug Deliv. Rev.*, 60, 1289, 2008.

[58] G. Marcon, L. Messori, P. Orioli, M. Cinellu, G. Minghetti, Reactions of gold(III) complexes with serum albumin, *Eur. J. Biochem.*, 270, 4655, 2003.

[59] D. S. Wyrick, S. G. Chaney, In vitro biotransformations of tetrachloro(d,l-trans)-1,2-diaminocyclohexaneplatinum(IV)(Tetraplatin) in rat plasma, *J. Label. Compd. Radio-pharm.*, 25, 349–357, 1988.

[60] Ž. D. Bugarčić, J. Bogojeski, B. Petrović, S. Hochreuther, R. Eldik, Mechanistic studies on the reactions of platinum(II) complexes with nitrogen- and sulfur-donor biomolecules, *J. Chem. Soc. Dalt.*, 41, 12329, 2012.

[61] A. Djeković, A. B. Petrović, Ž. D. Bugarčić, R. Puchtab, R. Eldik, Kinetics and mechanism of the reactions of Au(III) complexes with some biologically relevant

molecules, *J. Chem. Soc. Dalt.*, 41, 3633, 2012.

[62] M. Arsenijevic, V. Volarevic, A. Djekovic, T. Kanjevac, A. Tatjana, D. Nebojsa, D. Svetlana, Z. Bugarcic, *Med. Chem.*, 8, 2, 2012.

[63] S. L. Best, P. J. Sadler, Gold drugs: mechanism of action and toxicity, *Gold Bull.*, 29, 87, 1996.

[64] S. Hanessian, J. Wang, Hydrophilic analogs of (*R*,*R*)-diaminocyclohexane dichloro-platinum (DACH) and the influence of relative stereochemistry on antitumor activity, *Can. J. Chem.*, 71, 2102, 1993.

[65] L.Messori, G. Marcon, P. Orioli, Gold(III) Compounds as new family of anticancer drugs, *Bioinorg. Chem. Appl.* 1, 177, 2003.

[66] P. Calamai, S.Carotti, A.Guerri, T.Mazzei, L. Messori., E. Mini, P. Orili, G. P Speroni, Cytotoxic effects of gold (III) complexes on established human tumor cell lines sensitive and resistant to cisplatin. *Anticancer. Drug Des.*, 13, 67, 1998.

[67] P. Calamai, S. Carotti, A.Guerri, L.Messori, E.Mini, P.Orioli, G. P.Speroni, Biological properties of two gold(III) complexes: $AuCl_3$ (Hpm) and $AuCl_2$ (pm) *J. Inorg. Biochem.*, 66, 103, 1997.

[68] V. Volarevic, M. Milovanovic, A. Djekovic, Ž.D. Bugarcic, N. Arsenijevic, Cytotoxic effects of selected gold(III) complexes on the Murine BCl-1 B lineage leukeamia cell line, *J. Exp. Clin. Res.* 13, 99–102, 2012.

[69] E. Bouwman, B. Douziech, L. Gutierrez-Soto, M. Baretta, W. L. Driessen, J. Reedijk, G. Mendoza-Diaz, Co(II), Ni(II), and Zn(II) compounds of the new tridentate ligand *N*,*N*-bis(2-ethyl-5-methyl-imidazol-4-ylmethyl)aminopropane (biap) .X-ray structures of biap·H_2O, [Co(biap)(NCS)(OAc)], [Ni(biap)(NCS)(OAc)], [Ni(biap)

$(NCS)_2(MeCN)]$, (MeCN), and $[Ni(biap)_2](BF_4)_2(EtOH)$, *Inorg. Chim. Acta*, 304, 250, 2000.

[70] C. T. Brewer, G. Brewer, M. Shang, W. R. Sheidt, I. Muller, Bonding of halogenated arenes in photogenerated (arene)$M(CO)_5$ complexes (M = Cr, Mo, W), *Inorg. Chim. Acta*, 278, 197, 1998.

[71] A. Steenbergen, E. Bouwman, G. A. DeGraaff, W. L. Driessen, J. Reedijk, P. Zanello, Copper co-ordination compounds of a chelating imidazole–thioether ligand. The molecular structures of [1,3-bis(5-methyl-4-imidazolyl)-2-thiapropane]–bis (nitrato)-copper(II)andbis[1,3-bis(5-methyl-4-imidazolyl)-2-thiapropane]copper(II)-bis- (tetrafluoro-borate)-ethanol, *J. Chem. Soc. Dalt. Trans.*, 3175, 1990.

[72] S. Martinez-Carrera, The crystal structure of imidazole at –150°C, *Acta Cryst.*, 20, 783, 1966.

[73] G. Berthier, L. Praud, and J. Serre, Quantum aspects of Heterocyclic Compounds in Chemistry and Biochemistry, E. D. Bergman, B. Pullman (Ed.), *Israel Academy of Science*, Jerusalem, 40, 1970.

[74] J. Ohmori, M. Shimizu-Sasamata, M. Okade, and S. Sakamoto, Novel AMPA Receptor Antagonists: Synthesis and structure−activity Relationships of 1-hydroxy-7-(1*H*-imidazol-1-yl)-6-nitro-2,3(1*H*,4*H*)-quinoxalinedione and related compounds, *J. Med. Chem*., 39, 3971, 1996.

[75] M. Megumu, K. Susumu, Y. Fujio, Cadmium-113 NMR of cadmium(II) complexes with ligands containing N-donor atoms. Dependence of the chemical shift upon the ligand basicity, chelate ring size, counter anion, and cadmium concentration, *Inorg. Chim.*, 25, 964, 1986.

[76] K. Barbarossou, A. E. Aliev, I. P. Gerothanassis, J. Anastassopoulou, T. Theophanides, Natural Abundance ^{15}N CP MAS NMR as a Novel Tool for Investigating Metal Binding to Nucleotides in the Solid State, *Inorg. Chem.*, 40, 3626, 2001.

[77] K. Aoki, Crystallographic studies of interactions between nucleotides and metal ions. II. The crystal and molecular structure of the 1:1 complex of cadmium(II) with guanosine 5'-phosphate, *Acta Crystallogr.*, B32, 1454, 1976.

[78] S. K. Katti, T. P.Seshardi, M. A.Viswamitra, Structure of disodium guanosine 5'-phosphate heptahydrate, *Acta Crystallogr.*, B37, 1825, 1981.

[79] C. L. Barnes, S.W. Hawkinson, structure of disodium guanosine 5'-phosphate heptahydrate, *Acta Crystallogr.*, B38, 812, 1982.

[80] M. E. A. Churchill, R. G. Pritchard, and M. Helliwell, Structure of barium guanosine 5'-monophosphate, *Acta Crystallogr.*, C48, 1223, 1992.

[81] K. Eichele, R. E. Wasylishen, Indirect 113Cd, 14N spin-spin coupling constants as a structural probe of solid cadmium thiocyanate complexes, *Angew. Chem., Int. Ed. Engl.*, 31, 1222, 1992.

[82] R. K. Harris, A. C. Oliveiri, Quadrupolar effects transferred to spin-12 magic-angle spinning spectra of solids, *Prog. NMR Spectrosc.*, 24, 435, 1992.

[83] B. Krebs, G. Henkel, Transition-metal thiolates: from molecular fragments of sulfidic solids to models for active centers in biomolecules, *Angew. Chem. Int. Ed. Engl.*, 30, 769, 1991.

[84] H. Fleischer, Structural chemistry of complexes of $(n-1)d^{10}ns^{m}$ metal ions with β-N-donor substituted thiolate ligands (m = 0, 2), *Coord. Chem. Rev.*, 249, 799,

2005.

[85] E. S. Raper, Complexes of heterocyclic thionates. Part 1. Complexes of monodentate and chelating ligands, *Coord. Chem. Rev.*, 153, 199, 1996.

[86] P. D. Akrivos, Recent studies in the coordination chemistry of heterocyclic thiones and thionates, *Coord. Chem. Rev.*, 213, 181, 2001.

[87] A. A. Isab, M. S. Hussain, Carbon-13NMR and IR Studies of copper(I) complexes of the-NHCS group in five-and six-membered heterocyclic rings, *Transit. Met. Chem.*, 11, 298, 1986.

[88] A. A. Isab, Complexation of silver nitrate with imidazolidine-2-thione and its derivatives, *Transit. Met. Chem.*, 17, 374, 1992.

[89] J. S. Casas, E. G. Martinez, A. Sanchez, A. S. Gonzalez, J. Sordo, U. Casellato, R. Graziani, Complexes of Ag(I) with 1-methyl-2(3*H*)-imidazolinethione. The crystal structure of tris[1-methyl-2(3*H*)-imidazolinethione]-silver(*I*) nitrate, *Inorg. Chim. Acta*, 241, 117, 1996.

[90] A. A. Isab, M. S. Hussain, Synthesis, ^{13}C NMR and IR spectroscopic studies of gold(I) complexes of imidazolidine-2-thione and its derivatives, *Polyhedron*, 4, 1683, 1985.

[91] A. A. Isab M. S. Hussain, Complexation of imidazolidine-2-thione and its derivatives with gold (I) cyanide, J. Coord. Chem, 15, 125, 1986.

[92] S. Ahmad, A. A. Isab, H. Perzanowski, Ligand scrambling reactions of cyano (thione)-gold(I) complexes and determination of their equilibrium constants, *Can. J. Chem.*, 80, 1279, 2002.

[93] A. A. Isab H. Perzanowski, ^{1}H, ^{13}C and ^{199}Hg NMR studies of the

—NHCS-containing ligands with mercuric halides, *Polyhedron*, 15, 2397, 1996.

[94] Z. Popovic, G. Pavlovic, D. Matkovic-Calogovic, Z. Soldin, M. Rajic, D. Vikic-Topic, D. Kovacek, Mercury(II) complexes of heterocyclic thiones.: Part 1. Preparation of 1:2 complexes of mercury(II) halides and pseudohalides with 3,4,5,6-tetrahydro -pyrimidine- 2-thione. X-ray, thermal analysis and NMR studies, *Inorg. Chim. Acta*, 306, 142, 2000.

[95] U. Rajalingam, P. W. Dean, H. A. Jenkis, Solution multinuclear (^{31}P,^{111}Cd, ^{77}Se) magnetic resonance studies of cadmium complexes of heterocyclic aromatic thiones and the structure of [tetrakis(2(1*H*)-pyridinethione)cadmium] nitrate, $[Cd(C_5H_5NS)_4](NO_3)_2$, *Can. J. Chem.*, 78, 590, 2000.

[96] S. Ahmad, A. A. Isab, H. Perzanowski, Gold(I) complexes with tertiary phosphine sulfide ligands, *Transit. Met. Chem.*, 27, 782, 2002.

[97] S. Ahmad, A. A. Isab, and and M. Arab, Synthesis of silver(I) complexes of thiones and their characterization by ^{13}C, ^{15}N and ^{107}Ag NMR spectroscopy, *Polyhedron*, 21, 1267, 2002.

[98] B. B. Ivanova, M. Mitewa, Au(III) interaction with methionine and histidine containing peptides, *J. Coord. Chem.*, 57, 217, 2004.

[99] L. Ronconi, L. Giovagnini, C. Marzano, F. Bettìo, R. Graziani, G. Pilloni, D. Fregona, Gold Dithiocarbamate Derivatives as potential antineoplastic agents: Design, spectro- scopic properties, and in vitro antitumor activity, *Inorg. Chem.*, 44, 1867, 2005.

[100] M.B. Dinger, W. Henderson, Organogold(III) metallacyclic chemistry. Part 4. Synthesis, characterization, and biological activity of gold(III)-thiosalicylate and

-salicylate complexes, *J. Organomet. Chem.*, 560, 233, 1998.

[101] A. A. Isab, B. Al-Maythalony, M. I.M. Wazeer, ^{1}H, ^{13}C NMR and UV spectroscopy studies of gold(III)-tetracyanide complex with L-cysteine, glutathione, capto-pril, L-methionine and DL-seleno-methionine in aqueous solution, *Inorg. Chim. Acta*, 363, 3244–3253, 2010.

[102] K. N. Kouroulis, S. K. Hadjikakou, N. Kourkoumelis, M. Kubicki, L. Male, M. Hursthouse, S. Skoulika, A. K. Metsios, V. Y. Tyurin, A. V. Dolganov, E. R. Milaeva, N. Hadjiliadis, Synthesis, structural characterization and *in vitro* cytotoxicity of new Au(III) and Au(I) complexes with thioamides, *Dalt. Trans.*, 10446–10456, 2009.

[103] B. Đ. Glišić, M. I. Djuran, Z. D. Stanić, S. Rajković, Oxidation of methionine residue in Gly-Met dipeptide induced by $[Au(en)Cl_2]^+$ and influence of the chelated ligand on the rate of this redox process, *Gold Bull.*, 47, 33–40, 2014.

[104] Yanan Chi, W. Chu, Y. Wang, S. Wang, J. Du, J. Zhang, S. Li, G. Zhou, X. Qin, C. Zhang, **S**ynthesis, characterization and cytotoxicity of the Au(III) complexes with cyclic amine-based dithiocarbamate ligands, *Inorg. Chem Commun.* 30, 178–181, 2013.

[105] G. B. Morelle Negom Kouodom, M. Celegato, M. Crisma, S. Sitran, D. Aldinucci, F. Formaggio, L. Ronconi, D.Fregona, Rational design of gold(III)-dithiocarbamato peptidomimetics for the targeted anticancer chemotherapy, *J. Inorg. Biochem*, 117, 248– 260, 2012.

[106] D. Mirjana, Đ.Živadin, D. Bugarćić, F. Heinemann, R. Eldik, Substitution versus redox reactions of gold(III) complexes with L-cysteine, L-methionine and

glutathione, *Dalt. Trans.*, 43, 3911– 3921, 2014.

[107] H. Scheffler, Rational design of gold(III)-dithiocarbamato peptidomimetics for the targeted anticancer chemotherapy, *Polyhedron*, 29, 66–69, 2010.

[108] D. E. Jenkins, R. E. Sykora, Z. Assefa, Synthesis, X-ray crystallography, and photo-luminescence studies of four coordinate gold(I) complexes with the weak Lewis base tri-2-furyl phosphine ligand, *Inorg. Chim. Acta*, 406, 293–300, 2013.

[109] K. P. Bhabak, B. J. Bhuyan, G. Mugesh, Bioinorganic and medicinal chemistry: Aspects of gold protein complexes, *Dalton. Trans*., 40. 2099, 2011.

[110] F. K. Keter, I. Guzei, M. Nell, W. E. Van Zyl, J. Darkwa, Phosphinogold(I) dithiocarbamate complexes: effect of the nature of phosphine ligand on anticancer properties., *Inorg. Chem.*, 53, 2058–67, 2014.

[111] N. S. Jamaludin, Z.-J. Goh, Y. K. Cheah, K.-P. Ang, J. H. Sim, C. H. Khoo, Z. A. Fairuz, B. A. Halim, S. W. Ng, H.-L. Seng, E. R. T. Tiekink, Phosphanegold(I) dithio- carbamates, R3PAu[SC(=S)N((i)Pr)CH2CH2OH] for R = Ph, Cy and Et: role of phosphane-bound R substituents upon in vitro cytotoxicity against MCF-7R breast cancer cells and cell death pathways, *Eur. J. Med. Chem.*, 67, 127–41, 2013.

[112] H. Tapiero, D.Townsend, K.Tew, The antioxidant role of selenium and seleno-compounds, *Biomed. Pharmacother.*, 57, 134–144, 2003.

[113] S. E. Jackson-Rosario W. T. Self, Targeting selenium metabolism and selenoproteins: novel avenues for drug discovery, *Metallomics*, 2, 112–6, 2010.

[114] L. Letavayová, V. Vlcková J. Brozmanová, Selenium: from cancer prevention to DNA damage., *Toxicology*, 227, 1–14, 2006.

[115] A. Molter, J. Rust, C. W. Lehmann, G. Deepa, P. Chiba, and F. Mohr, Synthesis,

structures and anti-malaria activity of some gold(I) phosphine complexes containing seleno- and thiosemicarbazonato ligands., *Dalton Trans.*, 40, 9810–20, 2011.

[116] R. Abdulah, K. Miyazaki, M. Nakazawa, H. Koyama, Chemical forms of selenium for cancer prevention, *J. Trace Elem. Med. Biol.*, 19, 141–50, 2005.

[117] B. Al-maythalony, M. I. M. Wazeer, A. A. Isab, M. Shaikh, S. Altuwaijri, Antibacterial Activities of glycine and histidine complexes of $Cd(SeCN)_2$ and $Hg(SeCN)_2$, *Bioinorg. Chem. Appl.*, 2013, 1–8, 2013.

[118] A. A. Isab, S. Ahmad, Complexation of (trimethylphosphine) gold(I) with selenones, *Trans. Met. Chem.*, 31, 500–503, 2006.

[119] W. Rao, M. J. Koh, P. Wai, H. Chan, W. Rao, S. Ming, J. Koh, P. Wai Hong Chan, Gold-Catalyzed Cycloisomerization of 1,6-Diyne Carbonates and Esters to 2,4a-Dihydro-1*H*-Fluorenes, *J. Org. Chem*, 78, 3183– 3195, 2013.

[120] K. Das Saha J. Dinda, Novel Gold(I) and Gold(III)-N-Heterocyclic carbene complexes: synthesis and evaluation of their anticance properties, *Organometallics*, 33, 2544–2548, 2014.

[121] F. Hackenberg, H. Müller-Bunz, R. Smith, W. Streciwilk, X. Zhu, M. Tacke, Novel Ruthenium(II) and gold(I) NHC complexes: synthesis, characterization, and evaluation of their anticancer properties, *Organometallics*, 32, 5551-5560, 2013.

[122] M. Pellei, V. Gandin, M. Marinelli, C. Marzano, M. Yousufuddin, H. V. R. Dias, C. Santini, Synthesis and biological activity of ester and amide-functionalized imidazolium salts and related water-soluble coinage metal N-Heterocyclic Carbene Complexes, *Inorg Chem.*, 51, 8973–9882, 2012.

[123] L. Messori, L. Marchetti, L. Massai, F. Scaletti, A. Guerri, I. Landini, S. Nobili, G.

Perrone, E. Mini, P. Leoni, M. Pasquali, C. Gabbiani, Chemistry and biology of two novel gold(I) carbene complexes as prospective anticancer agents," *Inorg. Chem.*, 53, 2396–23403, 2014.

[124] T. Zou, C. T. Lum, C.-N. Lok, W.-P. To, K.-H. Low, C.-M. Che, A binuclear gold(I) complex with mixed bridging diphosphine and bis(N-heter, *Angew. Chem. Int. Ed.*, v 53, 5810–5814, 2014.

[125] E. A. Allen, W. Wilkinson, The vibrational spectra of some dialkyl sulphide complexes of gold(III) anil gold(I) halides, *Spectrochim. Acta*, 28A, 2257–2262, 1972.

[126] F. K. Keter, I. A. Guzei, J. Darkwa, N-heterocyclic dithiocarbamate platinum(II) complexes: Unexpected transformation of dithiocarbamate to oxodithiocarbonate in phosphinoplatinum complexes in solution, *Inorg. Chem. comms.*, 27, 60–63, 2013.

[127] Stoe & Cie., *X-Area X-RED32. Stoe Cie GmbH, Darmstadt, Germeny*, 2009.

[128] G. M. Sheldrick, A short history of SHLEX, *Acta Cryst.*, A64, 112–122, 2008.

[129] A. L. Spek, Structure validation in chemical crystallography, *Acta Cryst.* D65, 148–155., 2009.

[130] P. A. Macrae, C. F., Bruno, I. J., Chisholm, J. A., Edgington, P. R., McCabe, P., Pidcock, E., Rodriguez-Monge, L., Taylor, R., van de Streek J. & Wood, Mercury CSD 2.0– new features for the visualization and investigation of crystal structures, *J. Appl. Cryst.*, 41, 466–470, 2008.

[131] M. Altaf, M. Monim-ul-Mehboob, A. A . Isab, V. Dhuna, G. Bhatia, K. Dhuna, S. Altuwaijri, The synthesis, spectroscopic characterization and anticancer activity of new mono and binuclear phosphanegold(I) dithiocarbamate complexes, *New J.*

Chem., 39, 377–385, 2015.

[132] D. A. Brown , W. K. Glass, M. A. Burke, The general use of IR spectral criteria in discussions of the bonding and structure oi metal dithiocarbamates, *Spectrochim. Acta*, 32, 137–143, 1976.

[133] M. Ali, L. Dondaine, A. Adolle, C. Sampaio, F. Chotard, P. Richard, F. Denat, A. Bettaieb, P. Le Gendre, V. Laurens, C. Goze, C. Paul, Anticancer Agents: Does a phosphonium behave l Like a gold(I) phosphine complex Let a Smart Probe Answer, *J. Med. Chem.*, 58, 4521-4528, 2015.

[134] D. C. Onwudiwe and P. a Ajibade, Synthesis, characterization and thermal studies of Zn(II), Cd(II) and Hg(II) complexes of N-methyl-N-phenyl dithiocarbamate: the single crystal structure of $[(C_6H_5)(CH_3)NCS_2]_4Hg_2$, *Int. J. Mol. Sci.*, 12,1964–78, 2011.

[135] K. K. Ooi, C. I. Yeo, K. Ang, A. M. Akim, Y.-K. Cheah, N. A. Halim, H.-L. Seng, a E. R. T. Tiekink, Phosphanegold(I) thiolates, $Ph_3PAu[SC(OR)=NC_6H_4Me_4]$ for R = Me, Et and iPr, induce apoptosis, cell cycle arrest and inhibit cell invasion of HT-29 colon cancer cells through modulation of the nuclear factor-κB activation pathway and ubiquitination., *J. Biol. Inorg. Chem.*, 20, 855–73, 2015.

[136] H. Nabipour, S. Ghammamy, S. Ashuri, S. Aghbolagh, Synthesis of a new dithio-carbamate compound and study of its biological properties, *J. org. Chem.* , 2, 75–80, 2010.

[137] F. Jian, Z. Wang, Z. Bai, X. You, H. Fun, K. Chinnakali, I. A. Razak, The crystal structure, equilibrium and spectroscopic studies of (dithiocarbamate), *Polyhedron*, 18, 3401–3406, 1999.

[138] M. Altaf, M. Monim-ul-mehboob, A. A. Seliman, A. A. Isab, V. Dhuna, G. Bhatia, K. Dhuna, Synthesis, X-ray structures, spectroscopic analysis and anticancer activity of novel gold(I) carbene complexes, *J. Organomet. Chem*., 765, 68–79, 2014.

[139] D. Paliwoda, P. Wawrzyniak, and A. Katrusiak, Polymer under Pressure, *J. Phys. Chem. Lett.*, 5, 2182–2188, 2014.

[140] J. B. Foley, A. Herring, B. Li, and E. V Dikarev, Photochemical reactivity of two gold(I) dinuclear complexes, *cis*/*trans*-(Au*p*NBT)$_2$dppee: Isomerization for the *cis*-(Au*p*NBT)$_2$- dppee isomer, radical substitution for *trans*-(Au*p*NBT)$_2$dppee, *Inorg. Chim. Acta*, 392, 300–310, 2012.

[141] J. D. S. Chaves, F. Neumann, T. M. Francisco, C. C. Corrêa, M. T. P. Lopes, H. Silva, A. P. S. Fontes, M. V. de Almeida, Synthesis and cytotoxic activity of gold(I) complexes containing phosphines and 3-benzyl-1,3-thiazolidine-2-thione or 5-phenyl-1,3,4- oxadiazole-2-thione as ligands, *Inorg. Chim. Acta*, 414, 85–90, 2014.

[142] Gandin, F. Tisato, A. Dolmella, M. Pellei, C. Santini, M. Giorgetti, C. Marzano, M. Porchia, C. S. Uniti, In vitro and in vivo anticancer Activity of copper(I) complexes with homoscorpionate tridentate tris(pyrazolyl)borate and auxiliary monodentate phosphine ligands, *J. Med. Chem* I2, 4745-60, 2014.

[143] W. Liu, K. Bensdorf, M. Proetto, U. Abram, A. Hagenbach, R. Gust, NHC gold halide complexes derived from 4,5-diarylimidazoles: Synthesis, structural analysis, and pharmacological investigations as potential antitumor agents, *J. Med. Chem*., 54, 8605–8615, 2011.

[144] C. Abbehausen, J. Peterson, F. De Paiva, .P. Corbi, B. Formiga, Y. Qu, N. Farrell, Gold(I)- phosphine-N-Heterocycles: Biological activity and specific (ligand) interactions on the C-terminal HIVNCp7 Zinc Finger, *Inorg Chem*., 52, 11280–11287, 2013.

[145] H. D. Velazquez, F. Verpoort, N-Heterocyclic carbene transition metal complexes for catalysis in aqueous media.,*Chem. Soc. Rev.*, 41, 7032–60, 2012.

[146] E. Schuh, P. Carolin, A. Citta, A. Folda, M. P. Rigobello, A. Bindoli, A. Casini, F. Mohr, Gold(I) carbene complexes causing yhioredoxin1 and thioredoxin 2 oxidation as potential anticancer agents, *J. Med. Chem*., 55, 5518–5528, 2012.

[147] X. Xu, S. H. Kim, X. Zhang, A. K. Das, H. Hirao, S. H. Hong, Abnormal N-Heterocyclic Carbene gold(I) complexes: Synthesis, structure, and catalysis in hydration of alkynes, *Organometallics*, 32, 164–171, 2013.

[148] P. Bippus, M. Skocic, M. A. Jakupec, B. K. Keppler, and F. Mohr, Synthesis , structures and in vitro cytotoxicity of some cationic cis-platinum(II) complexes containing chelating thiocarbamates, *J. Inorg. Biochem.*, 105, 462–466, 2011.

[149] M. K. Samantaray, C. Dash, M. M. Shaikh, K. Pang, R. J. Butcher, P. Ghosh, N. York, and U.States,Gold(III) N-Heterocyclic Carbene complexes mediated synthesis of β enaminones from 1, 3-dicarbonyl compounds and aliphatic amines, I*norg. Chem.*, 50, 1840–1848, 2011.

[150] R. Mitra, A. K. Pramanik, A. G. Samuelson, Seleno-Nucleobases and their Water-soluble ruthenium–arene half-sandwich complexes: Chemistry and biological activity, *Eur. J. Inorg. Chem.*, 5733–5740, 2014.

[151] J. Carlos and L. Rodríguez, Phosphine-gold (I) compounds as anticancer agents : General description and mechanisms of action, *anti-Cancer. Agent. Med. Chem*, 11, 921–928, 2011.

[152] M. I. M. Wazeer, A. A. Isab, H. P. Perzanowski, Solid-state NMR studies of 1,3-imidazolidine-2-selenone and some related compounds, *Magn. Reson. Chem.*, 41, 12, 1026–1029, 2003.

[153] S. E. Jackson-Rosario W. T. Self, Targeting selenium metabolism and selenoproteins: novel avenues for drug discovery, *Metallomics*, 2, 112–6, 2010.

[154] C. W. Lehmann, F. Mohr, A. Molter, Synthesis and structural studies of some gold(I) complexes containing selenoureato ligands, *Tetrahedron*, 68, 10586–10591, 2012.

[155] A.Bredenkamp, X. Zeng,F.Mohr, Metal complexes of an N-selenocarbamoyl benzamidine, *Polyhedron*, 33, 107–113, 2012.

[156] A. Molter, J. Rust, C. W. Lehmann, G. Deepa, P. Chiba, F. Mohr, Synthesis, structures and anti-malaria activity of some gold(I) phosphine complexes containing seleno- and thiosemicarbazonato ligands., *Dalton Trans.*, 40, 9810–20, 2011.

[157] B. Al-maythalony, M. I. M. Wazeer, A. A. Isab, M. T. Nael, Complexation of Cd $(SeCN)_2$ with imidazolidine-2-thione and its derivatives: Solid state, solution NMR and anti-bacterial studies, *Spectroscopy* 22, 361–370, 2008.

[158] L. Oehninger, M. Stefanopoulou, H. Alborzinia, J. Schur, S. Ludewig, K. Namikawa, A. Muñoz-Castro, R. W. Köster, K. Baumann, S. Wölfl, W. S. Sheldrick, and I. Ott, Evaluation of arene ruthenium(II) N-heterocyclic carbene complexes as organometallics interacting with thiol and selenol containing biomolecules., *Dalton Trans.*, 42, 1657–66,. 2013.

[159] N. Filipović, N. Polović, B. Rašković, S. Misirlić-Denčić, M. Dulović, M. Savić, M. Nikšić, D. Mitić, K. Anđelković, T. Todorović, Biological activity of two isomeric N-heteroaromatic selenosemicarbazones and their metal complexes, *Monatshefte für Chemie - Chem. Mon.*, 145, 1089–1099, 2014.

[160] M. I. M. Wazeer, A. A. Isab, Solution solid-state NMR studies of some cadmium–selenone complexes, *Spectrochim. Acta Part A*, 62, 880–885, 2005.

[161] A. Molter, F. Mohr, Gold complexes containing organoselenium and organotellurium ligands, *Coord. Chem. Rev.*, 254, 19–45, 2010.

[162] U. Anthoni, G. Borch, P. Klaboe, P. H. Nielsen, Tentative Assignments of fundamental vibrations of thio-and selenoamides. 1,2-Dimethyl-3-pyrazolidineselone, a cyclic selenohydrizide. Selenation of the thioamide group in theory and practice, *Acta Chem. Scand. A*, 36, 69–77, 1982.

[163] Stoe, Cie, X-Area V1.35 and X-RED32 V1.31 Software, Stoe and Cie GmbH, Darmstadt. Germany. 2006.

[164] SHELXS2014/6 (Sheldrick, 2008)

[165] D. Gallenkamp, T. Porsch, A. Molter, E. R. T. Tiekink, F. Mohr, Synthesis and structures of gold(I) phosphine complexes containing monoanionic selenocarbamate ester ligands, *J. Organomet. Chem.*, 694, 2380–2385, 2009.

[166] M. J. Mckeage, L. Maharaj, S. J. Berners-price, Mechanisms of cytotoxicity and antitumor activity of gold(I) phosphine complexes: the possible role of mitochondria *Coord. Chem. Rev*, 232, 127–135, 2002.

[167] G. Lupidi, L. Avenali, M. Bramucci, L. Quassinti, R. Pettinari, H. K. Khalife, H. Gali-muhtasib, F. Marchetti, C. Pettinari, Synthesis, properties, and antitumor effects

of a new mixed phosphine gold(I) compound in human colon cancer cells, *J. Inorg. Biochem.*, 124, 78–87, 2013.

[168] N. Pillarsetty, K. K. Katti, T. J. Hoffman, W. A. Volkert, K. V Katti, and H. Kamei, In vitro and in vivo antitumor properties of tetrakis ((trishydroxy-methyl)phosphine) gold(I) Chloride, *J. Med. Chem.*, I, 1130–1132, 2003.

[169] E. R. T. Tiekink, phosphinegold(I) thiolates pharmacological use and potential, *Bioinorg. Chem. Appl*, 1, 53–67, 2003.

[170] E. García-Moreno, A. Tomás, E. Atrián-Blasco, S. Gascón, E. Romanos, M. J. Rodriguez-Yoldi, E. Cerrada, M. Laguna, In vitro and in vivo evaluation of organometallic gold(I) derivatives as anticancer agents., *Dalton Trans.*, 45, 2462–75, 2016.

[171] M. I. M. Wazeer, A. A. Isab, A. El-rayyes, Solid state NMR study of 1,3-imidazolidine-2-thione, 1,3-imidazolidine-2-selenone and some of their N-substituted derivatives,, *Spectroscopy*, 18, 113–119, 2004.

[172] J. Foley, R. C. Fort, K. Mcdougal, M. R. M. Bruce, and A. E. Bruce, Electronic and steric effects in gold(I) phosphine thiolate complexes, *Met. Based Drugs*, 1, 405–417, 1994.

[173] SHELXS2014/6 (Sheldrick, 2008, Spek, 2009).

[174] SHELXL2014/6 (Sheldrick, 2015)..

[175] D. Trans, E. Vergara, E. Cerrada, C. Clavel, M. Laguna, Thiolato gold(I) complexes containing water-soluble phosphane ligands: a characterization of their chemical and biological properties, *Dalt. Trans.*, 40, 10927–10935, 2011.

[176] M. Baron, S. Bellemin-Laponnaz, C.Tubaro, M. Basato, S. Bogialli, A.Dolmella, Synthesis and biological assays on cancer cells of dinuclear gold complexes with novel functionalised di(N-heterocyclic carbene) ligands., *J. Inorg. Biochem.*, 141, 94–102, 2014.

[177] U. E. I. Horvath, L. Dobrzańska, C. E. Strasser, W. Bouwer Neé Potgieter, G. Joone, C. E. J. van Rensburg, S. Cronje, H. G. Raubenheimer, Amides of gold(I) diphosphines prepared from N-heterocyclic sources and their in vitro and in vivo screening for anticancer activity., *J. Inorg. Biochem.*, 111, 80–90, 2012.

[178] Stoe, Cie, X-Area V1.35 and X-RED32 V1.31 Software, Stoe and Cie GmbH, Darmstadt. Germany. 2006. SHELXS97 (Sheldrick, 1990).

[179] H. D. Flack, On enantiomorph-polarity estimation, *Acta Cryst*. A39, 876-881, 1983

[180] P. Flack, Wagner, Use of intensity quotients and differences in absolute structure refinement, *Acta Cryst*., B69, 249-259, 2013.

[181] M. C. Jahnke, T. Pape, F. E. Hahn, Ligand exchange at a Gold(I) Carbene Complex, *Z. Naturforsch.*, 68b, 467–473, 2013.

[182] R. Visbal, J. M. López-de-Luzuriaga, A. Laguna, and M. C. Gimeno, Three-coordinate gold(I) N-heterocyclic carbene complexes:a new class of strongly luminescent derivatives., *Dalt. Trans.*, 43, 328–334, 2014.

[183] K. Singh, Y. Kumar, P. Puri, C. Sharma, K. R. Aneja, Metal-based biologically active compounds: Synthesis, spectral, and antimicrobial studies of cobalt, nickel, copper, and zinc complexes of triazole-derived schiff bases, bioinorg. *Chem. Appl.*, 2012, 1-9, 2012.

[184] S. Nobili, E. Mini, I Landini, C. Gabbiani, A. Casini, L. Messori, Gold compounds as anticancer agents: Chemistry, cellular pharmacology, and preclinical studies, *Med. Res. Rev*., 30, 550–580, 2009.

[185] A. Casti, R. Pedrido, Aurophilicity in gold(I) thiosemicarbazone clusters, *Dalton. Trans*., 41 ,1363–1372, 2012.

[186] A. Albert, C. Brauckmann, F. Blaske, M. Sperling, C. Engelhard, U. Karst, Speciation analysis of the antirheumatic agent Auranofin and its thiol adducts by LC/ESI-MS and LC/ICP-MS, *J. Anal. At. Spectrom.*, 27, 975, 2012.

[187] T. M. Simon, D.H. Kunishima, G. J. Vibret, A. lorber, Inhibitory effects of a new oral gold compounds on hela cell, *Cancer*, 44, 1965-1975, 1979.

[188] L. Maiore, M. Agostina, S. Nobili, I. Landini, E. Mini, C. Gabbiani, L. Messori, Gold(III) complexes with 2-substituted pyridines as experimental anticancer agents: Solution behavior, reactions with model proteins, antiproliferative properties, *J. Inorg. Biochem.*, 108, 123–127, 2012.

[189] A. Z. Mustafa M. Altaf, M. Monim-ul-Mehboob, M. Fettouhi, M.I.M. Wazeer, A.A. Isab, V. Dhuna, G. Bhatia, K. Dhuna, Tetrakis(1-3-diazinane-2-thione)platinum(II) chloride monohydrate complex: Synthesis, spectroscopic characterization, crystal structure and in vitro cytotoxic activity against A549, MCF7, HCT15 and HeLa human cancer lines, *Inorg. Chem. Commun.*, 44, 159–163, 2014

[190] P. K. Ghosh S. Saha, A. Mahaparta, Interaction of 2-aminopyrimidine with dichloro-[1-alkyl-2-(naphthylazo) imidazole]palladium(II) complexes: Kinetic and mechanistic studies, *J. Chem. Cent*., 1, 23–33, 2007.

[191] S. K. Bera S. K. Chandra, G.S. De, Substitution of Aqua Ligands from *cis*-[Pt(en)(H_2O)$_2$](ClO_4) and *cis*-[Pt(dmen)(H_2O)$_2$ (en=Ethylenediamine, dmen =N,N'-dimethylethylenediamine) by Glycine in Aqueous Medium- A Kinetic and Mechanistic Approach, *Int. J. Chem. Kinet*., 37, 4895–495, 2005.

[192] S. Ray, R. Sarkar, A. Chattopadhyay, A.K. Ghosh, Kinetic and mechanistic aspects of ligansubstitution on *cis*-diaqua (*cis*-1,2-diaminocyclohexane)platinum(II) with thglycine-containing dipeptides, *Progress in React. Kinet. Mech*., 39, 122–136, 2014.

[193] B.Đ. Glišić, U. Rychlewskab, M. I. Djuran, Reactions and structural characterization of gold (III) complexes with amino acids, peptides and proteins, *Dalton Trans*., 41, 6887–6901, 2012.

[194] P. M Yangyuoru, J.W. Webb, C.F. Shaw III, Glutathionato-S-Gold(III) complexes formed as intermediates in the reduction of auricyanide by glutathione *J. Inorg. Biochem*., 102, 584–593, 2008.

[195] A. J. Canumalla, N. Al-zamil, M. Phillips, A.A. Isab, C.F. SHaw III. Redox and ligand exchange reactions of potential gold(I) and gold(III)-cyanide metabolites under biomimetic conditions, *J. Inorg. Biochem*., 85, 67–76, 2001.

[196] M. Luty-Blocho, K. Paclawski, M. Wojnicki, K. Fitzner, The kinetics of redox reaction of gold(III) chloride complex ions with L-ascorbic acid, *Inorg. Chim. Acta,* 395, 189-196, 2013.

[197] W. J. Louw, W. Robb, Kinetics and mechanisms of reactions of gold(III) complexes. II. The formation and equilibrium hydrolysis of tetrabromoaurate(III), *Inorg. Chim. Acta*., 9, 33-37, 1974.

[198] S. S. Al-jaroudi, M. Fettouhi, M. I. M. Wazeer, A. A. Isab, Synthesis, characterization and cytotoxicity of new gold(III) complexes with 1,2-diaminocyclohexane: Influence of stereochemistry on antitumor activity, *Polyhedron*, 50, 434–442, 2013.

[199] S.S. Al-Jaroudi, M. Monim-ul-Mehboob, M.Altaf, M. Fettouhi, M.I.M.Wazeer, S. Altuwaijri, A. A. Isab, Synthesis, spectroscopic characterization, X-ray structure and electrochemistry of new bis(1,2-diaminocyclohexane)gold(III) chloride compounds and their anticancer activities against PC3 and SGC7901 cancer cell lines, *New J. Chem.*, 38, 3199, 2014

[200] S. Sahu, P. R. Sahoo, S. Patel, B. K Mishra, Oxidation of Thiourea and Substituted Thioureas, *J. Sulfur Chem.*, ifirst, 1-27, 2011.

[201] D. Chatterjee, S. Rothbart, and R. Van Eldik, Selective oxidation of thiourea with H_2O_2 catalyzed by [RuIII(edta)(H_2O)]: kinetic and mechanistic studies, *Dalton Trans*., 42, 4725–4729, 2013.

[202] A. A. Isab, S. Ahmad, Applications of NMR spectroscopy in understanding the gold biochemistry, *Spectroscopy*, 20, 109–123, 2006.

[203] A. A. Isab, S. Ahmad, A. R. Al-Arfaj, M. N. Akhtar, ^{13}C and ^{15}N NMR Studies of the interaction of gold(I) thiolates with thiourea (^{13}C and ^{15}N Labelled), *J. Coord. Chem.*, 56 , 95–101, 2003.

[204] R. Crabtree. Organometallic chemiistry of Transitition Metals, *5th Edn.*, Wiley& Sons, New Jersey, 115–116, 2009.

[205] M. N. Akhtar, A. A.I sab, M. S. Hussain, A. R. Al-arfaj, Synthesis of thionato-(trimethylphosphine)gold(I) complexes, *Trans. Met. Chem*., 21, 553–555, 1996.

[206] J. A. Weyh, R.E. Hamm, The Aquation of the cis-Bis(iminodiacetato)chromate(III) and runs(fac)-Bis(methyliminodiacetato)chromate(III) Ions in Acidic Aqueous Medium. *Inorg. Chem.*, 8, 2298-2302, 1969.

[207] Z. D. Bugarcic, B.V. Djordjevic, Kinetics and mechanism of the reaction of platinum(II) complexes with thioglycolic acid, *Monatshefte Fur Chemie*., 129, 1267-1274, 1998.

[208] A. Akbari, A.Samie, Kinetic Study on 1,10-phenantroline reaction with *cis*-[Pt(*p*-$FC_6H_4)_2(SMe_2)_2$] Complex, *Chem. Mater. Eng*., 1, 111-115, 2013.

[209] A. Samanta, G. K. Ghosh, I. Mitra, S. Mukherjee, J. C. Bose, S. Mukhopadhyay, W. Linert, S. C. Moi, Ligand substitution reaction on a platinum(II) complex with bio-relevant thiols: kinetics, mechanism and bioactivity in aqueous medium, *RSC. Adv*., 4, 43516, 2014.

[210] D. Fan, C. Yang, J. D. Ranford, and J. J. Vittal, Chemical and biological studies of gold(III) complexes with uninegative bidentate N–N ligands, *Dalt. Trans.*, 4749–4753, 2003.

[211] M. Bortoluzzi, A.Scrivanti, A. Reolon, E.Amadio, V.Bertolasi, Synthesis and characterization of novel gold(III) complexes with polydentate N-donor ligands based on the pyridine and triazole heterocycles, *Inorg. Chem. Commun.*, 33, 82–85, 2013.

[212] S. L. Best, Z. Guo, M. I. Djuran, P. J. Sadler, [Au(dien)Cl]Cl_2: exchange phenomena observed by ^{1}H and ^{13}C NMR spectroscopy, *Met. Based Drugs*, 6, 261–269, 1999.

[213] B. B. Zmejkovski, J. Trifunovi, A. Savi, D. Stankovi, A. Damjanovi, Z. Jurani, G. N. Kalu, T. J. Sabo, Gold(III) complexes with esters of cyclohexyl-functionalized, *J. Inorg. Biochem.*, 128, 146–153, 2013.

[214] J. Zhang, W. Lu, R. W. Sun, C. Che, Organogold(III) supramolecular polymers for anticancer treatment, *Angew. Chem. Int. Ed.*, 51, 4882–4886, 2012.

[215] M. Serratrice, M. A. Cinellu, L. Maiore, M. Pilo, A. Zucca, C. Gabbiani, A. Guerri, I. Landini, S. Nobili, E. Mini, and L. Messori, Synthesis, structural characterization, solution behavior, and in vitro antiproliferative properties of a series of gold complexes with 2-(2 ′-Pyridyl)benzimidazole as Ligand: comparisons of Gold(III) versus Gold(I) and Mononuclear versus Binuclear Derivatives, *Inorg Chem.*, 51, 3161–3171, 2012.

[216] R. February, Gold(Ill) compounds as new family of anticancer drugs, *Bioinorg. Chem. Appl.*, 1, 177–187, 2003.

[217] C. Gabbiani, A. Guerri, M. A. Cinellu, and L. Messori, Dinuclear Gold(III) complexes as potential anticancer agents: structure , reactivity and biological profile of a series of gold(III) oxo-bridged derivatives, *J. open Crystallogr.*, 3, 29–40, 2010.

[218] J. F. Vollano, S. Al-Baker, J. C. Dabrowiak, J. E. Schurig, Comparative antitumor studies on platinum(II) and platinum(IV) complexes containing 1,2-diaminocyclo-hexane., *J. Med. Chem.*, 30, 716–719, 1987.

[219] S. Zhu, W. Gorski, D. R. Powell, J. A. Walmsley, Synthesis , structures , and electrochemistry of gold(III) ethylenediamine complexes and interactions with guanosine 5′-monophosphate, *Inorg Chem.*, 45, 688–2694, 2006.

[220] C. D. Sanghvi, P. M. Olsen, C. Elix, S. Bruce, D. Wang, Z. Georgia, D. M. Shin, K. I. Hardcastle, C. E. Macbeth, and J. F. Eichler, Antitumor properties of five-coordinate gold(III) complexes bearing substituted polypyridyl ligands, *J. Inorg. Biochem.* 128, 68–76, 2013.

[221] M. Monim-ul-mehboob, M. Altaf, M. Fettouhi, A. A. Isab, M. I. M. Wazeer, M. N. Shaikh, S. Altuwaijri, Synthesis , spectroscopic characterization and anti-cancer properties of new gold(III)– alkanediamine complexes against gastric, prostate and ovarian cancer cells; crystal structure of [$Au_2(pn)_2(Cl)_2]Cl_2$. H_2O, *Polyhedron*, 61, 225–234, 2013.

[222] M. A. Rawashdeh-omary, M. A. Omary, H. H. Patterson, and R. V May, Oligomerization of $[Au(CN)_2]^-$ and $[Ag(CN)_2]^-$ ions in solution via ground-state aurophilic and argentophilic bonding, *J. Am. Chem. Soc.*, 122, 10371–10380, 2000.

[223] K. J. Harris and R. E. Wasylishen, A ^{13}C and ^{15}N solid-state NMR study of structural disorder and aurophilic bonding in Au(I) and Au(III) cyanide complexes, *Inorg. Chem.*, 48, 2316–2332, 2009.

[224] X. Wang, Y. Wang, J. Yang, X. Xing, J. Li, L. Wang, Evidence of significant covalent bonding in $[Au(CN)_2]^-$, *J. Am. Chem. Soc.*, 131, 16368–16370, 2009.

[225] L. H. Skibsted, in: A. G. Sykes(Ed.), Advances in Inorganic and Bioinorganic Mechanism, *Academic Press, New York*, 4, 137-183, 1986.

[226] R. Pearson, F. Basolo, Mechanisms of Inorganic Reactions, 2nd Edition, *Wiley & Sons, New York,* 139- 141; 410- 414, 1967.

[227] B. P. Marco Bortoluzzi, Gino Paolucci, The roles of ligands proton affinity, π-back donation and metal fragment hardness on the Au–N bond in N-donor heterocycles gold(III) complexes, *Polyhedron*, 29, 767–772, 2010.

[228] W. Y. Mason, H. B. Gray, Electronic structures and spectra of square-planar Complexes, *J. Amer. Chem. Soc.*, 7, 5721–5729, 1968.

[229] M. A. Ivanov, M. V. Puzyk, Spectroscopic and electrochemical properties of dichloro-diimine complexes of Au(III) and Pt(II) with 1,4-diazine derivatives, J. *Russ. Gen. Chem.*, 76, 843–848, 2006.

VITAE

Name	:Adam Ahmed Abdallah Sulaiman
Nationality	: Sudanese
Date of Birth	: December 31, 1979
E-mail	: adamahmed@kfupm.edu.sa, adamchemi@gmail.com.
Address	: KFUPM, Dhahran 31261, Saudi Arabia
Academic Background	: B.Sc.(Hon.), AL-Neelain University, Sudan
	M.Sc. in Applied Chemistry, University of Gezira, Sudan

PUBLICATIONS

1. Muhammad Altaf , M. Monim-ul-Mehboob , **Adam A.A. Seliman** , Anvarhusein A. Isab ,Vikram Dhuna , Gaurav Bhatia, Kshitija Dhuna, Synthesis, X-ray structures, spectroscopic analysis and anticancer activity of novel gold(I) carbine complexes. *Journal of Organometallic Chemistry* 765 (2014) 68-79.
2. **Adam A. A. Seliman**, Muhammad Altaf, Abdel-Nasser Kawde, Mohammed I. M. Wazeer and Anvarhusein A. Isab, NMR, and Kinetic Studies of the Interactions of [Au(cis-DACH)Cl]Cl and [Au(cis-DACH)2]Cl with Potassium Cyanide in Aqueous Solution. *Journal of Coordination Chemistry*, Vol 67, No. 21, (2014), 3431–3443.
3. Muhammad Altaf, M. Monim-ul-Mehboob, **Adam A.A. Seliman**, Manzar Sohail, Mohammed I.M. Wazeer, Anvarhusein A. Isab, L. Li, V. Dhuna, G. Bhatia, K. Dhuna, Synthesis, characterization and anticancer activity of gold(I)complexes that contain tri-tert-butylphosphine and dialkyl dithiocarbamate ligands. *European Journal of Medicinal Chemistry* 95 (2015) 464-472.
4. Khalid H. Omer, **Adam A. A. Seliman**, Muhammad Altaf , Naike Casagrande , Donatella Aldinucci and Anvarhusein A. Isab Synthesis, characterization and anticancer activity of gold(III) complexes with (1R,2R)-1,2-diamino-cyclohexane *Journal of Polyhedron.*102 (2015) 773-781.
5. **Adam A. A. Seliman**, Khalid H. Omer, Abdel-Nasser Kawde aM. I. M. Wazeer, Muhammad Altaf, Musa M. Musa and Anvarhusein A. Isab, Spectroscopic Studies of Interactions of the Potential Anticancer [Au(*cis*-DACH)Cl_2]Cl and

[Au(*cis*-DACH)$_2$]Cl$_3$ complexes with Biologically Relevant Thiones *J. Coord. Chem.* **in progress**.

6. **Adam A. A. Sulaiman[1]**, Muhammad Altaf[2], Anvarhusein A. Isab[1], Abdullah Alawad[3], Saleh Altuwaijri[4], Saeed Ahmad[5]. Synthesis, Characterization and *in vitro* Cytotoxicity of Gold(I) Complexes of (2-aminoethyl)diphenylphosphine and Dithiocarbamates. ***Monatshefte für Chemie***, in progress**.**
7. Khalid H. Omera, **Adam A. A. Selimana**, Hassan A. Al-Mohsina, Abdel-Nasser Kawdea, Mohamed Altafb, Mohammed I. M. Wazeera and Anvarhusein A. Isaba* Study of the interaction of some potential anticancer gold(III) complexes with biologically important thiols using NMR, UV-Vis and Electrochemistry. *Inorganica Chim Acta* in progress.
8. Said S. Al-Jaroudi, Shipra Yadav, Farukh Arjmand, **Adam A. Seliman**, Ali Alhoshani, Muhammad Altaf, H. M. Korashy and Anvarhusein A. Isab. DNA binding, molecular docking studies, in vitro cytotoxic evaluations and biological structure–activity relationship of dithiocarbamate phosphine gold(I)complexes. Ready to submit.

PATENTS

1. Anvarhusein A. Isab, Muhammad Altaf, M. Monim-ul-Mehboob, **Adam A.A. Seliman** New gold(I) complexes with t-butyl phosphine and dialkyl dithiocarbamate ligands, ***US Patent 0266909Al, 2015.***

CONFERENCE PAPERS

1. **Adam A. A. Seliman** and A. A. Isab, "New Gold(I) Complexes with t-butyl phosphine and Dialkyl-dithiocarbamate Ligands: Synthesis, Spectroscopic Characterization, and In vitro Cytotoxic Evaluation against A549, HeLa New Gold(I) Complexes with t-butyl phosphine and Dialkyldithiocarbamate Ligands" the 5th Scientific Conference for Students of Higher Education, Riyadh, KSA, April 28 to May 2, **2014**.

2. **Adam A. A. Seliman** and **A. A. Isab**, "NMR and kinetic studies of the interactions of [Au(cis-DACH)Cl_2]Cl and [Au(cis-DACH)2]Cl_3 with potassium cyanide in aqueous solution" 3rd International Conference and Exhibition on Laboratory Technology (IABTECH), Manama, Kingdom of Bahrain, Oct, 28-30, **2014**.

Awards

- The 5th Scientific Conference for Students of Higher Education, Riyadh, KSA, May, 2014

APPENDIX